Energy Research and Development Division
FINAL PROJECT REPORT

Laboratory Testing and Field Measurement of Plug-in Electric Vehicle (PEV) Grid Impacts

Prepared for: California Energy Commission
Prepared by: San Diego Gas & Electric and Quanta Technology

MARCH 2015
CEC-500-2015-093

PREPARED BY:

Primary Authors:
Gil Montes, SDG&E
Donna Miyasako-Blanco, SDG&E
Farid Katiraei, Quanta Technology
Saman Alaeddini, Quanta Technology
Tim Chang, Quanta Technology
Bahman Koosha, Quanta Technology
Joseph Chongfuangprinya, Quanta Technology

San Diego Gas & Electric
8316 Century Park Ct.
San Diego, CA 92123
www.sdge.com

Contract Number: 500-11-007

Prepared for:

California Energy Commission

Kiel Pratt
Contract Manager

Fernando Pina
Office Manager
Energy Systems Research Office

Laurie ten Hope
Deputy Director
ENERGY RESEARCH AND DEVELOPMENT DIVISION

Robert P. Oglesby
Executive Director

ACKNOWLEDGEMENTS

Gil Montes, San Diego Gas & Electric

Donna Miyasako-Blanco, San Diego Gas & Electric

Farid Katiraei, Quanta Technology

Saman Alaeddini, Quanta Technology

Tim Chang, Quanta Technology

Bahman Koosha, Quanta Technology

Joseph Chongfuangprinya, Quanta Technology

PREFACE

The California Energy Commission Energy Research and Development Division supports public interest energy research and development that will help improve the quality of life in California by bringing environmentally safe, affordable, and reliable energy services and products to the marketplace.

The Energy Research and Development Division conducts public interest research, development, and demonstration (RD&D) projects to benefit California.

The Energy Research and Development Division strives to conduct the most promising public interest energy research by partnering with RD&D entities, including individuals, businesses, utilities, and public or private research institutions.

Energy Research and Development Division funding efforts are focused on the following RD&D program areas:

- Buildings End-Use Energy Efficiency
- Energy Innovations Small Grants
- Energy-Related Environmental Research
- Energy Systems Integration
- Environmentally Preferred Advanced Generation
- Industrial/Agricultural/Water End-Use Energy Efficiency
- Renewable Energy Technologies
- Transportation

Laboratory Testing and Field Measurement of Plug-in Electric Vehicle (PEV) Grid Impacts is the final report for the Contract Number 500-11-007, "Electric Vehicle Charging Simulator for Distribution Grid Feeder Modeling", a PIER project funded by the California Energy Commission and conducted by SDG&E.. The information from this project contributes to Energy Research and Development Division's Energy Systems Integration Program.

For more information about the Energy Research and Development Division, please visit the Energy Commission's website at www.energy.ca.gov/research/ or contact the Energy Commission at 916-327-1551.

ABSTRACT

San Diego Gas & Electric (SDG&E) and Quanta Technology simulated and measured the impacts of electric vehicles on electric distribution circuits. One of SDG&E's highly impacted circuits was chosen as the test bed and modeled in a Real Time Digital Simulator test setup. In addition, two electric vehicle simulators were designed and constructed to interface with the Real Time Digital Stimulator, allowing true power hardware-in-loop testing of plug-in electric vehicle impacts. Several studies were conducted with the Real Time Digital Stimulator and plug-in electric vehicle simulators to reflect various charging and transformer loading conditions with combinations of single and multiple plug-in electric vehicle customers at given locations.

A study was also conducted at an SDG&E site integrating 18 fleet and employee-use electric vehicle chargers with a photovoltaic system and a lithium-ion based energy storage system.

Keywords: Plug-In Electric Vehicle (PEV), PEV Impact, Level 2 Chargers, DC Fast Chargers, RTDS, PHIL, Distribution Test Bed, Hybrid systems

Please use the following citation for this report:

Montes, Gilbert (San Diego Gas & Electric); Katiraei, Farid (Quanta Technology). 2015. Laboratory Testing and Field Measurement of Plug-in Electric Vehicle Grid Impacts. California Energy Commission. Publication number: CEC-500-2015-093

LIMITATION OF LIABILITY

This report is prepared by SDG&E and Quanta Technology, LLC under Contract 500-11-007 with the California Energy Commission. Neither Quanta Technology, nor SDG&E, nor the California Energy Commission, nor any person acting on behalf of either:

1. Makes any warranty or representation, expressed or implied, with respect to the use of any information contained in this report, or that the use of any information, apparatus, method, test, or investigation process disclosed in this report may not infringe privately owned rights.

2. Assumes any liabilities with respect to the use of or for damage resulting from the use of any information, apparatus, method, test, or investigation process disclosed in this report.

TABLE OF CONTENTS

LIST OF FIGURES

LIST OF TABLES

EXECUTIVE SUMMARY

Introduction

California's electricity ratepayers are expressing considerable interest in purchasing plug-in electric vehicles (PEVs). PEVs are being deployed in numbers that require utilities to understand and address the impact of battery charging on the distribution grid. Charging a PEV can represent a significant load addition, and may result in a need to upgrade existing electric distribution facilities. To date, only paper studies were done to assess the grid impact of PEV charging.

Project Purpose

The primary purpose was to design a test environment to investigate the impact of PEV charging on San Diego Gas and Electric's (SDG&E) distribution grid. Because utilities must understand and address the impact of PEV battery charging, a technical goal was to simulate load and power quality effects of multiple PEVs charging to determine the impact on grid performance and operation. This project would generate information and create an adaptable simulator to help utilities configure their distribution system to avoid outages to ratepayers caused by the impacts of PEVs.

A separate task of this project aimed to demonstrate an integrated approach to PEV charging incorporating renewable generation, battery energy storage and smart charging. Although not integrally tied to the PEV simulator activities, this workplace charging demonstration would serve as a showcase of potential mitigation strategies for PEVs appearing on the distribution grid.

Project Process

SDG&E and Quanta Technology designed and assembled two PEV battery charging simulators using commercially available power supplies and inverter systems to replicate PEV charging patterns. The PEV simulators, along with a Real Time Digital Simulator (RTDS), constituted the primary hardware components of the simulation studies. Two PEV simulators were sought for study to represent a 10 kilowatt (kW) alternating current (AC) Level 2 charger and a 40kW Level 3 direct current (DC) Fast Charger. The PEV simulators included a regenerative design that enhanced simulation flexibility and allowed the simulators to feed power back to the grid. The RTDS setup was used to simulate distribution circuits and associated customer locations.

The project team conducted a survey of SDG&E distribution feeders, which are the distribution power lines emanating from utility substations. The feeders were ranked using an algorithm according to a set of selected criteria. A circuit with a 12 kilovolt (kV) feeder, 41 distributed photovoltaic (PV) systems and 14 customers with PEVs was selected for representative testing.

The team designed experiments to test the impacts of PEV charging on distribution circuits by varying several factors, such as the charging patterns and number of customers. The researchers also evaluated system impacts covering various types and sizes of PEV chargers installed on the representative distribution circuits. It was assumed that various types of PEV chargers were installed and used by residential customers or were installed at public locations.

The project also included a workplace PEV charging demonstration at an SDG&E site combining 18 fleet and employee-use charging stations integrated with a solar PV system and with a lithium-ion battery energy storage system (BESS). The objective of integrating the PEV charging stations with PV and the BESS in this hybrid system architecture was to demonstrate the system's load control and power management capabilities. These capabilities can eliminate resource intermittency and avoid circuit overloading due to extensive loading from PEV charging stations.

Project Results

The primary findings from the PEV simulator tests are summarized as follows:

- The main distribution grid impact of PEV charging was on the transformer current and power flow profile of the circuit. In some cases, the current through transformer was tripled. The smaller transformers, typically 25 kilovolt-amperes (kVA) experienced the highest overloads, while the larger transformers, typically 50 kVA and 100 kVA, had greater margins for accepting the additional demand of the PEV charging loads.
- Voltage drops on the secondary circuits from the increased demand were highly observable. If the voltage on secondary circuits was very close to the lower band of the acceptable voltages, additional load of the PEV chargers would reduce the voltage further beyond the acceptable range. The uncontrolled charging patterns showed a higher impact on the voltage.
- Since the controlled charging mostly occurred during late evening, voltage was higher at that time compared to the late afternoon or early evening. The impact on the secondary voltage drop was lower compared to the uncontrolled scenarios.
- In most tested cases, there was a smaller impact on the primary circuit voltages at 12 kV.

Overall, it was shown that the PEV simulator and the power hardware-in-the-loop test setup provided a flexible environment for testing the impact of PEVs on the service transformer and the primary or secondary circuits. Different circuit arrangements and multiple customer connection points could be represented in the model and test bed and rearranged to meet changes in circuit characteristics or changes in the nature of loads.

Although it was not a core objective of the project, the simulator setup was also found to have the capability to model the impacts of smart inverters on the distribution grid.

The workplace PEV charging demonstration showed that load control, peak shaving, and other power management capabilities can be achieved by integrating PEV charging stations with solar PV and a stationary energy storage system. The hybrid system architecture can eliminate resource intermittency and avoid circuit overloading from PEV charging. The analysis of performance data covering several months of operations have facilitated detailed examinations of system design and control behavior.

Benefits to California

The PEV distribution grid impact simulations and integrated PEV charging demonstration are adding to stakeholders' understanding of PEV distribution grid impacts and mitigation options. They are pointing to methods utilities can use to save ratepayers money and ways to expand customer options.

The testing and impact analysis of various types of PEV chargers on the distribution network is contributing to advancements in system planning and the investigation of mitigation solutions to ensure proper asset utilization.   The project has generated information and created an adaptable simulator to help utilities configure their distribution system to avoid outages to ratepayers caused by PEV impacts.

The workplace charging demonstration is aiding advancements in system planning, mitigation solutions, ensuring proper asset utilization, and producing a variety of consumer options for California's electricity ratepayers.

Findings from the laboratory simulations and field demonstration can also improve utility-industry collaboration in enhancing PEV charger design and in structuring possible charging tariff rates that encourage shifting PEV charging load to off-peak times.

SDG&E and Quanta Technology researchers have extensively shared their distribution survey methodology, simulator setup, and workplace charging results in several forums as detailed in Appendix F : Technology Transfer Activities. The team developed a user guide to describe how other utilities and researchers can use the PEV simulator for any potential testing applications involving electric vehicles. The team also identified possible future enhancement and added features for the simulator setup.

Through its development, the PEV simulator also demonstrated its applicability for testing smart inverter functions, including power curtailments, power factor adjustment, and reactive power compensation. Smart inverter testing can provide benefits to engineers in understanding and testing aspects of grid integration, and is an interesting and valuable aspect of the project for industry, the research community, and policymakers.

CHAPTER 1:
Design of an Electrical Vehicle Simulator

In this project, designing two Plug-in Electric Vehicle (PEV) simulators were targeted for laboratory testing and impact studies. The PEV Simulators were used to represent actual PEV charging load with various customers' charging patterns on service transformers.

The first prototype PEV Simulator had the capability of emulating operation of one (up to) 10 kW Level 2 charger. It provided various options for creating customized charging profiles or selecting from a list of pre-programmed typical charging profiles such as: 3.3 kW (Chevy Volt), 5.2kW (Nissan LEAF), and 9.8kW (Tesla Roadster). The second PEV simulator represented one (up to) 40 kW DC Fast Charger. Simplified building blocks of the two PEV Simulators are shown in Figure 1 and Figure 2.

Figure 1 - Block Diagram of the PEV Simulator Rack 1 (Level 2 Charger)

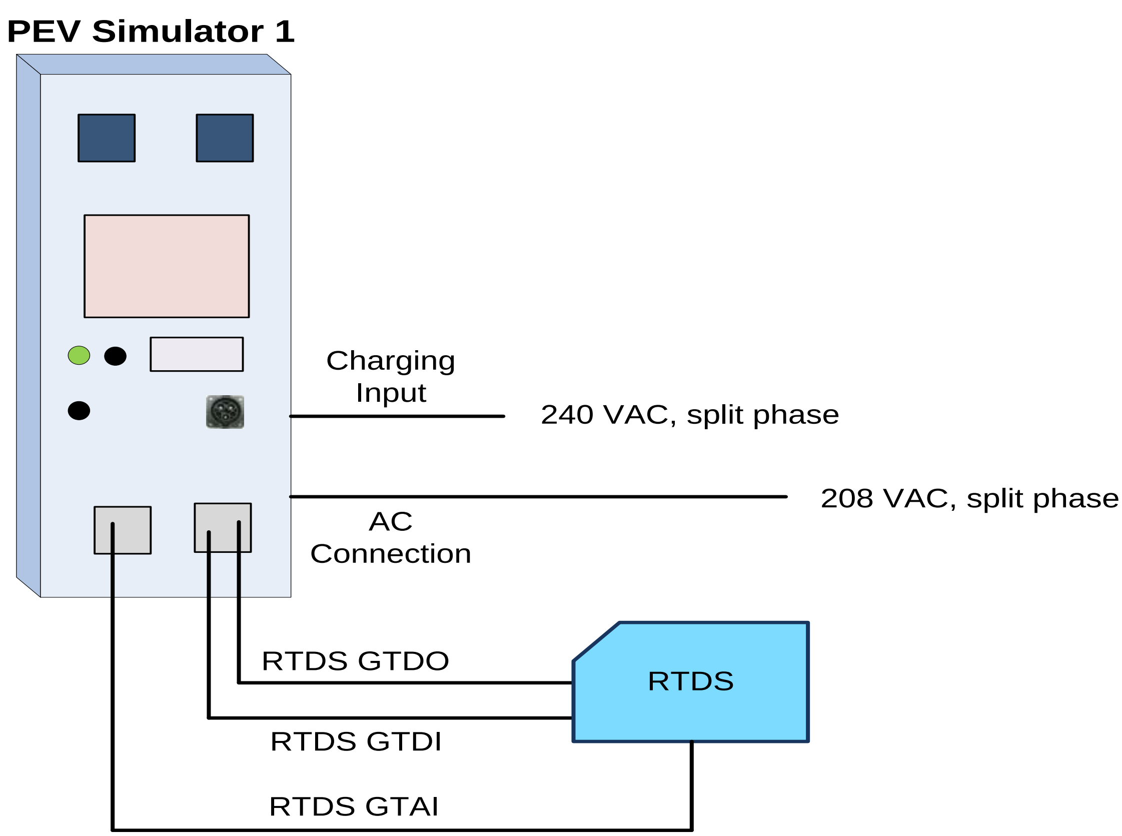

The Level 2 Charger, which was the common charger expected to be used by residential customers, was individually controlled to represent two types of customer charging behaviors, namely:

1) Uncontrolled charging pattern (representing customers with random charging style)

2) Price-driven charging pattern (incentive based charging style).

The level 3 DC Fast Charger was used to represent typical fast PEV chargers installed at public facilities (parking lots) and commercial buildings. The charging pattern was selective either as a controlled (time of use) or uncontrolled charger.

Both PEV charger simulators were designed with power re-generative capability to avoid enormous power dissipation as a result of PEV charging and discharging cycles. During the tests, the discharge power was re-circulated back to the grid from output terminals, providing a round trip efficiency of greater than 96%.

Figure 2 - Block Diagram of the PEV Simulator Rack 2 (DC Fast Charger)

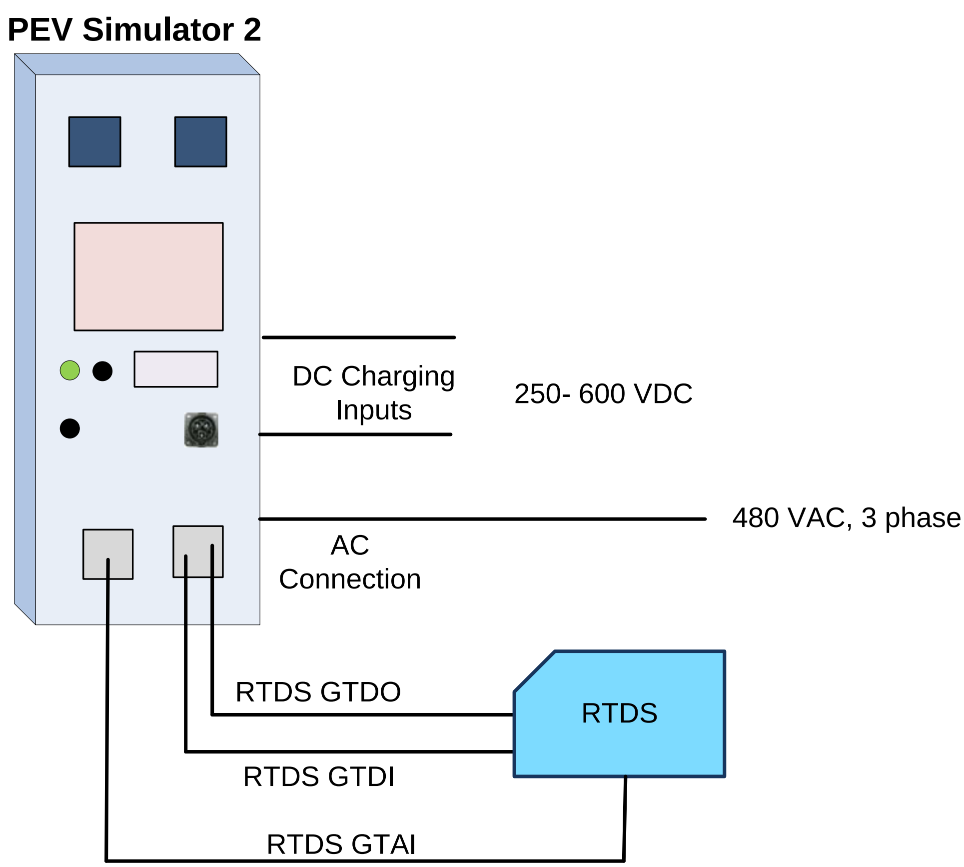

The major components of the Level 2 Charger of the PEV Simulator were as follows:

- Electrical Input: Power terminal, PEV charger plug (240 V, single-phase)
- Electrical Output: Interface terminals for low level voltage and current signals for RTDS (±10V), and power supply terminals for control circuits and power re-generative option (back to the lab grid at 208V, phase to phase)
- AC Measurement Devices: stand-alone Power Quality (PQ) meters, and a digital PQ card for RTDS measurements
- Control and Interface Units: Programmable Logic Controller (PLC), HMI screen, and analog/digital I/O cards
- Mechanical Selectors on the Enclosure: E-Stop button, Start button, Input selector switch

The major components of the DC Fast Charger of the PEV Simulator were as follows:

- Electrical Input: Power terminals (two electronically isolated DC inputs, 250- 600 VDC)
- Electrical Output: Interface terminals for low level voltage and current signals for (±10V), and power supply terminals for control circuits and power re-generative option (back to the lab grid at 480V, 3 phases)
- AC and DC Measurement Devices: stand-alone AC and DC types PQ meters, and a digital PQ card for RTDS measurements
- Control and Interface Units: PLC, HMI screen, analog/digital I/O cards
- Mechanical Selectors on the Enclosure: E-Stop button, Start Button

The EV Simulator 1 represented one Level 2 Charger. The PEV Simulator 2 represented one DC Fast Charger as well as the equivalent EV charging behavior. The electrical quantities representing a user selected charging profiles (voltage, current, active and reactive power) and the State of the Charge (SOC) of the battery were measured and converted to low level signals (±10V) for interface to the RTDS.

1.1 Mechanical Design

The PEV charger simulators were housed in Hammond server rack enclosures. The PEV charger rack 1 is approximately 2.19m high x 0.6m wide x and 0.8m deep (7′ 2.2″ H x 1′ 11.6″ W x 2′ 7.5″ D). The total weight of the rack 1 is about 220kg (485lb). The PEV DC Fast Charger simulator is approximately 2.24m high x 0.76m wide x and 1.07m deep (7′ 2.6″ H x 2′ 5.9″ W x 3′ 6.1″ D). The total weight of this rack is about 345kg (760lb).

Each of the PEV charger simulators has a hinged front panel and removable side and back doors for ease of maintenance and repair. The front panel allows direct access to the user interface of some of the internal components; see Figure 3 to Figure 5.

Figure 3 – PEV Level 2 Charger Enclosure

Figure 4 – PEV DC Fast Charger Enclosure

Figure 5 – PEV Level 2 Charger with a RTDS Rack

For the PEV Level 2 Charger Simulator, users were able to select two methods of connecting the EV simulator to their system using a selector switch. They could either connect to the J1772 receptacle using commonly used Level 2 EVSEs or they could use the terminal connectors near the bottom of the unit to connect to a 240 V power outlet.

The electrical connection for the PEV DC Fast Charger was mainly accommodated through power terminals due to the high current rating. Two DC charging channels were incorporated that can operate in parallel or individually. The re-generative power was re-cycled back to the grid at 480 V using an isolated transformer. Both the DC power input terminals and the AC output terminals were measured and converted to low level signals. Most control capabilities for adjusting the charging level were implemented through communications with power conversion systems.

Continuous readings of current, voltage, power and other relevant metrics were available from the Power Quality Meter (PQM). The user could update the PLC internal programming with new charging profiles and connect the unit to a network using the I/O interface on the front panel. The I/O interface featured a USB 2.0 port as well as two Ethernet ports. The Ethernet ports could be used to gather data from the PQM and, if required, change some of the internal settings. Pilot lights were provided to let the user know if the unit was in live operation.

An emergency stop button had been installed to the front panel to ensure that the unit could be promptly shut down in case of an emergency. The height of the HMI unit and locations of control pushbuttons were selected properly, giving the operator a comfortable position from which to view and interact with the unit (especially the HMI and the PQM). The entire units were on coasters to allow the units to be moved to different areas and test labs.

In PEV Simulator racks, the front panel had several display screens including the large Human-Machine Interface (HMI) screen and the smaller LCD screens of the power quality meters (PQM's). The pushbuttons for rack startup (green pushbutton), emergency start (red pushbutton), and the input selector switch, as well as the pushbuttons related to HMI screen were located in the middle of the front panel.

Figure 6 – PEV Simulator Rack 1 Front Panel

Once the unit was in place, the user should have opened all four doors using the provided keys. The user was required to make a detailed examination of all the power cable terminal connections (all cables 8 AWG and higher). If a connection was found to be loose, the user would have been required to tighten it. Checking the connections of control wiring would not have been necessary.

Figure 7 – (a) Rear View (b) Front View of Simulator Rack 1

(a)

(b)

1.2 Electrical Design

The PEV Simulator Racks were designed to re-generate power. In the PEV Simulator 1, AC power input was passing through line filters and an isolation transformer, then rectified to DC and inverted back to AC on a separate output circuit. In the PEV Simulator 2, the DC power inverted to AC at 480 V and was injected to the grid after passing through an isolation transformer. The re-generative approach allowed utilizing variable load at the power ratings of various chargers, but did not actually need to dissipate extensive amounts of power.

PEV Simulator Rack 1 had the following specifications:

- AC connection cables (at the back):
  - 208 V (two phase), 50 A
  - 120 V (single phase), 10 A
- Charging input (at the back):
  - 240 V (two phase), 35 A
- Ethernet Connection
- Front connections:
  - RTDS Digital IN
  - RTDS Digital Out
  - RTDS Analog out
  - EV Plug
- System limitations:
  - Maximum charging power: 10 kW
  - Minimum charging power: 1 kW
  - Maximum "Maintain Charge": 1 kW
  - Minimum "Maintain Charge": 0.5 kW
  - Simulation time: > 45 seconds, incorporating the time scale (total simulation time with multiplier should be greater than 45 sec)
  - Delay between simulations: 30 seconds (user adjustable with minimum 30 seconds)
  - Time multiplier range: 1 - 99

PEV Simulator Rack 2 had the following specifications:

- AC connection cables (at the front):
  - 480 V (three phase), 15 A (per phase)
  - 120 V (single phase), 10 A
- Charging inputs (at the front):
  - Two isolated 250- 600 VDC, 36 A
- System limitations:
  - Maximum charging power: 40 kW

The remainder of the specifications was the same as Rack 1.

The Level 2 Charger Simulator represented up to 10 kW of on-board chargers with selectable and programmable charging profiles. The maximum charging time was dependent on the selected size option. Some examples are given below.

- For 10 kW size:
  - PHEV: 1.5 hrs (SOC* - 0% to full)
  - BEV: 3.5 hrs (SOC – 20% to full)

- For 3.3 kW size:
  - PHEV: 3 hrs (SOC* - 0% to full)
  - BEV: 7 hrs (SOC – 20% to full)

The DC Fast Charger simulator represented up to 40 kW (40 A) of off-board chargers. The estimated charge time for a 20 kW off-board charger was:

- PHEV: 22 min. (SOC* - 0% to 80%)
- BEV: 1.2 hrs. (SOC – 20% to 100%)

It should be noted that ideal charge times indicated above assume 90% efficient chargers. The PEV Simulator is intended to be regenerative to avoid unnecessary power dissipation.

An overall block diagram of the power circuit for the level 2 EV simulator is shown in Figure 8. The input connections for the Level 2 EV simulator are selectable either as a regular power outlet or an EV power plug. The regular outlet terminals are protected through internal EVSE components for protection and safety purposes, similar to typical components of EVSEs.

However, the connection to the DC Fast Charger simulator is only allowed through a 480 VAC outlet. The main reason is the difference in type of charging power with or without the EVSEs in this case. The EV simulator with fast charging capability represents characteristics of both on-board and off-board chargers. An overall block diagram of the power circuit for the level 3 EV simulators is depicted in Figure 9.

Figure 8 – Electrical Block Diagram of the EV Simulator Rack 1

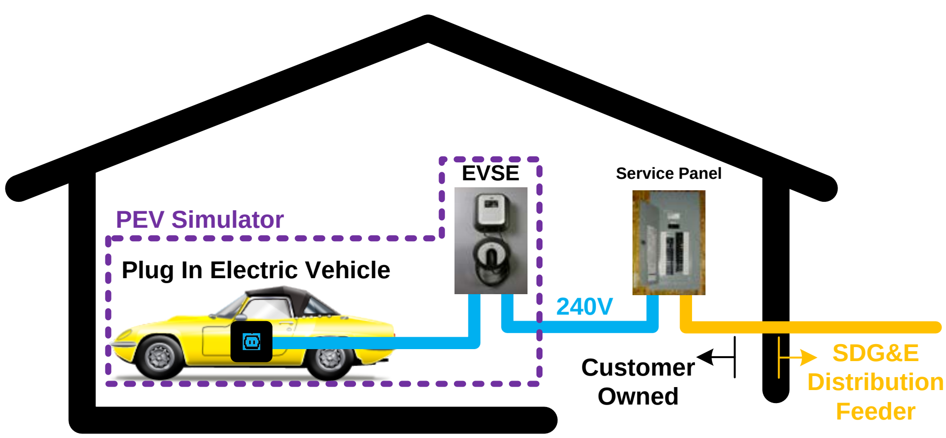

Figure 9 - Electrical Block Diagram of the EV Simulator Rack 2

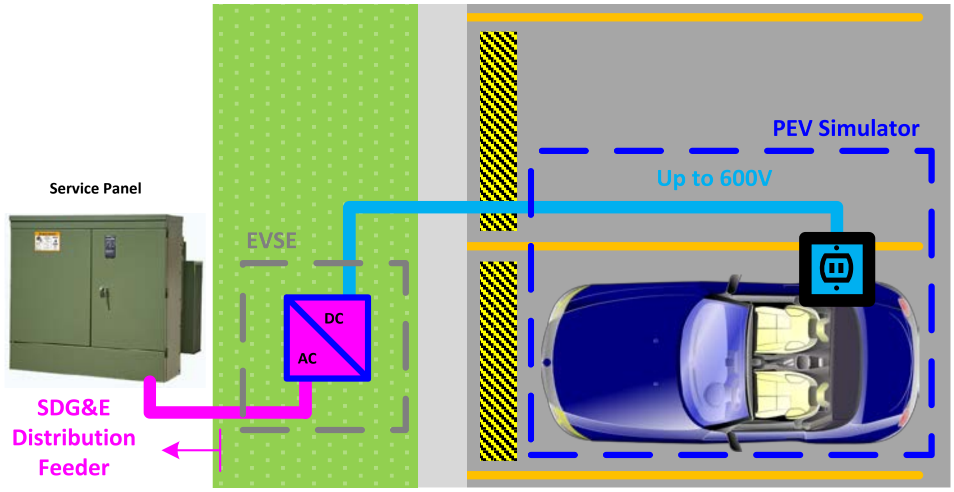

The power circuit design of the EV simulator incorporated the regenerative aspects of the power delivery to the device. The design aim had been to circulate back as much power consumed by the unit while accurately representing the charging characteristics of the combined EV charger and EV battery components. This allowed reducing the power dissipation by the units and enhanced the round trip efficiency of the simulators for use in an indoor laboratory environment.

1.2.1 Simulator Schematic

Figure 10 and Figure 11 outline the high level hardware architecture of the Level 2 and DC Fast Charger simulators.

Figure 10 – Hardware Architecture of Level 2 Charger Simulator

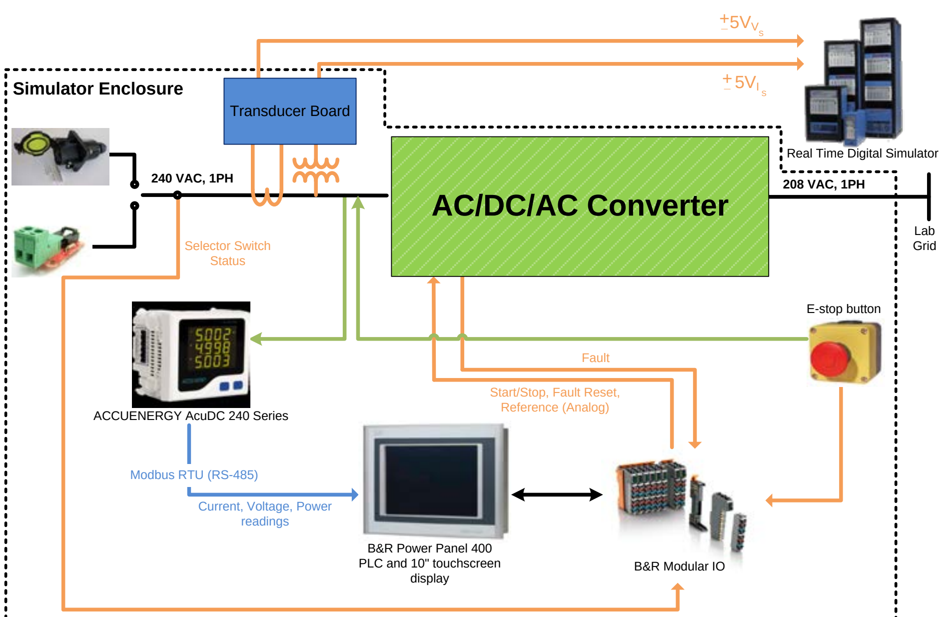

Figure 11 – Hardware Architecture of DC Fast Charger Simulator

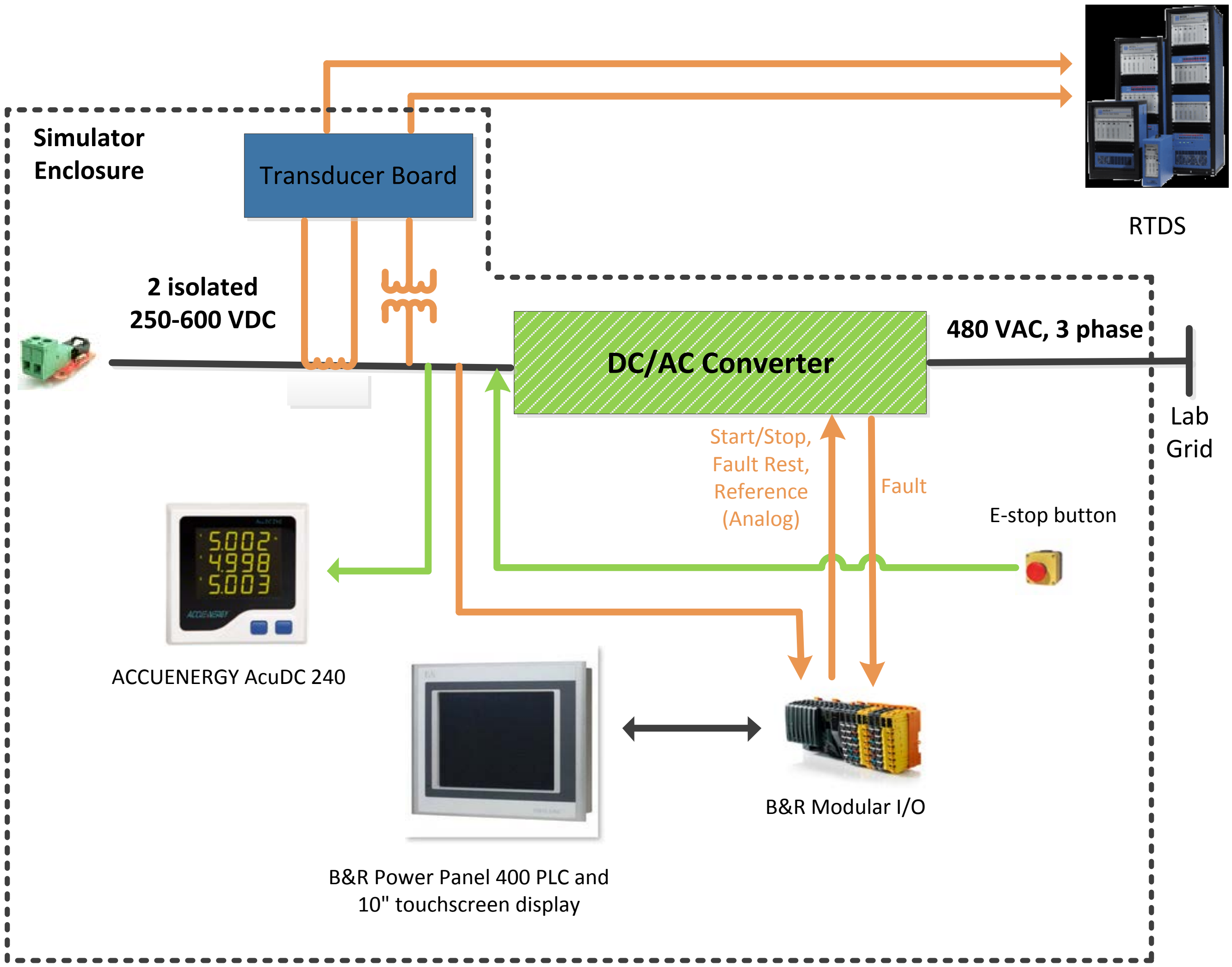

The EV simulator was designed to model an electric vehicle and on-board or off-board chargers for laboratory testing purposes. The main characteristics of the simulation environment included:

- User selectable EV battery state of charge
- Scalable charging time , with overall energy consumption remaining unchanged
- User selectable charging profile - charging start time and duration of charge are specified by the user
- User selectable charging tariff – includes Time of Use – TOU calculations
- The level 2 EV simulator can be connected directly to regular 240 V receptacles or plugged into commercial EVSEs

    - A manual selector was used to switch between the receptacle terminal and plug-in connection from EVSE

- The DC Fast Charger simulator can be connected to two electronically-isolated DC voltage, 250-600 VDC

1.2.2 Programmable Logic Controller-based Control

A combined programmable logic controller and interface device was selected in order to reduce the complexity of the design. This all-in-one controller and interface consisted of the following components:

- Basic Programmable Logic Controller (PLC) with recipe selections
- Human Machine Interface (HMI) – a 10″ Touch Screen Panel
- Input and output channels
- Optional data logging

The control system was responsible for actively communicating user selected simulation parameters to the corresponding devices in the EV simulator. The HMI also dynamically displayed real time metering information during the simulation. The overall structure required simple access to the control system's main program if there was a need to modify application programs, recipe profiles, or the screen visualization interface. This controller was ideal for storing process data recipes as well as application controller files. It provided additional analog and digital input/output channels and could accommodate extra communication protocol cards to communicate with other devices if necessary.

The requirements of the controller were divided into three distinct pre-simulation, simulation, and post-simulation modes. In the pre-simulation mode, the controller required appropriate internal memory allocation for the user's pre-stored charging profiles as well as sample pricing information. The user was able to modify pre-stored charging patterns if desired over time. Next, the user communicated a minimum of seven desired study parameters using various available options such as the HMI touch screen or other remote device interface. Following the input of the seven parameters, the simulator was ready for starting a 'simulation mode'.

Once prompted, the controller accessed its internal memory for the given user inputs and started the simulation. The controller transmitted a master launch to initiate simulator hardware start and then actively directed hardware parameters to match the user selected charging pattern in real time. The controller was also responsible for dynamically monitoring any internal faults in the system and was programed to safely shutting down the EV simulator when prompted.

Finally, the controller collected all necessary metering data as well as the simulation start-up parameters in order to save an output summary file in the post-simulation mode. The user could simply insert a USB key into the EV simulator prior to start of the simulation for detailed study summary upon completion. An overview of all necessary connection points to the combined controller and HMI system is represented in Figure 12.

Figure 12 – Control System Architecture and Interface for the PEV Charger Simulator

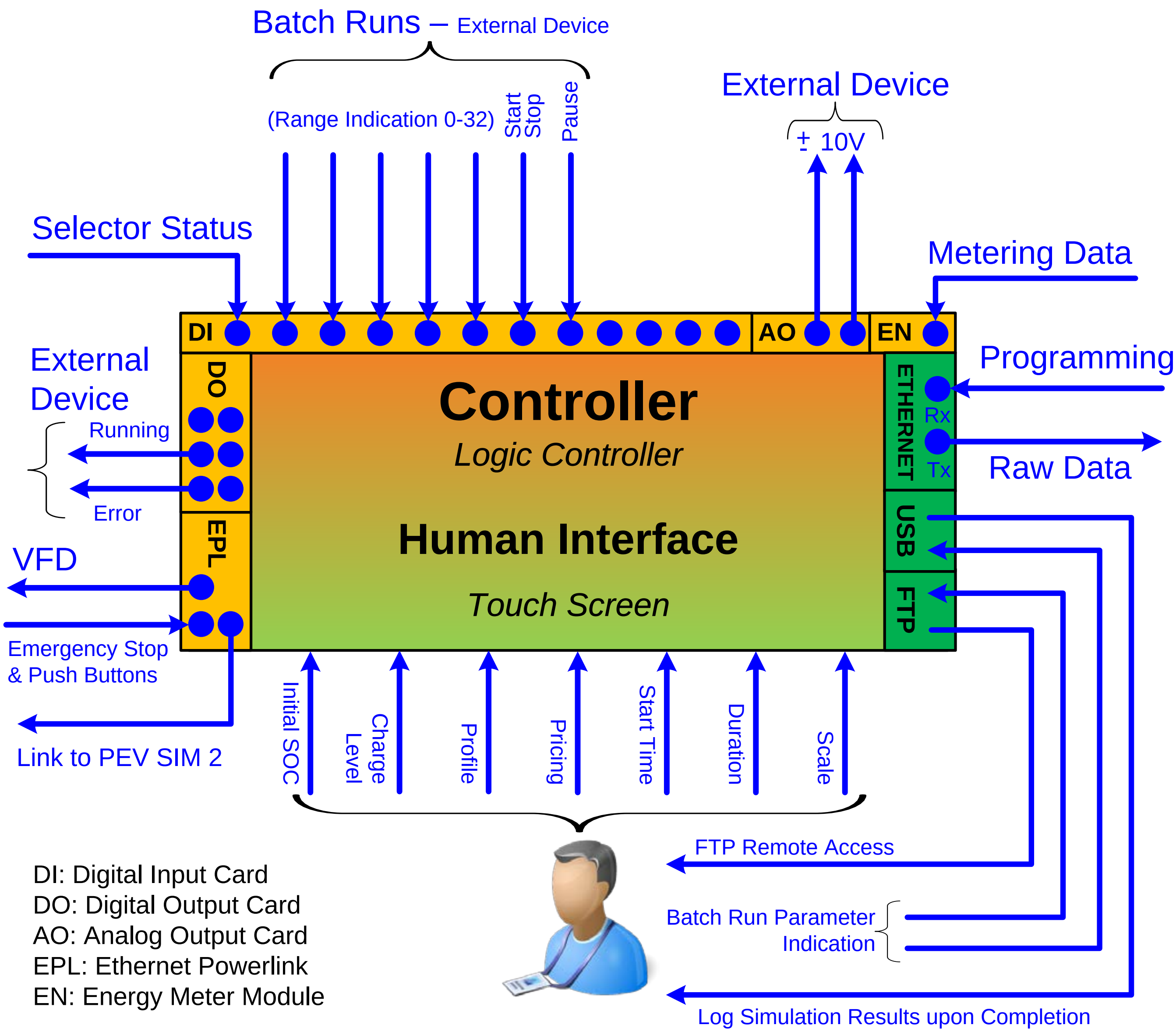

The PEV Simulators were designed to operate from the front panel (HMI) or remotely through the RTDS connection and/or a remote desktop.

Once the design and implementation of the PEV Simulator racks completed, Factory Acceptance Testing and Site Acceptance Testing were performed to verify operation and performance of the racks according to the proposed tests as described in the following sections.

CHAPTER 2:
Distribution Survey

A survey of existing SDG&E distribution systems was conducted to identify a circuit most likely to be impacted by plug-in electric vehicles, so that a test bed could be designed to replicate and analyze the impacted system. For this purpose, the data collection focus was on the circuits that currently included the largest number of PEV installations. The circuit, designated Circuit A, was identified as being the most likely to be impacted and was selected for modeling in RTDS.

2.1 Circuit Selection Criteria

In order to provide a basis for the test bed design, a representative circuit was selected by considering not only its likelihood of being impacted by high penetration of PEV customers but also its representativeness in terms of similarities of circuit characteristics, expected growth rate and number of existing PEV installations with those of other circuits.

SDG&E provided basic circuit characteristics for the top 11 circuits that had the most number of PEV customers at the time of study. The included circuit features were:

- Voltage level
- Associated substation
- Circuit capacity in amps
- Service transformer count and their total rated capacity per circuit
- Customer count and composition (residential, commercial, and industrial customers) per circuit
- Circuit length (overhead vs. underground)
- 2012 circuit peak load
- Number of PEV installations per circuit
- Type of voltage control devices on a circuit (for example: fixed/switched shunt capacitors, and voltage regulators)

In addition, detailed information of 1,276 existing PEV installations (as of January 2013) was provided as a supplementary database. The information provided in this database included:

- PEV installation locations (city, geographical coordinates, and circuit)
- PEV information (make, model, and year)
- Battery information (type, capacity, charging voltage, and maximum charging rate)

- Electric Vehicle Supply Equipment (EVSE) information (type, voltage, and maximum amp rating)

The map in Figure 13 shows the concentration of the PEV installations in the SDG&E system territory as of October 2012 (timeframe of the circuit selection). The locations were identified by four categories of single or multiple PEV customers per transformer and areas with combined PV generation and PEV load on the same transformer.

Figure 13 - PEV Customer Concentration in SDG&E System Territory - October 2012

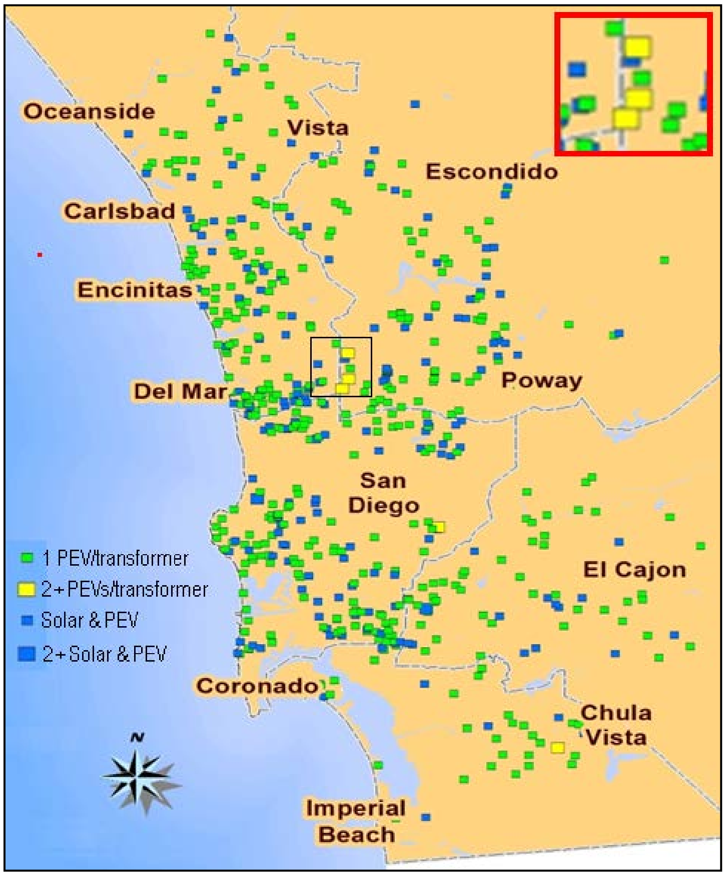

A "fuzzy logic" inference algorithm system was developed to rank the likelihood of high PEV adoption for the top 11 circuits. The top ranked circuit was selected and reviewed for characteristic selection and development of the test bed design. The representative circuit reflected the common characteristics of the impacted areas as identified for those top ranked circuits. The test bed was utilized as the base for analyzing and evaluating the impact presence of PEV customers and various charging patterns on distribution systems operation from several aspects which included:

- Exceeding equipment thermal loading
- Changes in the circuit voltage profile and potential for low voltage issues
- Increase in transformer loss of life and shortening of maintenance periods

- Possible voltage imbalance
- Affecting harmonic distortion levels

The test bed circuit was developed based on the common characteristics as identified and reported for the top ranked circuit(s). To capture the effect of actual charging patterns, the test system incorporated scaling up the simulated PEV charging according to a target number of PEV customers per service transformer and at various locations. The extracted PEV charging patterns was utilized to determine both circuit level impacts and individual component level impacts.

2.2 Circuit Selection Approach

In order to provide a basis for the design of a test bed replicating impacted areas, a representative circuit, designated Circuit A in subsequent documentation, was selected by considering not only its likelihood of being impacted by high penetration of PEV charging, but also its representativeness in terms of existing PEV installations. For example, if a circuit in the PEV early adopting region had significantly more PEVs already installed than its neighboring circuits, this circuit was not as representative as one that had similar PEV installations as its neighboring circuits. Ideally, detailed data such as customer income level and their willingness to advocate environment protection was used to analyze the PEV adoption likelihood. However, due to the limitation in obtaining this sort of information, the survey study was performed by extracting underlying implicative information from available data and utilizing the information to select representative circuits.

The five extracted input attributes used in the survey are outlined below:

1. <u>PEV Regional Adoption Rate</u>: The percent of PEVs from the substation feeding the studied circuit (out of total 1276 existing PEVs). The more PEVs the feeding substation support, the more likely the customers in the area were adopting PEVs, especially at the early stages.
2. <u>PEV Adoption Diversity Factor</u>: The reciprocal of the percent of PEVs on the circuit over the total number of PEVs the feeding substation supported. The larger the factor was, the smaller PEV percentage the circuit had in the same substation. In other words, the smaller the PEV concentration on the circuit was, the more representative this circuit was in terms of its PEV adopting pace.
3. <u>Circuit Length</u>: The longer the circuit was, the more concerns with regard to voltage violation it had when more PEV installations were in place, especially where locations of PEV installations were at a customer's premise, outside of utility control.
4. <u>PEV Circuit Adoption Rate</u>: The percent of residential customers owning PEVs. Currently, all the PEV customers own only one PEV. The number of PEVs represented the number of customers owning a PEV.
5. <u>PEV Load Factor</u>: The percent of PEV charge load related to the 2012 circuit peak load. Its magnitude was represented by the product of the number of PEVs on the circuit and the power draw of a Nissan LEAF. This was a reasonable assumption as:
    - The Nissan LEAF dominated SDG&E's service territory in most early adopting circuits.

- The maximum PEV charging rate was 3.3kW for Chevy Volt and 3.7kW for Nissan LEAF - the difference was not significant.
- In many cases the exact model was unknown.

These five extracted attributes covered the likelihood of PEV adoption both at the regional level and circuit level; included the potential impact of PEVs on circuit loading and voltage profile; and also took into consideration the circuit representativeness among all possible circuits in the SDG&E territory.

Based on the current data availability, it was not statistically significant to quantify a threshold to determine different levels of PEV adoption likelihood. Therefore, a fuzzy inference system was developed to rank the likelihood of high PEV adoption for the top 11 circuits.

A brief introduction of the fuzzy inference system is presented as follows. Detailed tutorials about fuzzy logic and fuzzy inference systems can be found online or in any fuzzy logic reference book. Fuzzy logic allowed for approximate values and inferences as well as incomplete or ambiguous data (fuzzy data) as opposed to only relying on crisp data [1]. A membership function was the tool to define how each input was mapped to the degree of membership of each fuzzy category. Fuzzy inference was the process of formulating the mapping from a given input to an output using fuzzy logic. The mapping provided a basis from which decisions could be made, or patterns discerned [2].

For the purpose of this analysis, the input data was first normalized to the range of [0, 1] to avoid any potential bias due to different input variable magnitude. Then, a commonly used triangle membership function was applied for both input and output variables. Basic "if-then" rules were used to define the mapping from circuit features to the likelihood of a circuit being impacted by high penetration of PEV charging. The analysis then aggregated the output from different rules, and used the most popular centroid method to "de-fuzzify" the aggregated fuzzy set into a single number, which was used as the final score of the circuit's likelihood of being exposed to high PEV penetration impact. A more detailed explanation and an example of the calculation are presented in Appendix A.

2.3 Identified Circuits

The final score and ranking of the top 11 candidate circuits, which were considered for system replication, are listed in Table 1, along with the values for the five extracted input attributes. The detailed methodology and raw data for these five input attributes are presented in Appendix A and 0 respectively for review.

Table 1 - Circuit Ranking and Values for Attributes

Circuit ID	# PEV	Regional Adoption Rate	Circuit Adoption Rate	Adoption Diversity Factor	Circuit Length	Load Factor	Score	Rank
A	14	4.94%	0.81%	4.50	19,953	7.41%	0.572	1
B	23	5.17%	1.05%	2.87	46,848	4.36%	0.565	2
C	17	5.17%	0.74%	3.88	30,203	4.21%	0.526	3
D	12	4.94%	0.35%	5.25	37,472	2.53%	0.504	4

Circuit ID	# PEV	Regional Adoption Rate	Circuit Adoption Rate	Adoption Diversity Factor	Circuit Length	Load Factor	Score	Rank
E	11	3.92%	0.40%	4.55	42,646	2.70%	0.501	5
F	11	3.92%	0.42%	4.55	27,682	4.95%	0.499	6
G	11	3.92%	0.24%	4.55	41,352	2.32%	0.489	7
H	15	2.59%	0.74%	2.20	34,032	3.21%	0.453	8
I	11	1.10%	0.35%	1.27	54,086	2.93%	0.408	9
J	11	1.10%	0.30%	1.27	36,690	2.85%	0.377	10
K	11	1.65%	0.33%	1.91	27,458	2.47%	0.371	11

This ranking was derived based on the aggregated consideration of the five different extracted input attributes. Even though the number of existing PEVs (#PEV) were not directly used as an input for the fuzzy inference algorithm, the final ranking of the top 11 circuits were generally consistent with their number of PEVs in the system. One example exception was that circuit A with 14 PEVs was ranked as No.1 but circuit H with 15 PEVs was ranked much lower.

Three of the five attributes (Regional Adoption Rate, Adoption Diversity Factor, and Circuit Length) were not directly associated with the number of PEVs on a given circuit. Although the two remaining attributes (Circuit Adoption Rate and Load Factor) were derived from the number of existing PEVs on the circuit, they were normalized by different features. Therefore, it was reasonable to claim that the ranking was not biased by one single factor, the number of PEVs, even though the derived circuit ranking was consistent with its ranking.

Circuit A was selected for further analysis in order to extract circuit characteristics and to understand PEV charging patterns. The top four ranked circuits were fed by two substations. Circuit B and C are associated with a common substation, while circuit A and D were from another common substation. If more circuits were to be selected for study, it would be recommended to select circuits from different substations to ensure their representativeness.

It is worth noting that all the 11 candidate circuits were among the ones with the highest PEV penetration at the time of study, they did not represent circuits with no PEV customers or with few PEV installations. It would be misleading to draw conclusions how closely the selected circuit represented other circuits. However, the score of each circuit listed in Table 1 provided a good view of the likelihood of high PEV impact based on current adoption rates. This same methodology can be applied to all the circuits in the SDG&E system to calculate their corresponding scores if needed.

2.4 Selected Circuit (Circuit A)

Circuit A was one of four feeders off substation #1 in SDG&E's distribution system. The circuit was rated at 12.0 kV with a downstream power flow of 5.3MW. The feeder featured one 1.2Mvar shunt capacitor, 41 distributed PV sources, and 14 customers with plug-in electric vehicles. Four adjacent feeders and one cap bank at the substation bus represented a total 26.4MW and 15.1Mvar load neighboring the study circuit. The layout of the feeder (from SynerGEE) is shown in Figure 14. The feeder is split into two sections, with the top section (shown in left) continuing to the bottom section (shown in right).

Figure 14 - Feeder Layout

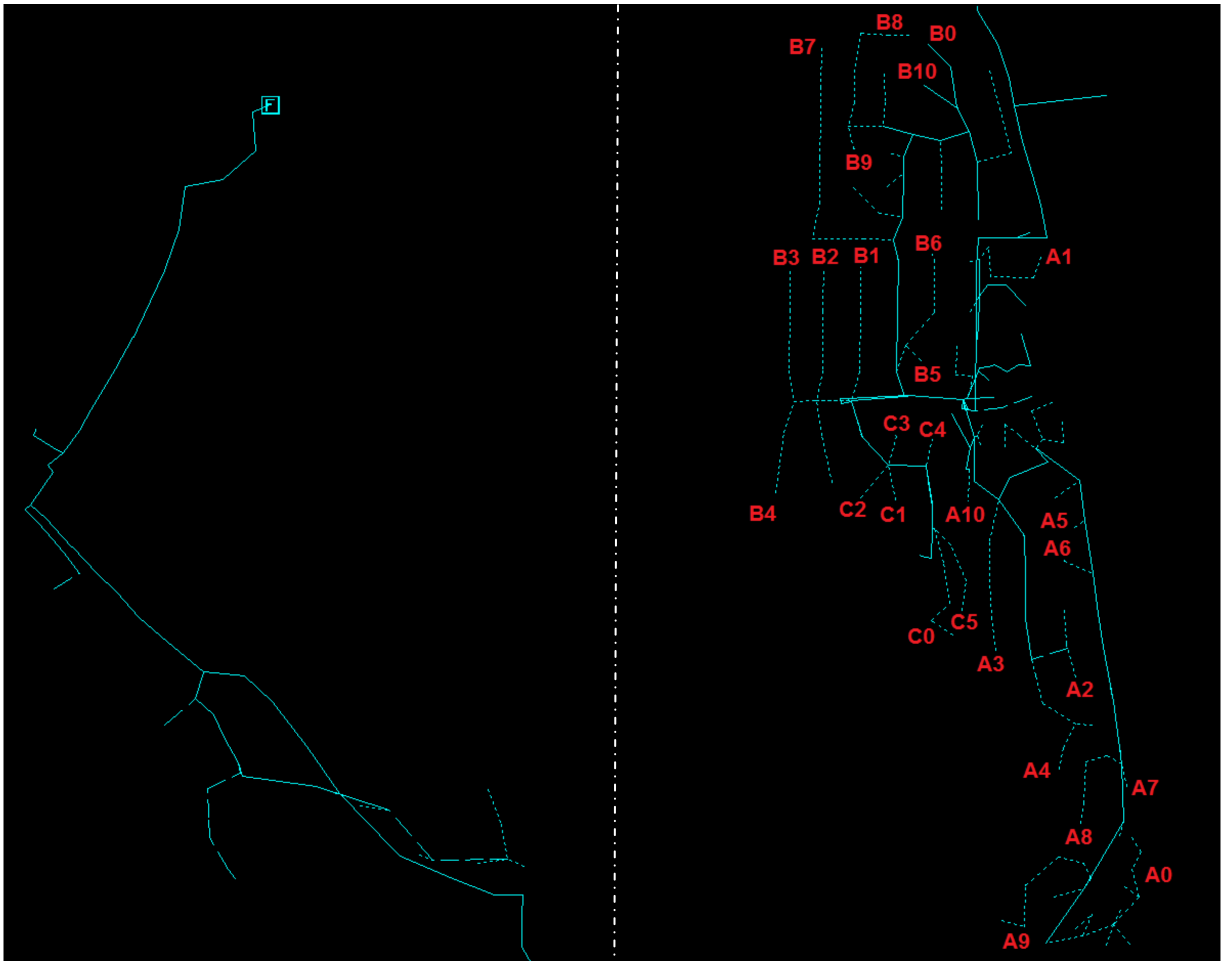

To aid in branch identification, each branch was clustered into three main areas (A, B, C) defined in the geographic feeder layout as shown in Figure 14. The one-line diagram of the feeder with the area designation is shown in Figure 15. Feeder segment lengths (in miles) are indicated with arrows and the real power, reactive power and per-unit voltages associated with each segment are shown in red text.

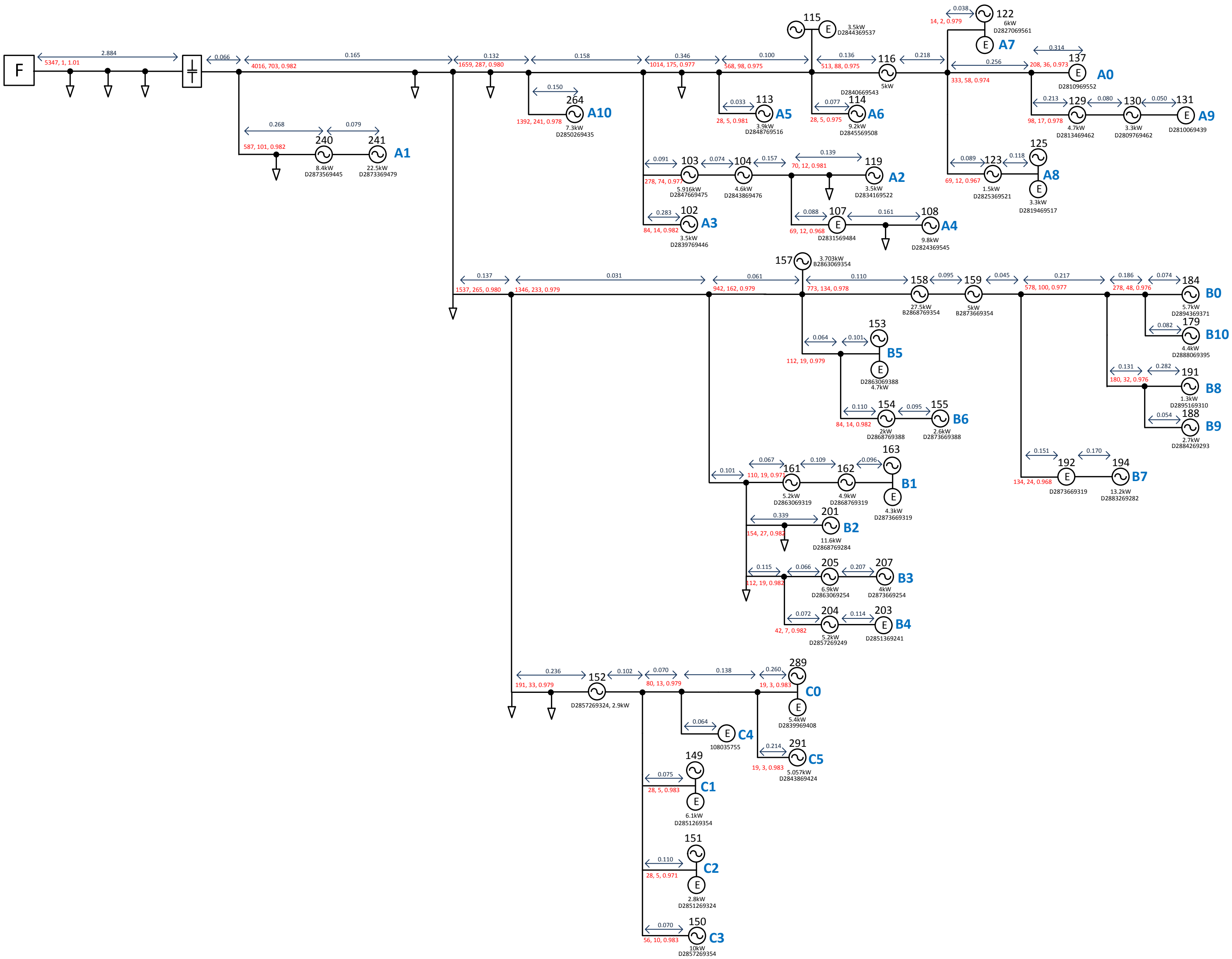

Figure 15 – Circuit A One-line Diagram with Segment Designation and Power Flow Data

CHAPTER 3:
Test Bed Design

The benchmark test bed was built with characteristics as close as possible to the selected distribution circuit A, as identified in the distribution system survey. The test bed had the ability to integrate the PEV Simulator units. This test bed also provided the means for changing the circuit load and configurations to vary the voltage profile and investigate the impact of PEV charging load under various operating scenarios.

A Real Time Digital Simulation (RTDS) setup with a minimum two rack system was proposed to build an accurate model of the representative circuit A (primary network). This model made up the core of the test bed. The secondary networks and customer connections were modeled and represented in a third RTDS rack, interfaced through customer service transformers. The RTDS setup provided the flexibility and accuracy needed to represent the distribution circuit characteristics while accounting for changing loads and customer profiles, and managing an interface to PEV Simulator measurements. The circuit model can be changed and re-adjusted according to typical differences in the nature of the circuits from various regions in the SDG&E territory. The flexibility in re-configuration brought the added value to the project design and future needs for impact evaluation. In addition, any individually monitored profiles from distributed resources on a circuit (solar generation, energy storage, etc.) could be properly incorporated in the RTDS-based test bed for complex system integration analysis.

An overall block diagram of the proposed RTDS-based test bed is shown in Figure 16. This chapter outlines the specifications of the test bed and the details of the RTDS model. The chapter also describes the peripheral equipment, interfacing devices, and the arrangement required for assembling the test setup along with a list of proposed test cases, experimental approaches and data/measurement suggestions for testing the PEV impact under realistic distribution circuit loading conditions.

Figure 16 – Overall Test Bed Setup Using RTDS

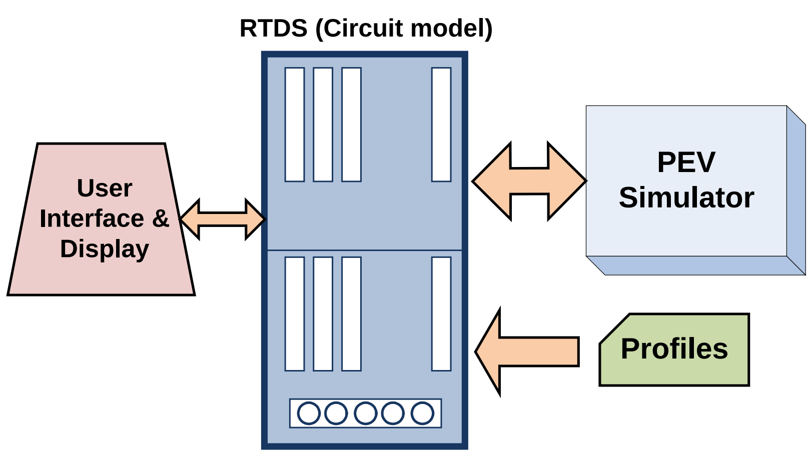

3.1 Model Creation

The RTDS hardware allowed for a limited number of electrical nodes; therefore, several parts of the system were aggregated to fit within the capacity of two RTDS racks. The basic approach to system reduction was to lump loads at major nodes, and lump lines in PI sections. Because the objective was to investigate the effect of plug-in electric vehicles on the feeder, the EV locations were prioritized in the determination of major nodes. Whenever possible, everything in the direct upstream path of an EV location was explicitly modeled, while everything downstream or not in the direct path of an EV location was lumped. The PV sources were also either aggregated or individually represented if they shared some connection points with EVs. A detailed explanation of the primary system modeling methodology is given in Appendix C: Primary System Modeling Methodology Details – Page C-1.

An example of the aggregation approach is shown in Figure 17. Here, the four PVs at the end of the line (184, 179, 191, 188) were lumped at one bus, while all segment lengths up to EV192 were explicitly modeled as PI sections. PV158 and PV159 were modeled at their proper locations due to their locations in the direct upstream path of EV192.

Figure 17 - Circuit Aggregation Approach

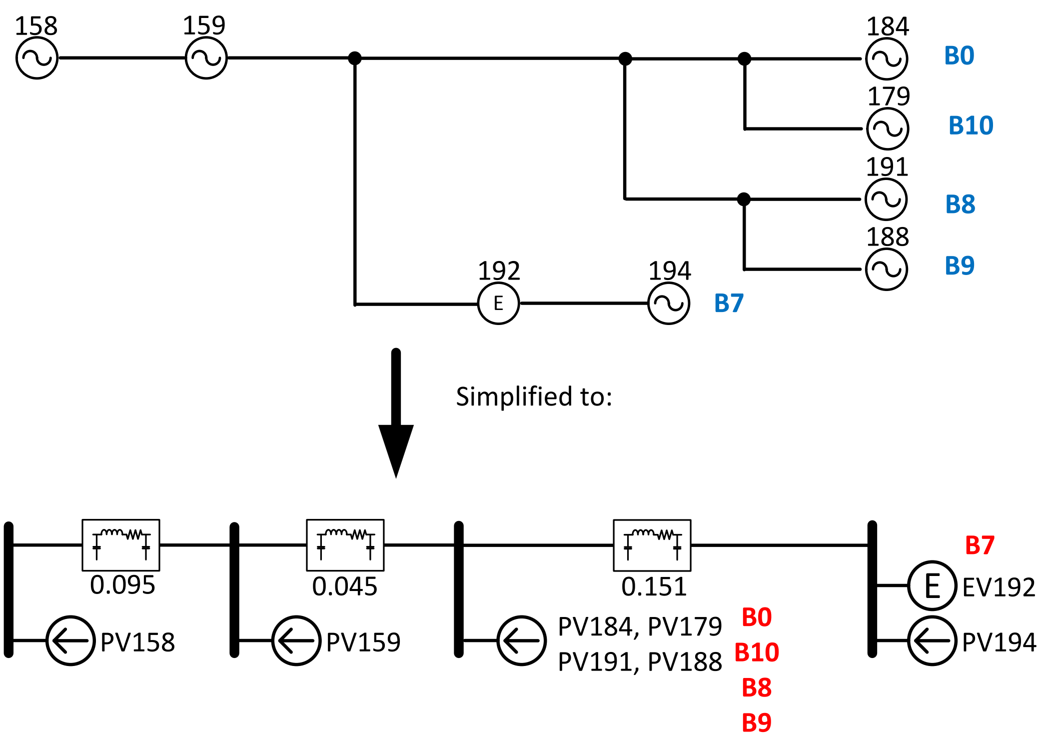

The aggregated system modeled in RTDS is shown in Figure 18. Due to the size of the system, two subsystems were required to accurately represent the primary circuit on the two RTDS racks. A fictitious transformer was included between Bus 7 and Bus 101 to allow data transfer between the two subsystems.

Figure 18 - RTDS System Layout of Circuit A

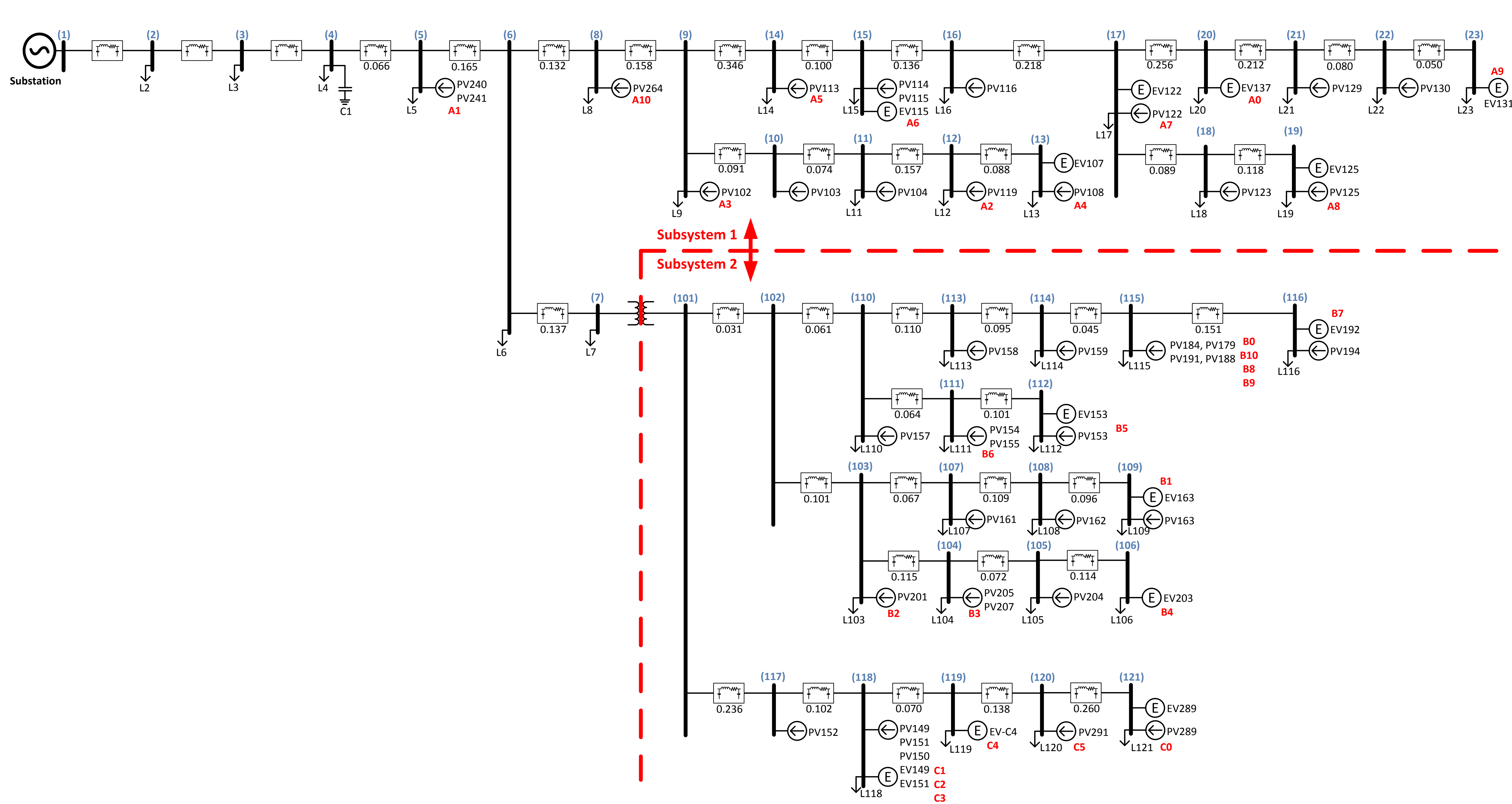

The line and load parameters for the model in the RTDS are given in Table 2 for Subsystem 1 and Table 3 for Subsystem 2.

Table 2 - RTDS Model Line and Load Parameters (Subsystem 1)

PI Section Parameters					
Line Segment	**Miles**	**Res+ (ohm)**	**Ind+ (ohm)**	**Res0 (ohm)**	**Ind0 (ohm)**
Source	0.000	0.031900	0.451700	0.012400	1.312800
PI0102	1.310	0.250033	0.573773	0.621225	2.142196
PI0203	2.122	0.225291	0.575745	0.453092	2.406409
PI0304	0.763	0.422867	0.575111	0.640325	2.299604
PI0405	0.066	0.036435	0.049553	0.055172	0.198138
PI0506	0.165	0.083497	0.106254	0.145088	0.411552
PI0608	0.132	0.115837	0.030388	0.333860	0.147070
PI0809	0.158	0.138938	0.036448	0.400441	0.176399
PI0914	0.346	0.303303	0.079567	0.874168	0.385082
PI1415	0.100	0.087750	0.023020	0.252910	0.111410
PI1516	0.138	0.140841	0.036300	0.262089	0.059538
PI1617	0.218	0.207943	0.054011	0.479460	0.164612
PI1720	0.256	0.261895	0.067500	0.487355	0.110710
PI2021	0.213	0.198095	0.097447	0.639269	0.213807
PI2122	0.080	0.081478	0.021000	0.151622	0.034443
PI2223	0.050	0.050827	0.013100	0.094583	0.021486
PI1718	0.089	0.074685	0.052885	0.335150	0.125860
PI1819	0.118	0.107806	0.057108	0.371678	0.127785
PI0910	0.091	0.079939	0.020971	0.230397	0.101493
PI1011	0.074	0.064815	0.017003	0.186809	0.082291
PI1112	0.157	0.137774	0.036143	0.397088	0.174922
PI1213	0.088	0.078798	0.041472	0.270037	0.092627

Load Parameters						
Load	**Load (kW)**			**Load (kVAR)**		
	A	**B**	**C**	**A**	**B**	**C**
L2	46	62	62	8	14	2
L3	89	90	90	16	13	6
L4	54	46	46	34	32	23
L5	291	141	155	51	25	27
L6	233	342	236	40	59	40
L8	111	99	57	19	17	10
L9	14	85	1	3	15	1
L14	129	103	214	22	18	37
L15	27	28	0	5	5	0
L16	28	27	1	5	4	0
L17	27	28	0	4	5	0
L20	27	0	208	5	0	36
L21	0	70	0	0	12	0
L22	0	14	0	0	3	0
L23	0	14	0	0	2	0
L18	28	0	0	5	0	0
L19	41	0	0	7	0	0
L10	55	0	0	9	0	0
L11	0	0	28	0	0	4
L12	0	70	56	0	12	10
L13	69	0	0	12	0	0

Table 3 - RTDS Model Line and Load Parameters (Subsystem 2)

PI Section Parameters						Load Parameters						
						Load	Load (kW)			Load (kVAR)		
Line Segment	Miles	Res+ (ohm)	Ind+ (ohm)	Res0 (ohm)	Ind0 (ohm)		A	B	C	A	B	C
PI0607	0.137	0.047000	0.028000	0.163000	0.046000	L7	55	70	66	9	12	11
PI101102	0.031	0.026000	0.007000	0.075000	0.033000							
PI102110	0.061	0.054000	0.014000	0.154000	0.068000	L110	19	19	19	3	3	3
PI110113	0.110	0.097000	0.025000	0.279000	0.123000	L113	0	0	28	0	0	5
PI113114	0.095	0.083000	0.022000	0.239000	0.106000	L114	0	29	0	1	5	0
PI114115	0.045	0.039000	0.010000	0.113000	0.050000	L115	179	190	210	30	33	36
PI115116	0.151	0.273000	0.073000	0.503000	0.196000	L116	137	0	0	24	0	0
PI110111	0.048	0.116000	0.031000	0.214000	0.084000	L111	0	84	0	0	14	0
PI111112	0.101	0.182000	0.048000	0.335000	0.131000	L112	0	28	0	0	5	0
PI102103	0.101	0.089000	0.023000	0.256000	0.113000	L103	28	112	154	5	19	27
PI103107	0.067	0.122000	0.032000	0.224000	0.087000	L107	41	0	0	7	0	0
PI107108	0.109	0.112000	0.029000	0.208000	0.047000	L108	41	0	0	7	0	0
PI108109	0.096	0.098000	0.025000	0.183000	0.042000	L109	28	0	0	5	0	0
PI103104	0.115	0.208000	0.056000	0.383000	0.150000	L104	0	70	0	0	12	0
PI104105	0.072	0.072000	0.019000	0.134000	0.030000	L105	0	28	0	0	5	0
PI105106	0.114	0.117000	0.030000	0.217000	0.049000	L106	0	14	0	0	2	0
PI101117	0.236	0.155000	0.054000	0.385000	0.114000							
PI117118	0.102	0.105000	0.027000	0.195000	0.044000	L118	27	56	28	5	10	5
PI118119	0.070	0.072000	0.019000	0.134000	0.030000	L119	28	14	0	5	2	0
PI119120	0.138	0.142000	0.037000	0.265000	0.064000	L120	0	0	19	0	0	3
PI120121	0.260	0.450000	0.041000	0.000000	0.001000	L121	0	0	19	0	0	3

For the purpose of test bed development and introducing the EV connection points, a modeling approach was proposed for representing the secondary network, residential houses and EVSE terminals.

Across SDG&Es territory, secondary systems were either overhead or underground. Most of the secondary systems on circuit A were underground; however, it was determined that the tests completed would have been more beneficial for the investigation if a mix of overhead and underground secondary networks were considered. Below is a summary of typical characteristics for secondary networks based on a review of SDG&Es distribution circuits.

Overhead: Typical XFMR Size either 25 kVA or 50 kVA			
Size of Transformer	**25 kVA**	**50 kVA**	**100 kVA**
Number of Customers	7	13	23
Number of EV Customers	1-2	1-2	2 or 3
Secondary Line Size	1/0 AL	1/0 AL	1/0 AL
Service Drop	#2 AL	#2 AL	#2 AL
Secondary Line Length	150 ft	150 ft	150 ft
Service Drop Length	50 ft	50 ft	50 ft
Underground: Typical Size is 50 kVA or 100 kVA			
Size of Transformer	**25 kVA**	**50 kVA**	**100 kVA**
Number of Customers	7	13	23
Secondary Line Size	3/0 AL	3/0 AL	3/0 AL
Service Drop	3/0 AL	3/0 AL	3/0 AL
Secondary Line Length	100 ft	100 ft	100 ft
Service Drop Length	50 ft	50 ft	50 ft

Based on transformer loading data extracted from the customer database for the representative circuit A, the average peak kVA and number of customers for each transformer are given in the table below in Table 4:

Table 4 – Average Number of Customers per Transformer

XFMR Averages (all XFMR)			XFMR Averages (EV only)		
Size	Peak KVA	#Customers	Size	Peak KVA	#Customers
150	26.84	4.83	-	-	-
100	31.54	23.78	-	-	-
75	30.77	17.88	-	-	-
50	24.87	12.43	50	36.01	14.50
25	17.64	7.38	25	16.04	7.50

A schematic diagram of the secondary network representation is shown in Figure 19. Each secondary system was characterized by the service transformer size, the number of customers on the transformer, the number of customers with EVSEs and the cable size and length. The combined length of a secondary line and service drop cable was introduced by equivalent impedances between the secondary of the transformer and the customer connection point.

Figure 19 – Schematic Diagram of the Secondary Systems

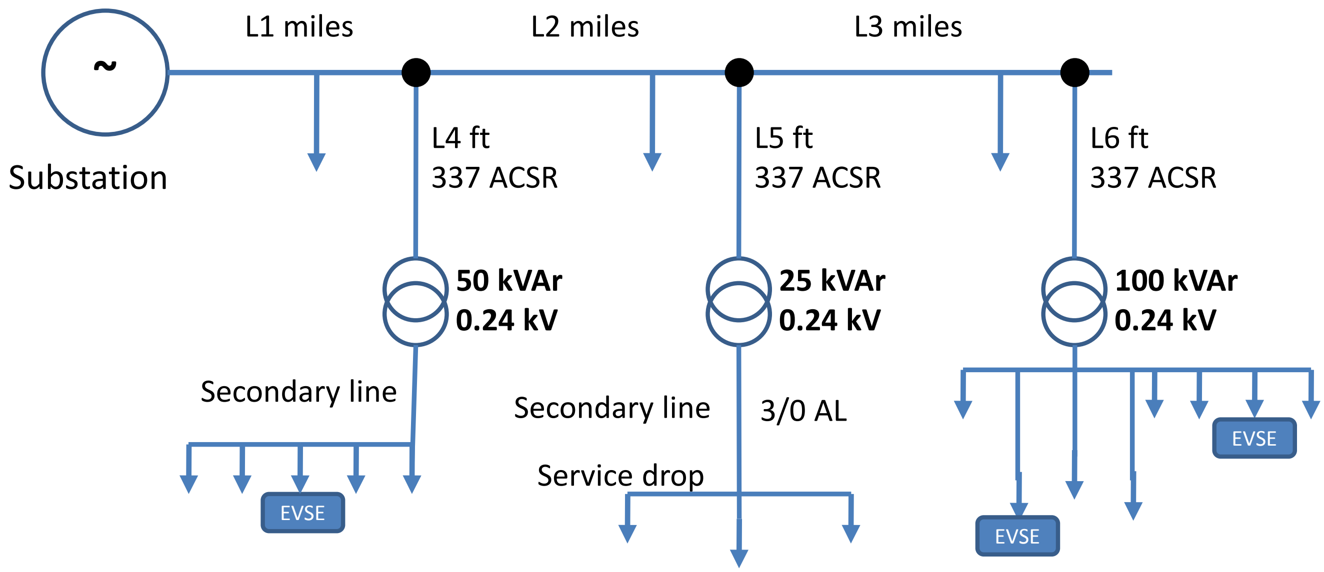

The following combination of regular and EV customers were selected and applied in the modeling of the secondary systems in RTDS:

- 25 kVA service transformer: up to 7 customers, including 1 or 2 customers with level 2 EVSEs
- 50 kVA service transformer: up to 13 customers, including 1 or 2 customers with level 2 EVSEs
- 100 kVA service transformer: up to 23 customers, including 2 to 3 customers with level 2 EVSEs

To determine an equivalent impedance, all underground cables or overhead conductors were assumed 3/0 AL size. The estimated line/cable lengths are:

- 150 ft secondary line length
- 50 ft service drop length

The above cable lengths and gauges introduce an equivalent impedance of (0.023 + j 0.0052) ohms between the secondary of the transformer and a customer connection point. The impedance was modeled as lump sum resistive and inductive elements in series. Because some of the secondary loads were aggregated, the service transformer size was selected according to the closest kVA rating that can serve the total maximum load at specific service bus with consideration of up to 120% possible overloading.

As an example, at Bus 15 in the RTDS model, the total load was 55 kW and 10 kvar (56 kVA). A service transformer size of 50 kVA was chosen for serving the load. In addition to about 12.5 kW of installed

PV sources, there is an EV customer on this bus. The secondary model for this bus is shown in Figure 20.

Figure 20 – Secondary System Model for the Combination of Load EV and PV at Bus 15

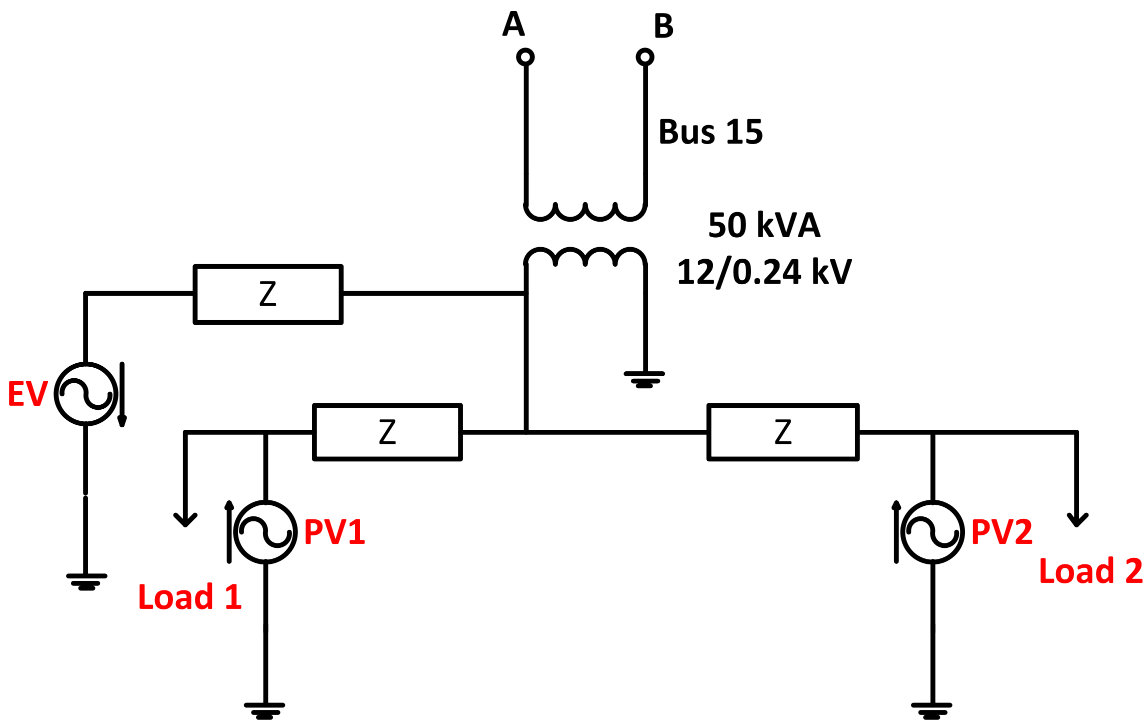

The type of connections and total customer loads per bus in the RTDS model are given in Appendix D. 0 explains a benchmark that was used to test the secondary system representation in RTDS. An EV customer or a PV system is modeled as a current source. The measurement for current magnitude was taken from the expected power consumption (or generation) of the EV or PV system.

3.2 Model Validation

Three performance characteristics were used to verify that the modeled RTDS system accurately reflects Circuit A from SynerGEE. These were three phase (TPH) and single line to ground (SLG) fault currents, 3-phase voltages (or single phase when appropriate), and real and reactive power flow at nodal locations. The comparison of fault currents from SynerGEE to RTDS is shown in Table 5, and the comparison of voltage and power flows is shown in Table 6.

The fault currents observed in RTDS were consistently higher than reported by SynerGEE, but still close with under 7% error. The discrepancy was due to the impedance of the inter-subsystem transformer which was added to allow data to be exchanged between subsystems.

The voltage comparison shows a maximum of 0.8% error, but overall, the SynerGEE and RTDS measurements agree quite well. The RTDS real and reactive power flow readings were also fairly consistent with their SynerGEE counterparts.

Table 5 - SynerGEE and RTDS Comparison (Fault Current)

SynerGEE and RTDS Comparison (I fault)							
Bus	Miles	TPH Fault (kA)			SLG Fault (kA)		
		SynerGEE	RTDS	%error	SynerGEE	RTDS	%error
4	4.195	2855	2968	4.0%	1558	1658	6.4%
6 (to 8) 6 (to 7)	4.426	2703	2758	2.0%	1479	1498	1.3%
9 (to 10) 9 (to 14)	4.716	2485	2566	3.3%	1373	1407	2.5%
15	5.162	2248	2302	2.4%	1263	1273	0.8%
17 (to 20) 17 (to 18)	5.518	2042	2095	2.6%	1181	1187	0.5%
20	5.774	0	x	N/A	1144	1133	1.0%
22	6.067	0	x	N/A	1075	1110	3.3%
18	5.607	0	x	N/A	1146	1177	2.7%
10	4.807	2443	2508	2.7%	1353	1376	1.7%
12	5.038	0	2368	N/A	1304	1303	0.1%
101 (to 102) 101 (to 117)	4.563	2656	2688	1.2%	1461	1485	1.6%
102 (to 110) 102 (to 103)	4.594	2609	2666	2.2%	1438	1478	2.8%
110 (to 113) 110 (to 111)	4.655	2545	2624	3.1%	1407	1442	2.5%
115	4.905	0	x	N/A	1344	1300	3.3%
111	4.703	0	x	N/A	1367	1441	5.4%
103 (to 107) 103 (to 104)	4.695	0	x	N/A	1397	1428	2.2%
108	4.871	0	x	N/A	1353	1394	3.0%
105	4.839	0	x	N/A	1337	1402	4.9%
118	4.901	2436	2348	3.6%	1383	1307	5.5%
119	4.971	2387	2302	3.6%	1366	1289	5.6%
120	5.109	0		N/A	1342	1291	3.8%

Table 6 - SynerGEE and RTDS Comparison (VPQ)

SynerGEE and RTDS Comparison (VPQ)									
Bus	Miles	V3PH (pu)			P (kW)		Q (kVAR)	
		SynerGEE	RTDS	%error	SynerGEE	RTDS	SynerGEE	RTDS
4	4.195	1.021	1.021	0.0%	4609	4936	812	812
6 (to 8)	4.426	1.018	1.017	0.1%	1659	1675	287	298
6 (to 7)					1537	1849	265	248
9 (to 10)	4.716	1.016	1.014	0.2%	278	283	47	53
9 (to 14)					1014	1022	175	177
15	5.162	1.013	1.011	0.2%	513	517	88	90
17 (to 20)	5.518	1.012	1.010	0.2%	333	336	58	31
17 (to 18)					69	55	12	15
20	5.774	1.016	1.010	0.6%	98	98	17	21
22	6.067	1.016	1.010	0.6%	14	14	2	3
18	5.607	1.005	0.998	0.7%	41	41	7	9
10	4.807	1.016	1.014	0.2%	223	226	38	41
12	5.038	1.006	1.014	0.8%	69	68	12	16
101 (to 102)	4.563	1.018	1.016	0.2%	1346	1469	233	258
101 (to 117)					191	192	33	34
102 (to 110)	4.594	1.018	1.016	0.2%	942	950	162	167
102 (to 103)					404	517	70	91
110 (to 113)	4.655	1.016	1.015	0.1%	773	779	134	137
110 (to 111)					112	113	19	24
115	4.905	1.006	1.013	0.7%	137	138	24	29
111	4.703	1.020	1.015	0.5%	28	28	5	6
103 (to 107)	4.695	1.009	1.015	0.6%	110	111	19	26
103 (to 104)					112	112	19	26
108	4.871	1.009	1.002	0.7%	28	28	5	6
105	4.839	1.020	1.014	0.6%	14	14	2	3
118	4.901	1.018	1.015	0.3%	80	51	13	14
119	4.971	1.018	1.015	0.3%	38	38	6	9
120	5.109	1.022	1.028	0.6%	19	19	3	4

The voltage profile and feeder real and reactive power flow at selected buses reported by SynerGEE and measured in RTDS are shown in Figure 21, Figure 22, and Figure 23. The maximum difference in node voltages between SynerGEE and RTDS is around 0.8%. The real and reactive power flow curves match well.

Figure 21 - Voltage Profile

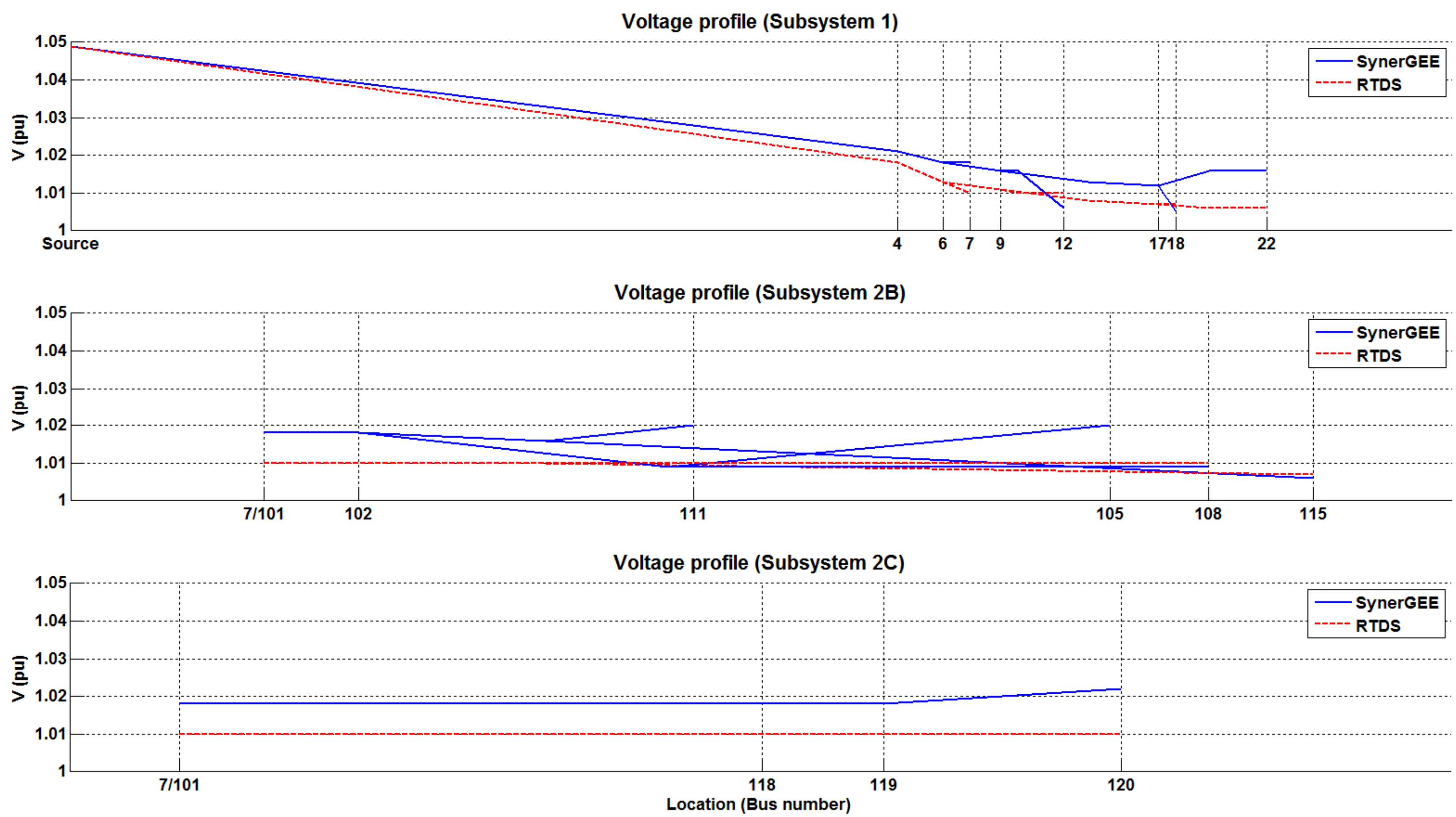

Figure 22 - Real Power Flow

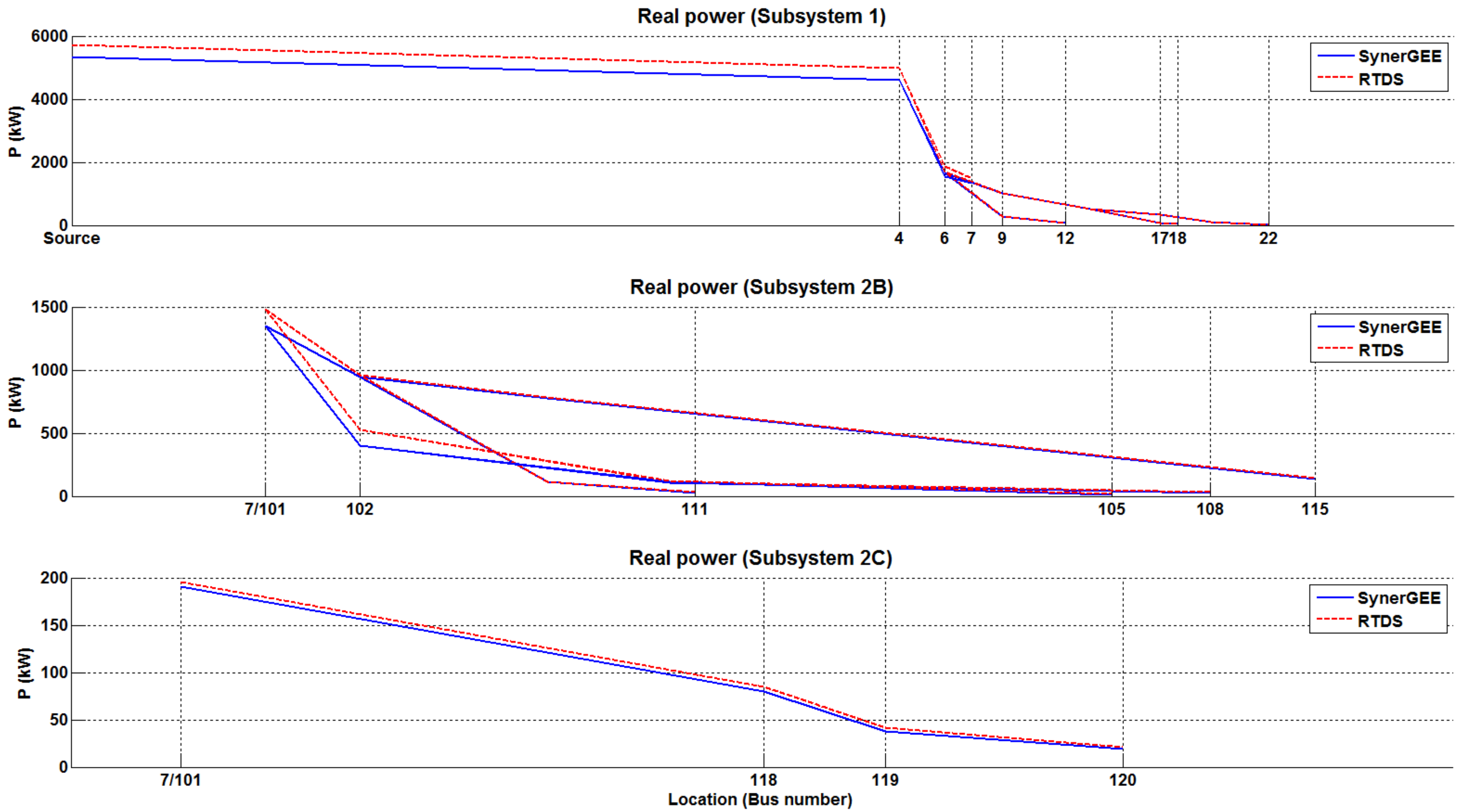

Figure 23 - Reactive Power Flow

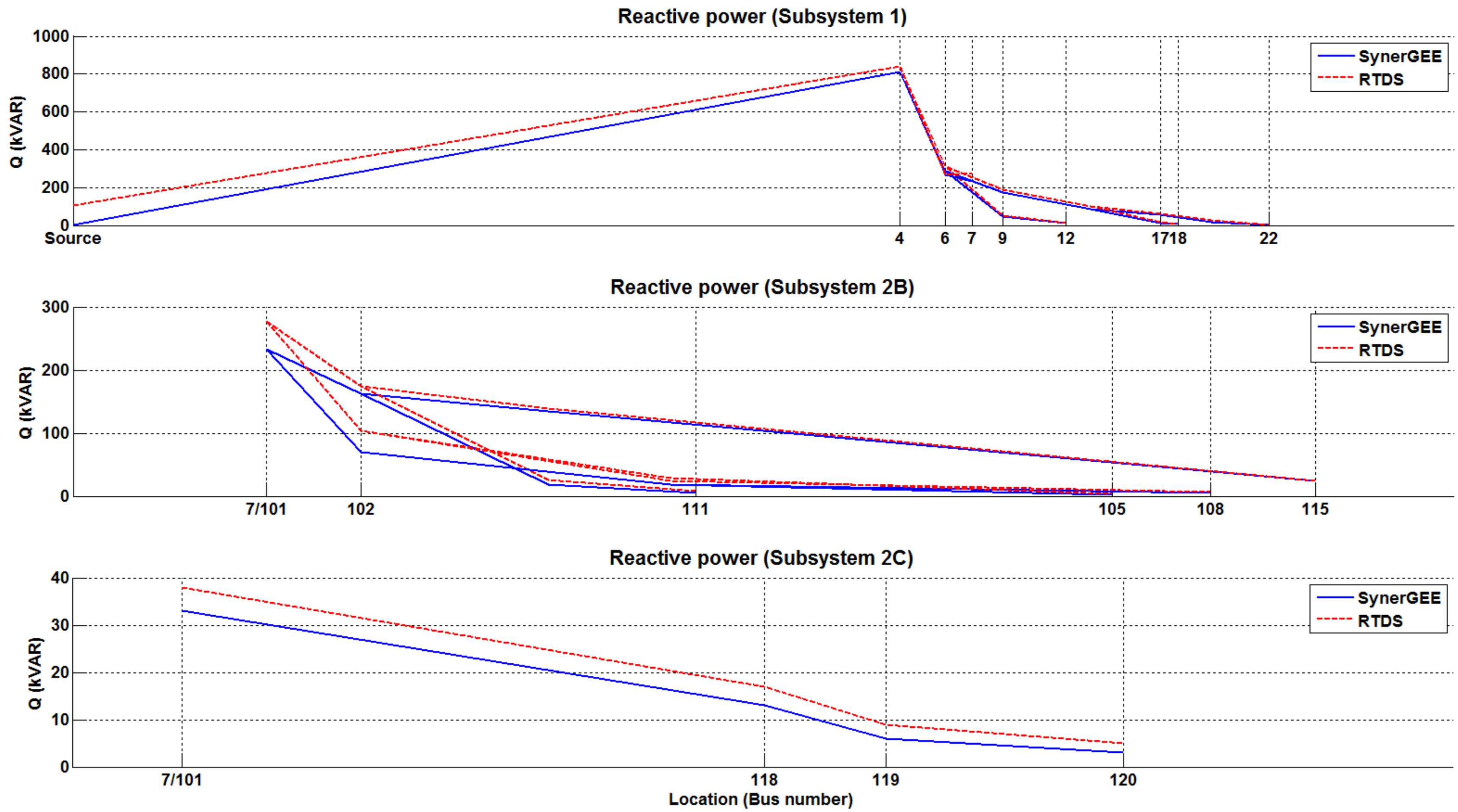

3.3 Test Bed Setup

In order to select a representative distribution circuit for benchmark, the top ranked distribution circuits were selected as part of an investigation and distribution system survey of the electric vehicles adoption patterns [5]. The common characteristics of the circuits were reviewed and a circuit with a high number of PEV customers was selected for the benchmark design. The benchmark circuit was simulated on a three-rack RTDS platform which is part of a Power Hardware-In-Loop (PHIL) test setup. The primary network (12 kV circuits) was modeled on two RTDS racks. The third RTDS rack was used for modeling of the secondary (low voltage) network and the customer interconnection. The instantaneous voltage measurements at the point of interconnection of the selected PEV chargers, corresponding to customers EVSE, were determined through RTDS simulation of the circuit. The PEV charging voltages (grid voltages at the point of connection) were amplified and used to drive the PEV Simulators. The power consumptions and current waveforms from the PEV Simulators were measured and fed back to the RTDS to be reflected in the circuit loading.

In order to determine both circuit level and individual customer level impacts of PEV charging load, the testing and investigations incorporated scaling up the number of PEV customers per service transformer. Due to the limitations in the number of PEV Simulators, the large scale representation of PEV chargers on the circuit was limited to the loading characteristics associated with either of the two PEV Simulators. However, the starting/ending of the charging patterns was adjusted (delayed) to achieve a diversified customer behavior.

A proposed laboratory test set-up detailing all required equipment is shown in Figure 24. The main components were:

- **Four RTDS Racks** – for simulating the distribution circuit and associated loads, and providing signal interfaces for closed loop operation
- **Two PEV Simulators** – to represent PEV charging conditions
- **Two Grid Simulators** (240 V single phase and 480 V three phase) - to amplify the low level signals from the RTDS
- **Feeder Protection Relays**
- **One Capacitor Controller**
- **Three Voltage and Current Amplifiers** – for interface of secondary level voltages and currents
- **110V DC Power Supply**
- **Ethernet Switches**
- **Computer Station**

The closed loop connection between the RTDS and PEV Simulators is defined as below:

- Low level signals representing the voltage measurements for the selected locations of PEV charging units were sent from the RTDS GTAO card to the grid simulators
- Grid simulators amplified the voltages and provided the power source for the PEV Simulators at 240 V and 480V levels corresponding to Level 2 and Fast Chargers, respectively.
- The output current measurements from the PEV Simulators in the form of low level voltage signals were captured and sent to the GTAI card on the RTDS as input feedback
- Additional digital input and output signals between the RTDS (GTDI, GTDO) and each PEV Simulator were utilized for running multiple automated simulations (batch simulations).

The user has the ability to test the behavior of protective and control devices within SDG&E's distribution circuits by passing the output of the RTDS simulation results to the relay rack with the aid of amplifiers. Furthermore, all devices have the ability to communicate with a designated RTDS computer through a common Ethernet switch.

Figure 24 – Laboratory Test Set-Up

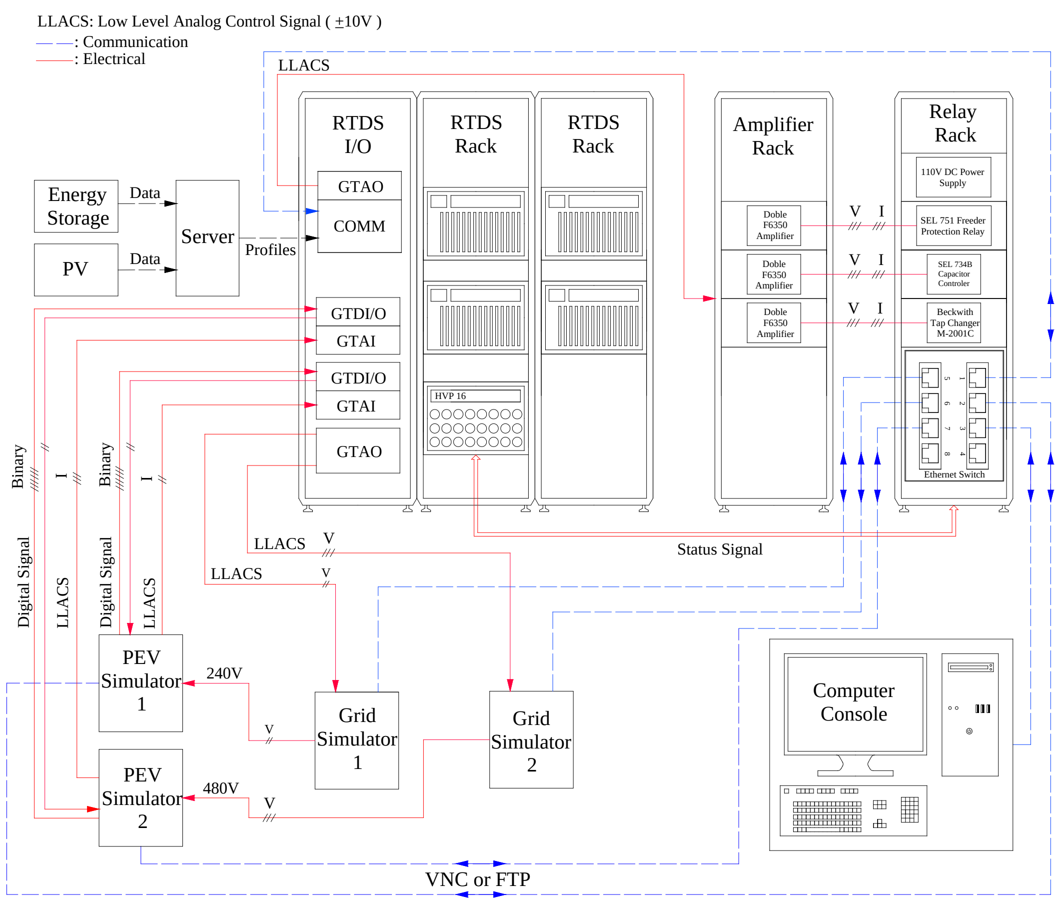

CHAPTER 4:
Test Plan and Test Results

This section provides the test results of investigating the impact of the increase in penetration of PEV (and the corresponding increase in charging demand) on the distribution systems, including service transformers, circuit devices and voltage/power flow profiles of the circuits. The representative Circuit A, used in the study, is shown in Figure 25.

Figure 25 – Test Circuit Layout

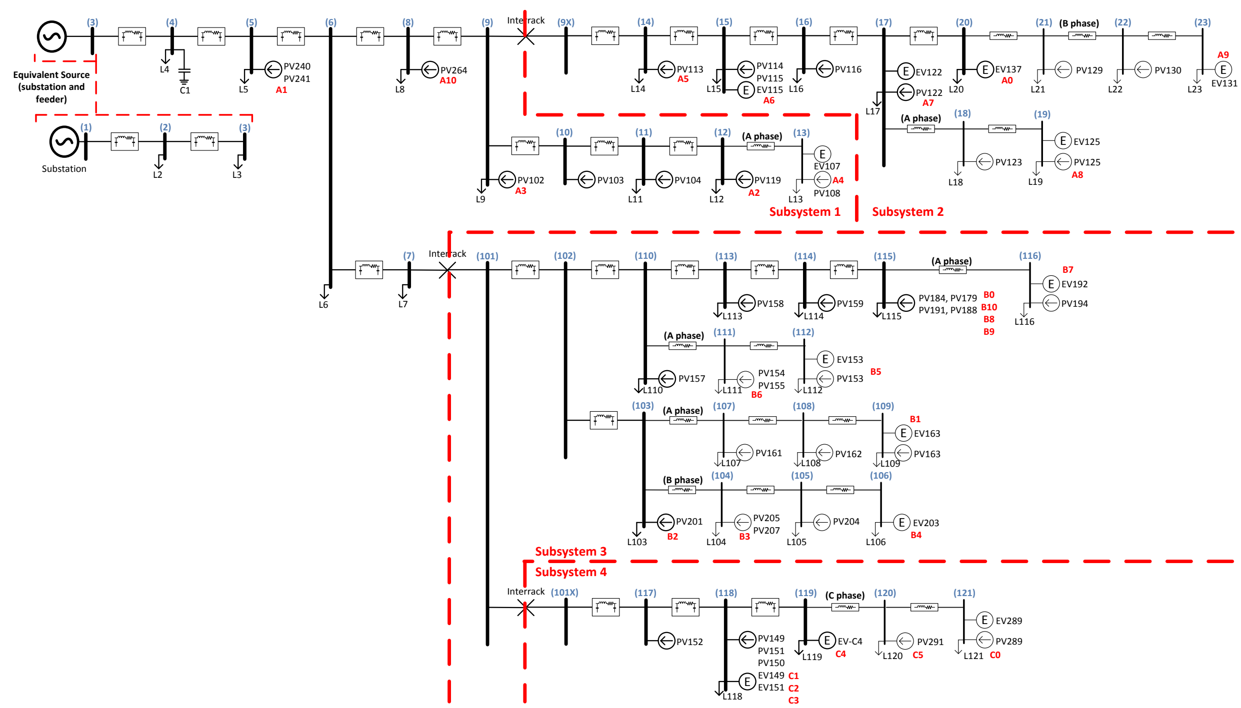

4.1 Modeling

Two types of PEV chargers were investigated:

- AC Level 2 Charger at 240 V (up to 9.8kW)
- DC Fast Charger (up to 40kW).

Residential EV chargers were represented by the AC 240 V model and comprise the bulk of this study. The DC Fast Chargers were tested at two locations: Bus 5 representing a shopping mall, and Bus 118 representing a school, as candidate locations for future deployment of DC Fast Chargers.

The circuit under study had multiple PEV customers, as well as several solar PV inverter installations (roof-top PV). The loads, PV, and EV units were modeled on a secondary low voltage (240 V) circuit, connected between phases through two 12.47kV-to-0.120kV windings. PV and EV were represented by current sources connected between the two windings (240 V) and loads were connected phase to ground (120V). For single phase loads, only a single 12.47kV-to-0.24kV service transformer was used. Transformer impedances were set to Z = 2.5% with X/R ratio of 15.

The load exceeded the transformer kVA rating at numerous secondary locations due to the load lumping methodology used to model the circuit in RTDS – not every secondary location on the circuit was modeled. The secondary circuit locations which featured existing PV or EV systems, or for which had strong potential for the addition of PV or EV systems, were given priority for explicit modeling. The loads along the circuit were lumped into the secondary circuit transformers at the defined buses. For the cases where the lumped load greatly exceeded the transformer rating, the loads were split so that a portion would remain on the high voltage (primary) side of the transformer, reducing the actual kVA through the transformer to within rated values of transformers. A typical representation of a secondary circuit is shown in Figure 26 below.

Figure 26 – Low Voltage (240 V) Secondary Circuit

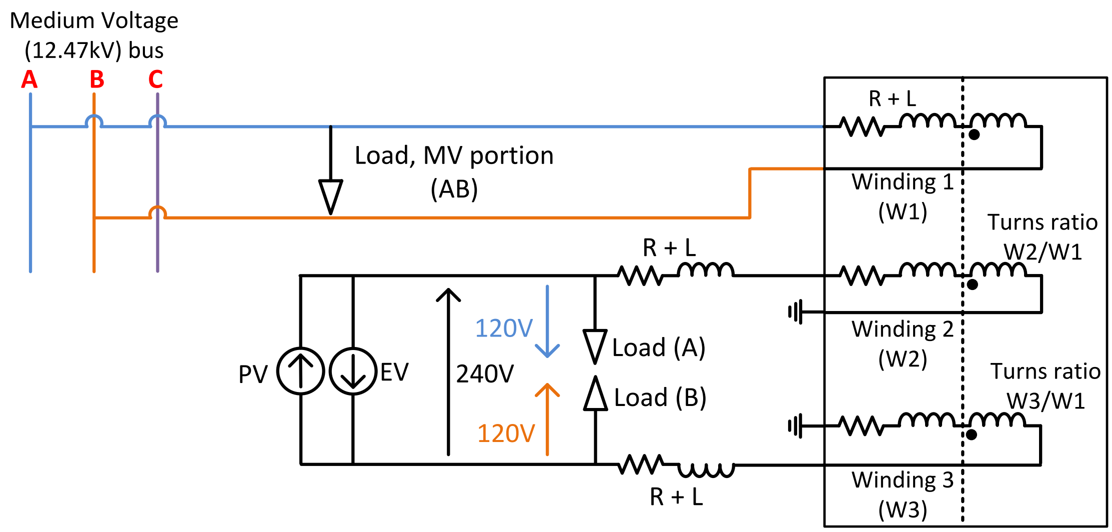

Circuit A was modeled with 28 secondary circuits, 14 of which had existing EV customers.

Two sets of EV customer sizes were chosen for the study, one with completely random distribution and one with random distribution with a set percentage of each size:

- **Set 1**: Random distribution of 3.3kV, 5.8kV, 6.6kV, and 9.8kV EV sizes
- **Set 2**: 4x 3.5kV (~28%), 8x 6.8kV (~58%), 2x 9.8kV (~14%)

Three sets of EV charging times were selected, with random distribution between specified start and end times:

- **Always On**: EV was charged from 4:00 pm through to 4:00 am the next morning
- **Uncontrolled Operation**: Start times from 4:00 pm to 6:00 pm, end times range from 10:00 pm to 4:00 am the next morning
- **Controlled Operation**: Start times from 9:00 pm to 12:00 am, end times from 3:00 am to 6:00 am the next morning

In addition to the fourteen (14) existing customers with EV, values were assigned for all secondary circuits to simulate the case that all transformers would feature EV charging. Customer loads, number of PEVs and PV sizes in the circuit are given in Table 7 and Table 8. The existing EV customers are shaded in the tables.

Table 7 – RTDS Transformer, Load, PV, and EV Parameters (Subsystem 1 and 2)

	Transformer Parameters			Load and PV			EV Size		EV Charging Time			
Bus #	XFMR kVA		Connection	Total Load		Total PV	Set 1	Set 2	Uncontrolled Charging		Controlled Charging	
	Rated	Actual		kW	kVAR	kW	kW	kW	Start	End	Start	End
2			ABC	170	23							
3			ABC	269	34							
4			ABC	146	90							
5			ABC	587	102	30.9						
6			ABC	810	139							
7			ABC	191	32							
8			ABC	267	46	7.3						
9			ABC	100	19	3.5						
10	50	70	A	55	9	5.9	9.8	3.5	17:00	01:30	21:30	04:00
11	50	35	C	28	4	4.6	6.6	6.8	17:00	00:30	23:30	03:00
12			BC	126	22	3.5						
13	100	88	A	69	12	9.8	3.3	3.5	16:30	22:30	23:00	05:00
14			ABC	446	77	3.9						
15	50	41	AB	55	10	12.7	3.3	6.8	16:00	00:30	21:00	04:30
16	50	41		56	9	5.0	5.8	9.8	17:00	01:00	00:00	03:00
17	50	41	AB	55	9	6.0	5.8	3.5	16:30	23:30	23:30	03:00
20	100	82	AC	235	41		6.6	6.8	18:00	01:00	21:00	05:00
21	100	89	B	70	12	4.7	5.8	6.8	16:30	03:00	23:00	05:00
22	25	16	B	14	3	3.3	9.8	3.5	16:30	03:00	21:30	06:00
23	25	18	B	14	2		3.3	6.8	17:00	22:30	22:00	03:00
18	50	35	A	28	5	1.5	3.3	6.8	16:00	22:00	22:00	03:30
19	50	32	A	41	7	3.3	5.8	9.8	16:30	23:30	23:30	05:00

Table 8 – RTDS Transformer, Load, PV, and EV Parameters (Subsystem 3 and 4)

Bus #	Transformer Parameters			Load		PV	EV Size		EV Charging Time			
	XFMR kVA		Connection	Total Load		Total PV	Set 1	Set 2	Uncontrolled Charging		Controlled Charging	
	Rated	Actual		kW	kVAR	kW	kW	kW	Start	End	Start	End
110			ABC	57	9	3.7						
113	50	35	C	28	5	27.5	6.6	6.8	16:00	02:00	00:00	04:30
114	50	36	B	29	6	5.0	5.8	6.8	16:30	01:30	23:30	05:00
115			ABC	579	99	14.1						
116	100	82	A	137	24	13.2	6.6	3.5	17:30	23:30	21:00	05:30
111	100	108	B	84	14	4.6	5.8	6.8	16:00	23:00	22:00	03:00
112	50	35	B	28	5	4.7	5.8	6.8	17:30	02:30	21:30	05:00
103			ABC	294	51	11.6						
107	50	52	A	41	7	5.2	5.8	3.5	17:30	00:00	00:00	04:00
108	50	52	A	41	7	4.9	6.6	6.8	18:00	03:00	21:00	05:00
109	50	35	A	28	5	4.3	9.8	6.8	17:30	22:30	22:30	06:00
104	100	89	B	70	12	10.9	9.8	9.8	17:00	02:30	21:00	03:30
105	50	35	B	28	5	5.2	5.8	3.5	18:00	23:30	23:30	05:30
106	25	17	B	14	2		9.8	9.8	17:00	00:30	23:30	05:00
117						2.9						
118A	50	41	AB	55	10	9.5	6.6	6.8	18:00	01:30	00:00	04:00
118B	50	46	BC	260	10	9.5	9.8	6.8	16:30	02:00	23:00	05:30
119	50	53	AB	42	7		6.6	3.5	17:30	04:00	00:00	03:00
120	25	24	C	19	3	5.1	9.8	6.8	17:30	00:30	00:00	05:30
121	25	24	C	19	3	5.4	5.8	6.8	16:00	02:30	22:00	03:30

The test system had the capability to select a starting time and ran through the charging profile, looping back to the beginning at 12:00 am, until it was commanded to stop. The PV output followed a high-fluctuation solar radiation profile which covered a complete day (24 hours). It was assumed that all PVs on the circuit were using the same profile. The PV outputs were scaled according to the profile shown in Figure 27. PV data was obtained from SDG&E's Solar Carport installation and corresponded to measurements for a selected day (July 9, 2013).

Figure 27 – 24-Hour PV Profile Scaling

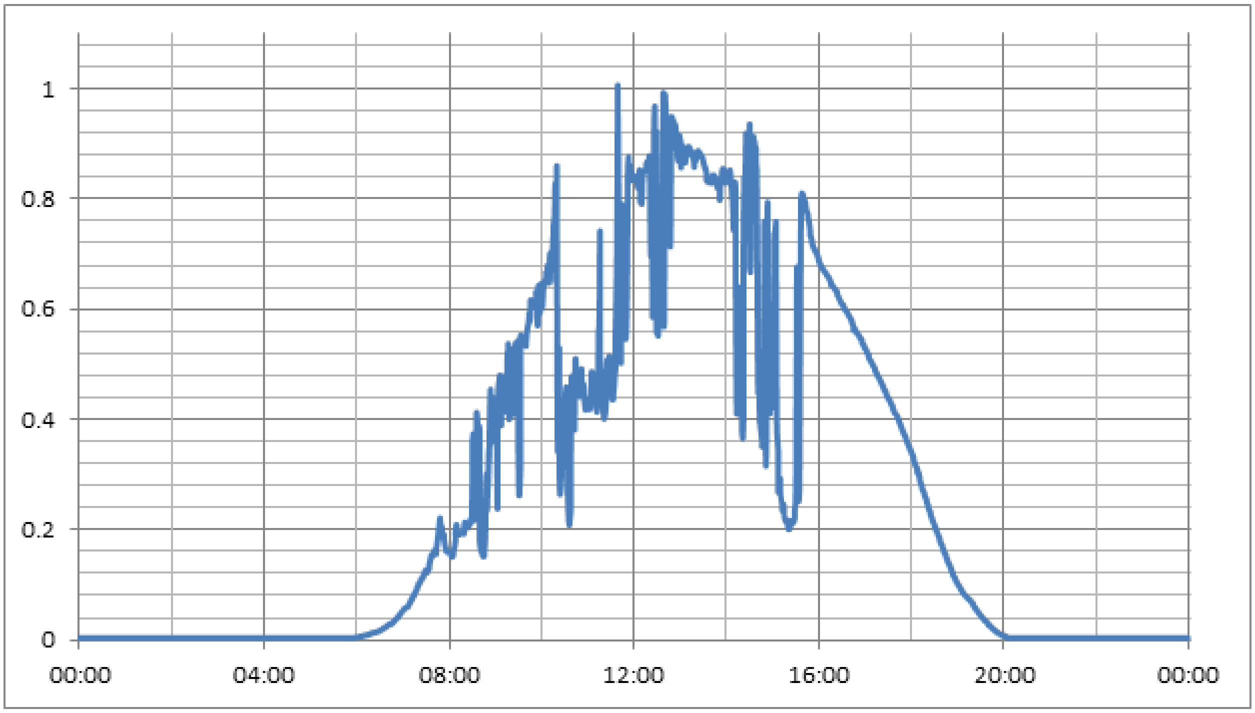

The loads were scaled according to a pre-programmed 24-hour profile, provided by SDG&E as a typical profile for the circuit under study. The load profile is shown in Figure 28.

Figure 28 – 24-Hour Load Profile Scaling

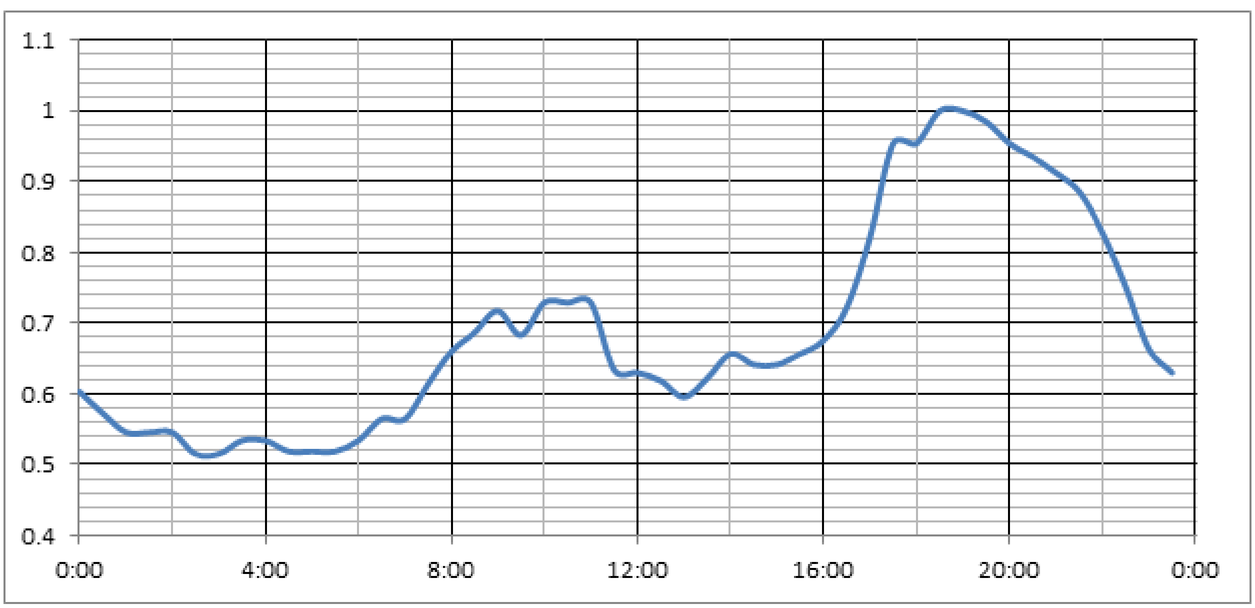

The voltage at the beginning of the test circuit was adjusted individually for the three phases according to (1):

$$V(pu) = \frac{4\frac{S_{bus}}{S_{base}} + 121}{120} \quad \textbf{(1)}$$

Where:

S_{bus} = MVA at beginning of test system

S_{base} = 5.2 MVA, apparent power flow into test system under full load condition

This was based on SDG&E's load tap changer (LTC) control strategy, which adjusted the voltage reference based on the circuit loading through the substation transformer. Because the first part of the circuit segments and some loads were lumped together, the voltage adjustment was applied per phase to account for the unbalanced voltage conditions downstream of the LTC point.

4.2 Test Plan

The test plan was divided into offline (RTDS only) and online (RTDS in conjunction with Grid and PEV Simulators) sections.

4.2.1 Offline Tests

The offline tests established a baseline performance of the modeled Circuit A in RTDS and verified the controls for load, PV, and residential EV operation. All test cases were run for a 24-hour loop in accelerated time, where 1-second real time was equivalent to 1-minute of simulation time. All relevant offline tests were conducted using EV Set 1 (random distribution) and either uncontrolled or controlled charging times. The proposed tests were:

- Baseline circuit performance with fixed maximum loads
- Circuit performance with varying loads and integration of PV
- Full system test with varying loads, PV output, and EV active with all existing customers
- Full system test with varying loads, PV output, and EV active on all transformer secondary circuits

4.2.2 Online Tests

The online tests included the operation of the Grid and PEV Simulations for use in conjunction with the RTDS in a closed loop. The RTDS sent voltage waveform data through its Analog Output to the Grid simulator. The Grid simulator in turn, amplified this signal and fed into the PEV Simulator, replicating the 240 V environment the PEV Simulator would normally operate in. Finally, the PEV Simulator generated a current signal and output to the RTDS, bringing the effect of the charging vehicle back into the computer (RTDS) model. The schematic diagram of the test setup is shown in Figure 29 below.

Figure 29 – RTDS Hardware in Loop Setup for Testing PEV Charging Impact

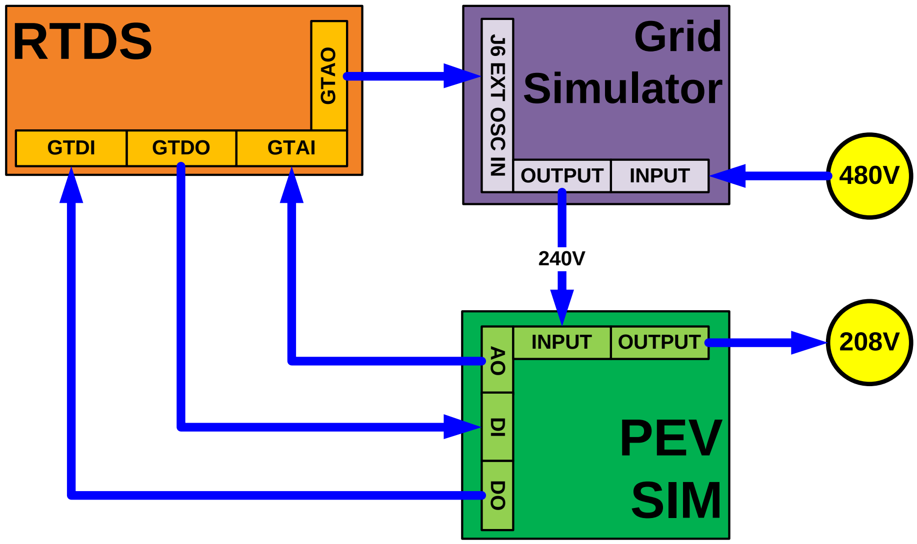

Online tests included both cases run in real time and in 24-hour accelerated time (1 minute real time was equal to 1 hour simulation time). Online tests were conducted with both EV Set 1 (random distribution) and Set 2 (random distribution with set percentages of each PV size), and all sets of charging times.

The following tests were conducted:

- Verification of closed loop operation with RTDS
- Analysis circuit performance with varying loads and integration of PV
- Verification of single EV operation
- Expansion of analysis to multiple EVs on a single transformer
- Full system test with all existing EV customers

Full system test with EV active on all transformer secondary circuits

4.2.3 Fast DC Charger Tests

The DC charger tests comprised two cases at full power (40kW) for 20 minutes in accelerated time. Two different locations were selected, representing a fast charger at a shopping mall and a second fast charger at a school. The majority of the Circuit A area was comprised of residential houses that were expected to have level 2 chargers.

4.3 Test Results for PEV Impact Evaluation

The full set of test results are detailed in the separate document titled *Appendix H: Grid Impact Testing and Data Analysis*. Highlights and representative cases are presented in this report.

4.3.1 Offline – Baseline Test with Variable Load and PV Profiles

This test covered circuit performance for a 24-hour period (starting from 8:00am) with SDG&E provided load profile and a high fluctuation PV profile, shown in Figure 27 and Figure 28 respectively. The test was run in accelerated time, with one-second real time set equivalent to 1 minute of simulation time. The voltage at all selected circuit locations is shown in Figure 30 along with the 24-hour load and PV profile. It was seen that voltage on the circuit varied from 0.97pu through 1.04pu, depending on location and loading. It was observed that the voltage characteristic was dominated by the varying load profile. The PV output fluctuation caused slight voltage variations during the daytime. Transformer voltages and currents are shown in Figure 31, Figure 32, Figure 33, and Figure 34. The impact on primary (12 kV level) voltages was minor, but sudden changes in the secondary voltages were seen in the profiles.

Figure 30 – Voltage at All Circuit Locations for Varying Load and PV Profile

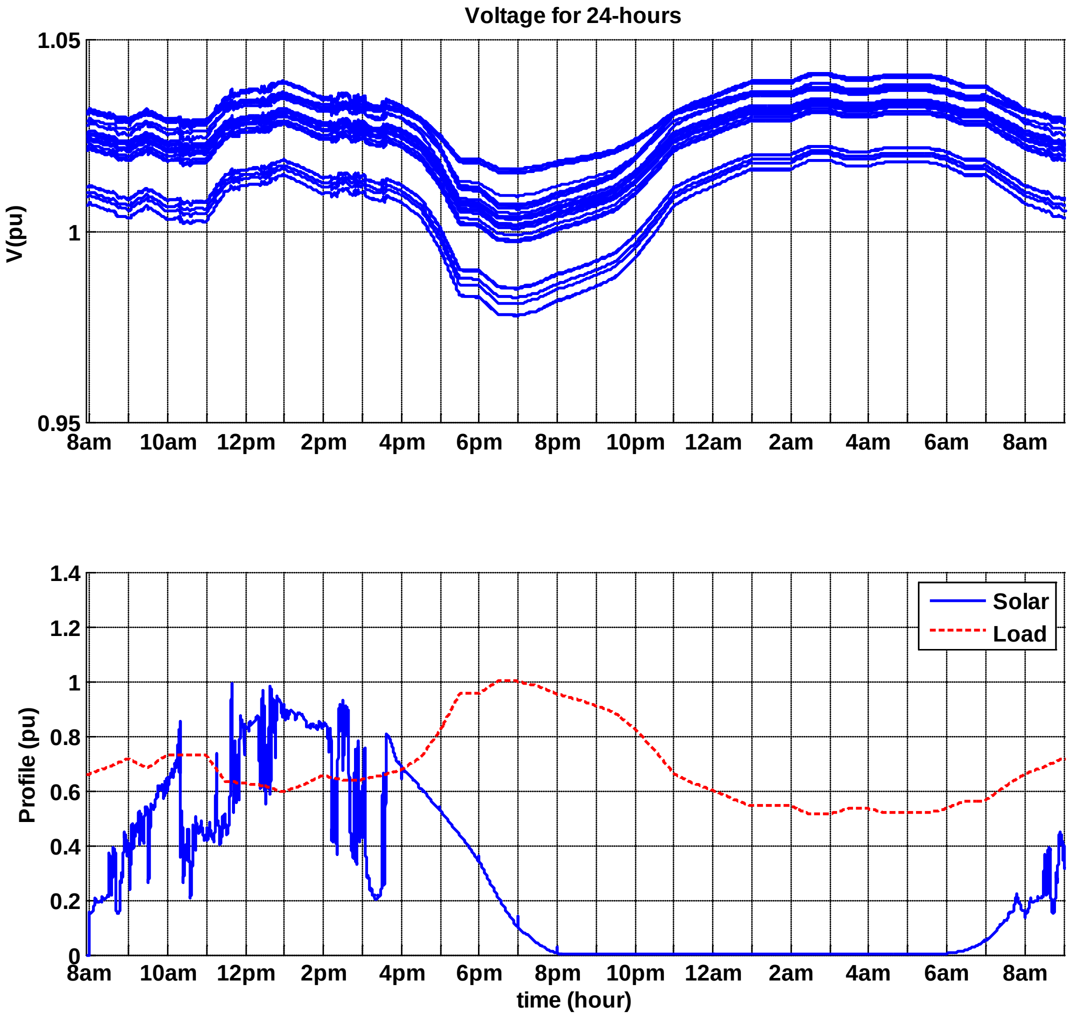

Figure 31 – Primary and Secondary Voltages and Current at 25 kVA Transformers

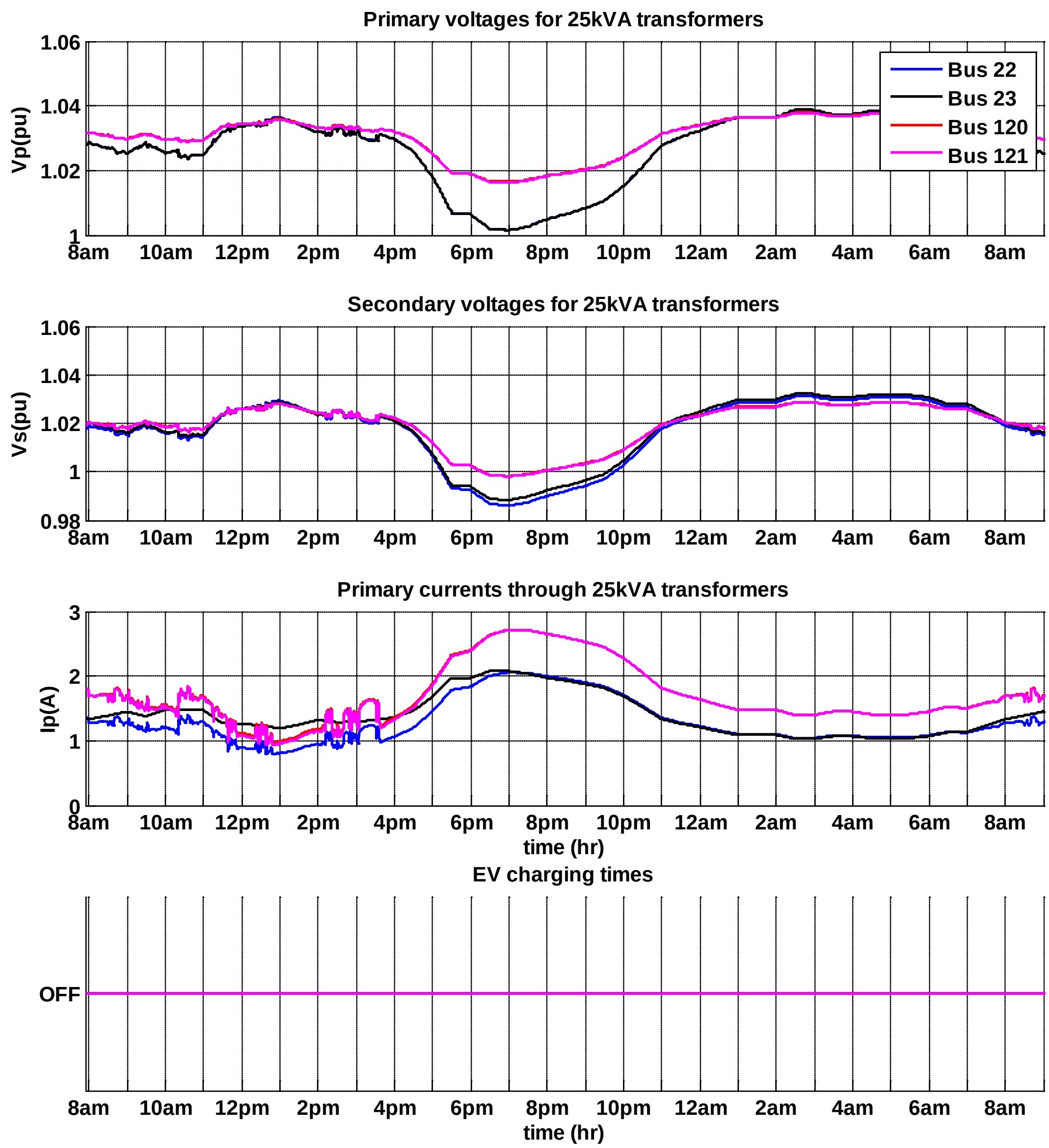

Figure 32 – Primary and Secondary Voltages and Current at 50 kVA Transformers (Subsystem 1)

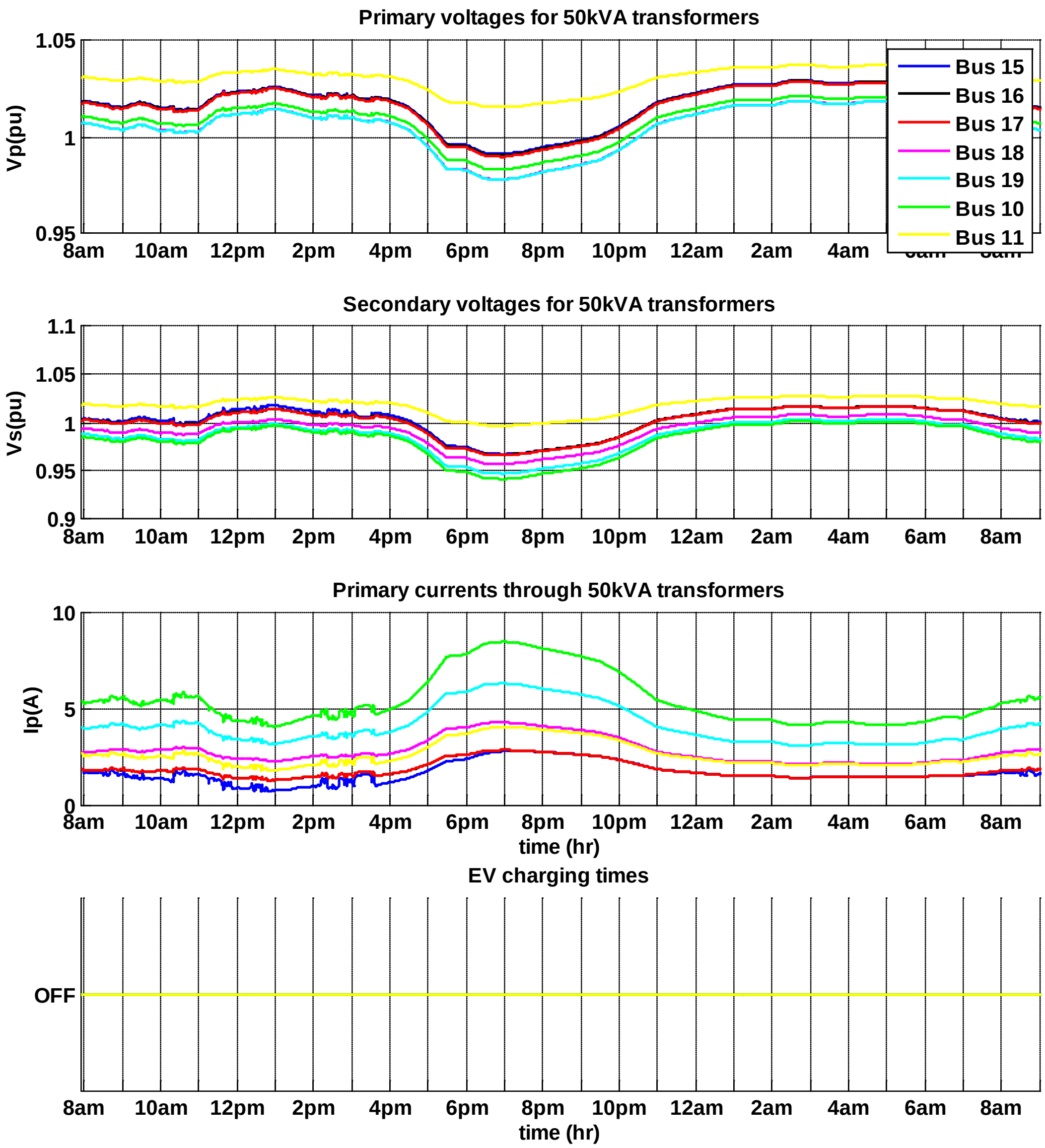

Figure 33 – Primary and Secondary Voltages and Current at 50 kVA Transformers (Subsystem 2)

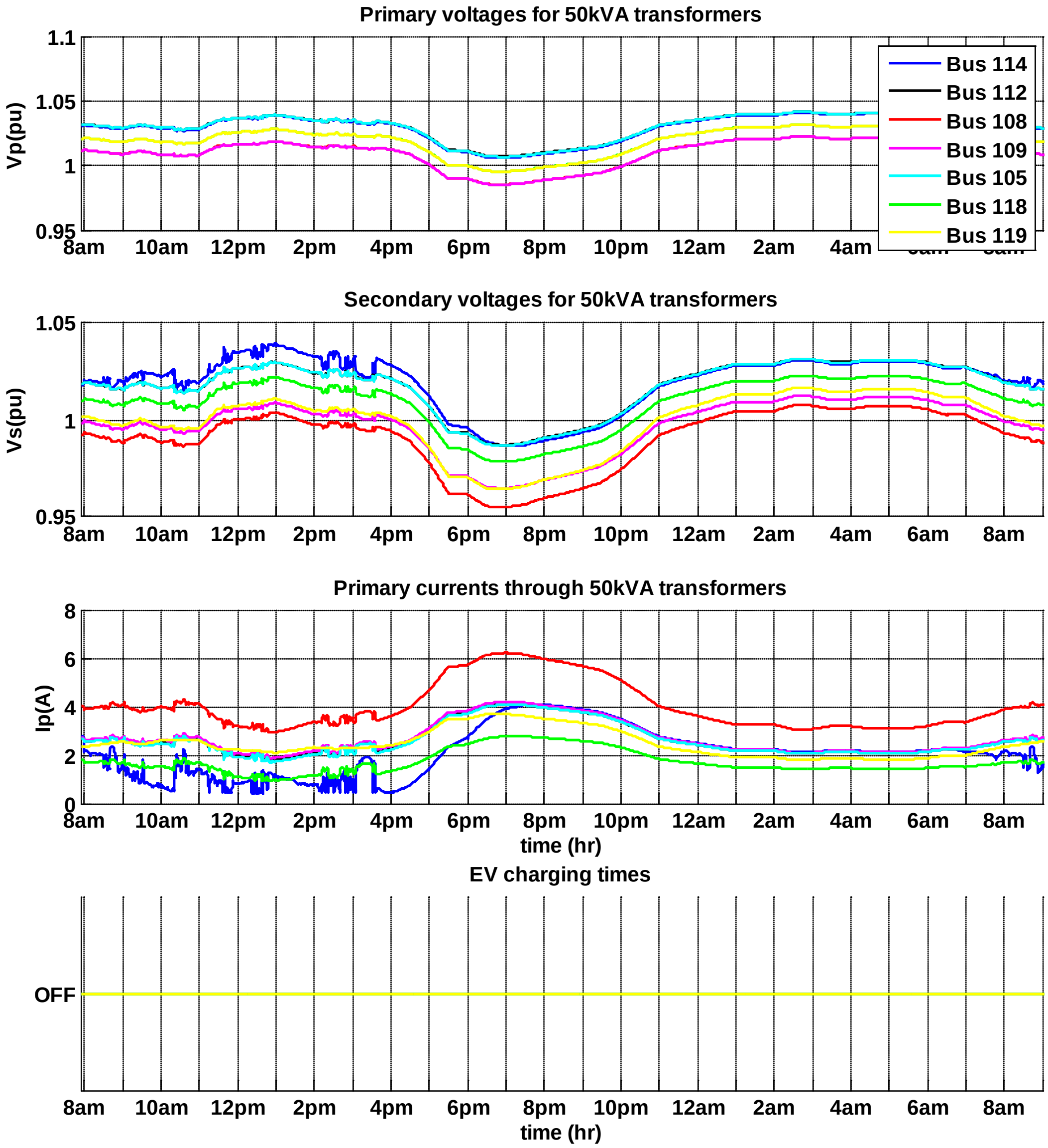

Figure 34 – Primary and Secondary Voltages and Current at 100 kVA Transformers

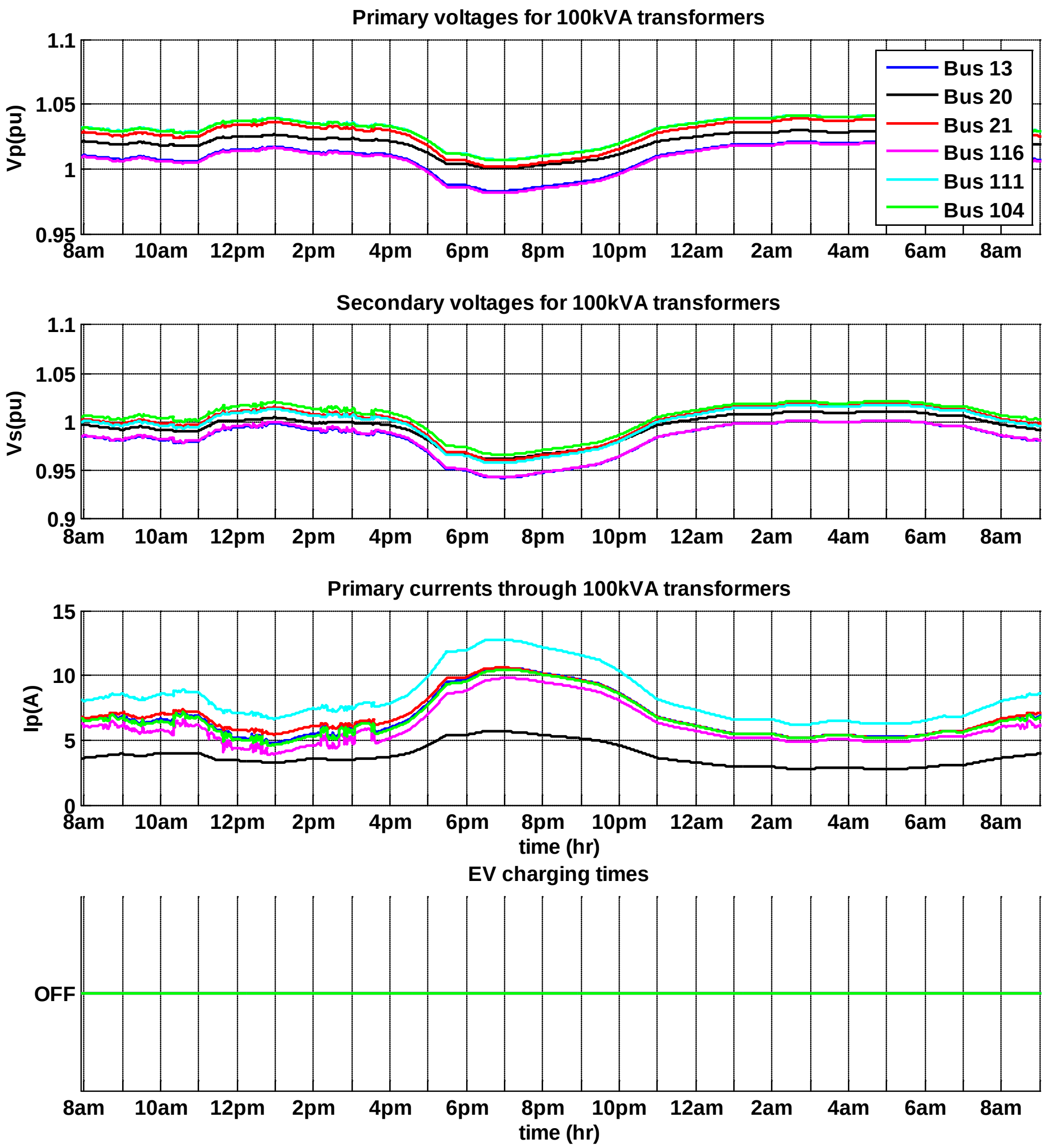

4.3.2 Offline – Full System with All Existing EV Customers (14 Total)

In this test, EV outputs were added at fourteen (14) existing customer locations. EV sizes and charging times were randomly assigned according to the following sizes and times:

- EV Set 1: random distribution of 3.3kW, 5.8kW, 6.6kW, 9.8kW EV sizes
- Uncontrolled Charging: 4:00 pm – 6:00 pm starting times, 10:00 pm – 4:00 am end times
- Controlled Charging: 9:00 pm – 12:00 am starting times, 3:00 am – 6:00 am end times

The details for EV sizes and charging times for both uncontrolled and controlled charging scenarios are given in Table 9.

Table 9 – EV Size and Charging Times Parameters for All Existing Customers (14)

	Transformer and EV Parameters						
Bus #	Transformer Rated kVA	Connection	Total EV kW	Uncontrolled Charging		Controlled Charging	
				Start	End	Start	End
13	100	A	3.3	16:30	22:30	23:00	05:00
15	50	AB	3.3	16:00	00:30	21:00	04:30
17	50	AB	5.8	16:30	23:30	23:30	03:00
20	100	AC	6.6	18:00	01:00	21:00	05:00
23	25	B	3.3	17:00	22:30	22:00	03:00
19	50	A	5.8	16:30	23:30	23:30	05:00
116	100	A	6.6	17:30	23:30	21:00	05:30
112	50	B	5.8	17:30	02:30	21:30	05:00
109	50	A	9.8	17:30	22:30	22:30	06:00
106	25	B	9.8	17:00	00:30	23:30	05:00
118A	50	AB	6.6	18:00	01:30	00:00	04:00
118B	50	BC	9.8	16:30	02:00	23:00	05:30
119	50	AB	6.6	17:30	04:00	00:00	03:00
121	25	C	5.8	16:00	02:30	22:00	03:30

4.3.2.1 Uncontrolled Charging

Voltages for the entire circuit for uncontrolled charging are shown in Figure 35. Transformer voltages and currents are shown in Figure 36, Figure 37, Figure 38, Figure 39. It should be noted that EV charging indicators are shown for all customers, even though only 14 customers have EV. It is observed that EV charging had a large effect on primary transformer current flow, but only a minor effect on the secondary transformer voltage. EV charging had no significant effect on the circuit voltage for the selected EV penetration level. As observed, the 25 kVA transformers were mostly affected by the additional loads of the EV chargers, due to low capacity margin to accommodate additional load.

Figure 35 – Voltage at All Circuit Locations for Varying Load and PV Profile (Uncontrolled Charging)

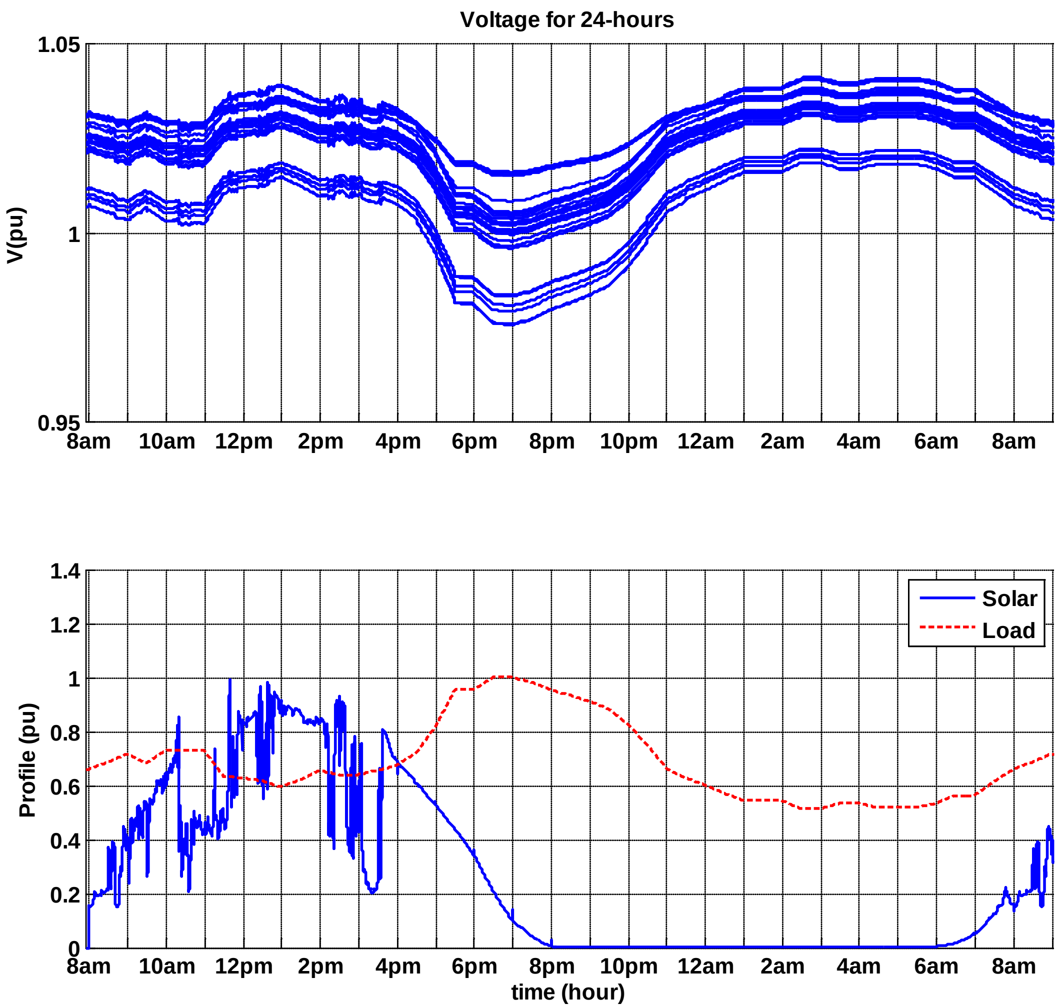

Figure 36 – Primary and Secondary Voltages and Current at 25 kVA Transformers (Uncontrolled Charging)

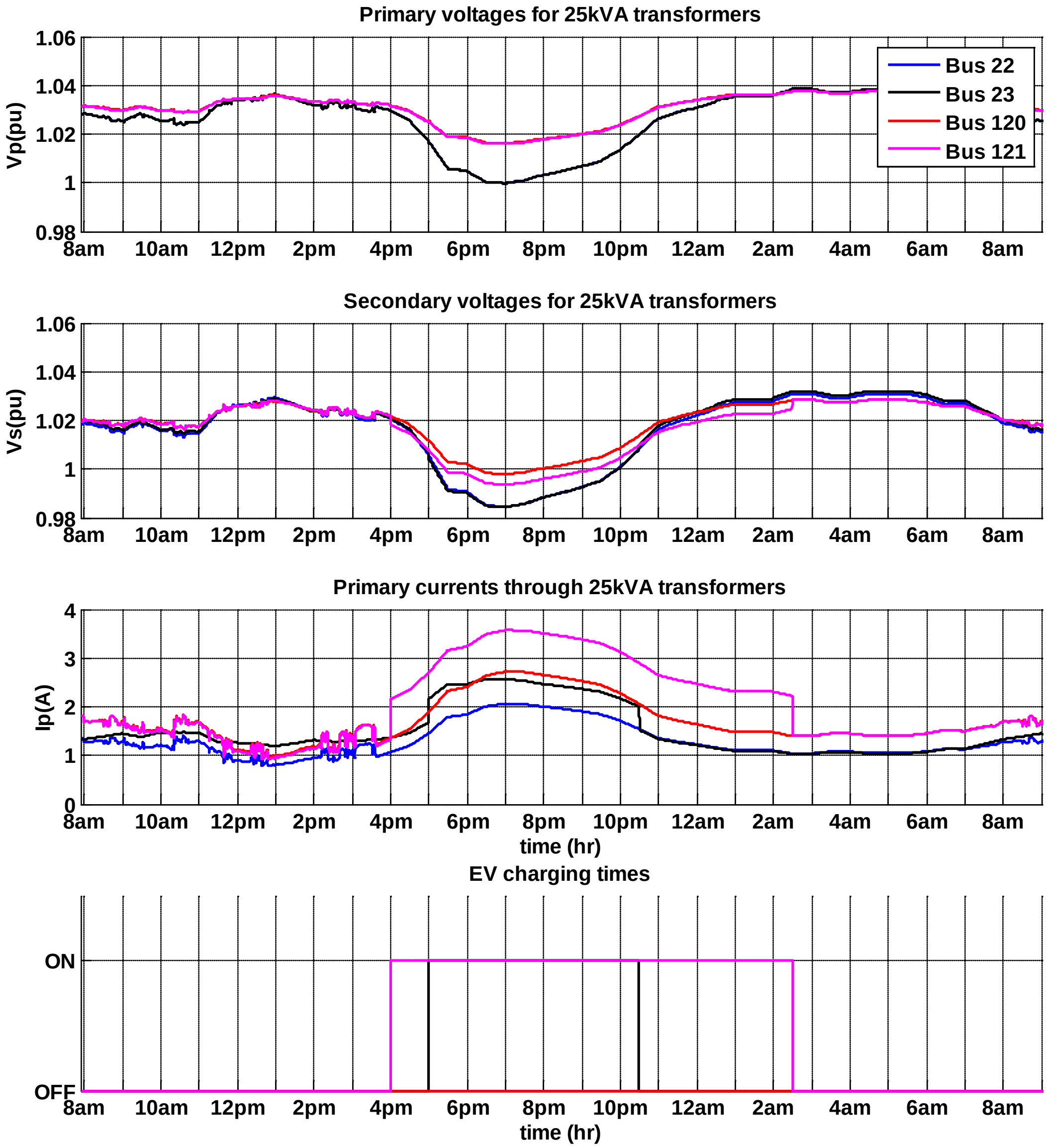

Figure 37 – Primary and Secondary Voltages and Current at 50 kVA Transformers (Subsystem 1) (Uncontrolled Charging)

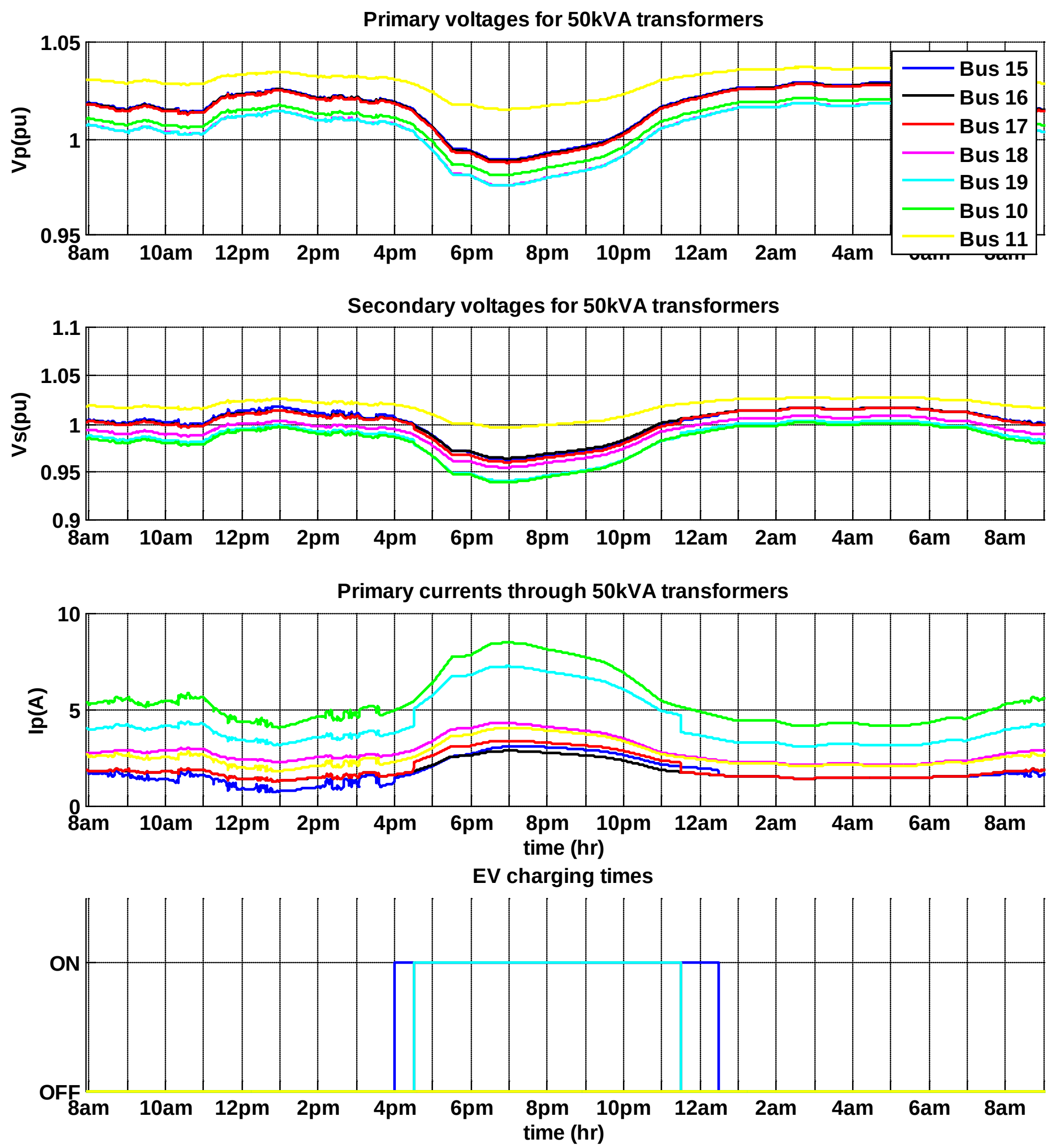

Figure 38 – Primary and Secondary Voltages and Current at 50 kVA Transformers (Subsystem 2) (Uncontrolled Charging)

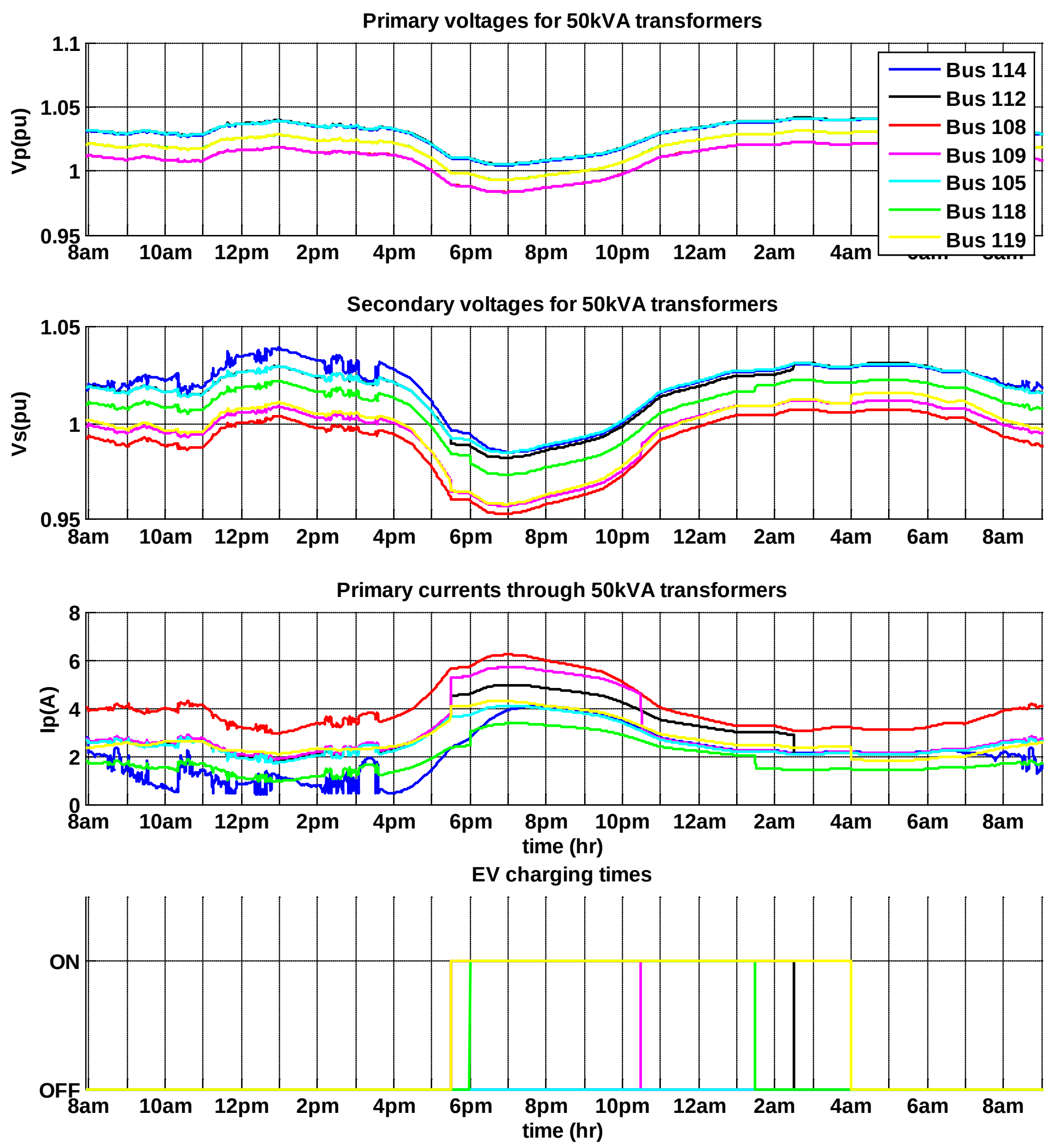

Figure 39 – Primary and Secondary Voltages and Current at 100 kVA Transformers (Uncontrolled Charging)

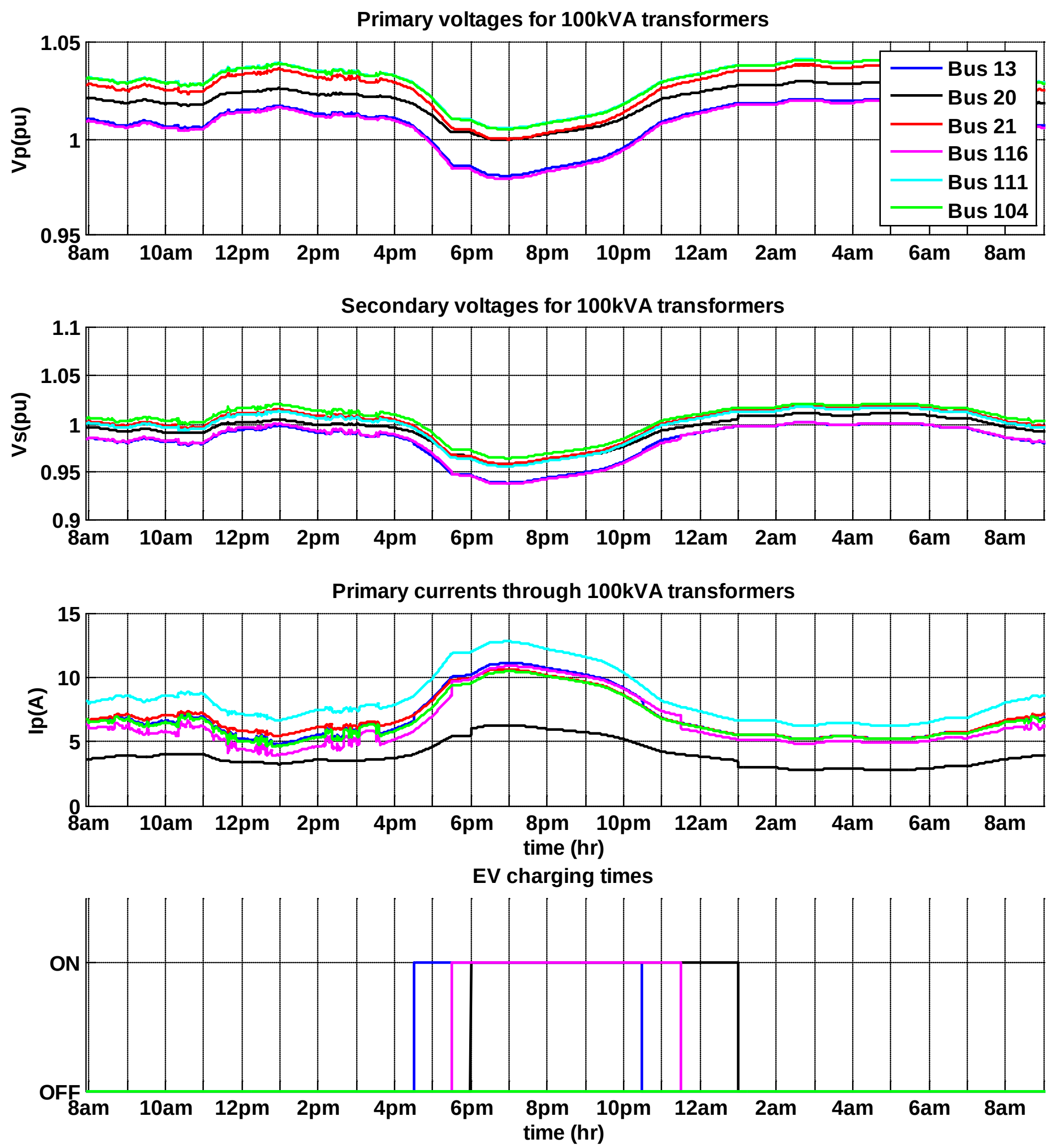

4.3.2.2 Controlled Charging

Plots for controlled charging are shown in Figure 40 through Figure 44. It was observed that EV charging had a large effect on primary transformer current flow, but only a minor effect on the secondary transformer voltage. However, due to the controlled characteristics of the charging profiles, the increase loading and change in power flow was shifted toward off-peak time of the system. EV charging had no significant effect on the circuit voltage at primary level. The secondary circuits experienced low voltage issues due to further drop in transformer voltages as a result of additional EV charging loads.

Figure 40 – Voltage at All Circuit Locations for Varying Load and PV Profile (Controlled Charging)

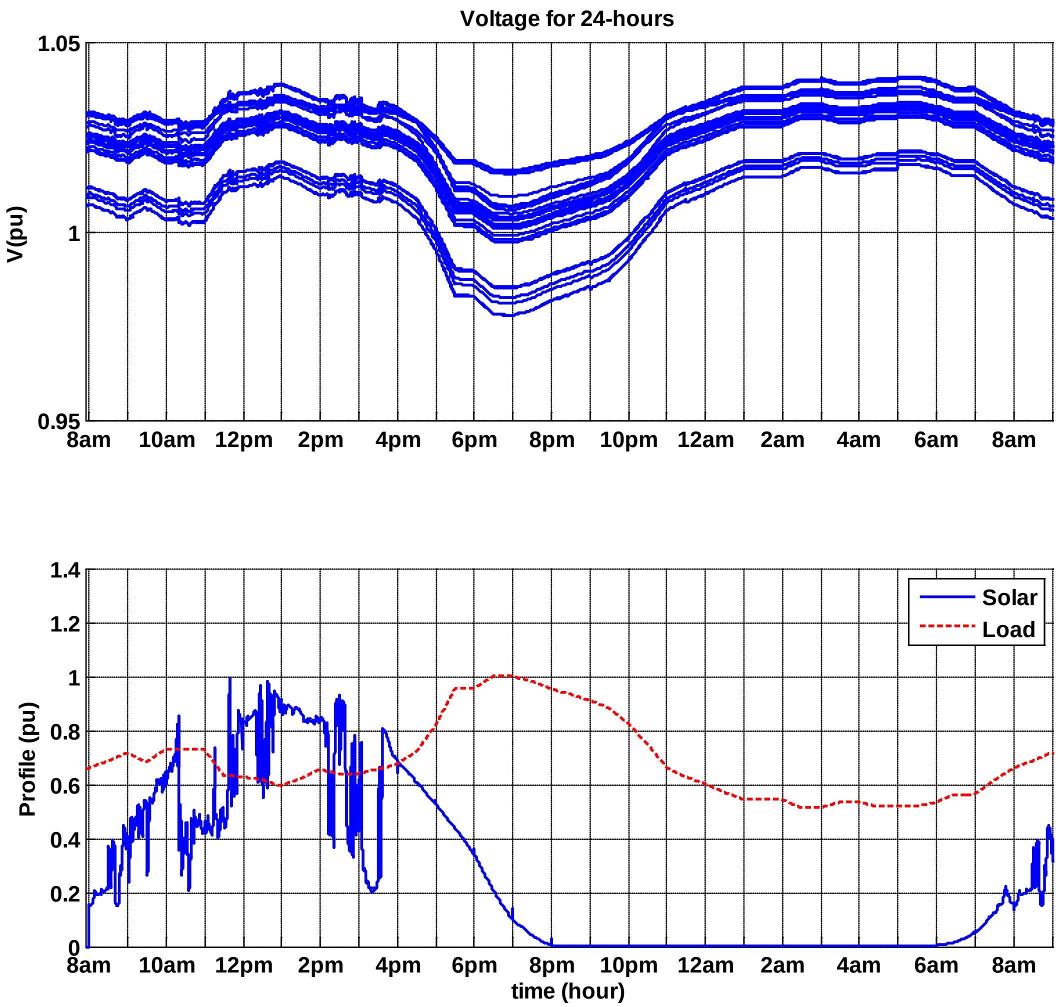

Figure 41 – Primary and Secondary Voltages and Current at 25 kVA Transformers (Controlled Charging)

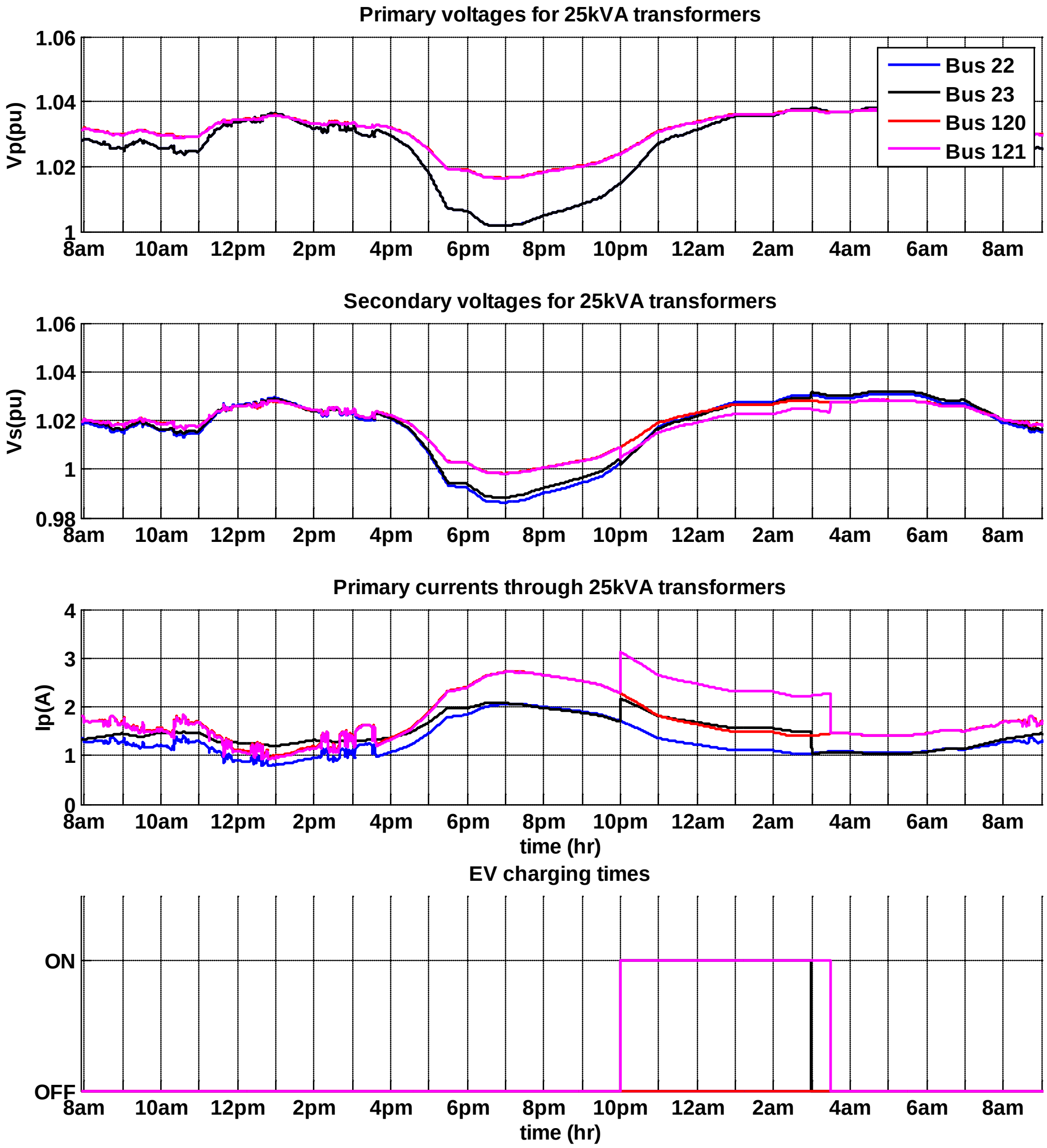

Figure 42 – Primary and Secondary Voltages and Current at 50 kVA Transformers (Subsystem 1) (Controlled Charging)

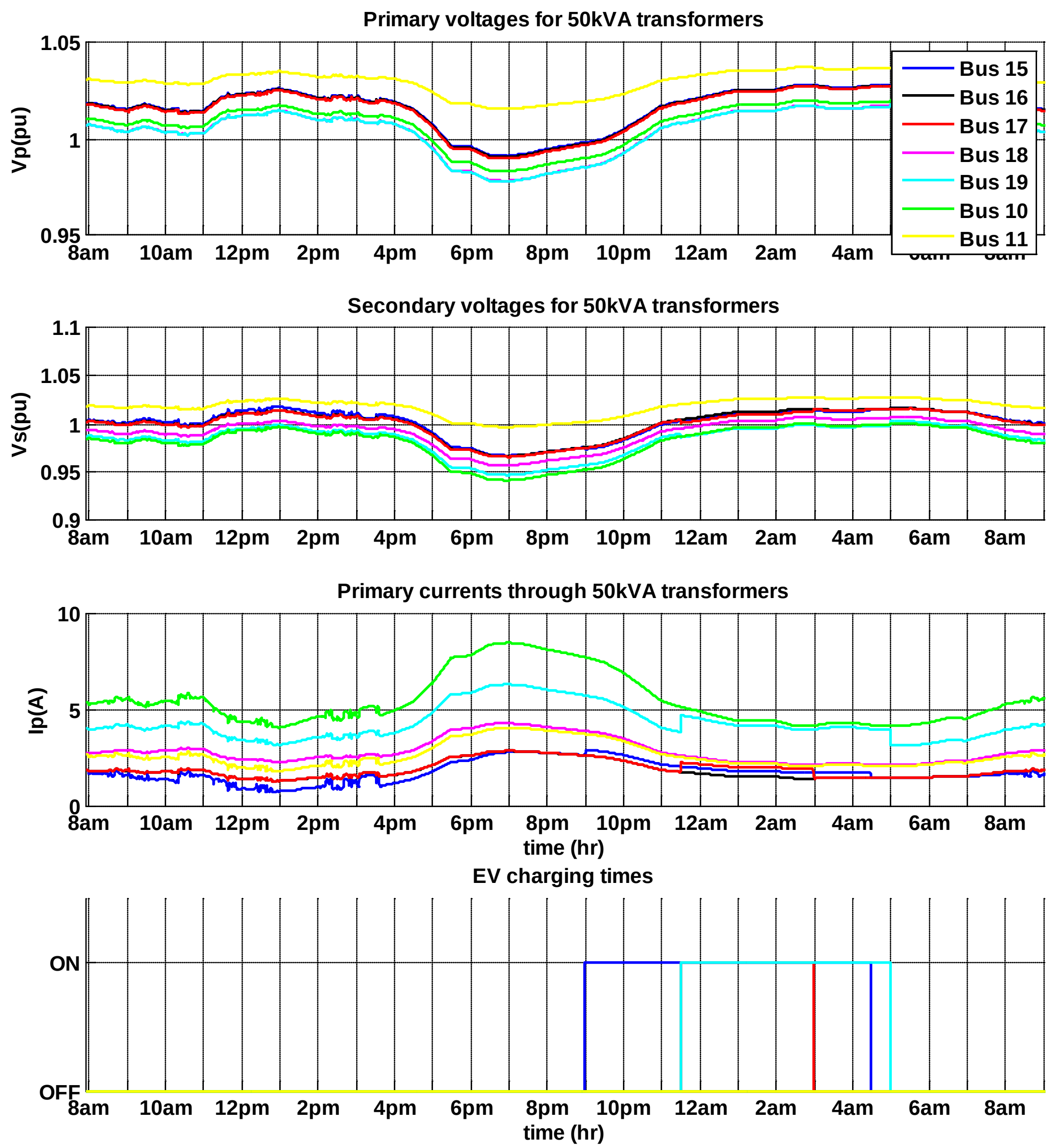

Figure 43 – Primary and Secondary Voltages and Current at 50 kVA Transformers (Subsystem 2) (Controlled Charging)

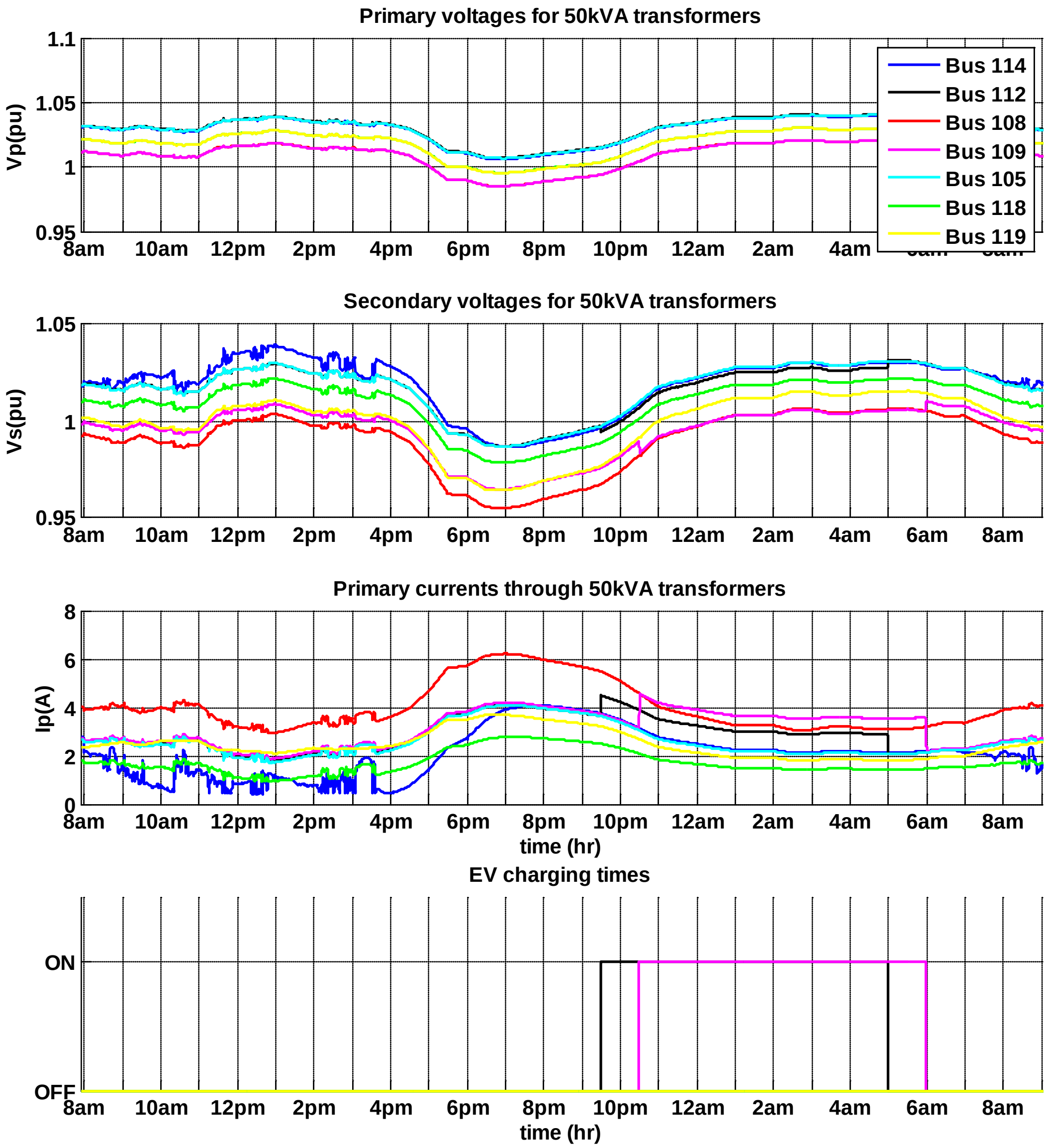

Figure 44 – Primary and Secondary Voltages and Current at 100 kVA Transformers (Controlled Charging)

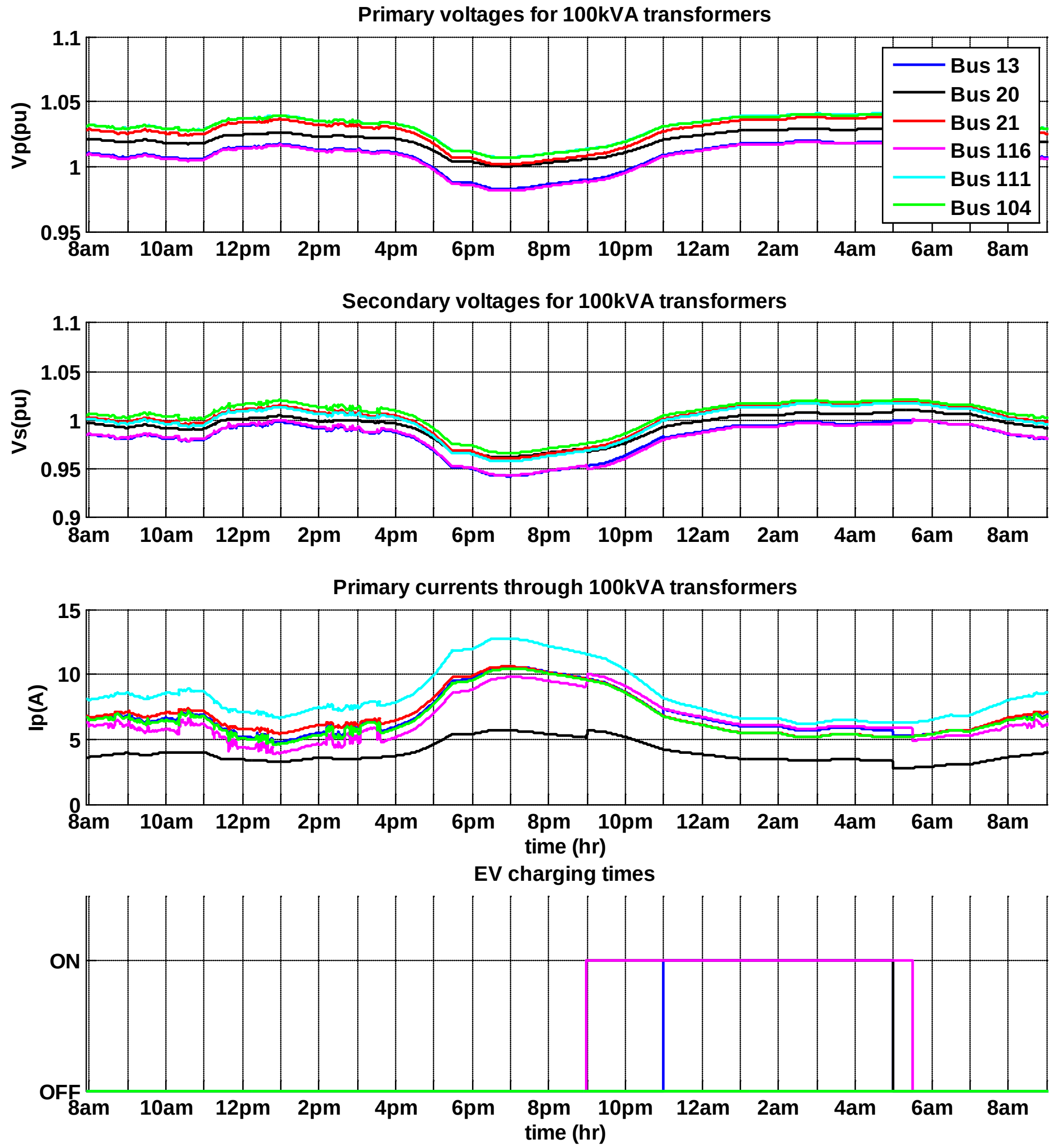

4.3.3 Offline – Full System with EV for All Customers (28 Total)

In this test, EV outputs were added to all customer locations (transformer secondary circuits). EV sizes and charging times were randomly assigned according to the following sizes and times:

- EV Set 1: Random distribution of 3.3kW, 5.8kW, 6.6kW, 9.8kW EV sizes
- Uncontrolled Charging: 4:00 pm – 6:00 pm starting times, 10:00 pm – 4:00 am end times
- Controlled Charging: 9:00 pm – 12:00 am starting times, 3:00 am – 6:00 am end times

The details for EV size and charging times for both uncontrolled and controlled charging scenarios are given in Table 10, with the original 14 EV customers being shaded.

Table 10 – EV Size and Charging Times Parameters for All Customers

	Transformer and EV Parameters						
Bus #	Transformer Rated kVA	Connection	Total EV kW	Uncontrolled Charging		Controlled Charging	
				Start	End	Start	End
10	50	A	9.8	17:00	01:30	21:30	04:00
11	50	C	6.6	17:00	00:30	23:30	03:00
13	100	A	3.3	16:30	22:30	23:00	05:00
15	50	AB	3.3	16:00	00:30	21:00	04:30
16	50	AB	5.8	17:00	01:00	00:00	03:00
17	50	AB	5.8	16:30	23:30	23:30	03:00
20	100	AC	6.6	18:00	01:00	21:00	05:00
21	100	B	5.8	16:30	03:00	23:00	05:00
22	25	B	9.8	16:30	03:00	21:30	06:00
23	25	B	3.3	17:00	22:30	22:00	03:00
18	50	A	3.3	16:00	22:00	22:00	03:30
19	50	A	5.8	16:30	23:30	23:30	05:00
113	50	C	6.6	16:00	02:00	00:00	04:30
114	50	B	5.8	16:30	01:30	23:30	05:00
116	100	A	6.6	17:30	23:30	21:00	05:30
111	100	B	5.8	16:00	23:00	22:00	03:00
112	50	B	5.8	17:30	02:30	21:30	05:00
107	50	A	5.8	17:30	00:00	00:00	04:00
108	50	A	6.6	18:00	03:00	21:00	05:00
109	50	A	9.8	17:30	22:30	22:30	06:00
104	100	B	9.8	17:00	02:30	21:00	03:30
105	50	B	5.8	18:00	23:30	23:30	05:30
106	25	B	9.8	17:00	00:30	23:30	05:00
118A	50	AB	6.6	18:00	01:30	00:00	04:00
118B	50	BC	9.8	16:30	02:00	23:00	05:30
119	50	AB	6.6	17:30	04:00	00:00	03:00
120	25	C	9.8	17:30	00:30	00:00	05:30
121	25	C	5.8	16:00	02:30	22:00	03:30

4.3.3.1 Uncontrolled Charging

Voltages for the entire circuit for uncontrolled charging are shown in Figure 45. Transformer voltages and currents are shown in Figure 46, Figure 47, Figure 48, and Figure 49. It was observed that EV charging had a large effect on primary transformer current flow (20% to 30% increase in loading). The effect on the secondary transformer voltages were in the 1-2% range. EV charging had a minor effect on the primary circuit voltages at 12 kV. The transformer size should match the expected EV charging loads.

Figure 45 – Voltage at All Circuit Locations for Varying Load and PV Profile (Uncontrolled Charging)

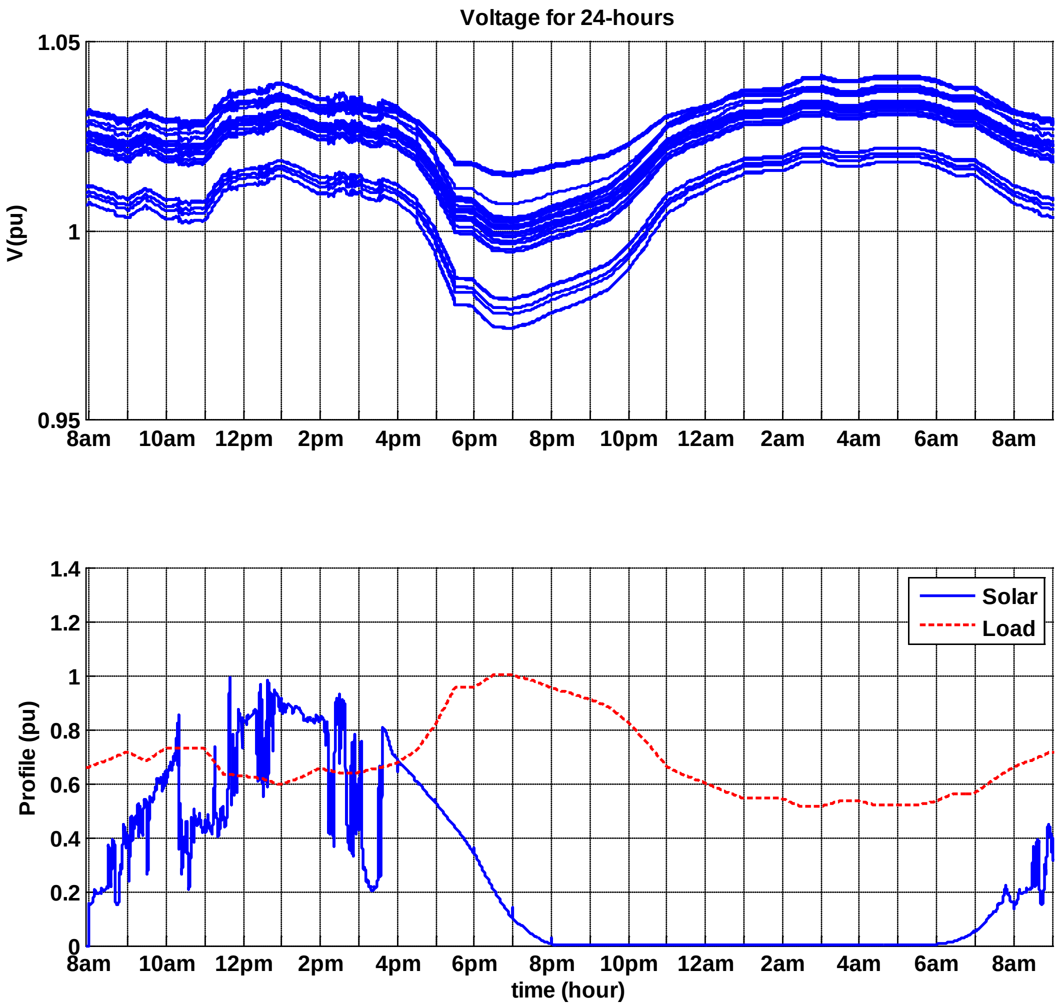

Figure 46 – Primary and Secondary Voltages and Current at 25 kVA Transformers (Uncontrolled Charging)

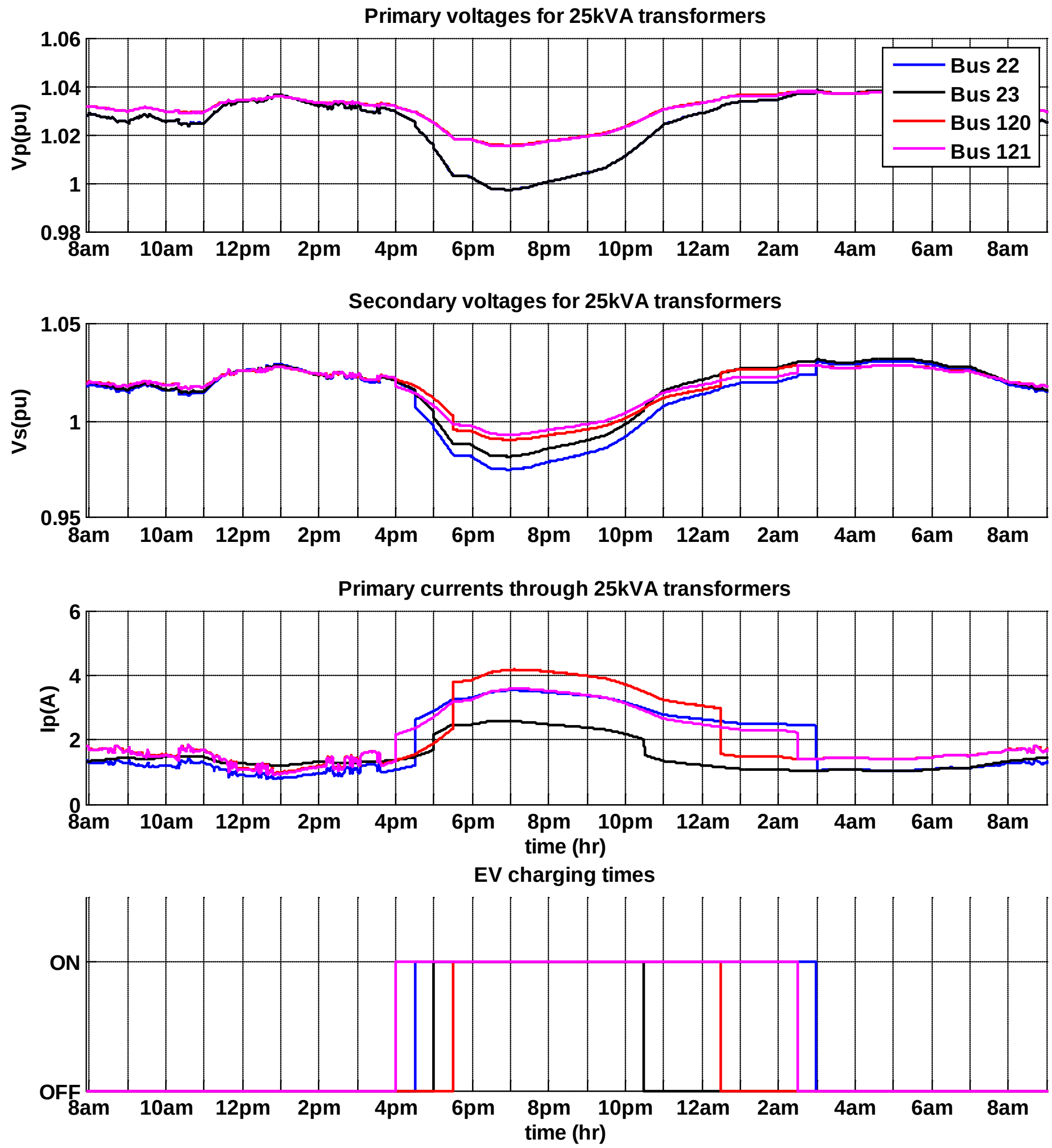

Figure 47 – Primary and Secondary Voltages and Current at 50 kVA Transformers (Subsystem 1) (Uncontrolled Charging)

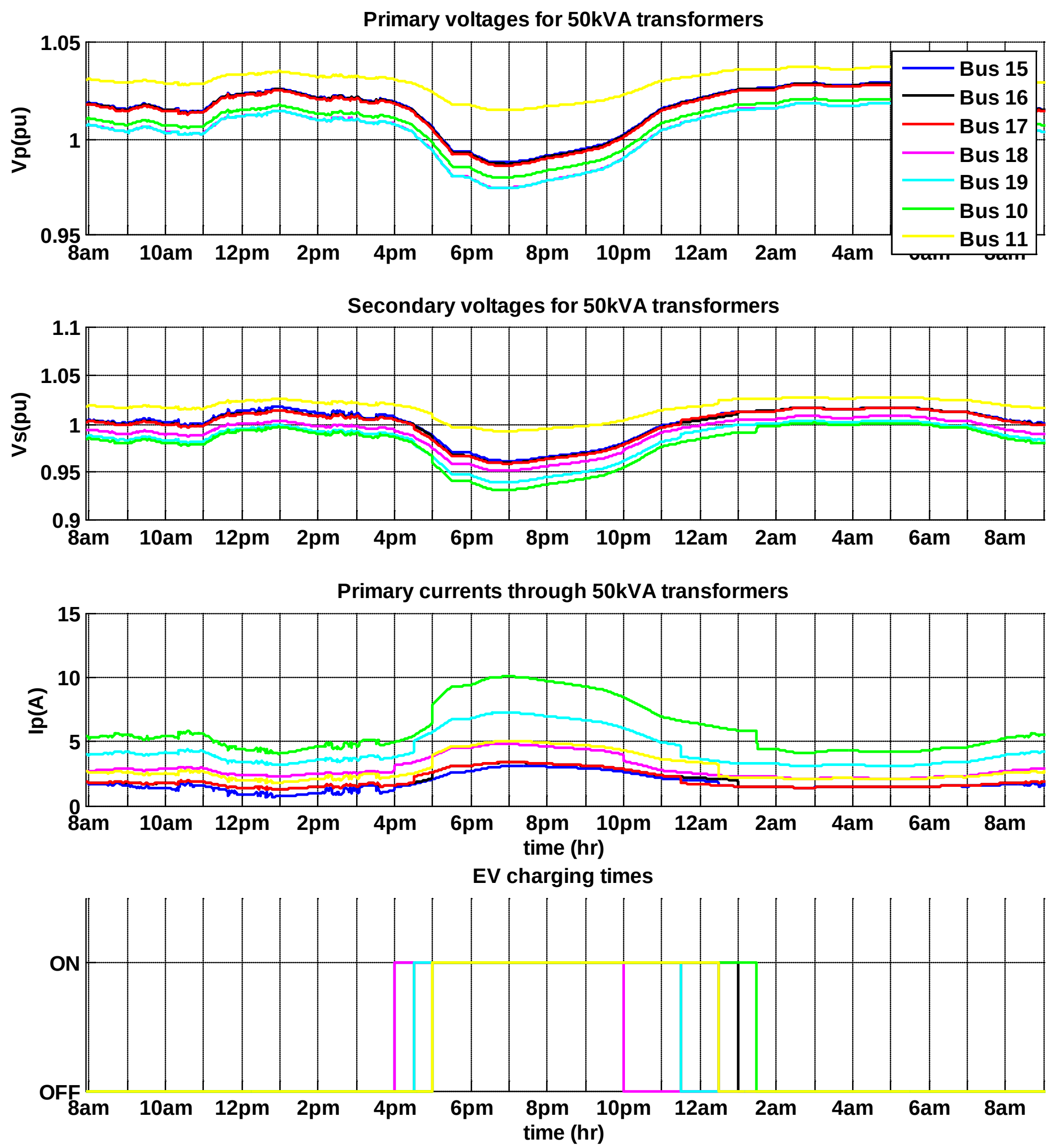

Figure 48 – Primary and Secondary Voltages and Current at 50 kVA Transformers (Subsystem 2) (Uncontrolled Charging)

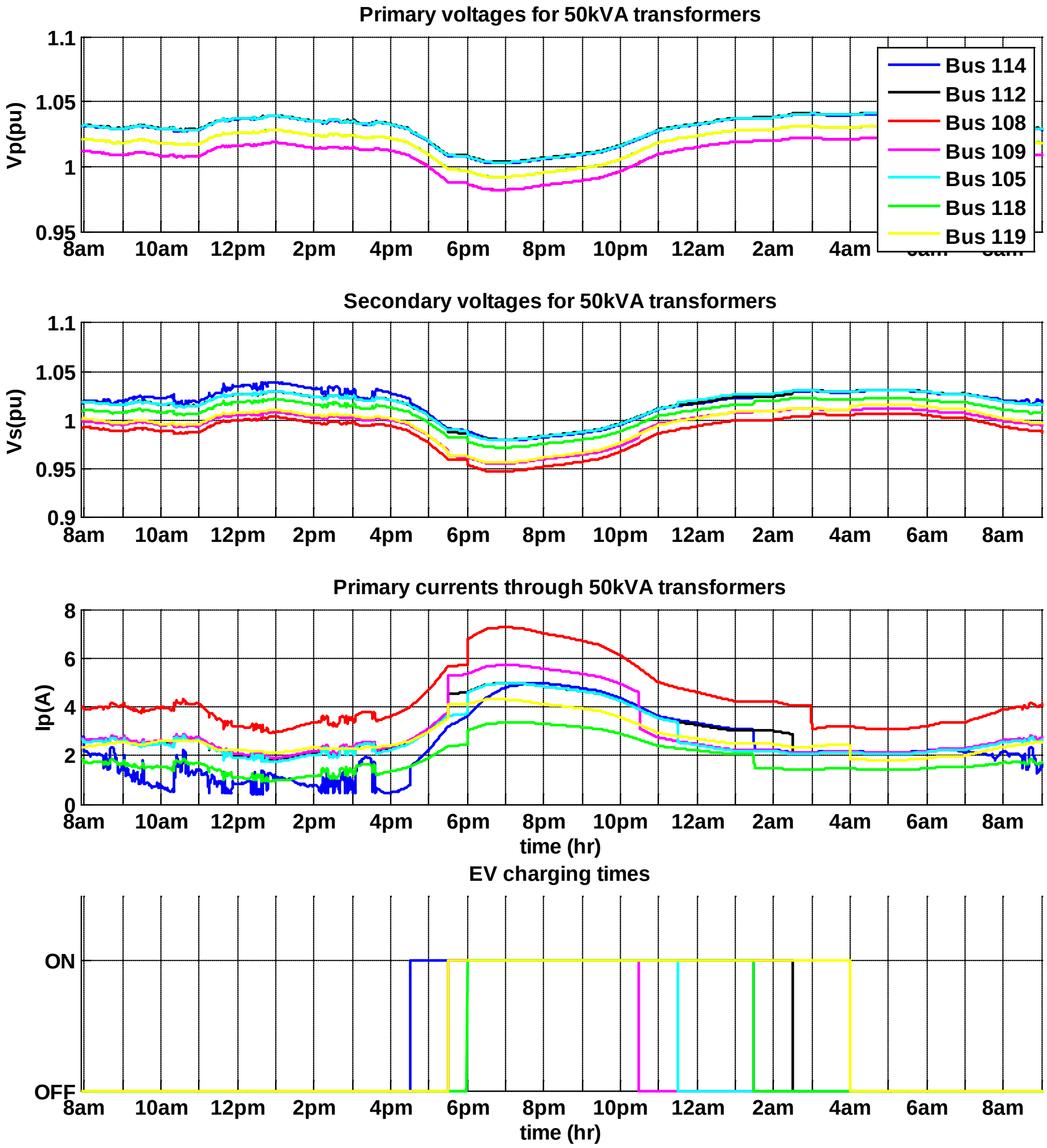

Figure 49 – Primary and Secondary Voltages and Current at 100 kVA Transformers (Uncontrolled Charging)

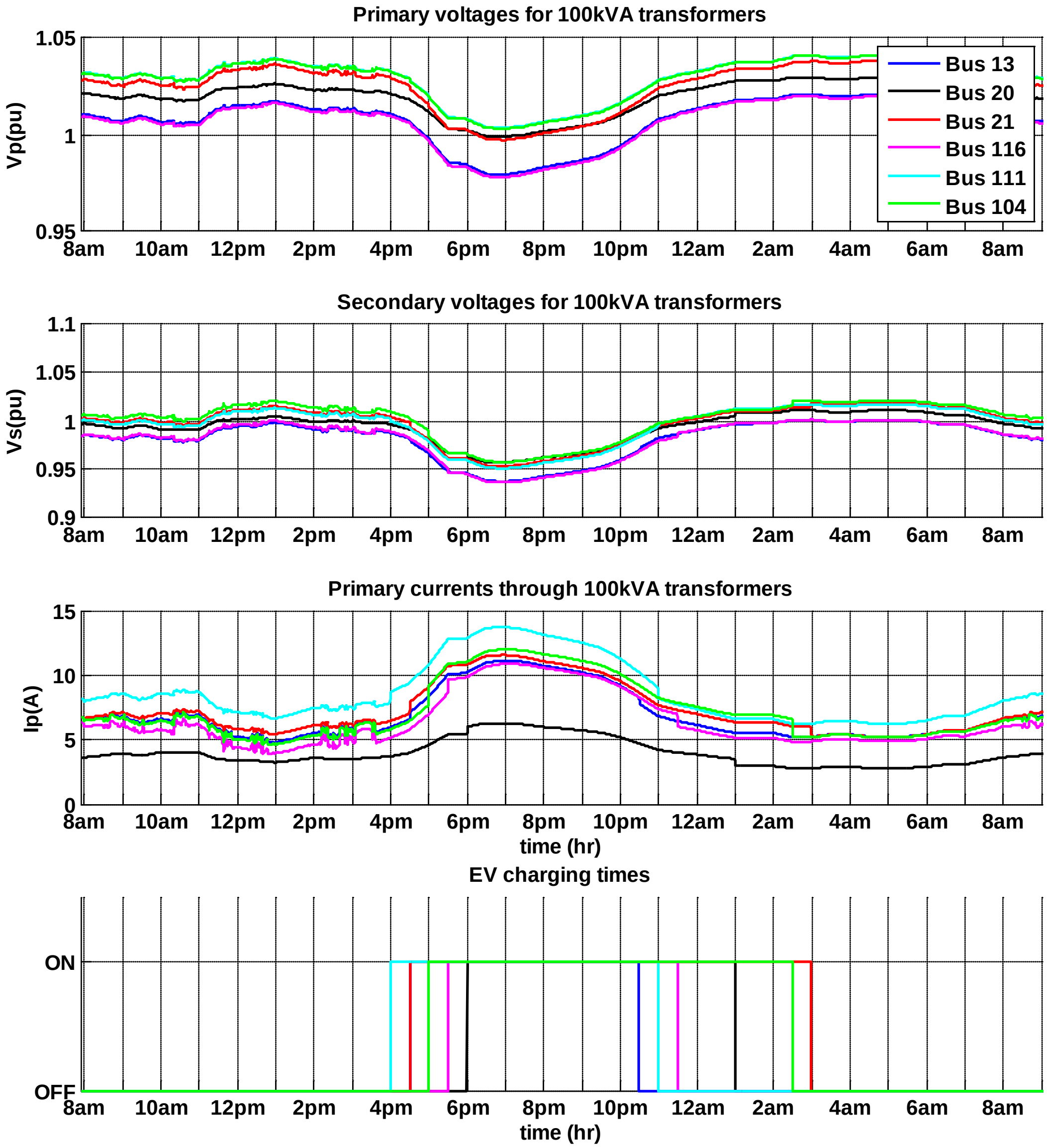

4.3.3.2 Controlled Charging

Plots for controlled charging are shown in Figure 50 through Figure 54. It was observed that EV charging had a large effect on primary transformer current flow, but only a minor effect on the primary transformer voltages at this penetration level. In addition, because the controlled charging mostly occurred during late evening time, voltage was higher at that time compare to the late afternoon or early evening. Hence, the impact on the secondary voltage drop was lower comparing to the un-controlled scenarios.

Figure 50 – Voltage at All Circuit Locations for Varying Load and PV Profile (Controlled Charging)

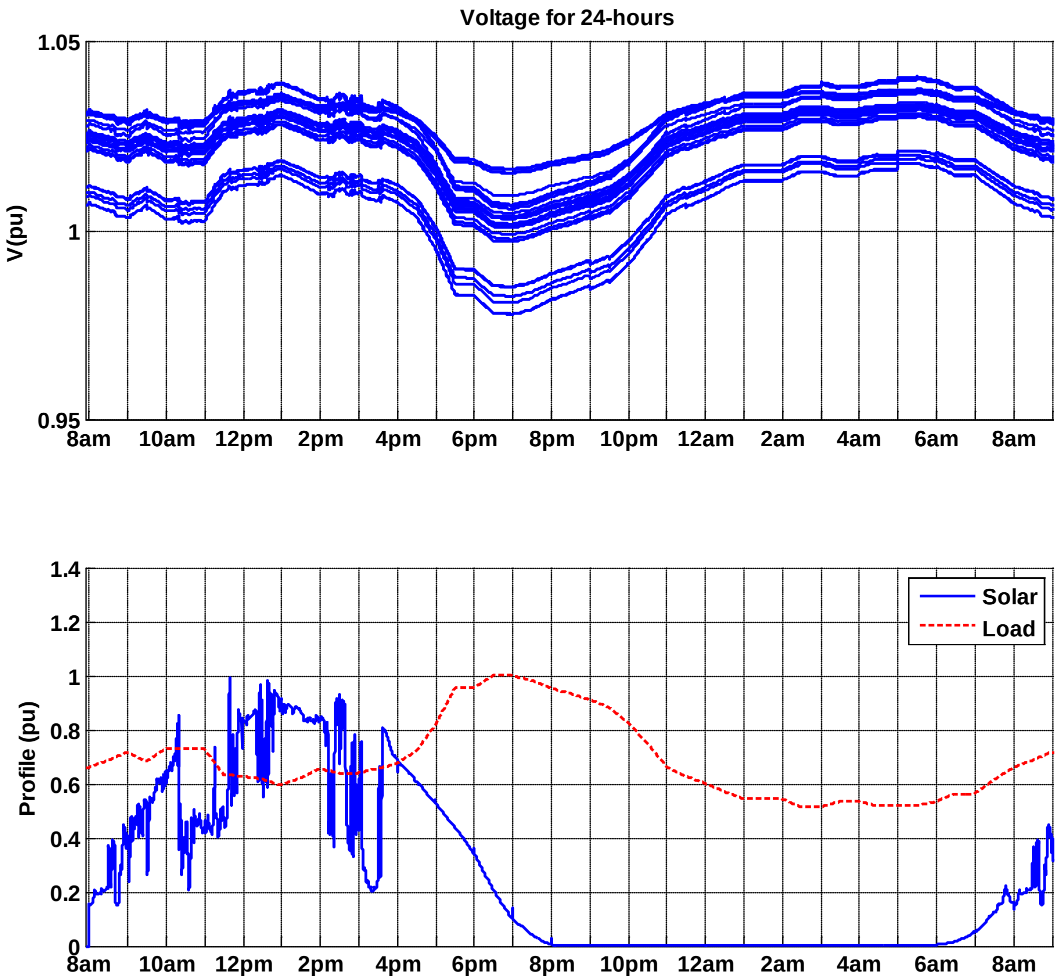

Figure 51 – Primary and Secondary Voltages and Current at 25 kVA transformers (Controlled Charging)

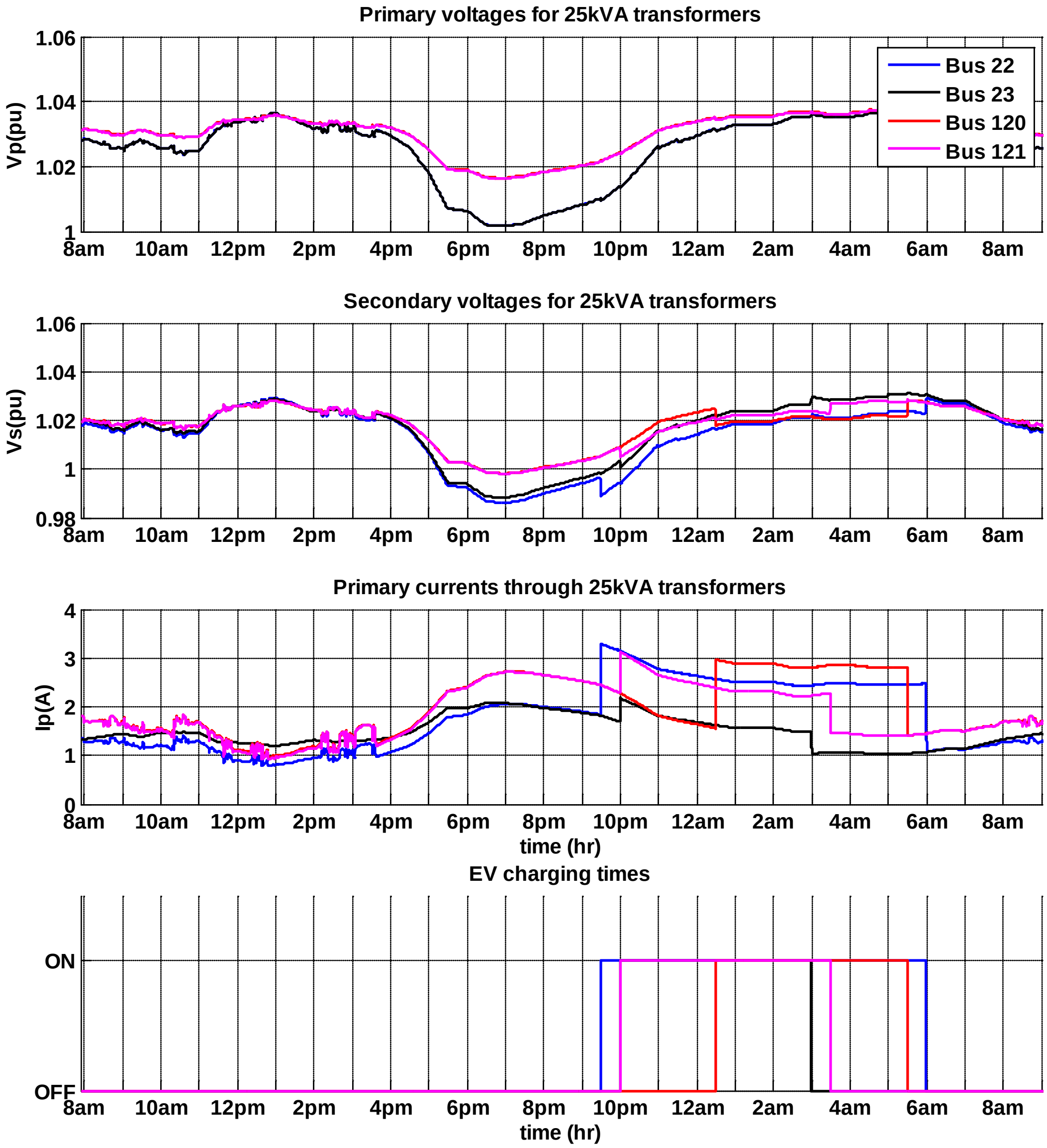

Figure 52 – Primary and Secondary Voltages and Current at 50 kVA transformers (Subsystem 1) (Controlled Charging)

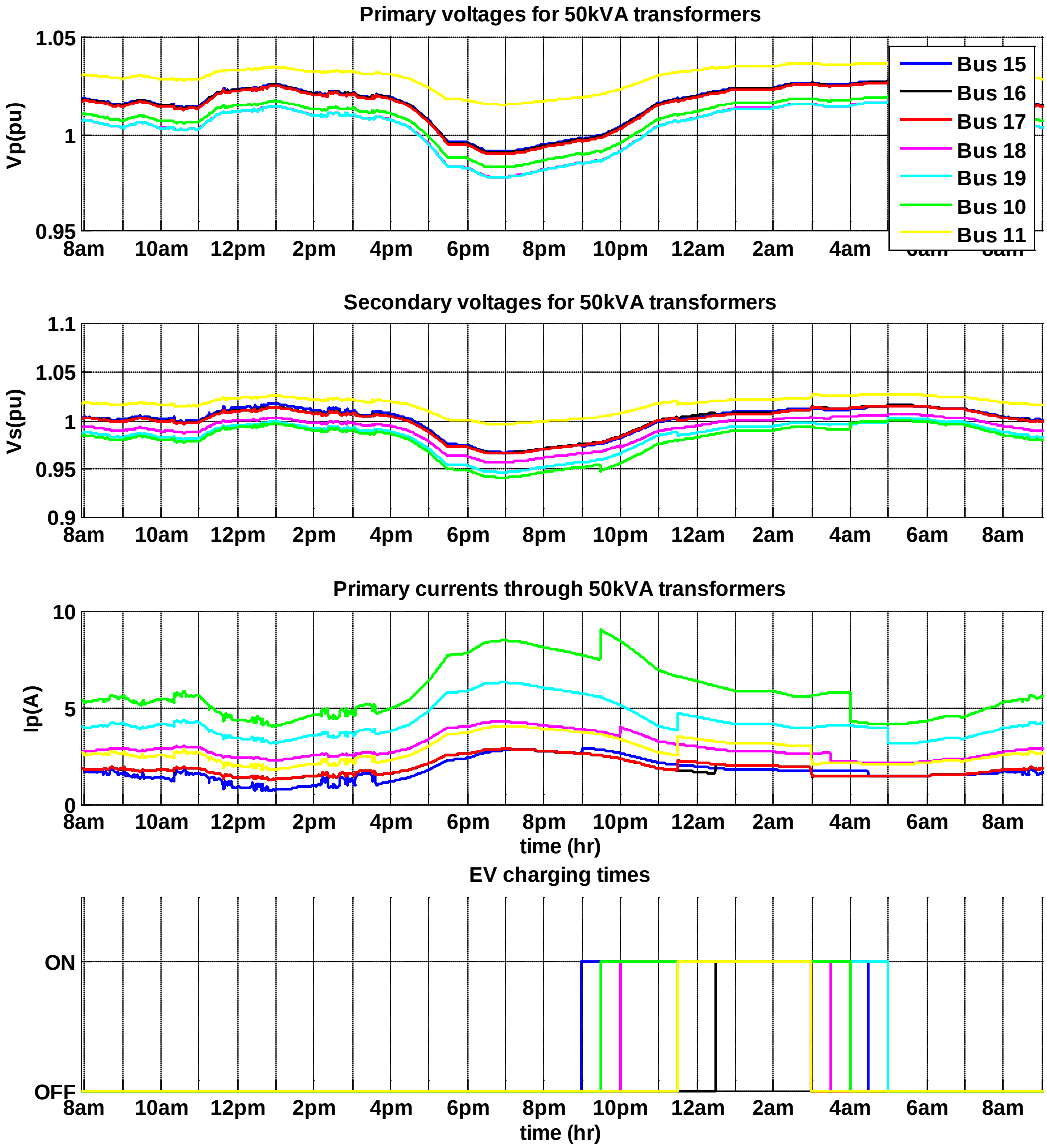

Figure 53 – Primary and Secondary Voltages and Current at 50 kVA Transformers (Subsystem 2) (Controlled Charging)

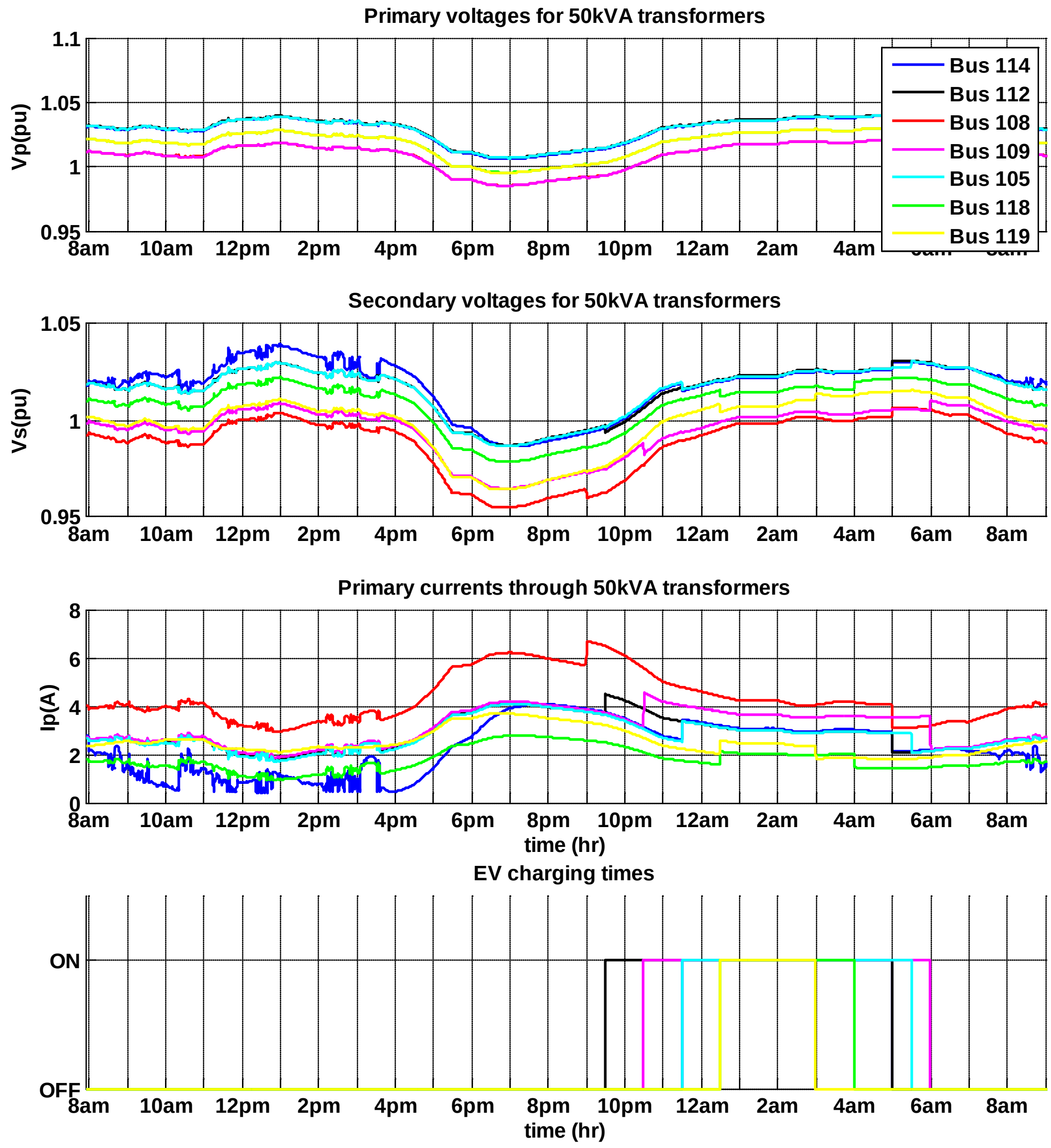

Figure 54 – Primary and Secondary Voltages and Current at 100 kVA Transformers (Controlled Charging)

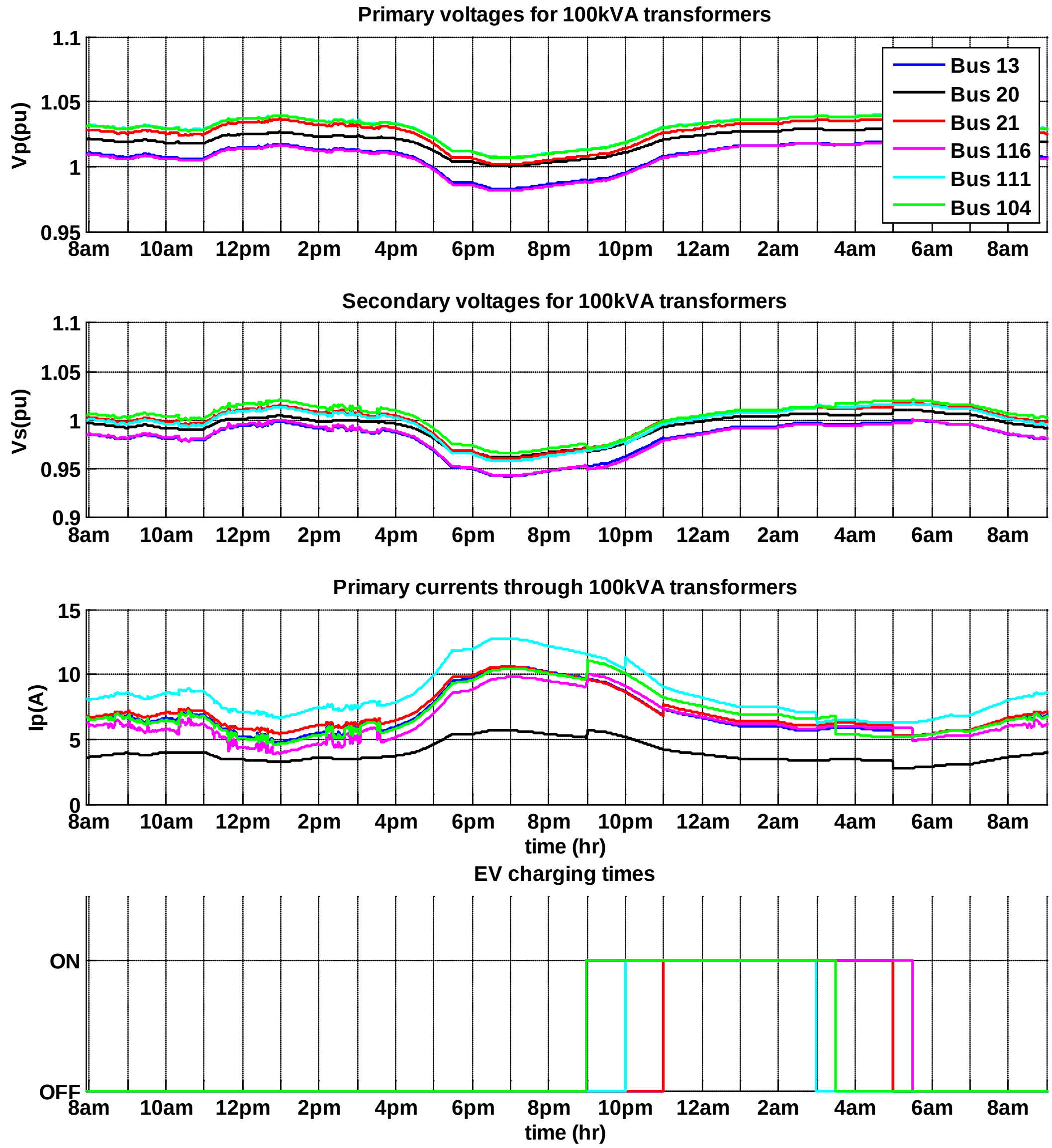

4.3.4 Online – Closed Loop Operation of PEV Simulator with Grid Simulator

This test verified operation of the closed loop and ability to communicate between the RTDS and the Power Hardware In the Loop (PHIL): Level 2 PEV Simulator and Grid Simulator. The schematic diagram of the test setup is shown in

Figure ***55***. Tests at different charging levels were performed to determine single level 2 PEV Simulator operation.

Figure 55 – RTDS Hardware In Loop Setup for Testing PEV Charging Impact

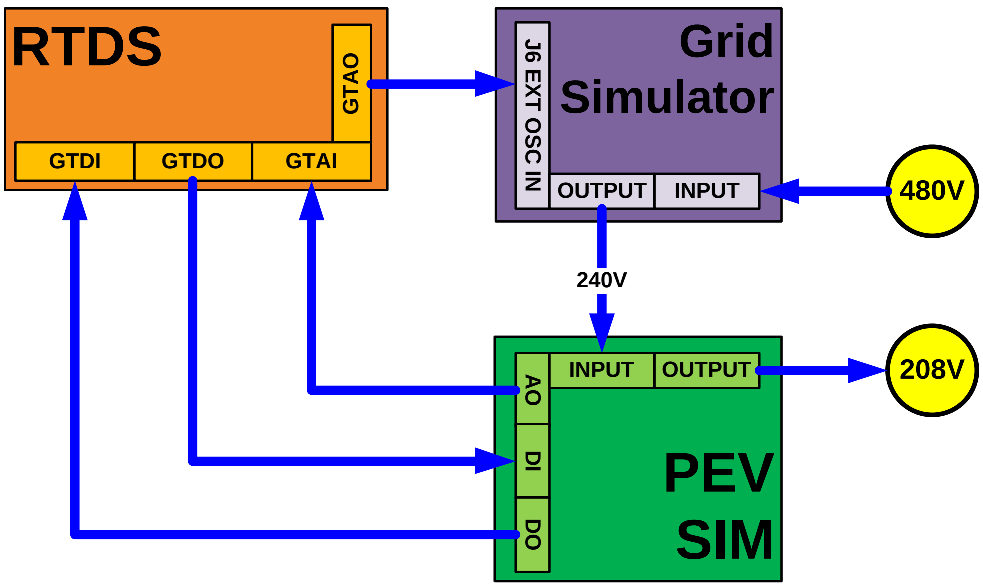

A 67 kVA grid simulator was used to amplify the secondary voltage measurement and feed into the PEV Simulator. The secondary voltage was provided by an RTDS analog card as a signal in the +/-10 V range and corresponded to the voltage at a selected service transformer from the simulated circuit under study. The grid simulator acted as a linear amplifier with a fixed gain to convert the low level signal to a 240 V range (variable) for the PEV Simulator. The effects of circuit voltage changes (e.g. due to load or local generation variations and/or capacitor switching transients) were reflected in the secondary measurements.

The PEV Simulator operated with the 240 V voltage from the grid simulator. Based on the selected charging level and charging profile, the charging current measurements from PEV Simulator were determined and fed back to the RTDS as low level signals. RTDS then used the feedback current and injected them into the system through the service transformer.

PEV charging profiles of 3.5 kW, 5.2 kW, 8.7 kW, and 9.6 kW were tested, representing different types of plug-in electric vehicles. The voltage and currents for a 9.6 kW PEV charging profile is shown in Figure 56 below to indicate the verification of the hardware in loop test setup.

Figure 56 – PEV Voltage (kV) and Current (kA, Scaled x10 for Comparison)

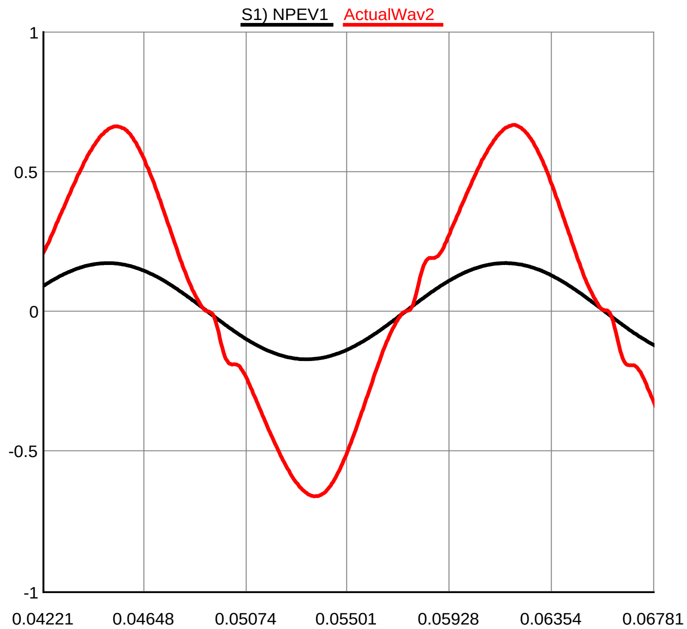

Similarly, the current injection into the service transformer as part of the model and input to RTDS are shown in Figure 57. A snapshot of the HMI screen for verification of the test case is also shown in Figure 58.

Figure 57 – Service Transformer Current (Red) and PEV Charging Current (Black) in kA

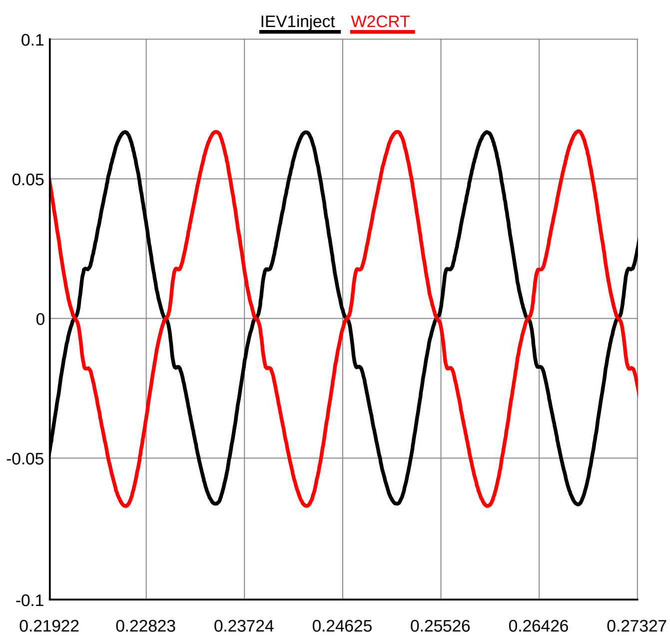

Figure 58 – RTDS Measurement of Currents (A) and Transformer Power (kW)

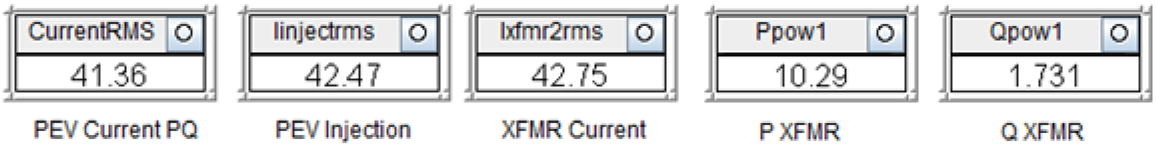

Figure 59 – Snapshot of the PEV HMI Screen for 9.6kW Charger

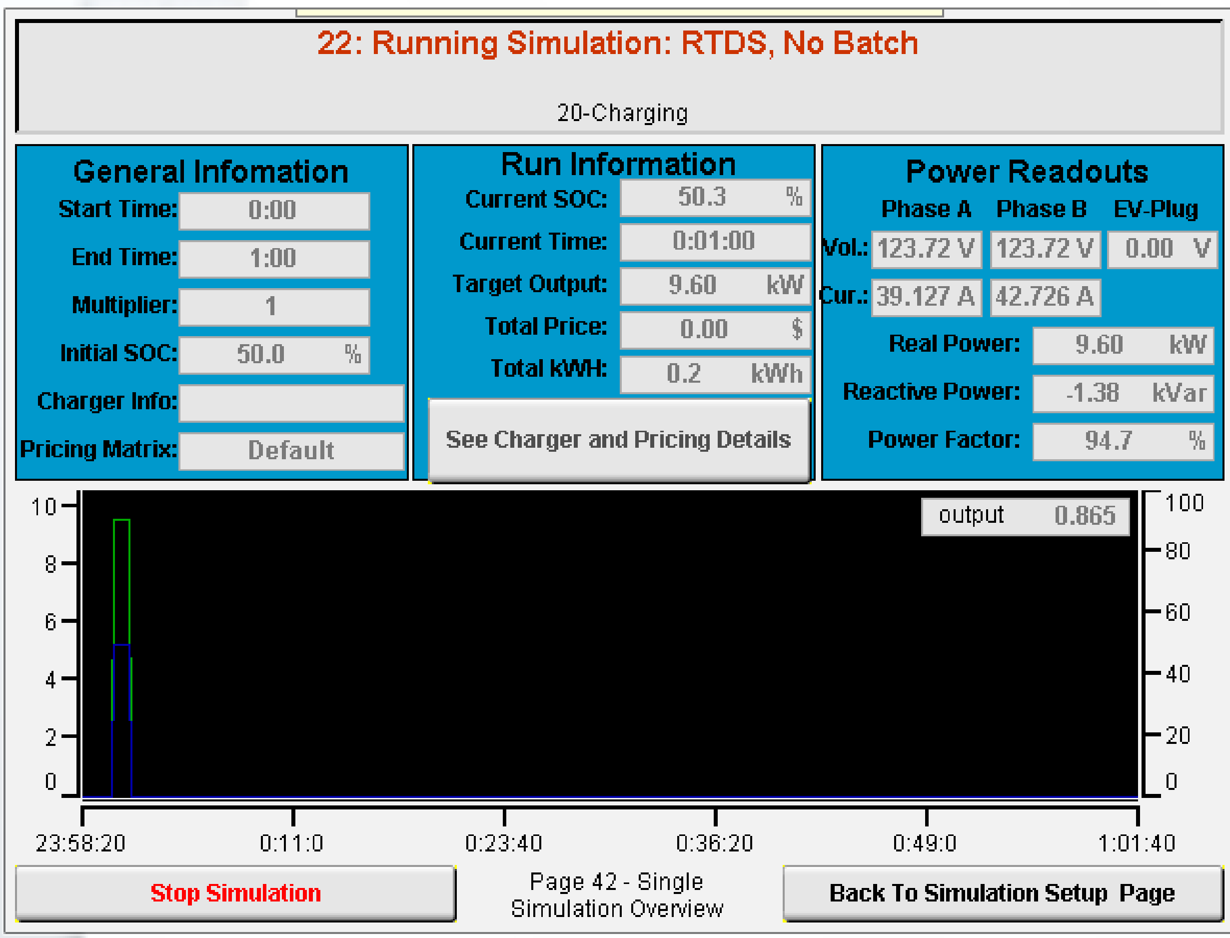

4.3.5 Online – Full System Test – All Customers Have EV (15 minutes real time)

This test covered a hypothetical scenario, where all transformers (excluding the three-phase loads on the first part of the system) had EV customers. The test was performed starting at 12:00pm. EV outputs were added at all (28) transformer secondaries. EV Set 1 (random distribution) defines the sizes and EVs are on for the entire 15 minute period. The details for EV size are given in Table 11, with the original 14 EV customers being shaded.

Table 11 – EV Size for All Potential Customers (28)

	Transformer Parameters			Load and PV			EV Size
Bus #	XFMR kVA		Connection	Total Load		Total PV	Set 1
	Rated	Actual		kW	kVAR	kW	kW
10	50.00	70.00	A	55.00	9.00	5.92	9.80
11	50.00	35.00	C	28.00	4.00	4.60	6.60
13	100.00	88.00	A	69.00	12.00	9.80	3.30
15	50.00	41.00	AB	55.00	10.00	12.70	3.30
16	50.00	41.00		56.00	9.00	5.00	5.80
17	50.00	41.00	AB	55.00	9.00	6.00	5.80
20	100.00	82.00	AC	235.00	41.00		6.60
21	100.00	89.00	B	70.00	12.00	4.70	5.80
22	25.00	16.00	B	14.00	3.00	3.30	9.80
23	25.00	18.00	B	14.00	2.00		3.30
18	50.00	35.00	A	28.00	5.00	1.50	3.30
19	50.00	32.00	A	41.00	7.00	3.30	5.80
113	50.00	35.00	C	28.00	5.00	27.50	6.60
114	50.00	36.00	B	29.00	6.00	5.00	5.80
116	100.00	82.00	A	137.00	24.00	13.20	6.60
111	100.00	108.00	B	84.00	14.00	4.60	5.80
112	50.00	35.00	B	28.00	5.00	4.70	5.80
107	50.00	52.00	A	41.00	7.00	5.20	5.80
108	50.00	52.00	A	41.00	7.00	4.90	6.60
109	50.00	35.00	A	28.00	5.00	4.30	9.80
104	100.00	89.00	B	70.00	12.00	10.90	9.80
105	50.00	35.00	B	28.00	5.00	5.20	5.80
106	25.00	17.00	B	14.00	2.00		9.80
118A	50.00	41.00	AB	55.00	10.00	9.50	6.60
118B	50.00	46.00	BC	260.00	10.00	9.50	9.80
119	50.00	53.00	AB	42.00	7.00		6.60
120	25.00	24.00	C	19.00	3.00	5.06	9.80
121	25.00	24.00	C	19.00	3.00	5.40	5.80

Voltages for the entire circuit for uncontrolled charging are shown in Figure 60. Transformer voltages and currents are shown in Figure 61 through Figure 64. Around noon time, PV production was strong. Due to reduction in load based on the given profile, voltage started to increase despite the presence of EV charging. The voltages showed about a 2% to 2.5% increase from the no EV condition. In a few locations, the voltage had passed 1.05 pu.

Figure 60 – Voltage at All Circuit Locations for Varying Load and PV Profile (12:00 pm Start)

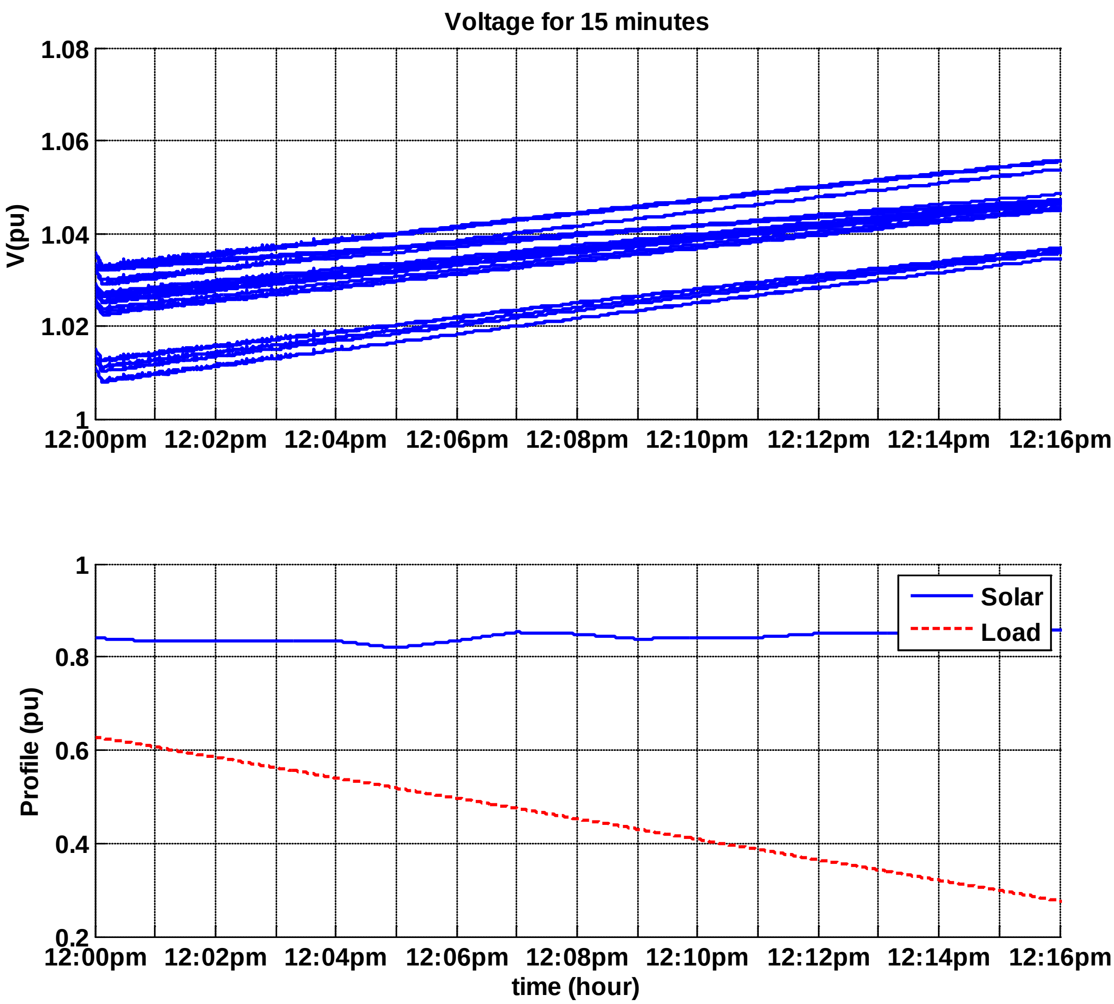

Figure 61 – Primary and Secondary Voltages and Current at 25 kVA Transformers (12:00 pm Start)

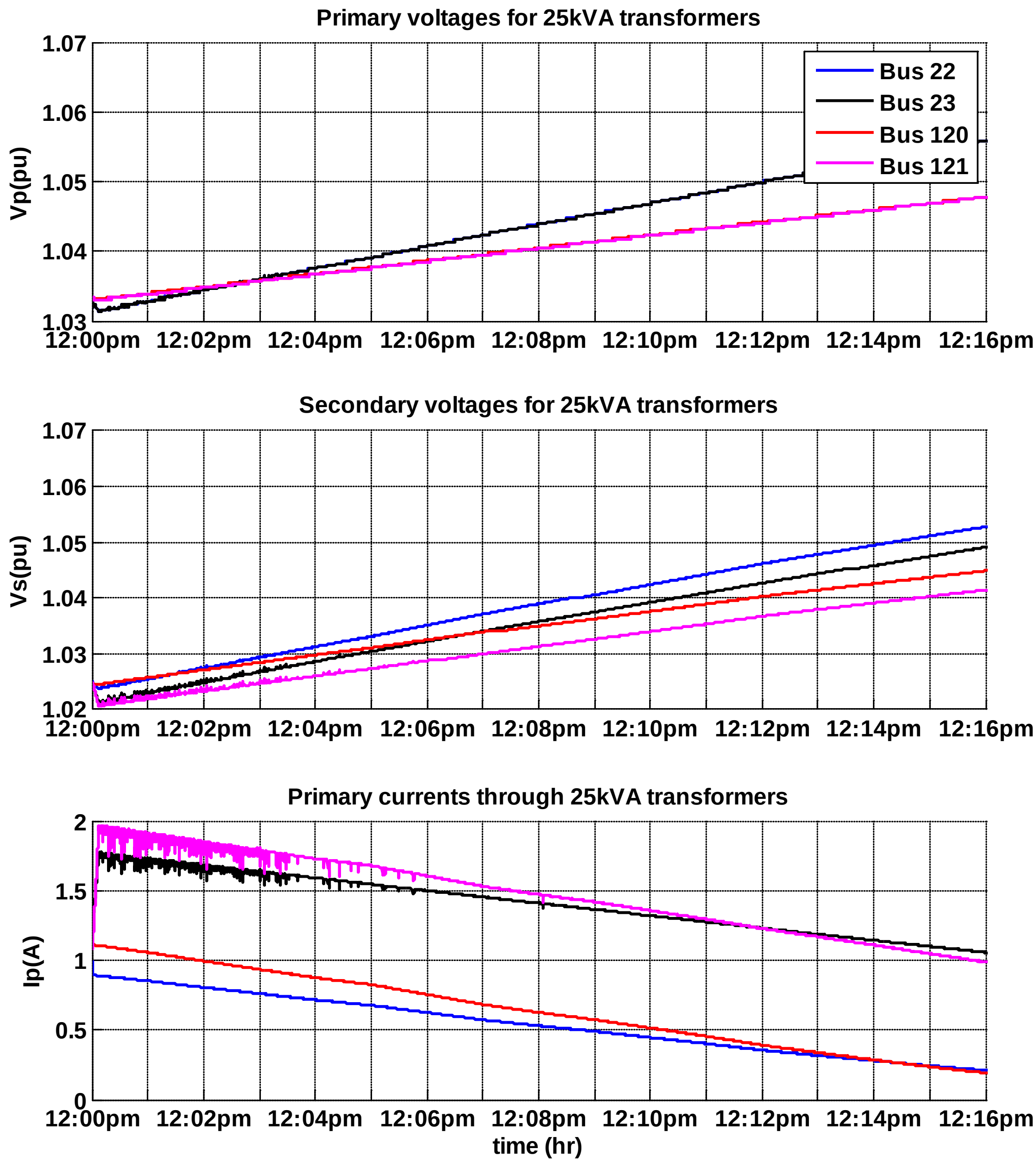

Figure 62 – Primary and Secondary Voltages and Current at 50 kVA Transformers (12:00 pm Start) Subsystem 1

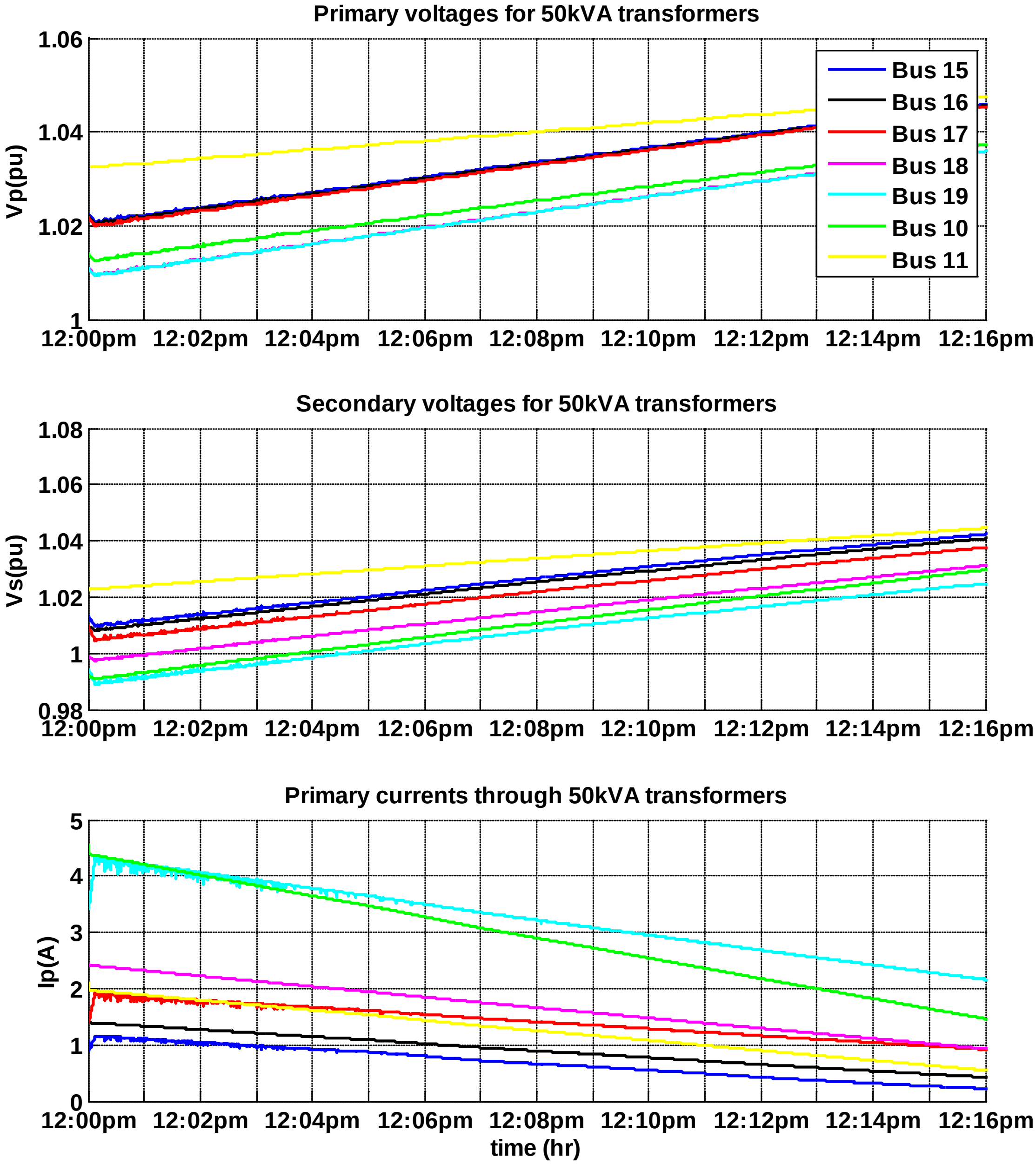

Figure 63 – Primary and Secondary Voltages and Current at 50 kVA Transformers (12:00 pm Start) Subsystem 2

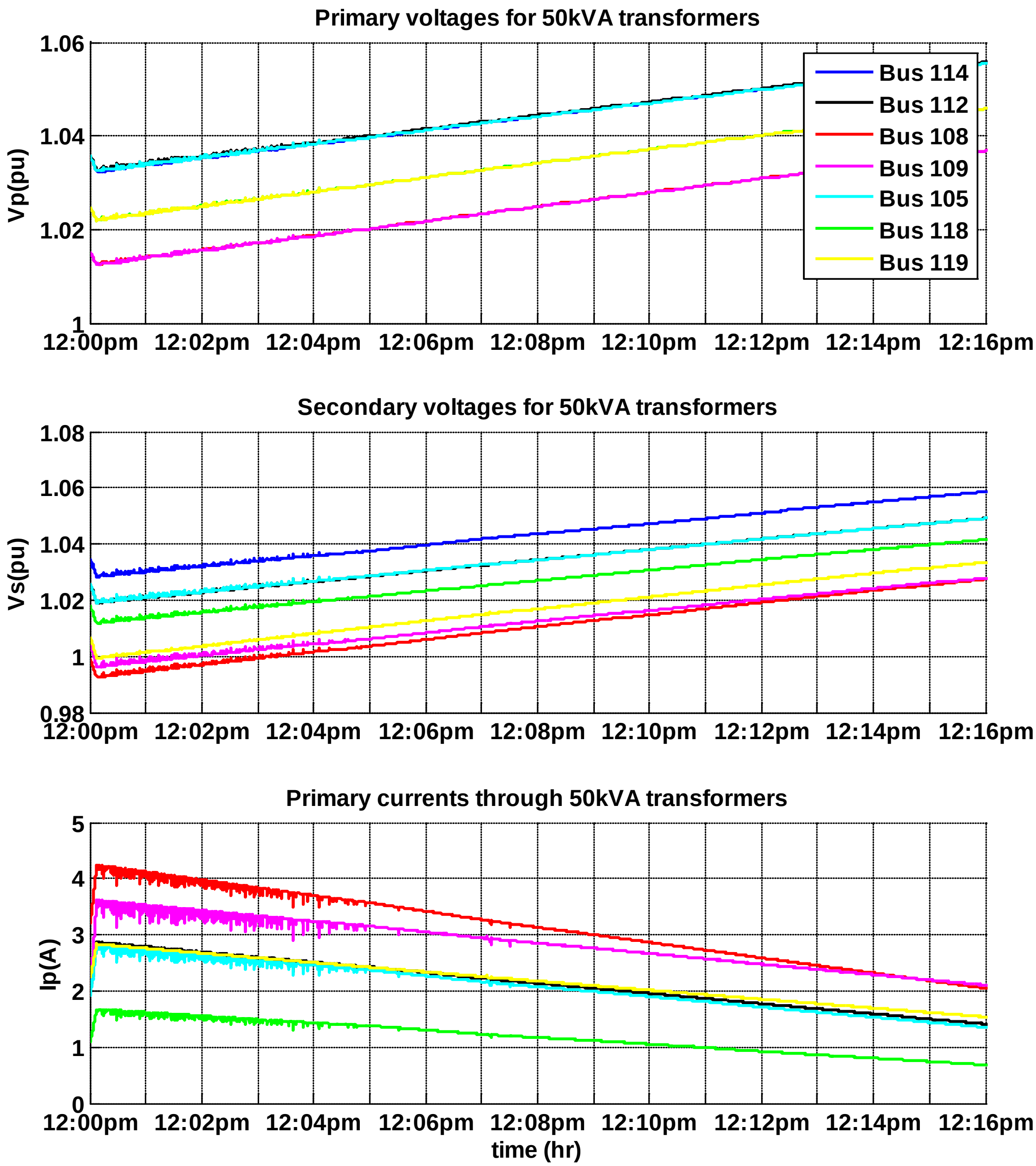

Figure 64 – Primary and Secondary Voltages and Current at 100 kVA Transformers (12:00 pm Start)

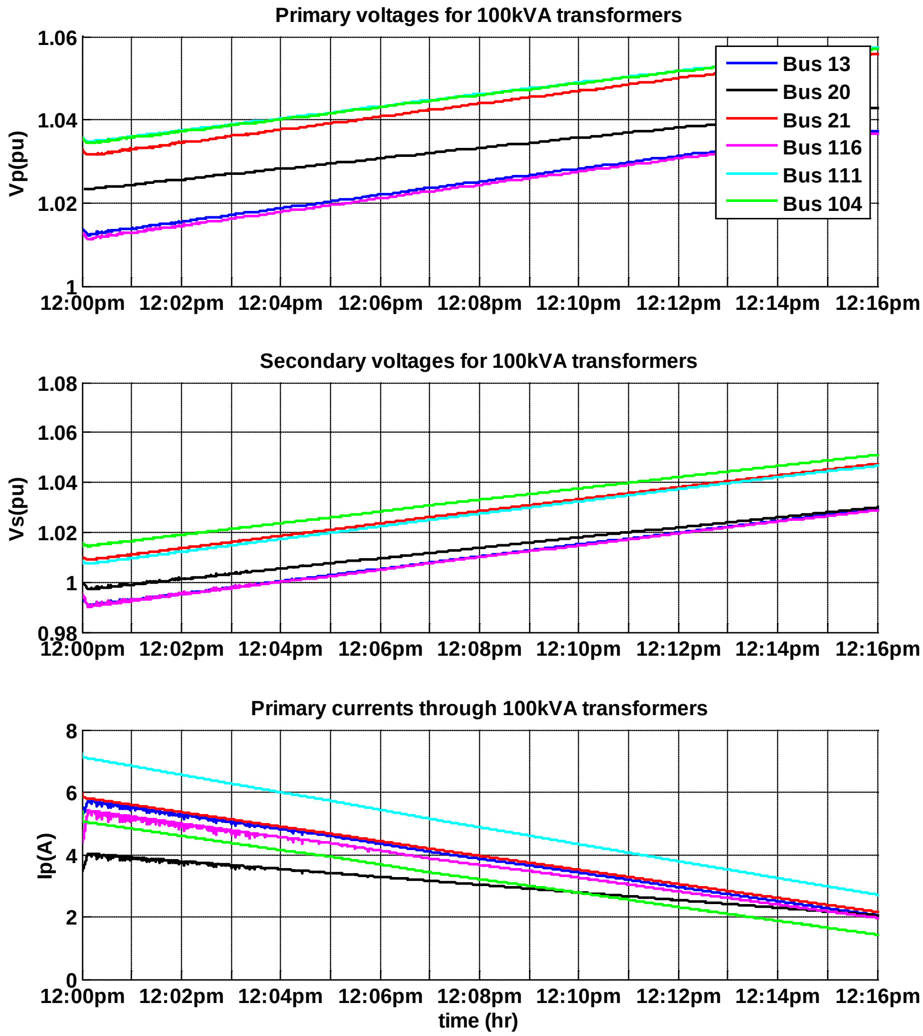

4.3.6 Online – Full System Test – All Customers Have EV (24 hours accelerated time)

In this test, EV outputs were added to all customer locations (transformer secondary circuits). EV sizes and charging times were randomly assigned according the following sizes and times:

- **EV Set 1:** Random distribution of 3.3 kW, 5.8 kW, 6.6 kW, 9.8 kW EV sizes
- **EV Set 2:** 4x 3.5 kV, 8x 6.8 kV, 2x 9.8 kV
- **Always On**: EV was charged from 16:00 (4:00pm) through to 4:00 (4:00am) the next morning
- **Uncontrolled Charging:** 4:00 pm – 6:00 pm starting times, 10:00 pm – 4:00 am end times

The details for both EV size sets and uncontrolled charging times are given in Table 12, with the original 14 EV customers being shaded.

Table 12 – EV size and charging times parameters for all customers

	Transformer Parameters			Load and PV			EV Size		EV Charging Time	
Bus #	XFMR kVA		Connection	Total Load		Total PV	Set 1	Set 2	Uncontrolled Charging	
	Rated	Actual		kW	kVAR	kW	kW	kW	Start	End
10	50	70	A	55	9	5.9	9.8	3.5	17:00	01:30
11	50	35	C	28	4	4.6	6.6	6.8	17:00	00:30
13	100	88	A	69	12	9.8	3.3	3.5	16:30	22:30
15	50	41	AB	55	10	12.7	3.3	6.8	16:00	00:30
16	50	41		56	9	5.0	5.8	9.8	17:00	01:00
17	50	41	AB	55	9	6.0	5.8	3.5	16:30	23:30
20	100	82	AC	235	41		6.6	6.8	18:00	01:00
21	100	89	B	70	12	4.7	5.8	6.8	16:30	03:00
22	25	16	B	14	3	3.3	9.8	3.5	16:30	03:00
23	25	18	B	14	2		3.3	6.8	17:00	22:30
18	50	35	A	28	5	1.5	3.3	6.8	16:00	22:00
19	50	32	A	41	7	3.3	5.8	9.8	16:30	23:30
113	50	35	C	28	5	27.5	6.6	6.8	16:00	02:00
114	50	36	B	29	6	5.0	5.8	6.8	16:30	01:30
116	100	82	A	137	24	13.2	6.6	3.5	17:30	23:30
111	100	108	B	84	14	4.6	5.8	6.8	16:00	23:00
112	50	35	B	28	5	4.7	5.8	6.8	17:30	02:30
107	50	52	A	41	7	5.2	5.8	3.5	17:30	00:00
108	50	52	A	41	7	4.9	6.6	6.8	18:00	03:00
109	50	35	A	28	5	4.3	9.8	6.8	17:30	22:30
104	100	89	B	70	12	10.9	9.8	9.8	17:00	02:30
105	50	35	B	28	5	5.2	5.8	3.5	18:00	23:30
106	25	17	B	14	2		9.8	9.8	17:00	00:30
118A	50	41	AB	55	10	9.5	6.6	6.8	18:00	01:30
118B	50	46	BC	260	10	9.5	9.8	6.8	16:30	02:00
119	50	53	AB	42	7		6.6	3.5	17:30	04:00
120	25	24	C	19	3	5.1	9.8	6.8	17:30	00:30
121	25	24	C	19	3	5.4	5.8	6.8	16:00	02:30

4.3.6.1 EV Profile Set 1, EV Always On

Voltages for the entire circuit are shown in Figure 65. Transformer voltages and currents are shown in Figure 66 through Figure 69. It was observed that EV charging had a large effect on primary transformer current flow, causing the secondary transformer voltage minor drop. EV charging had less effect on the circuit voltage.

Figure 65 – Voltage at All Circuit Locations for Varying Load and PV Profile (EV Set 1, Always On)

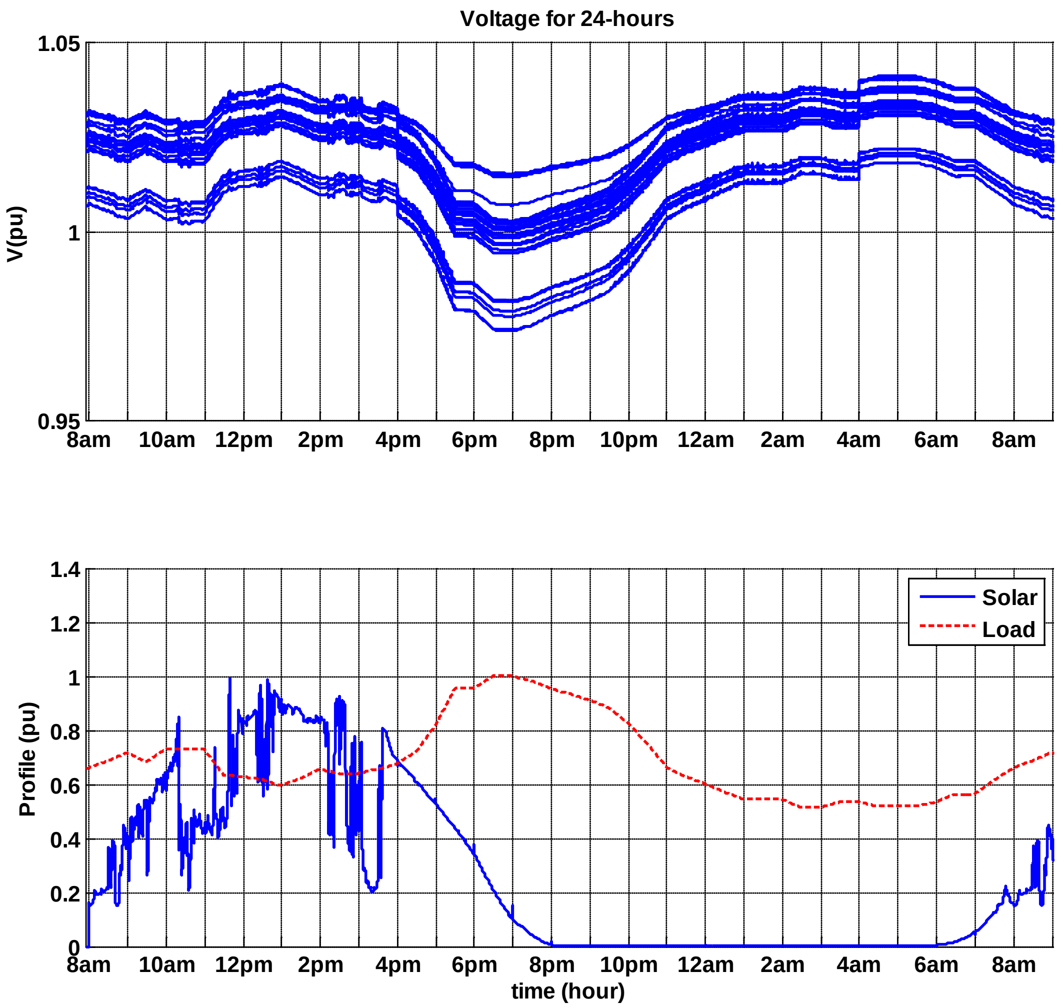

Figure 66 – Primary and Secondary Voltages and Current at 25 kVA Transformers (EV Set 1, Always On)

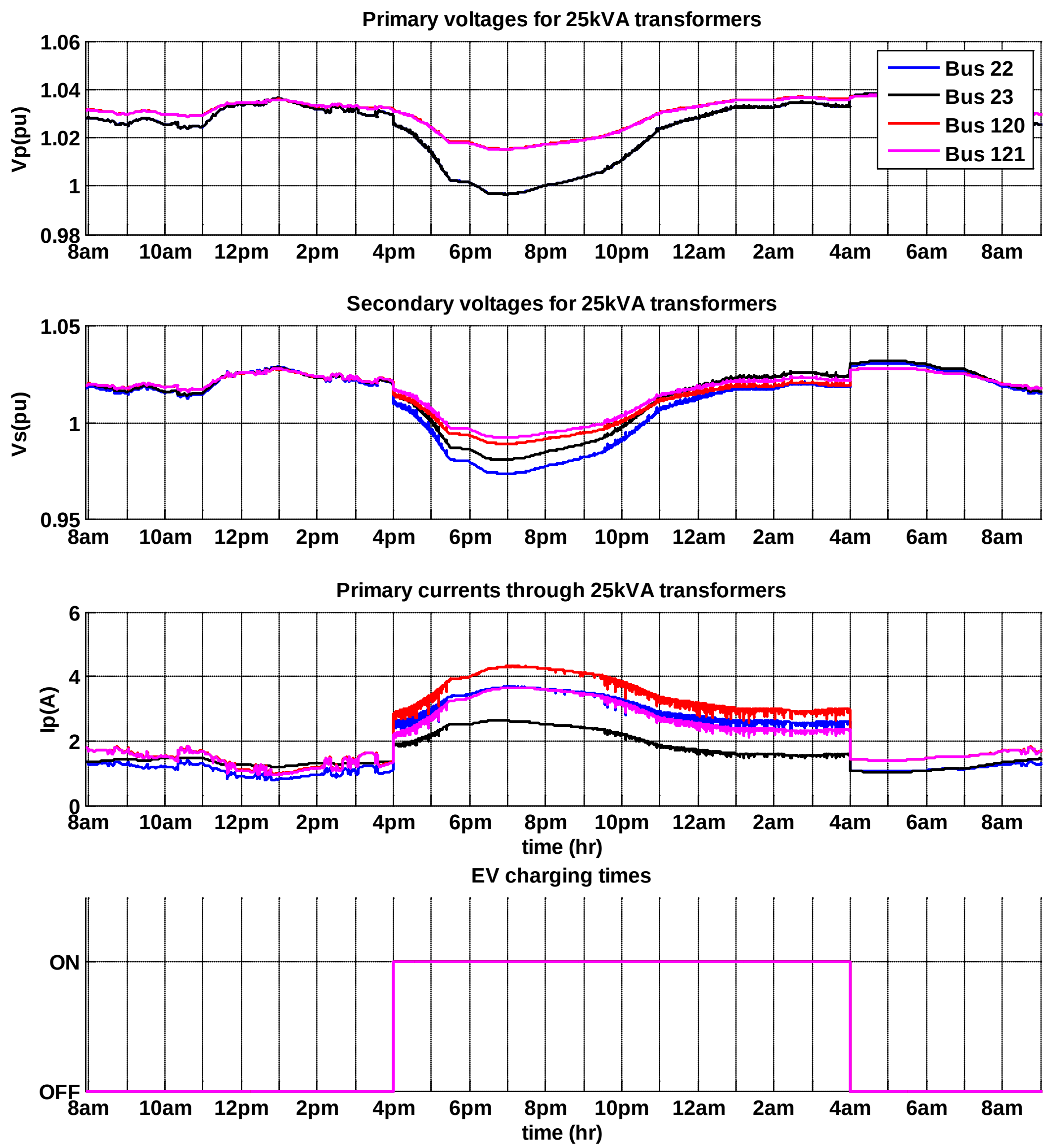

Figure 67 – Primary and Secondary Voltages and Current at 50 kVA Transformers – Subsystem 1 (EV Set 1, Always On)

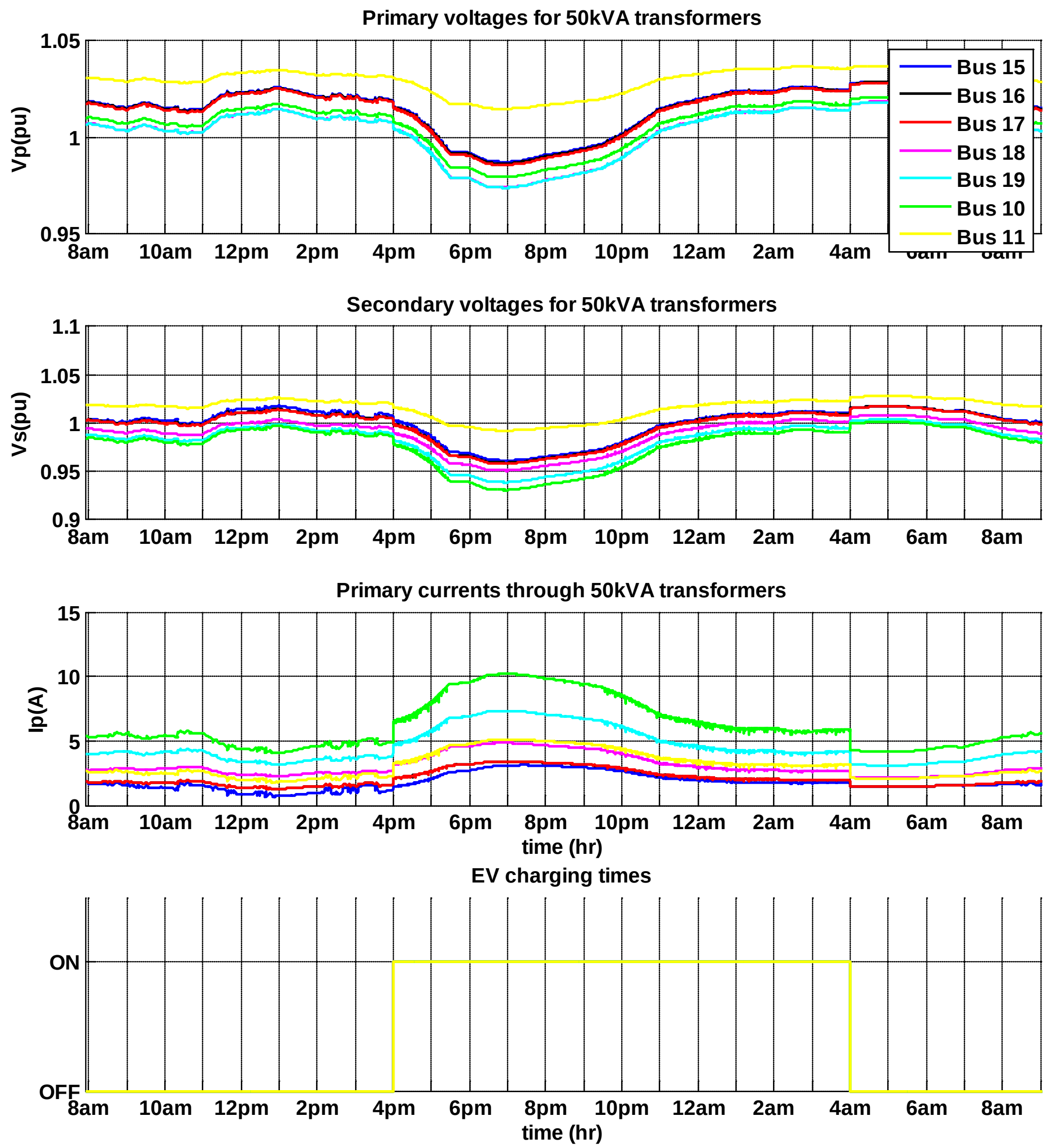

Figure 68 – Primary and Secondary Voltages and Current at 50 kVA Transformers – Subsystem 2 (EV Set 1, Always On)

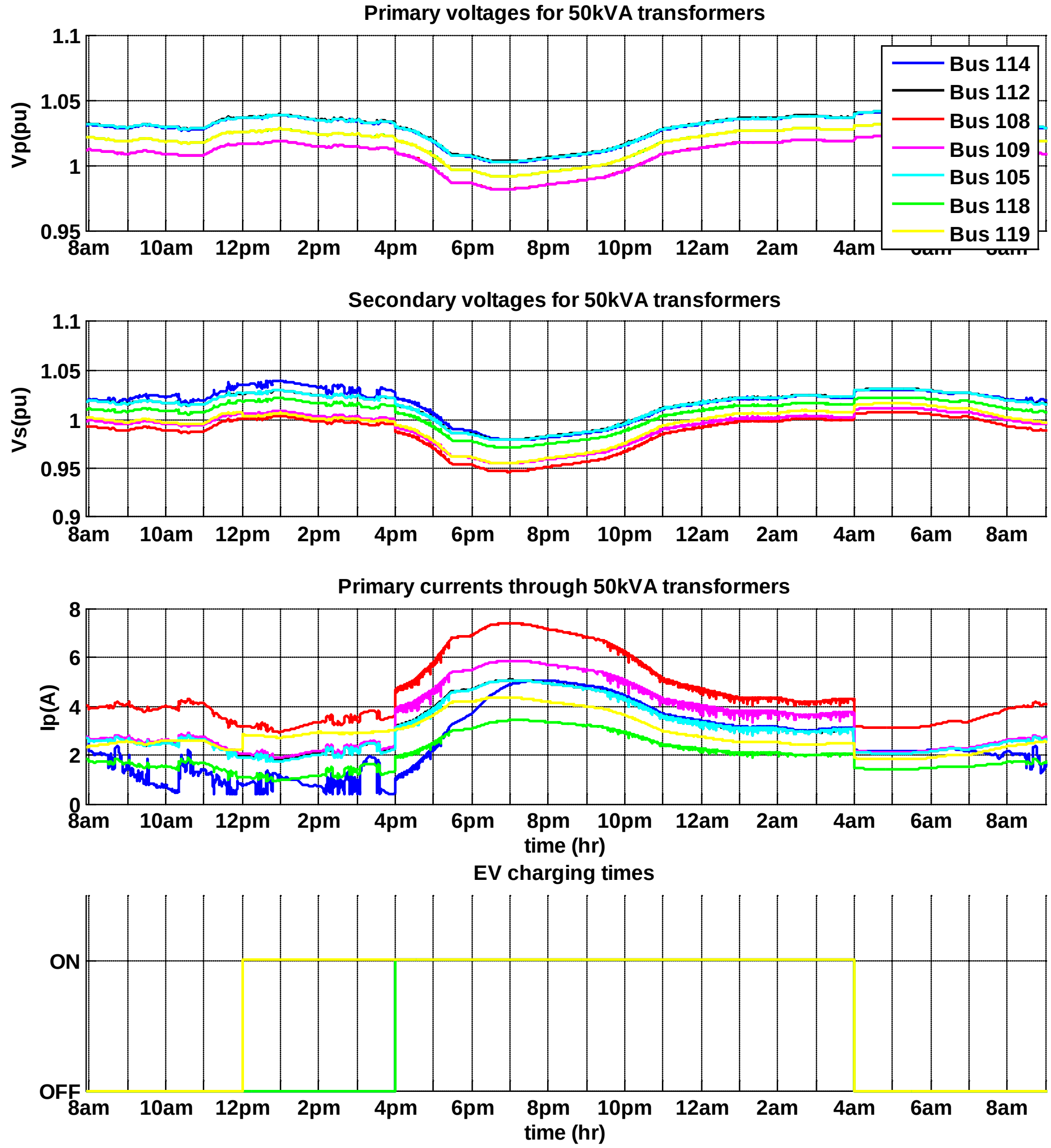

Figure 69 – Primary and Secondary Voltages and Current at 100 kVA Transformers (EV Set 1, Always On)

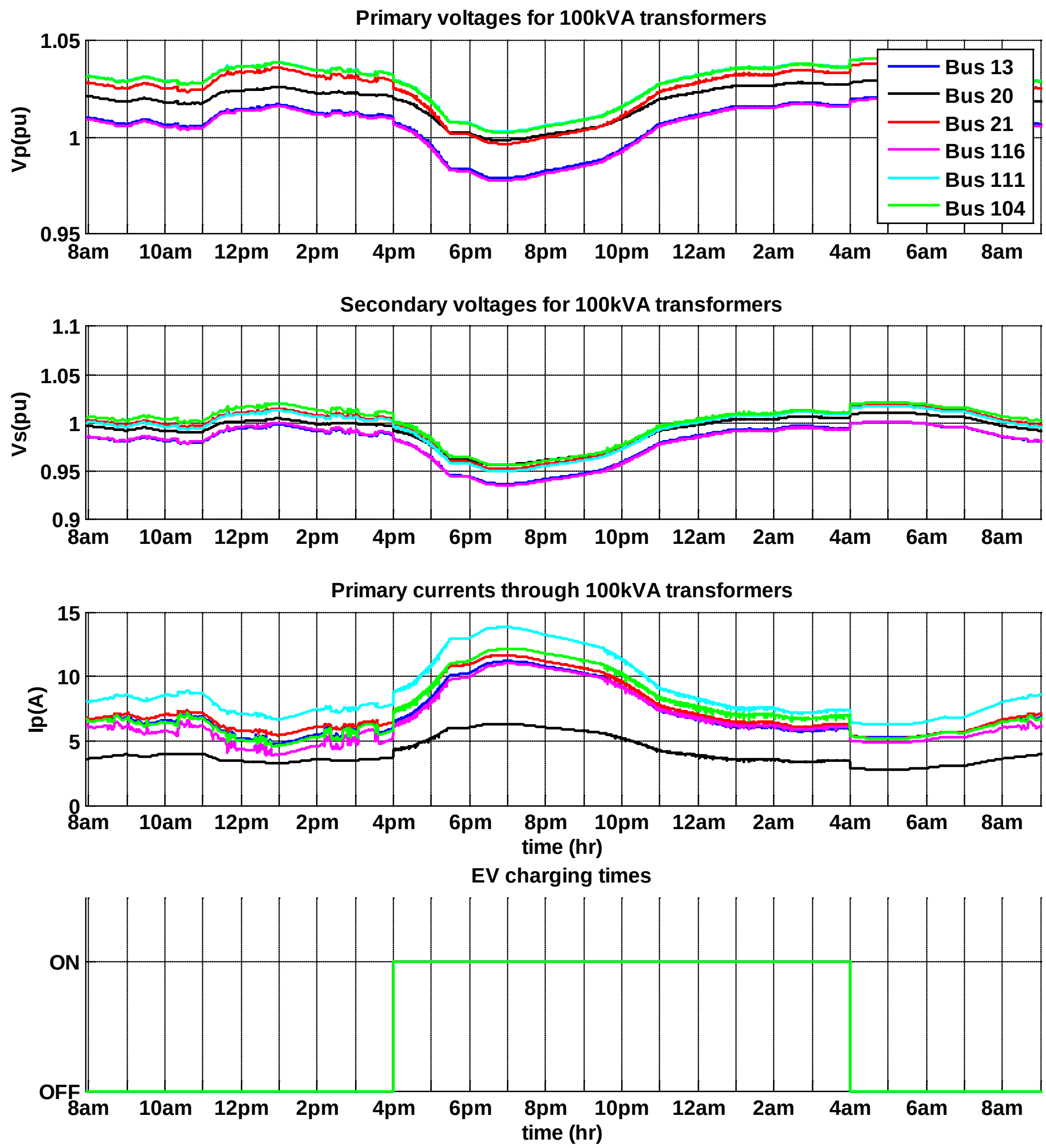

4.3.6.2 EV Profile Set 2, EV Always On

Voltages for the entire circuit are shown in Figure 70. Transformer voltages and currents are shown in Figure 71 through Figure 74. It was observed that EV charging had a large effect on primary transformer current flow, but only a minor effect on the secondary transformer voltage. EV charging had less effect on the primary circuit voltage.

Figure 70 – Voltage at All Circuit Locations for Varying Load and PV Profile (EV Set 2, Always On)

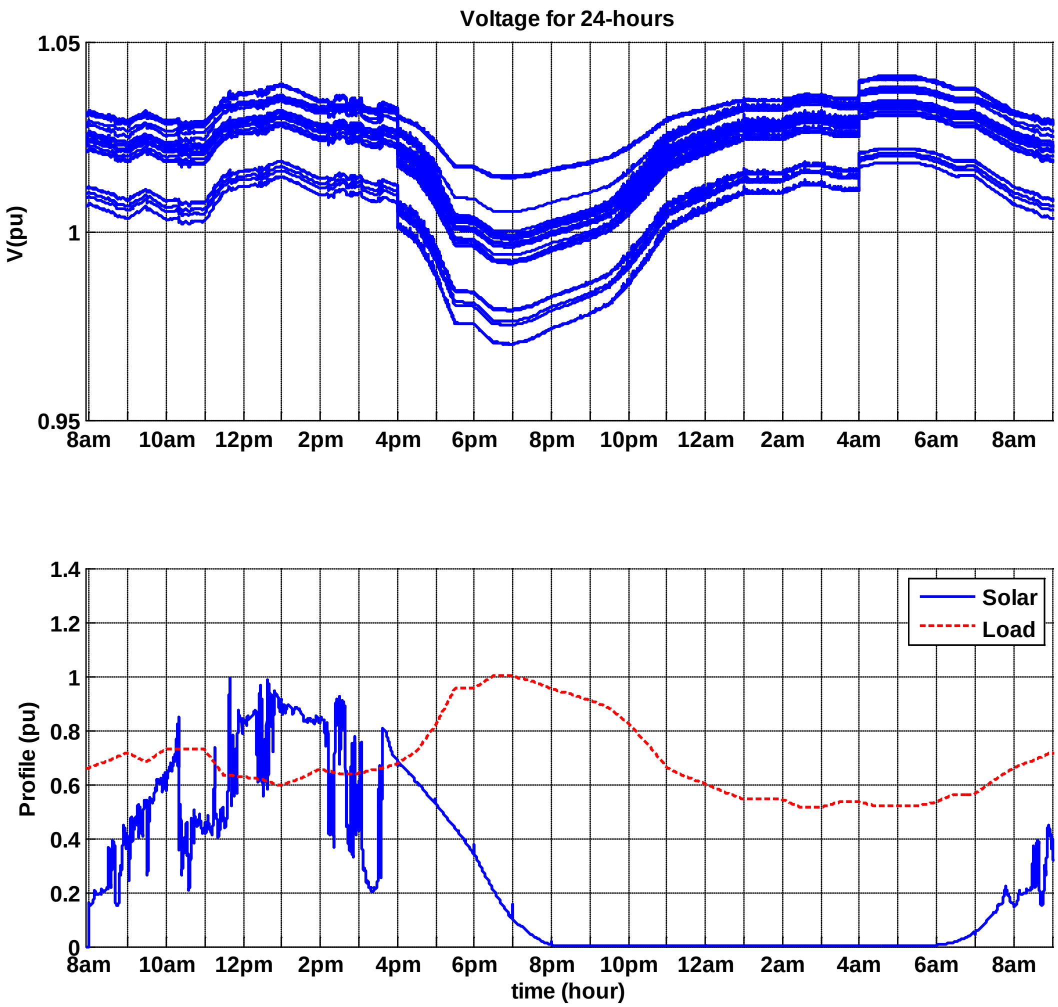

Figure 71 – Primary and Secondary Voltages and Current at 25 kVA Transformers (EV Set 2, Always on)

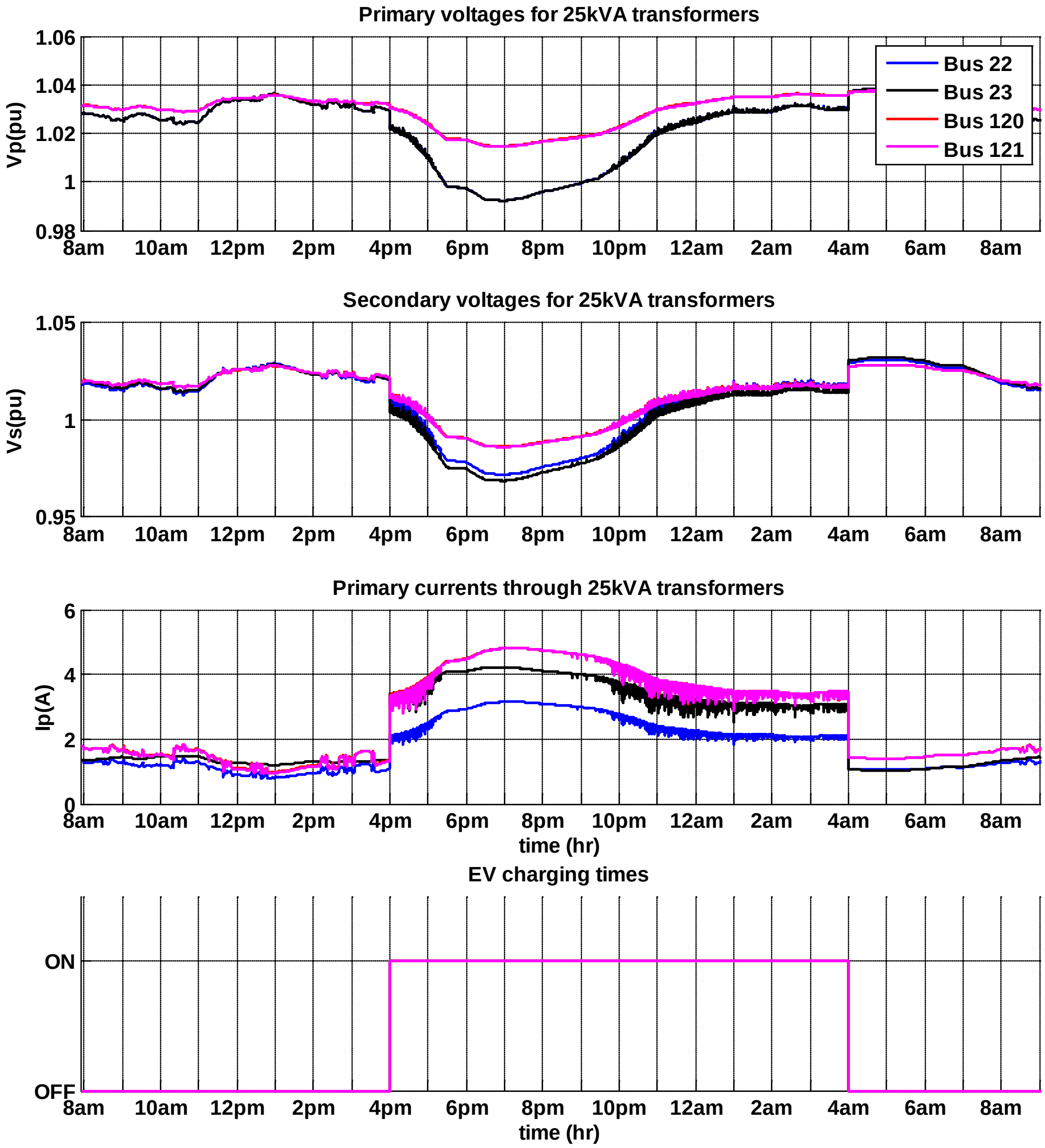

Figure 72 – Primary and Secondary Voltages and Current at 50 kVA Transformers – Subsystem 1 (EV Set 2, Always on)

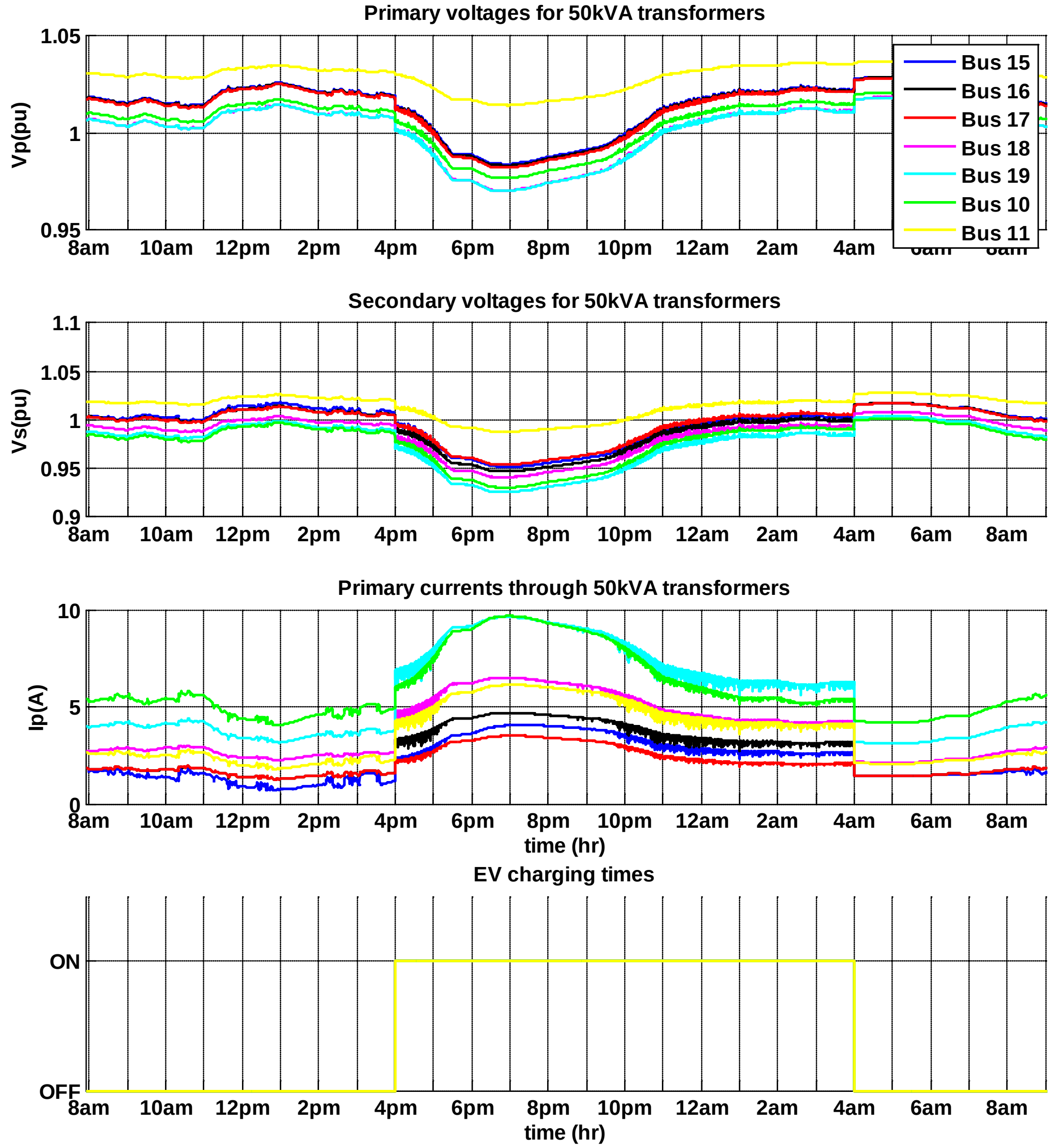

Figure 73 – Primary and Secondary Voltages and Current at 50 kVA Transformers – Subsystem 2 (EV Set 2, Always on)

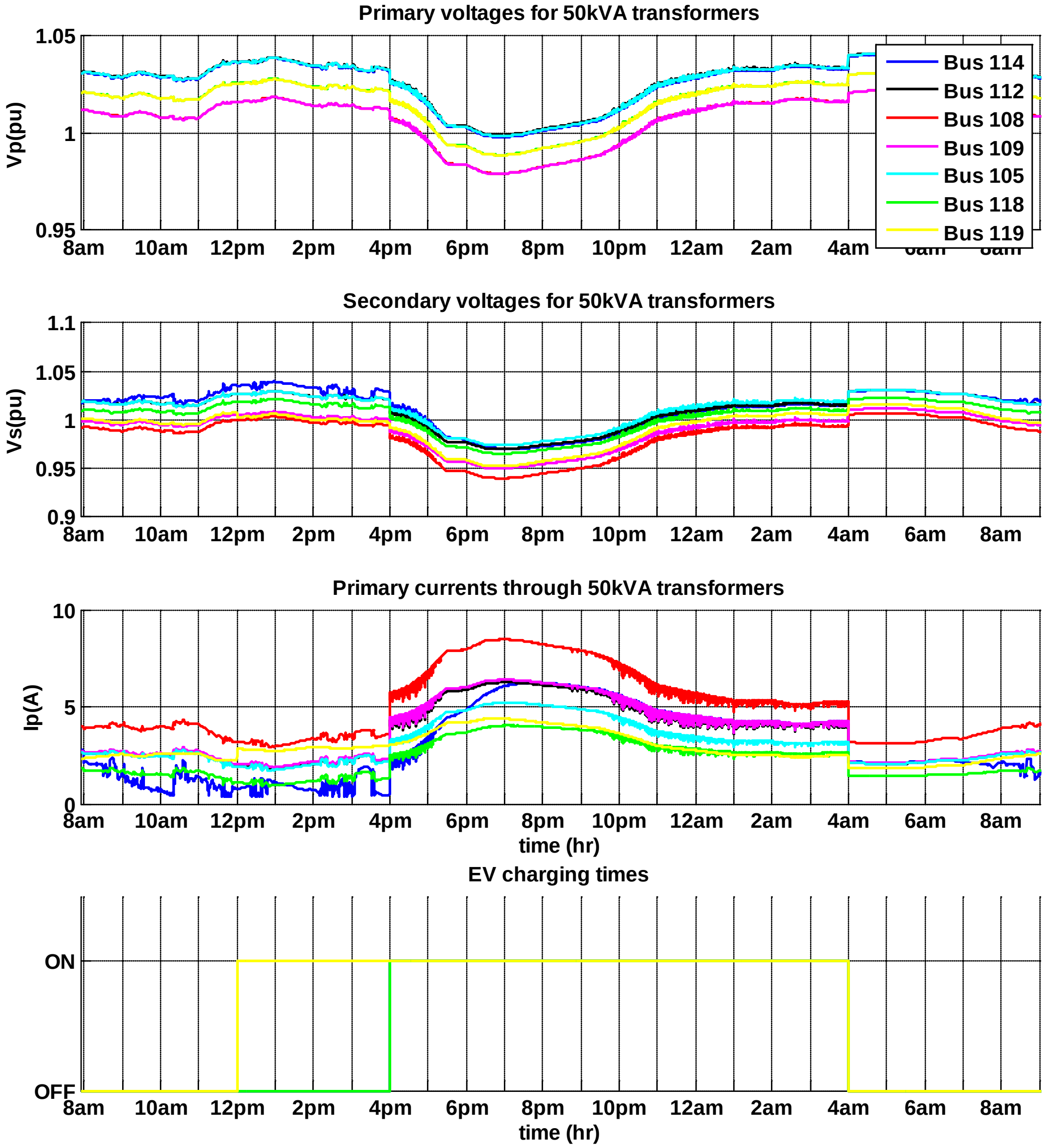

Figure 74 – Primary and Secondary Voltages and Current at 100 kVA transformers (EV Set 2, Always on)

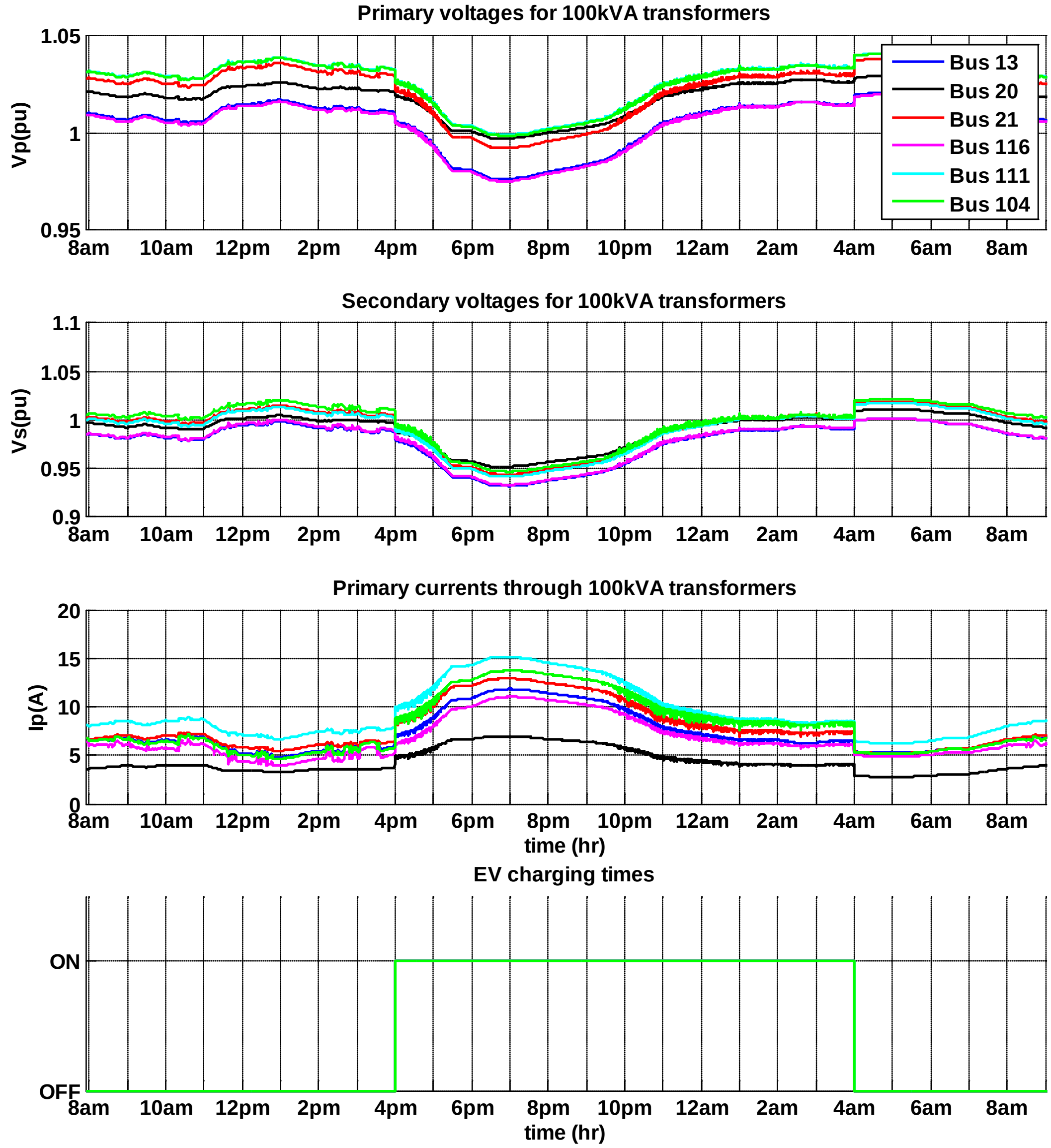

4.3.6.3 EV Profile Set 1, Uncontrolled Charging

Voltages for the entire circuit are shown in Figure 75. Transformer voltages and currents are shown in Figure 76 through Figure 79. It was observed that EV charging had a large effect on primary transformer current flow, but only a minor effect on the secondary transformer voltage. EV charging had less effect on the primary circuit voltages.

Figure 75 – Voltage at All Circuit Locations for Varying Load and PV Profile (EV Set 1, Uncontrolled Charging)

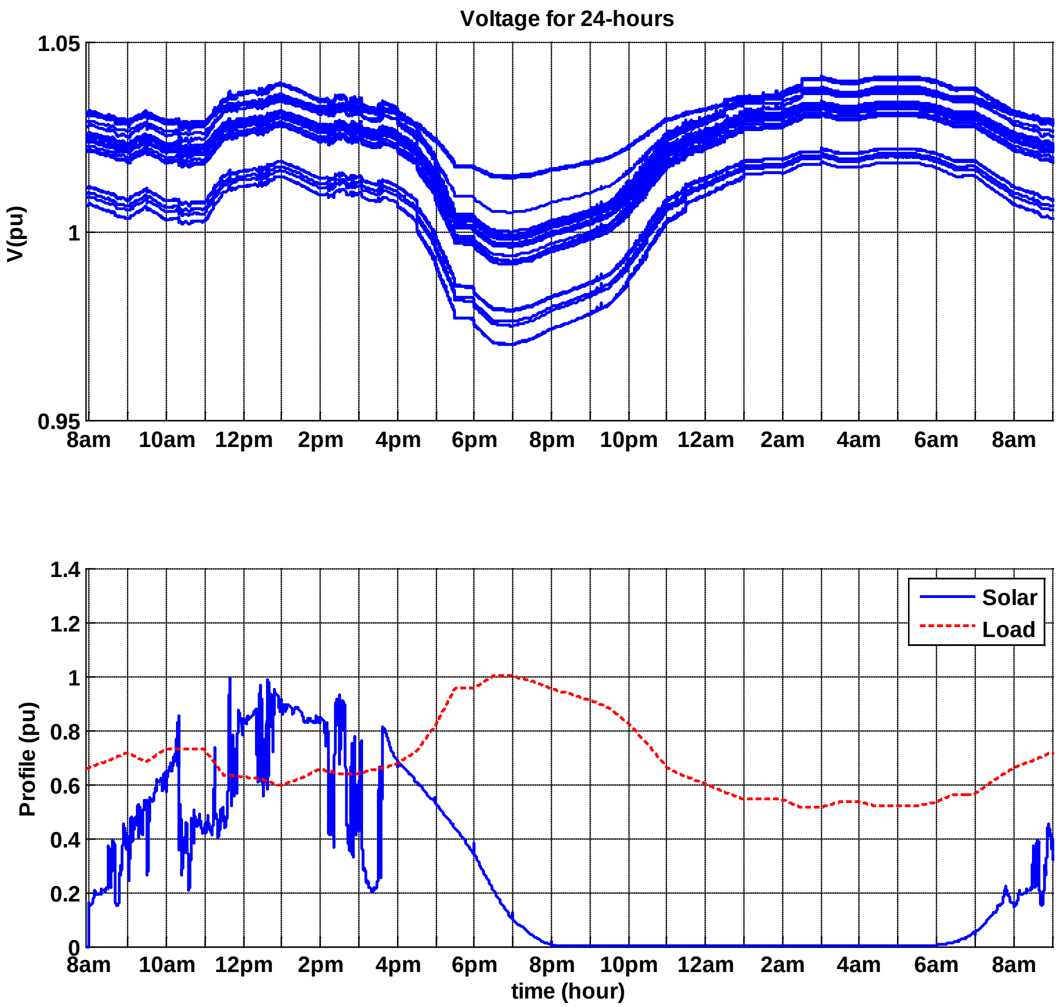

Figure 76 – Primary and Secondary Voltages and Current at 25 kVA Transformers (EV Set 1, Uncontrolled Charging)

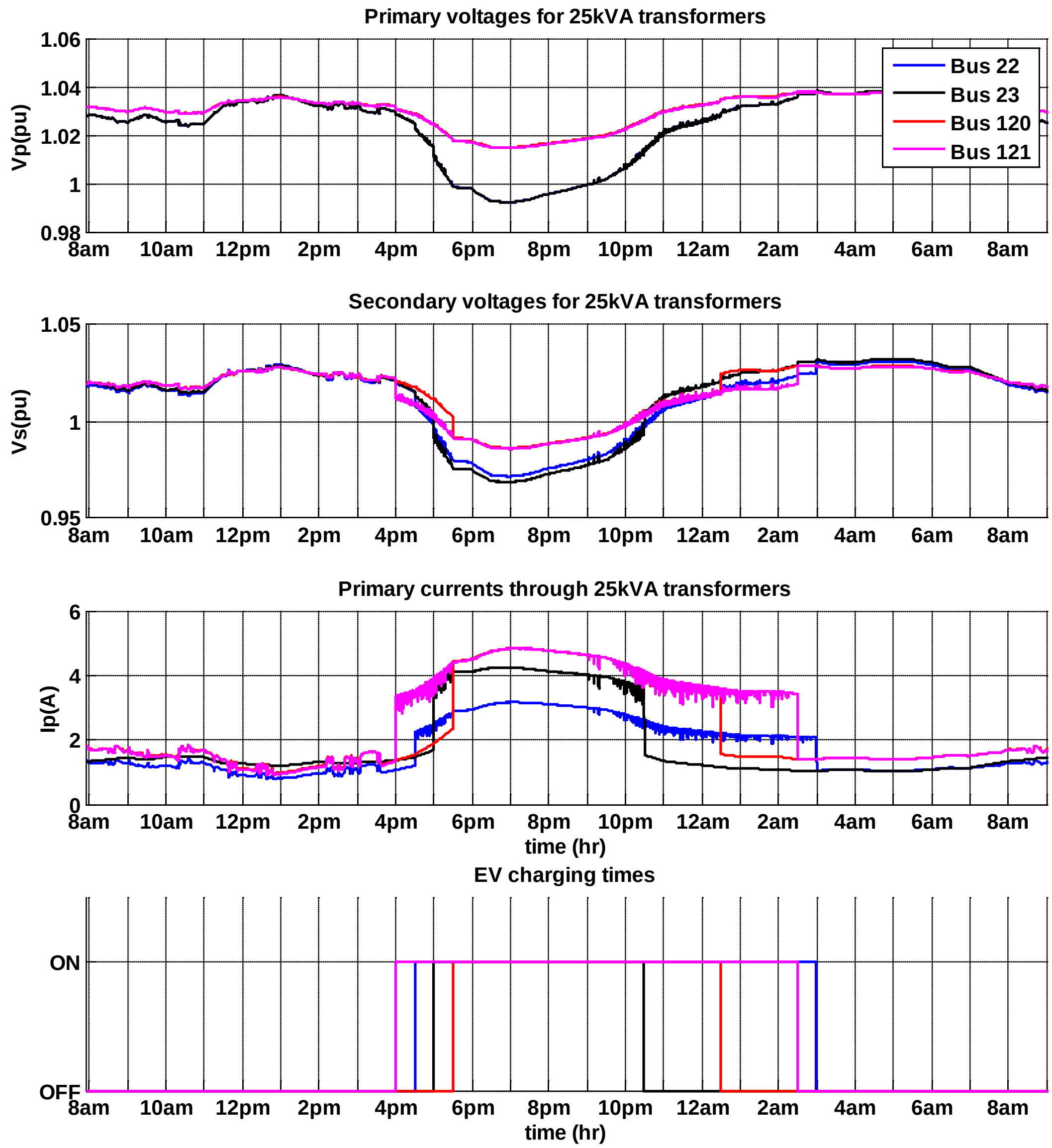

Figure 77 – Primary and Secondary Voltages and Current at 50 kVA Transformers – Subsystem 1 (EV Set 1, Uncontrolled Charging)

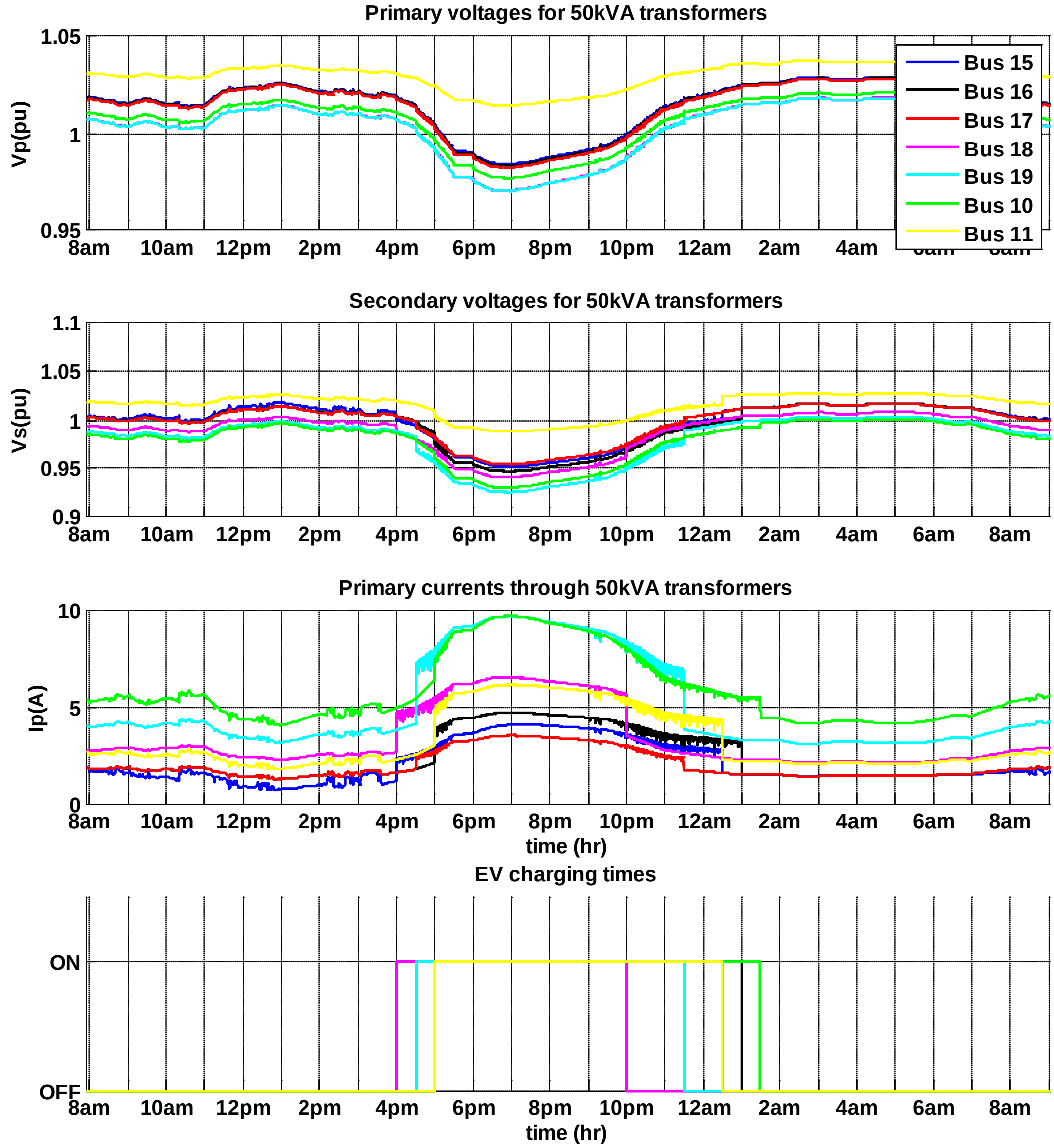

Figure 78 – Primary and Secondary Voltages and Current at 50 kVA Transformers – Subsystem 2 (EV Set 1, Uncontrolled Charging)

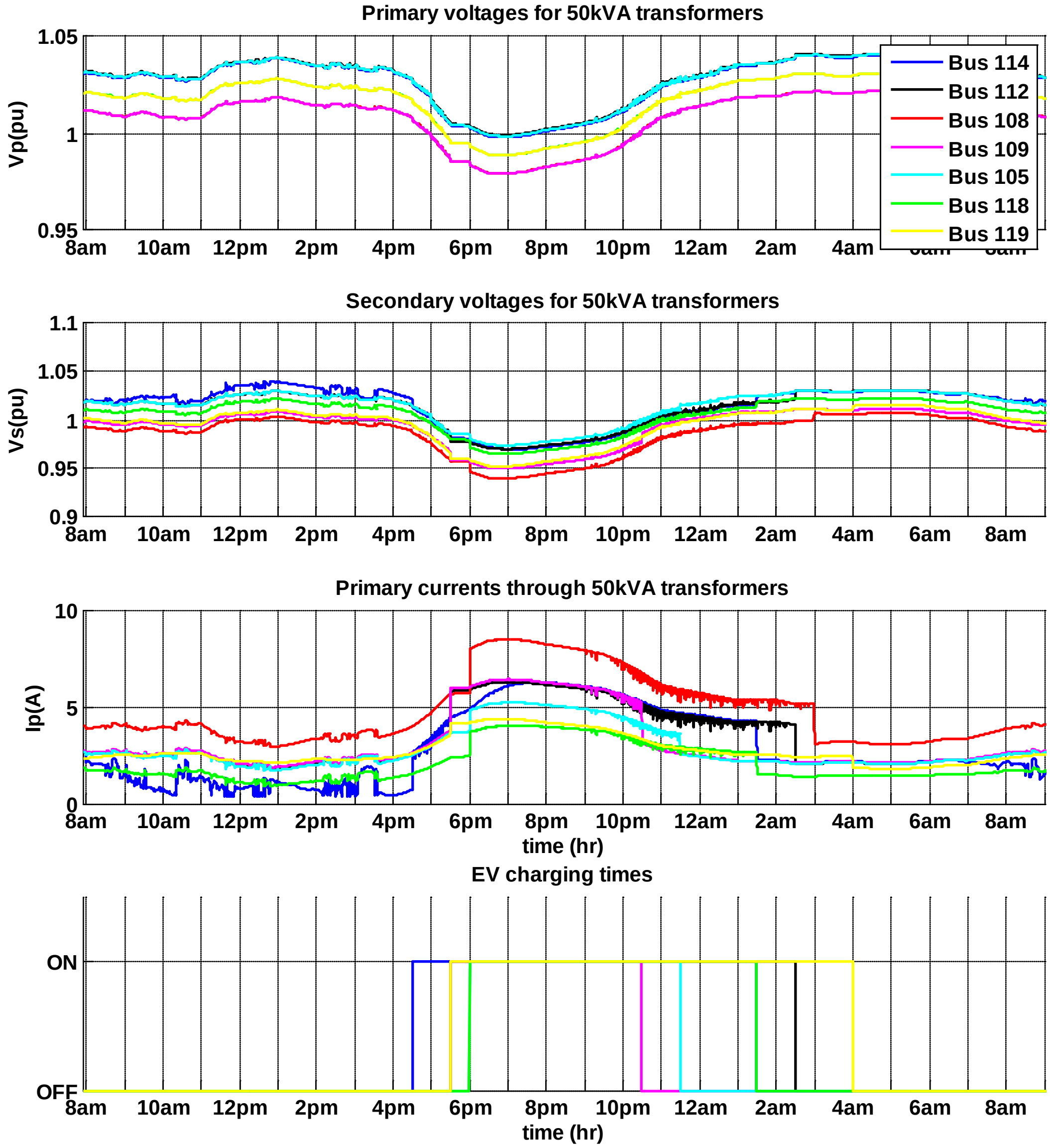

Figure 79 – Primary and Secondary Voltages and Current at 100 kVA Transformers (EV Set 1, Uncontrolled Charging)

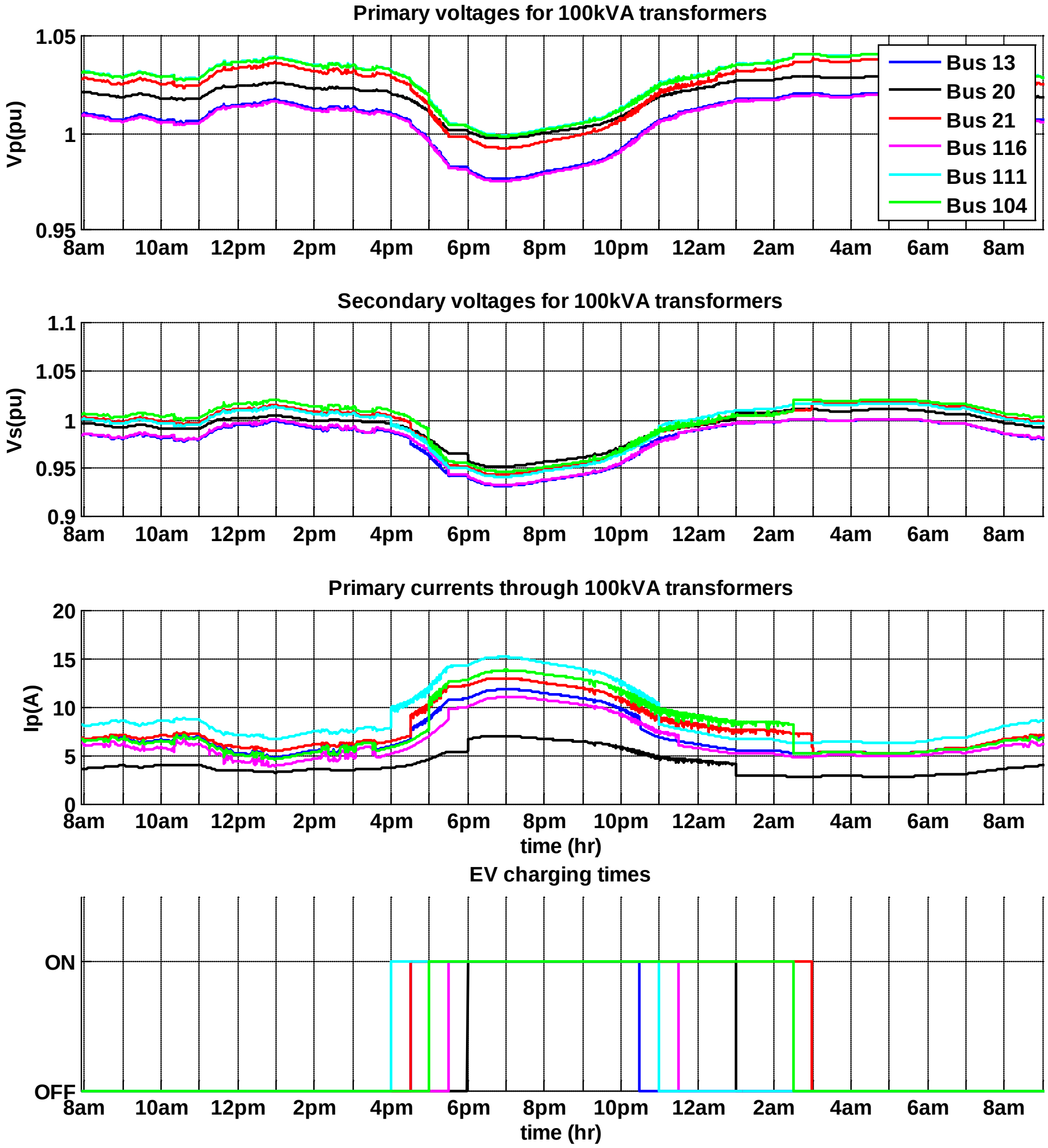

4.3.6.4 EV Profile Set 2, Uncontrolled Charging

Voltages for the entire circuit are shown in Figure 80. Transformer voltages and currents are shown in Figure 81 through Figure 84. It was observed that EV charging had a large effect on primary transformer current flow and the secondary transformer voltages. The voltage effect was mainly because EV charging occurred in the early evening time-frame where the system load was high and voltage was already closer to the lower bandwidth. In some cases, the loading had doubled. Additional loading reduced the voltage further. EV charging had less effect on the circuit voltage.

Figure 80 – Voltage at All Circuit Locations for Varying Load and PV Profile (EV Set 2, Uncontrolled Charging)

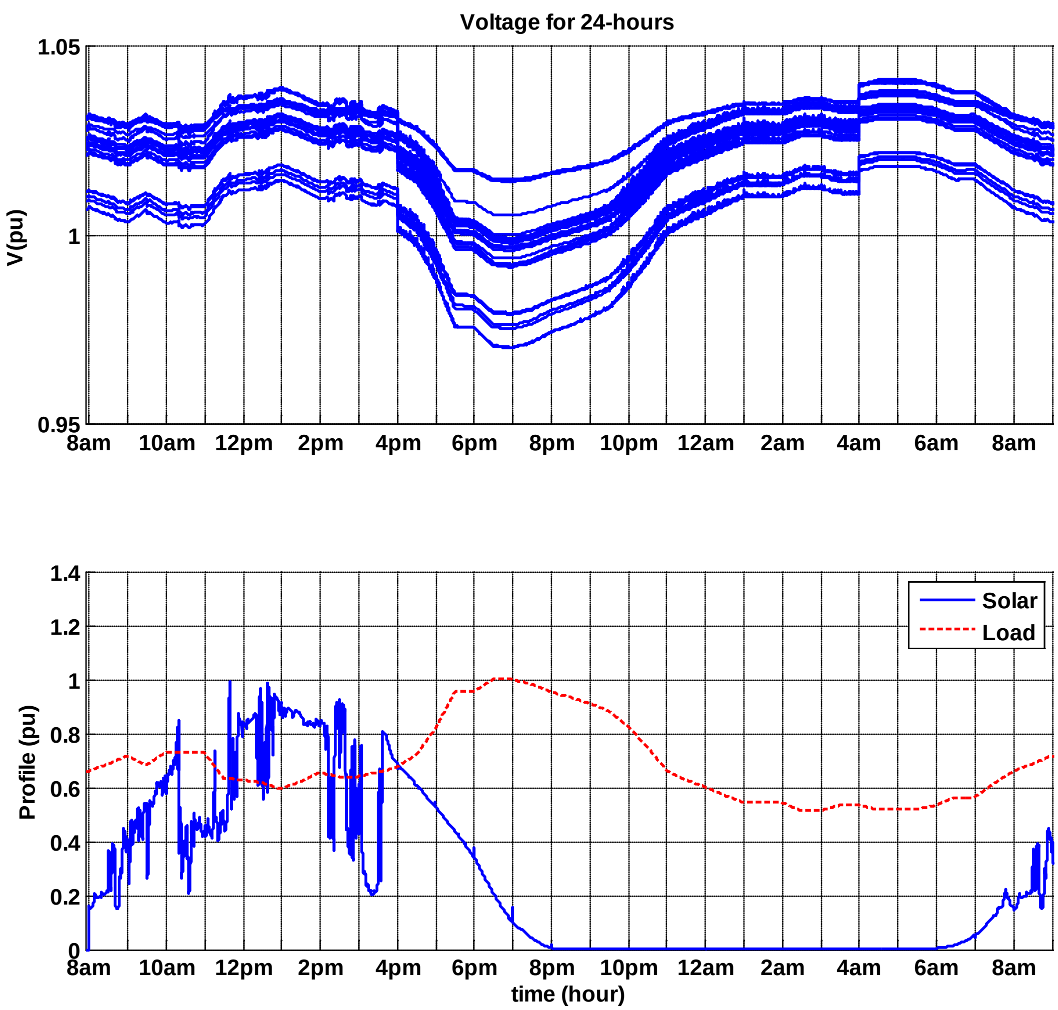

Figure 81 – Primary and Secondary Voltages and Current at 25 kVA Transformers (EV Set 2, Uncontrolled Charging)

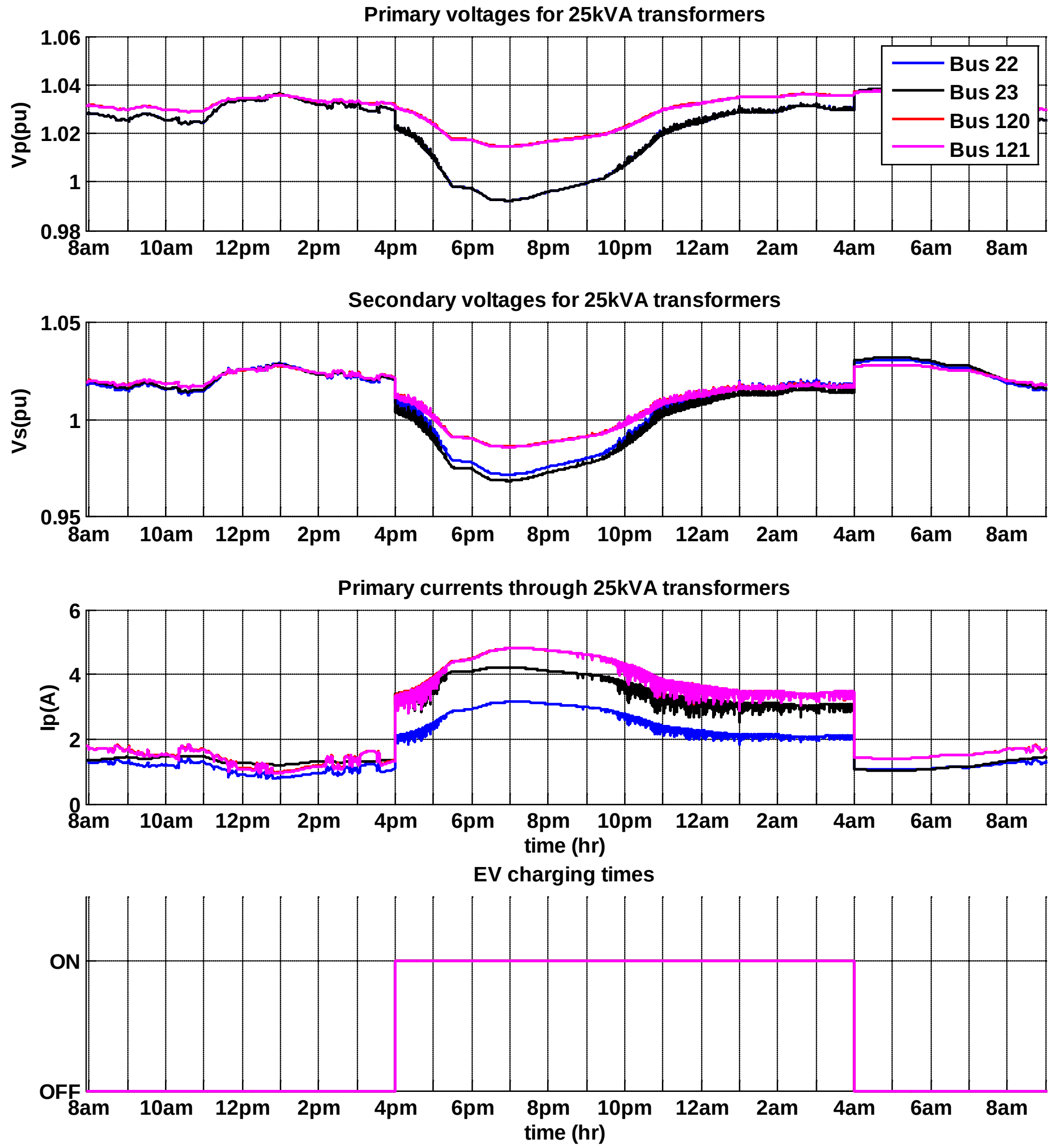

Figure 82 – Primary and Secondary Voltages and Current at 50 kVA Transformers – Subsystem 1 (EV Set 2, Uncontrolled Charging)

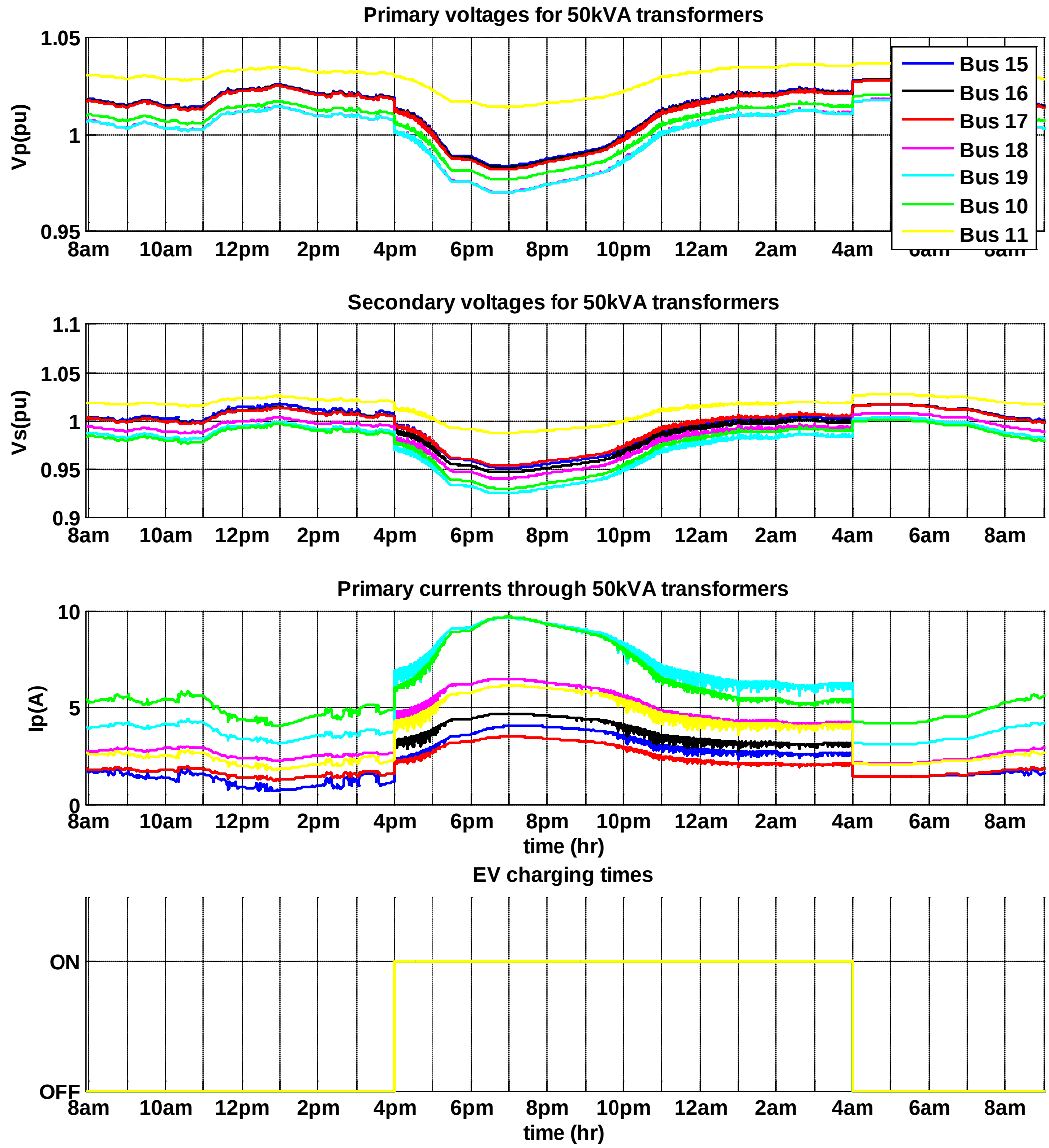

Figure 83 – Primary and Secondary Voltages and Current at 50 kVA Transformers – Subsystem 2 (EV Set 2, Uncontrolled Charging)

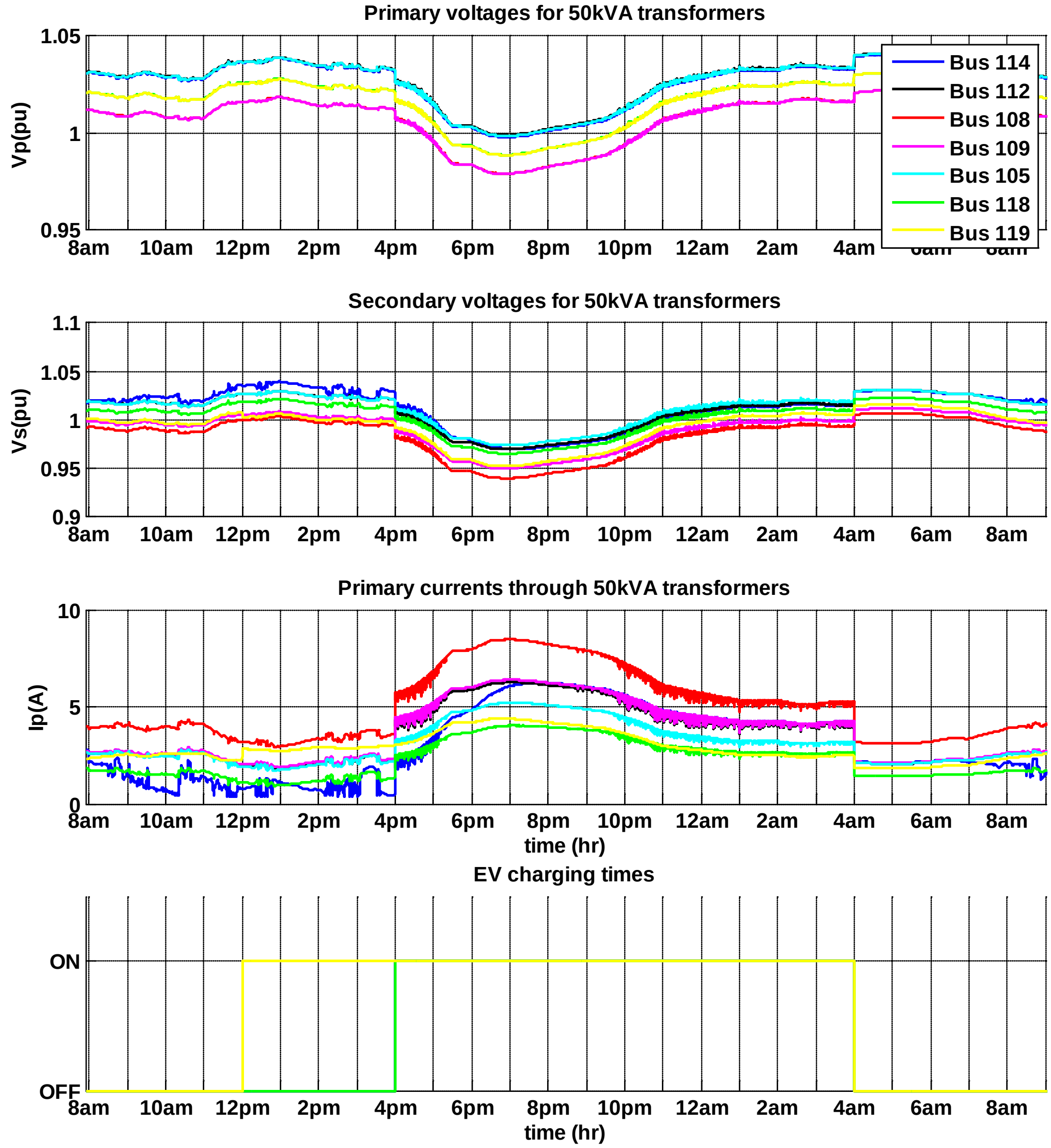

Figure 84 – Primary and Secondary Voltages and Current at 100 kVA Transformers (EV Set 2, Uncontrolled Charging)

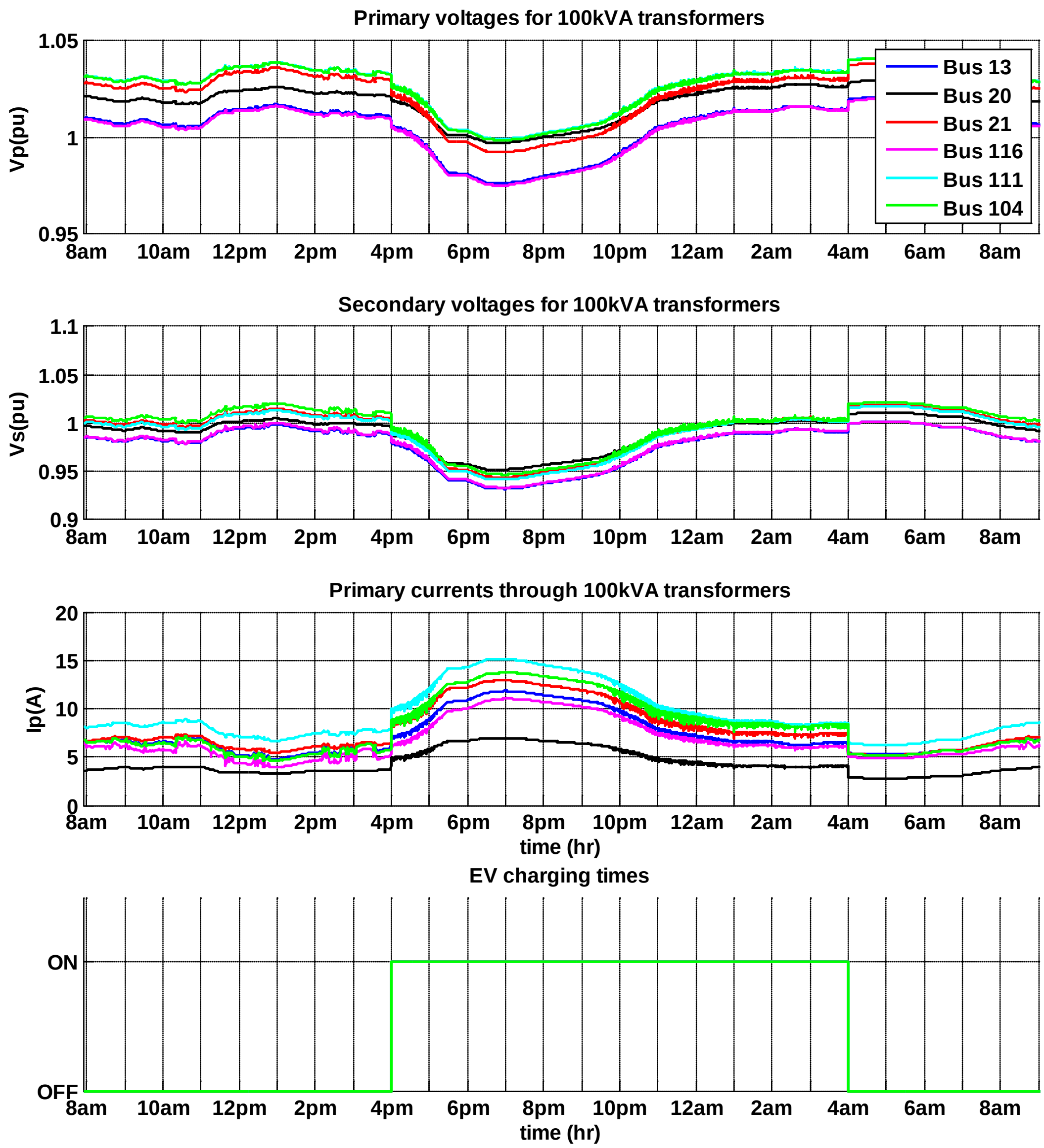

4.3.7 Online – Multiple EV on Single Transformer

These tests involved the connection of multiple EV customers to a single transformer location on the circuit. Loads were scaled according to the full 24-hour profile, and PV generation was disabled. Two locations were selected for the connection of the transformer, representing a 25 kVA and 50 kVA transformer. Start and end charging times were randomly selected for each individual EV customer according to the limits defined by the uncontrolled charging time. Size and charging details are shown in Table 13.

Table 13 – EV Size and Charging Times Parameters

Transformer and EV Parameters						
Bus #	Transformer Rated kVA	Connection	EV	EV size kW	Uncontrolled Charging Start	End
120	25	C	120[1]	5.8	17:30	00:30
			120[2]	5.8	16:30	22:30
109	50	A	109[1]	6.8	17:30	22:30
			109[2]	6.8	16:00	23:00
			109[3]	9.8	16:30	02:30
			109[4]	3.5	18:00	01:30
			109[5]	3.5	17:00	01:30

4.3.7.1 Bus 120, Uncontrolled Charging

The primary circuit voltage, transformer voltages, and transformer currents are shown in Figure 85. The effect of the staggered charging times of each EV customer is seen in the step decrease of secondary transformer voltage, and the step increase of transformer current. The transformer loading had tripled in some cases. The charging of EV customers had a large effect on transformer current flow and minimal effect on secondary transformer voltage. There was less effect on the primary circuit voltage.

Figure 85 – Voltages and Currents for Multiple EV Customers for Single Transformer at Bus 120

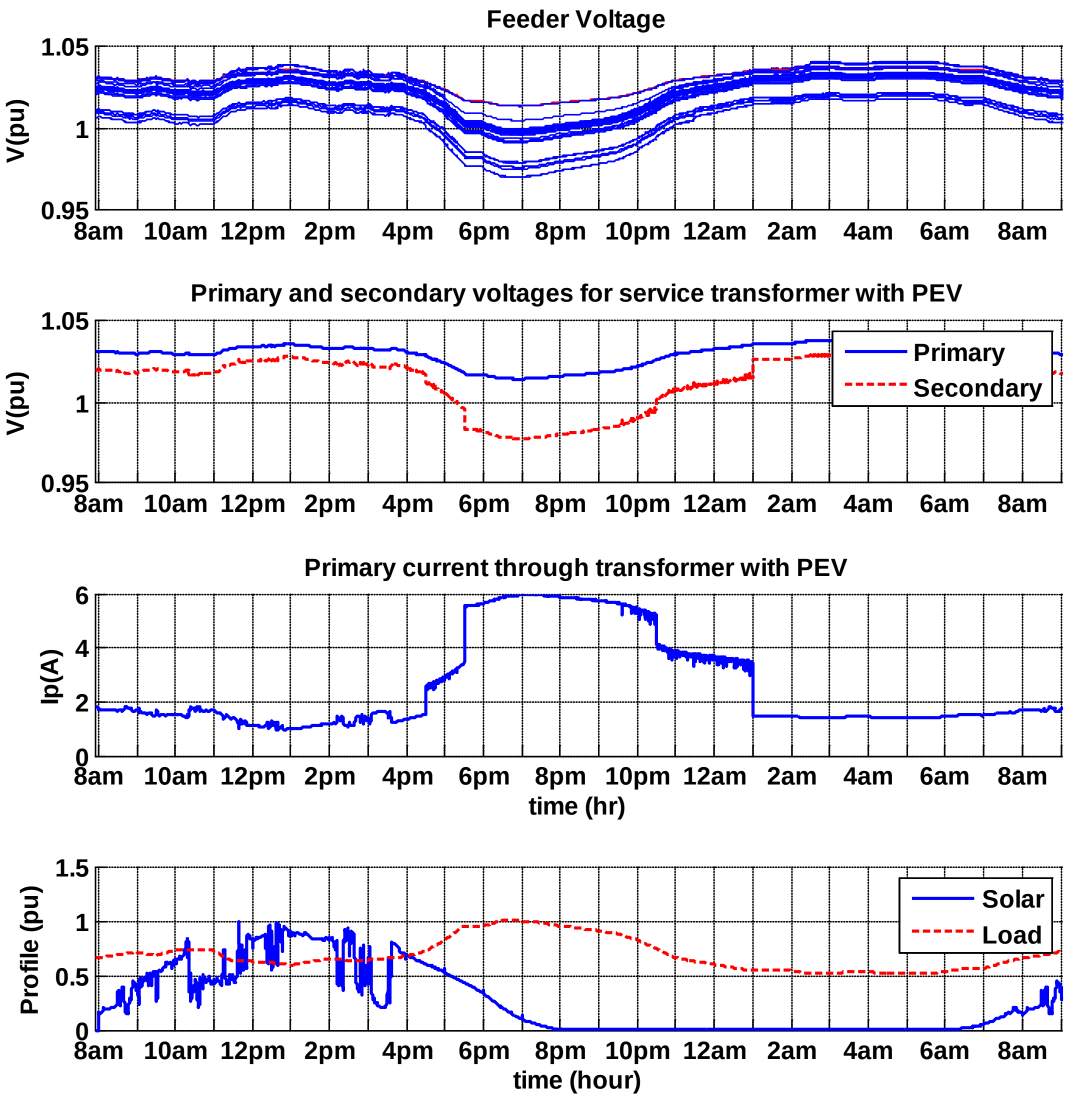

4.3.7.2 Bus 109, Uncontrolled Charging

The primary circuit voltage, transformer voltages, and transformer currents are shown in Figure 86. The effect of the staggered charging times for each EV customer is seen in the step decrease of secondary transformer voltage, and the step increase of transformer current. The charging of EV customers had a large effect on transformer current flow and secondary transformer voltage, with voltage dropping to nearly 0.9pu. There was less effect on the primary circuit voltage.

Figure 86 – Voltages and Currents for Multiple EV Customers for Single Transformer at Bus 109

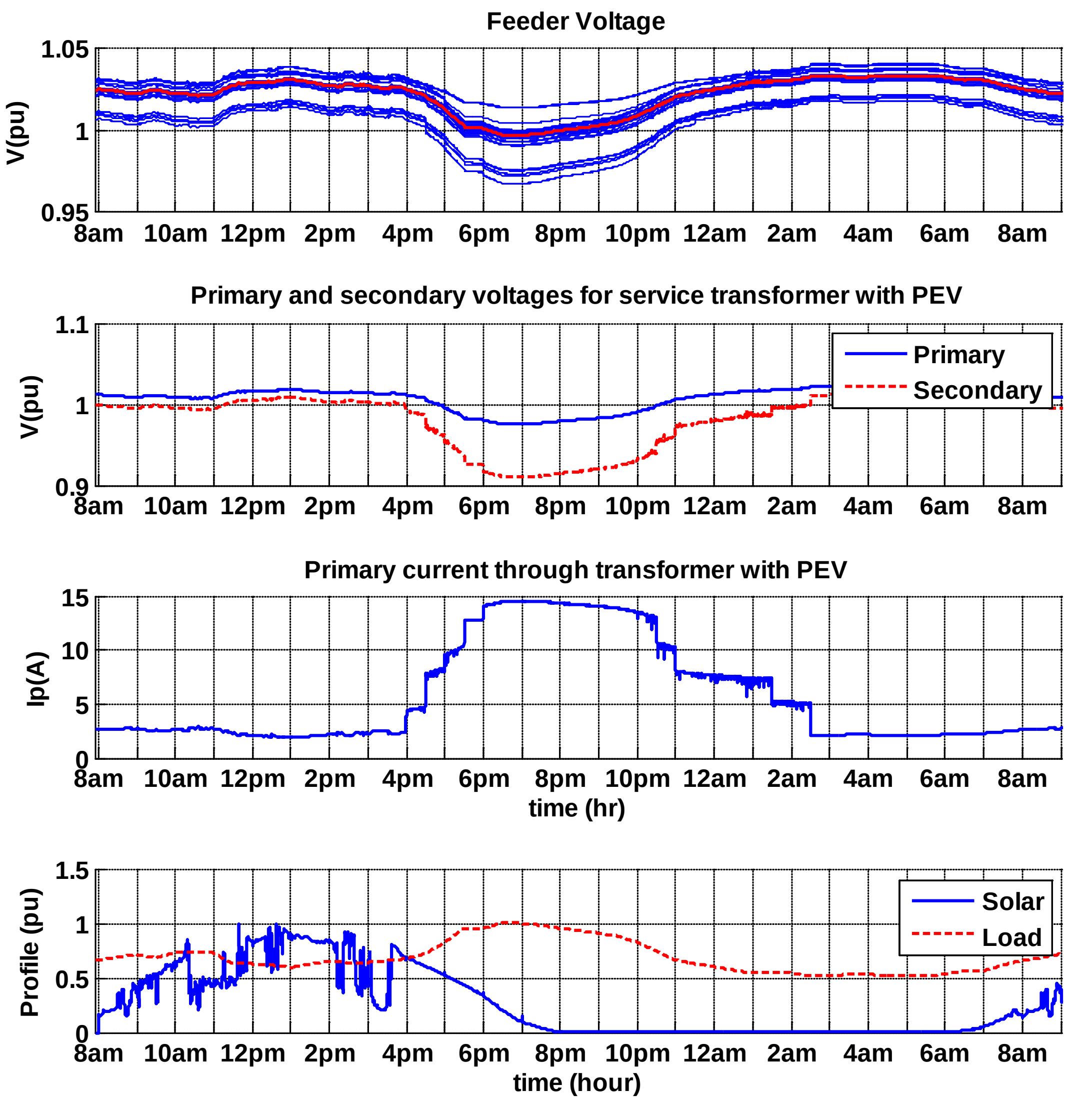

4.3.8 Online - Full System Test – Large EV

In all previous tests, the addition of EV had minimal effect on circuit and transformer primary side voltage, even when all secondary circuits had EV. The purpose of this test was to determine the size of aggregate EV at which the circuit would start to experience significant voltage issues (> 0.01pu). In this test, the EVs on all 28 secondary circuits were scaled according to existing proportions to aggregate sizes of 500kW and 1,000kW.

The circuit voltage and power flow at the substation are shown in Figure 87. It was seen that the change in real power flow at the substation changed by less than 400kW when the EV (rated at 500kW) was active. Similar results were seen for EV aggregate size of 1,000kW – the change in power flow was less than 400kW. This effect was due to the limitation of the transformer rating, which could not support more power flow to the secondary circuits.

Figure 87 – Voltages and Power Flow for 500kW Aggregate EV

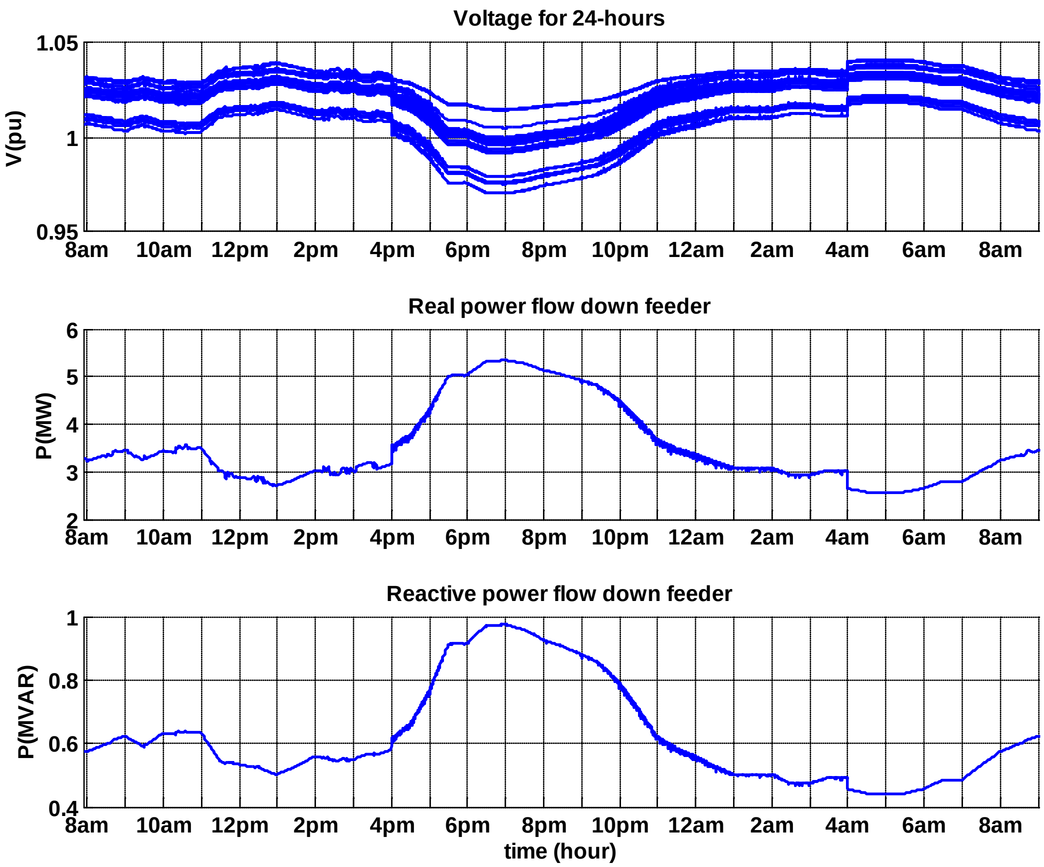

4.3.9 Online – DC Charger Test

Two locations were studied for the DC Fast Charger tests:

- **One DC Fast Charger at Bus 5**: Represented a shopping mall location, 40kW, 20 minutes active starting at 12:00 pm
- **One DC Fast Charger at Bus 118**: Represented a school location, 40kW, 20 minutes active starting at 12:00pm

The DC Fast Chargers were supplied through existing three phase transformers that carried other loads and customers. For both cases, it was assumed that DC Fast Charger was used during noon time.

4.3.9.1 DC Charger at Bus 5

The primary circuit voltage, secondary transformer voltage and currents, and real and reactive power flows into the EV charger are shown in Figure 88. It was seen that the effect of the EV on both primary and secondary voltages were insignificant. Bus 5 was relatively close to the substation, introducing a good candidate for deployment of DC Fast Chargers without adverse impact on the circuit.

Figure 88 – Voltages, Currents and Power Flow for DC EV Charger at Bus 5

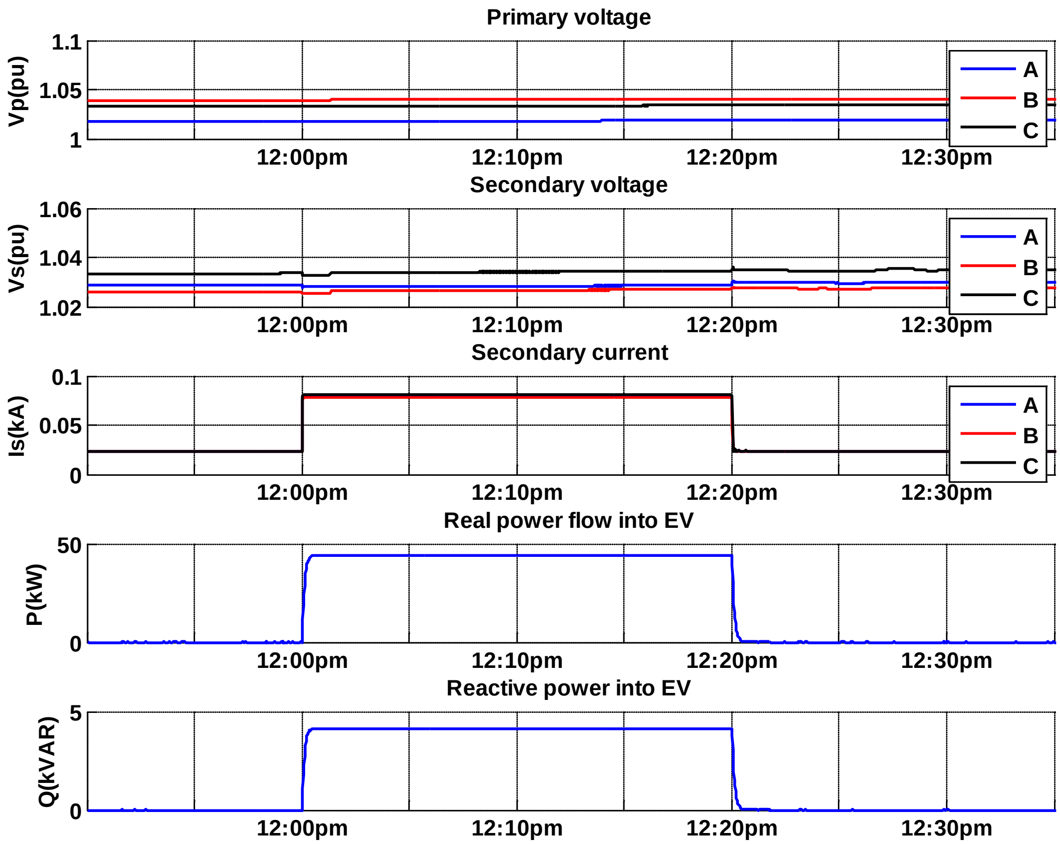

4.3.9.2 DC Fast Charger at Bus 118

The primary circuit voltage, secondary transformer voltage and currents, and real and reactive power flows into the EV charger are shown in Figure 89. It was seen that the effect of the EV charging on both primary and secondary voltages was insignificant.

Although this location was further away from the substation, the system was strong and impact on the voltages was negligible.

Figure 89 – Voltages, Currents and Power Flow for DC EV Charger at Bus 118

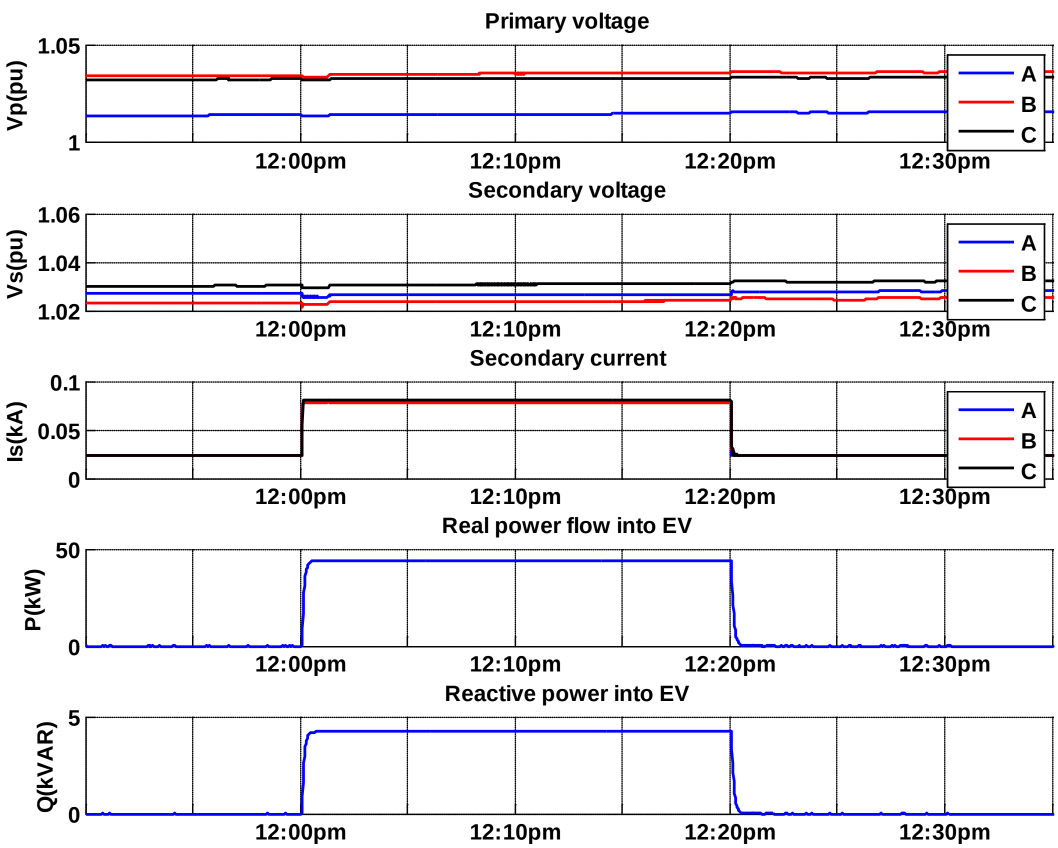

In summary, proposed locations were generally good candidates for deployment of DC Fast Chargers, with no expected impact on the voltages and/or operation of the circuit.

4.3.9.3 Smart Inverter Testing with PEV Simulator

During the design of the DC Fast Charger Simulator (PEV Rack 2), it was noted that this simulator could also be utilized for testing Smart Inverter capabilities with RTDS through power hardware in the loop simulation. PEV Rack 2 included two transformer-less (TL) three phase 480 V inverters. The inverters offered several control features through communication channels with the inverters, such as:

- Dynamic power factor adjustment
- Reactive power and voltage control
- Power curtailment

The remote control using communications with the two inverters were performed through a cluster controller as shown in Figure 90. The cluster controller used a proprietary protocol to communicate with the downstream inverters, but a Modbus protocol to communicate with outside world for receiving commands and transferring measurements and status.

Figure 90 - Communication Architecture for the Smart Inverter Tests

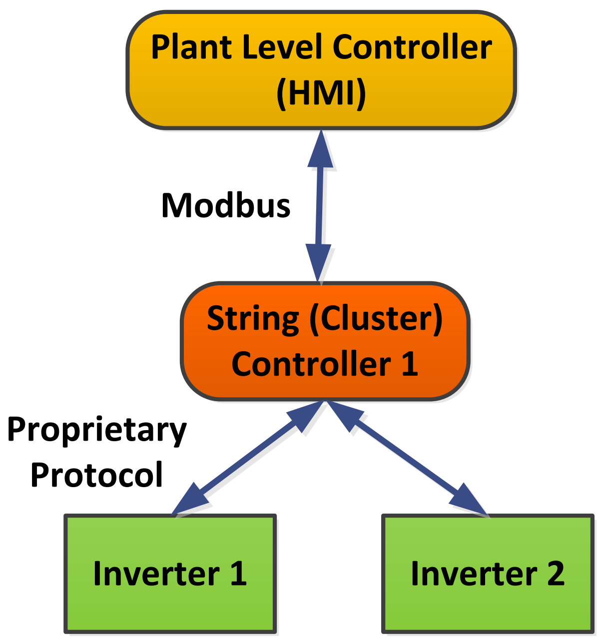

PEV Simulator Rack 2 used the above mentioned communication structure to exchange set-points and data measurements with the two inverters. A use control page was added to the HMI design which allowed specifying power factors and power curtailment set-points for the multiple inverter system (in this case, two inverters).

The HMI page for controlling the inverters and testing smart inverter features is shown in Figure 91. Customized Free-Control Mode and Customized Controlled Set-point Mode were the two control options that were specifically implemented for the inverter testing. As shown, the power curtailment set-point and power factor could be dynamically changed throughout a test. The information was communicated through the Mod-bus commands to the cluster controller in the EV Simulator Rack, and from there to the two inverters on the rack. Examples of data exchange with individual inverters are shown in Figure 92.

Figure 91 – HMI Page for Selection of Control Modes

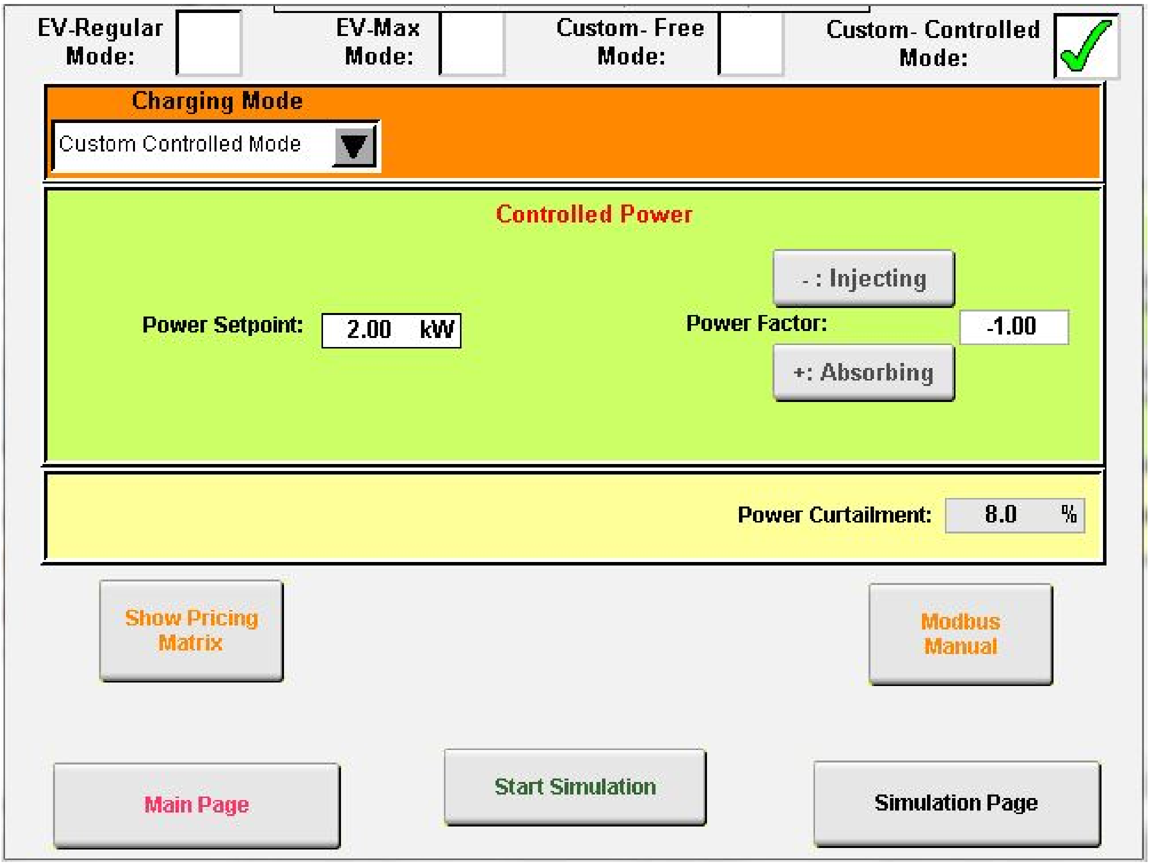

Figure 92 – Modbus Communications for Measurements and Commands

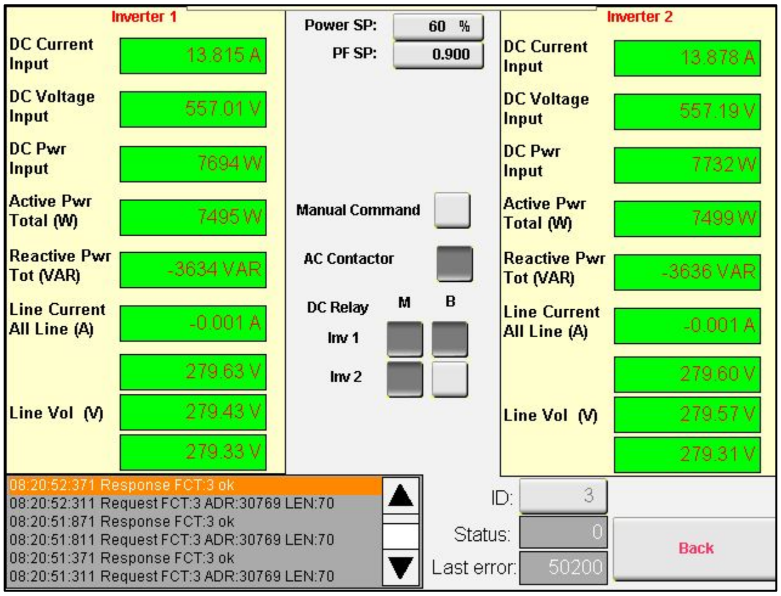

An example of custom control simulation for the inverter with 60% curtailment and -0.9 power factor (injecting reactive power) is shown below in Figure 93.

Figure 93 – Simulation Page for Custom Control of Inverters with Dynamic Power Factor

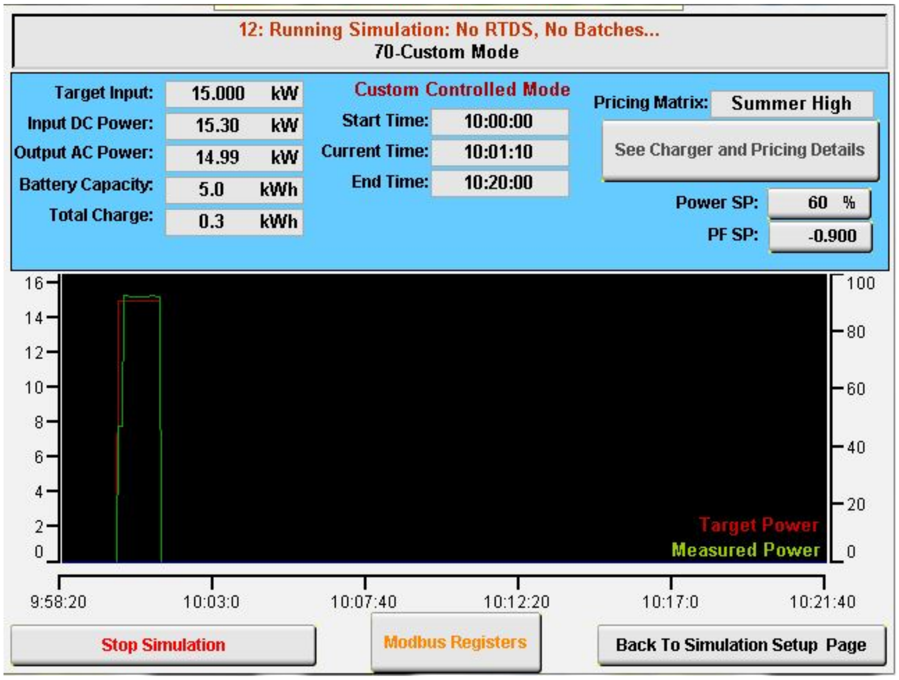

An example of the snapshot capture for inverter currents and voltages from the tests is shown in Figure 94.

Figure 94 - Voltage and Current Waveforms as Captured by RTDS Closed Loop Tests

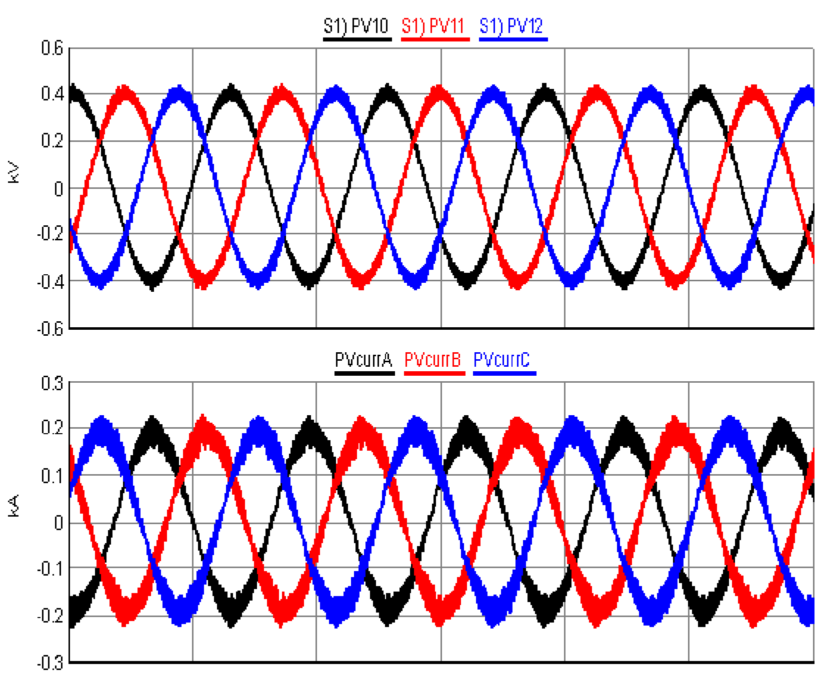

During the tests, it was noted that power curtailment had direct impact on the MPPT scheme of the inverters. The effect on the maximum power curve is shown below in Figure 95. The operating point had moved away from the maximum point of power tracking and power curve.

Figure 95 – Power Curve of the Inverters Under Power Curtailment

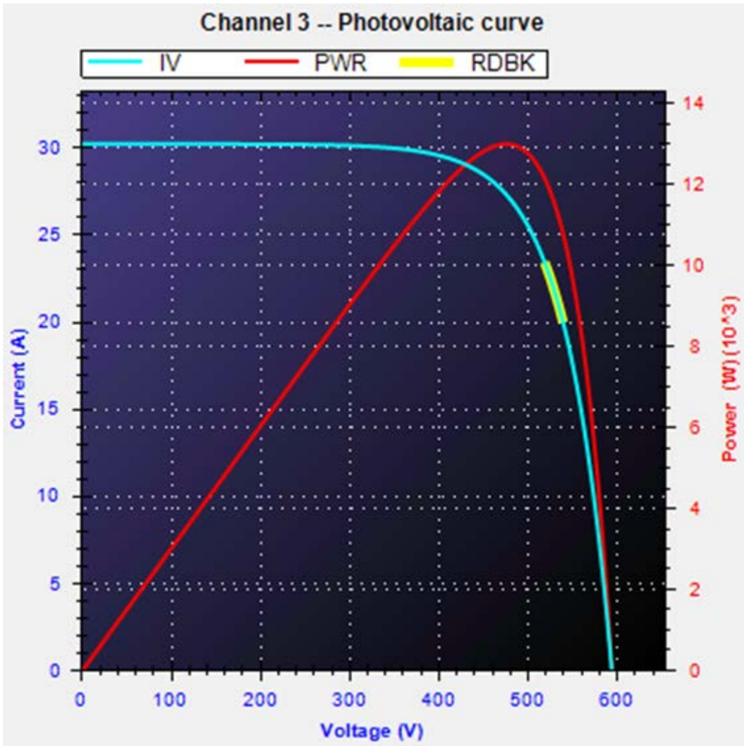

Several tests were introduced and examined with the test bed to verify the advanced features of the new generation of transformerless inverters including:

- Inverter operation at various power curtailment levels and variations in power factor
- Inverter operation with asymmetrical voltages or under unbalance loading conditions operation
- Fault current testing of the inverter and effect of controls and protections on the dynamic response of the inverter
- Performance during accidental islanding and TOV effect

As an example, the current and voltage waveforms captured from applying a single line to ground fault at the terminal of the inverters are shown in the Figure 96 below. As was observed, the inverters in this case had been able to ride through the fault and did not disconnect, since the voltage drop at the point of inverter connections was not large enough.

Figure 96 – Effect of Single Phase Fault at Terminal of Inverters on Voltages and Currents

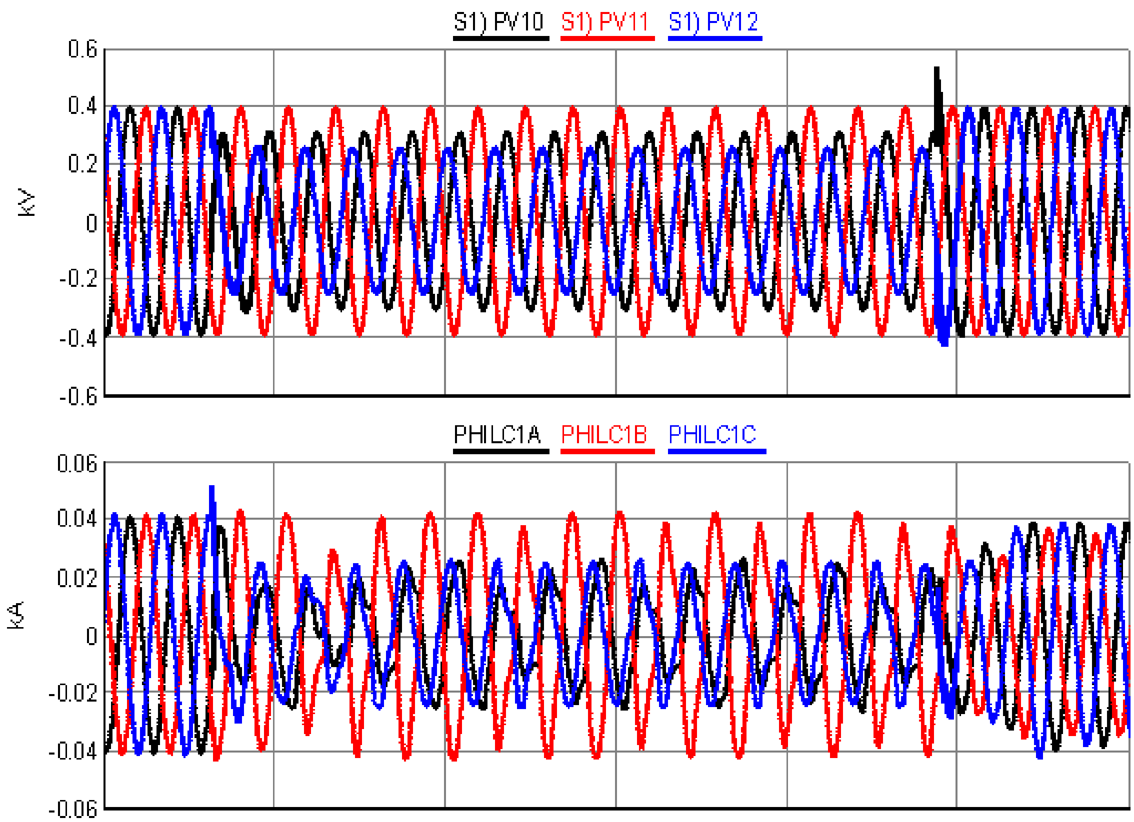

In addition, it was tested that several inverter parameters could be changed through the communications including the inverter protection settings and re-connection time delay for re-start after grid restoration. This was an advanced setting feature that was available on non-certified inverters and could be requested by utility customers to coordinate the protection settings with the utility requirements

CHAPTER 5:
Integration Studies Using a Hybrid PEV-PV and Energy Storage System

In this chapter, the integration of the electric vehicles with solar and energy storage was studied. An experimental field implementation of integrated design approaches for co-locating and effective utilization of distributed energy resources in conjunction with high concentration of PEV charging stations was conducted. The demonstration site was developed by integrating a Battery Energy Storage System (BESS) and a solar PV carport into the electrical system of a parking lot.

Typical and alternative approaches for supplying charging stations for electric vehicles in a commercial parking lot are represented in Figure ***97***.

Figure 97 – Conventional vs. Hybrid (Integrated) PEV Charging Station Design Approach

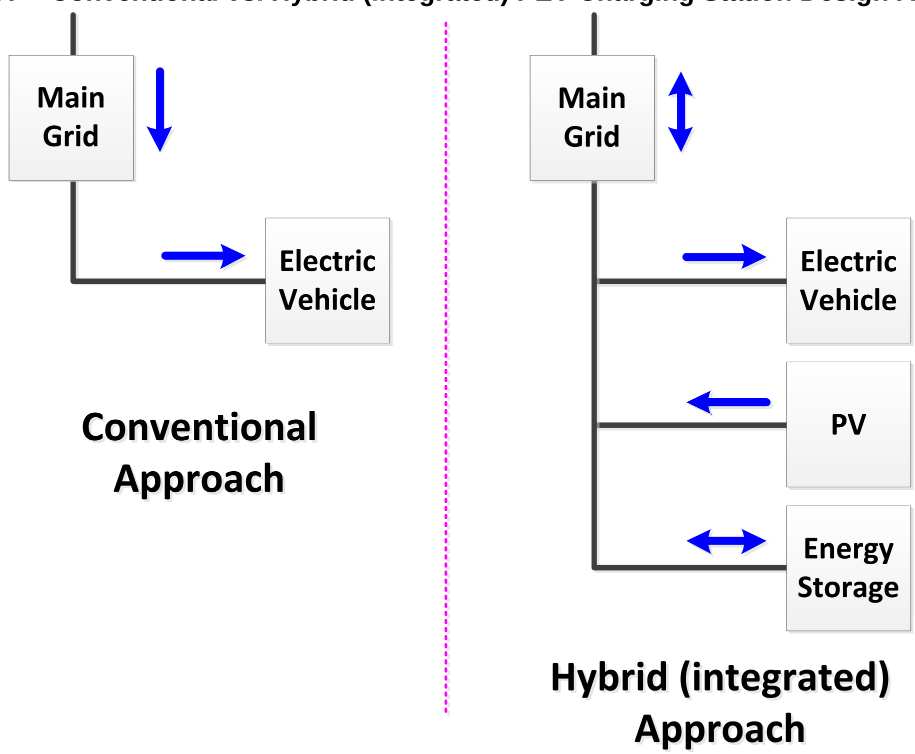

The hybrid approach utilizes a combination of distributed energy resources, solar PV generation units, and energy storage systems, to manage the additional loading introduced by PEV charging stations and to enhance the controllability of site loads from the main grid interconnection point.

5.1 Site Description

An SDG&E owned outdoor commercial parking lot was used to implement a hybrid demonstration site for the integration of multiple PEV charging stations with solar PV systems and battery energy storage units. The demonstration project provided an experimental set-up for design assessment and evaluation of integration approaches to mitigate impact of large concentrations of PEV charging stations on the local electric grid. The field measurements and data gathered from the demonstration readily enabled evaluation of the effectiveness of the proposed hybrid mitigation solution. Analysis of the field data was also used to assess performance of power management and energy balancing schemes of the BESS and the hybrid system to determine the requirements for future designs and to suggest proper controls for the battery energy storage unit. The results from the demonstration project quantifies the enhancing effect of adding active generation from renewable resources and managing capabilities of energy storage to coordinate large charging loads of electric vehicles.

For the purpose of this demonstration, SDG&E had re-arranged the infrastructure of an existing parking lot with multiple PEV charging stations to utilize as a real-world outdoor demonstration facility with actual customers (SDG&E Field PEV Fleet). This parking lot serves a main multi-building office complex, heavily utilized by utility employees during weekdays. The facility presently has over 10 level 2 charging stations, and 8 level one chargers. As part of the Energy Commission project, a 24 kW Photovoltaic (PV) system (solar carport) was added to one side of the parking lot. A 50 kW, 80 kWh battery energy storage system (BESS) was also re-located to the parking lot and was integrated into the main distribution panel supplying the electrical circuits to the PEV charging stations, shown in

Figure ***98***. All the charging stations, the solar carport, and the BESS are connected to same service transformer, making it a unique integrated and hybrid system. Each system is metered separately for the purpose of controls as well as monitoring and evaluation of system operations.

Figure 98 – Integration Test Site Single Line

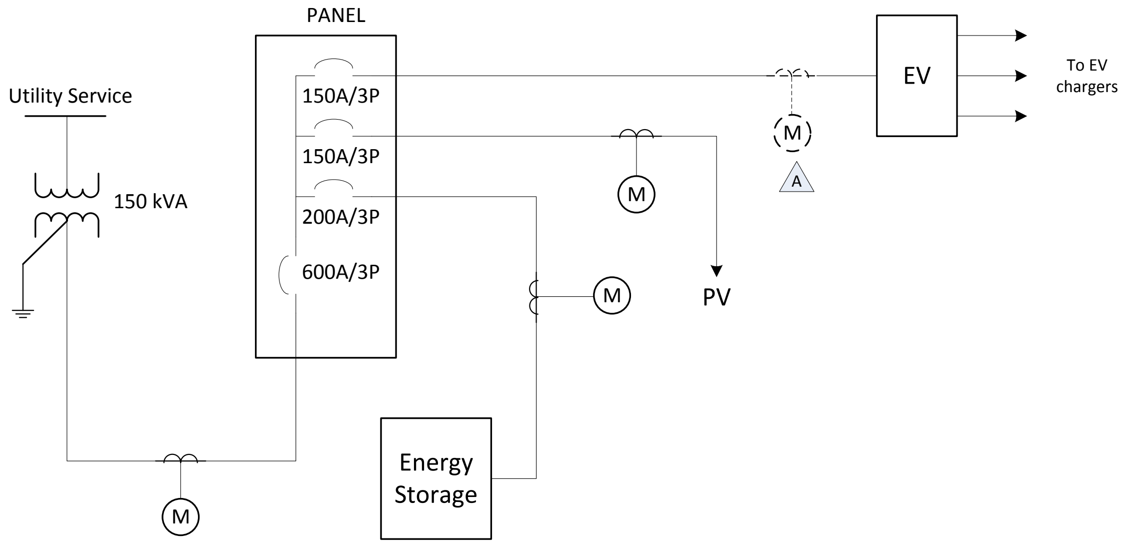

The site was equipped with power flow measurement devices for transformer load (M_Load), PV system (M_PV), PEV charging stations (M_EV), and battery storage unit (M_BESS). All the data provided in this report are based on the selected power flow convention as shown in Figure 99. The positive direction is defined as injection back to the distribution circuit. Therefore, the charging power of the battery will be reflected as a negative flow and its discharging power will appear as a positive flow. Similarly, power injected to the system will be positive. Metered data from the demonstration system has been primarily collected from April to November of 2013 for evaluation purposes. Additional site tests and data collection were scheduled and performed in June/July 2014.

Figure 99 – Integration Site Power Measurement Polarity

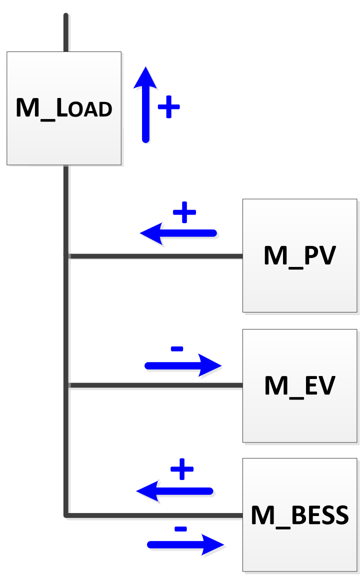

5.2 Studies Conducted and Results

5.2.1 Data Analysis Approach and Key Indicators

The data available from April to November of 2013 contains many variances and requires careful organization prior to any evaluation. Any suspicious data (bad metering or data transfer) was excluded from further evaluation. Bad data could be the result of either missing data (loss of metering communication) or when the energy storage was not operational (maintenance or installation stage). Also, testing multiple control modes of the energy storage and seasonal effects on the PV generation and PEV loading behavior resulted in the division of data. Lastly, due to limited PEV charging during weekends and holidays, the evaluation of the integration site performance for this report is focused primarily on weekdays. The available data was divided into three study cases, considering three steady-state load management levels of: 0kW (in November), 5kW (in July), and 10kW (in August). For these tests, the battery energy storage unit was set-up in 'Load Management' control mode based on measuring power flow through the service transformer to achieve a fixed power flow at the service transformer connection point, during the daytime. When there is PV generation and/or PEV charging load, the battery storage unit has to provide the balancing power based on the difference in generation and load, as compared with the user-selected load level.

Two scenarios within this study may have occurred:

- There is an overnight charge from midnight to 4:00 am at constant 5 kW level
- If the battery SOC goes below 25%, the load management control cannot be accomplished

The key indicators to monitor and analyze are:

- Initial and final SOC per day
- Percentage of time that control was successfully accomplished
- Average PV generation, PEV charging load, and the BESS cumulative charge and discharge energy per day
- Maximum rate of change of power at the service transformer level

Observations from the Control Mode and Operation During Weekend Days

Very little energy storage charge/discharge was observed for the duration of applying Case Study 1 on the weekends. The battery management system was either turned 'off' or it was in the 'idle' mode on weekends. No PEV charging was expected on non-working days and, therefore, all PV generation was back fed directly to the grid. Most PEVs are typically charged by Friday evening and are left idle until Monday morning (See Figure 100).

Figure 100 – Weekend Control Idle Mode (Saturday, November 2, 2013)

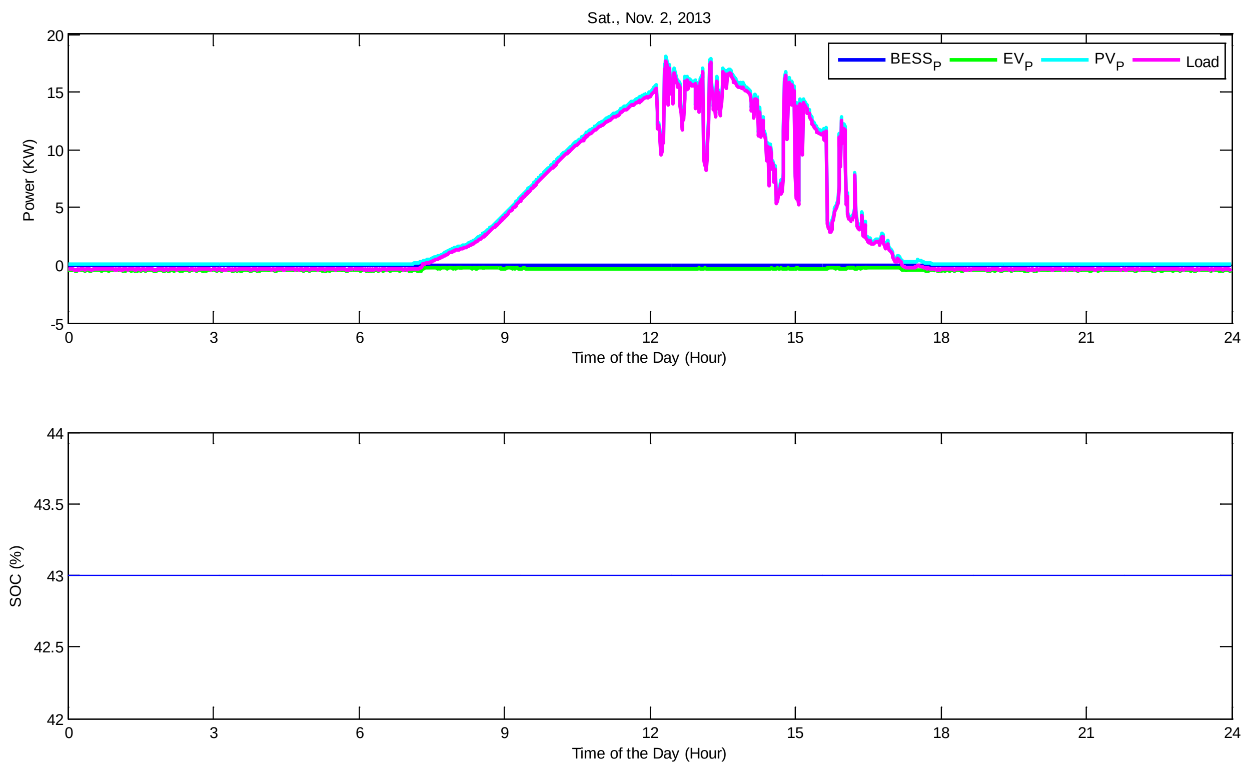

Observations from the Control Modes Applied During Weekdays

Due to the idle mode characteristic of weekend energy storage control, the focus of most analysis for the study cases was on the weekday datasets. The battery management system attempted to regulate the load at 0, 5, or 10 kW set-points during daytime by the use of 'Load Management' mode described in section 5.2.1. A fixed overnight charge schedule was applied in addition to the load management mode as part of the control strategy. This control ensured that the SOC of a depleted battery (due to the previous day operation) was raised above 50% state by early morning.

The BESS charging period was scheduled from midnight to 4:00 am at a constant power of 5kW, increasing the SOC by 20% at the end of this interval (See Figure 101).

Figure 101 – Weekday Control Load Management Mode (Tuesday, November 5, 2013)

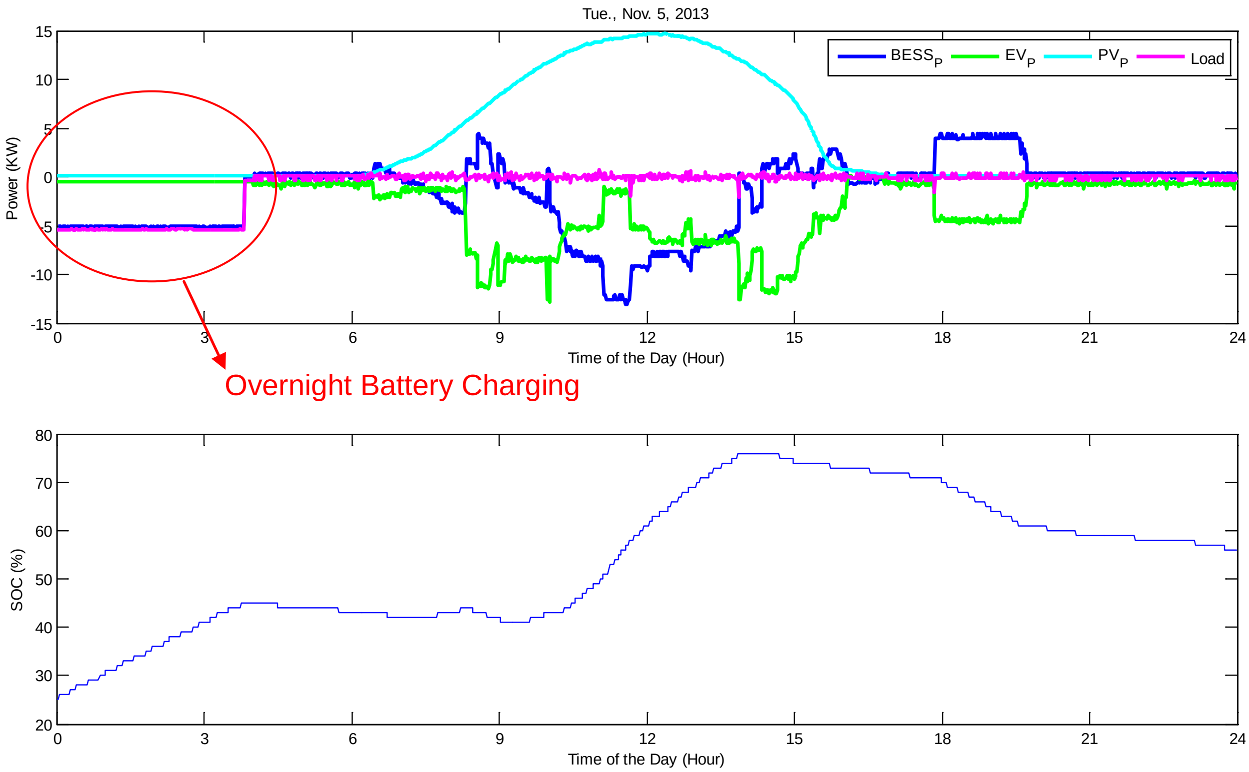

The objective for reviewing the three study cases was to select optimized set points for the energy storage to maximize the percentage of time that load management control can be accomplished. Due to major changes in the PV generation in different seasons and various days of the week, this report will be concluded by proposing the following set points described in ***Table 14*** in the recommendation section.

Table 14 – Seasonal Set-point Selection

Set-points	Summer		Winter	
	Weekend	Weekday	Weekend	Weekday
Load Management Limit (kW)	0 or 5 kW	N/A	10 kW or higher	N/A
Start of Day SOC (%)	35%	N/A	70%	N/A

5.2.2 Case Study 1 – Maintaining Load at 0 kW (November 2013)

The performance of the load management control at 0 kW was evaluated for the time period of November 2, 2013 – November 24, 2013. The objective was to monitor the success of the energy storage regulating load flow at 0 kW, to limit the power flow of the main transformer from the grid during the day. The mode was considered successful when the load meter reported an amount within the load profile variation of -500 to +500 watts (accounts for minor fluctuations). The daytime load management interval was considered from 6:00 am to 9:00 pm in order to exclude any unusual night activities, as well as the scheduled midnight charge (non-zero load).

Based on the performance analysis criteria given above, the energy storage load regulation of 0kW was successful for **65%** of the time for the selected 15 weekdays in case study 1. Table 15 provides daily success rate of the energy storage control system and a snapshot of best/worst days of operation.

Table 15 – Case Study 1: Daily Success Rate of Load Regulation (Weekdays)

Day in November	4	5	6	7	8	11	12	13	14	15	18	19	20	21	22
Success Rate (%)	67 %	99 %	99 %	79 %	90 %	70 %	52 %	43 %	78 %	33 %	66 %	30 %	67 %	33 %	66 %

Nov 5 (Best Day)	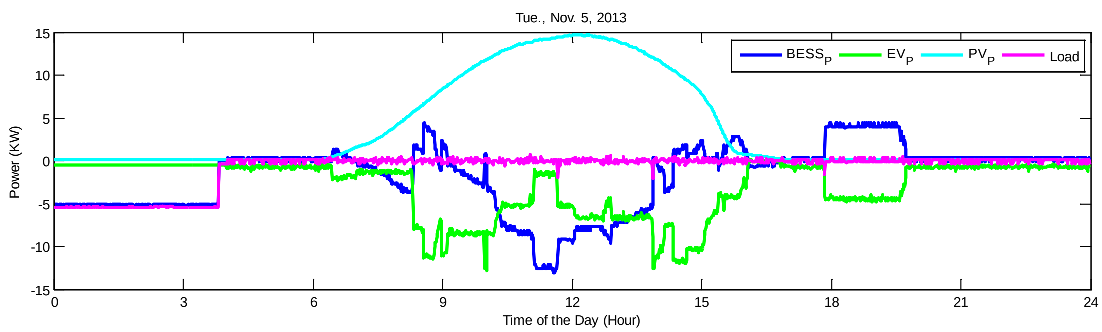
Nov 19 (Worst Day)	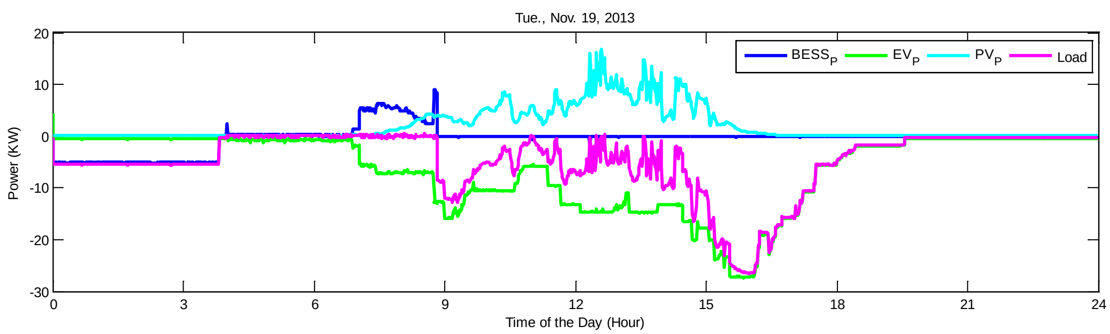

The average daily energy exchange for the BESS, main grid, PV generation, and PEV load is summarized in Table 16 below.

Table 16 – Case Study 1: Average Daily System Behavior

PV Generation (kWh)	PEV Charging (kWh)	BESS Charging (kWh)	BESS Discharging (kWh)	Load (+) (kWh)	Load (-) (kWh)
61.43	104.6	35.56	21.81	1.11	-54.34

The control objective for this period was to limit the load values to zero. The load expects a positive energy flow back to the grid, for instance, when PV generation is higher than PEV charging and the energy storage is fully charged (100% SOC). This positive flow was limited in the month of November as the PEV charge was considerably higher than PV generation (1.11 kWh daily average). The high load demand of 54.34 kWh was due to load management only being successful for 65% of the time, resulting in the main grid supporting the difference between PEV charging and PV generation for the rest of 35% of the day. It is also skewed by the fix scheduled overnight charge of the battery for 4 hours. Further investigation of the SOC levels is required to properly optimize the load management mode.

It was observed that the energy storage SOC management was critical for the success of the load management mode. Start of the Day SOC was defined as the battery state of charge at 4:00 am (end of the scheduled overnight charge). The average starting SOC for Case Study 1 was approximately 48%. End of the Day SOC was calculated at midnight, just prior to the scheduled overnight charge. The average End of Day SOC for Case Study 1 was approximately 28%. As supported by these results, it was expected that the end of day SOC be lower for this case, since the average PEV charging was considerably higher than PV generation. The energy storage was supposed to discharge the difference between PV generation and PEV load in order to keep the main grid contribution at zero (see Table 17).

Table 17 – Case Study 1: Start and End of Day SOC (Weekdays)

Day in November	4	5	6	7	8	11	12	13	14	15	18	19	20	21	22
Start of Day SOC	61%	45%	76%	55%	46%	51%	45%	44%	45%	46%	43%	45%	41%	45%	43%
End of Day SOC	25%	56%	35%	26%	33%	25%	24%	25%	26%	25%	25%	21%	25%	23%	26%

Furthermore, SOC distribution for the entire study case was calculated and presented in ***Table 18***. Expectation was to use the entire range of SOC in order to take full advantage of the battery cells. It was observed that the 20% extreme capacity range of the battery (SOC> 80% and SOC < 20%) were unavailable in November, during the commissioning stage. Therefore, the load management control was only able to utilize 60% charging capacity of the energy storage. However, ***Table 18*** shows that energy storage is observed to be chasing the difference between the PEV load and PV charge as it was below 40% SOC for more than 60% of the time, compared to less than 8% of time being above 60% charge. Initial observation of higher load than generation with the decrease of SOC from Start to End of the day suggest the battery required additional overnight charging to start the day with a higher SOC than 48%. This conclusion does not allow us to have the energy storage start at 100% charge in the morning as there will still be instances of PV generation larger than PEV load and therefore the energy storage requires charging the difference.

Table 18 – Case Study 1: Battery SOC Distribution

SOC Interval (%)	0-10	10-20	20-30	30-40	40-50	50-60	60-70	70-80	80-90	90-100
Operation (%)	0%	0%	38%	25%	23%	7%	3%	5%	0%	0%

Daily patterns showed a high PEV charging in early morning when employees returned their electric vehicles to the charging station as well as in the evening just before the end of working hours. With limited PV generation during these stages, the energy storage was expected to compensate a large difference between generation and load, and therefore, the SOC would drop dramatically. We expected the opposite effect of charging the energy storage in between these high PEV load periods (11:00 am to 3:00 pm) as PV generation was at its peak and the majority of electric vehicles connected to the charging station at 8:00 am were fully charged. With careful attention to all available data, it can be concluded that the SOC typically drops by 25% early in the morning and can increase by 40% in the afternoon. With PV generation dying down in the evening, the SOC was expected to drop considerably for the remainder of the day (See Figure 102).

Figure 102 – Battery Performance on Friday, November 8, 2013

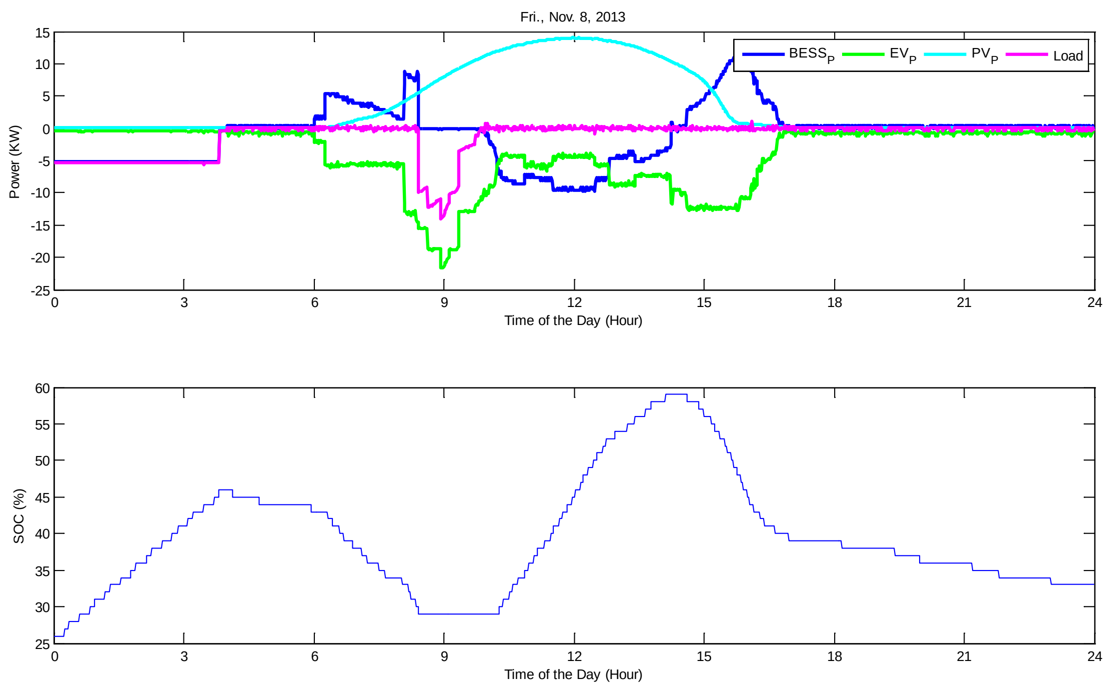

Based on the observations above, the start of the day target SOC should be considerably higher than the average 48% to optimize the amount of time load management mode that could be achieved. A set of recommended start of the day SOCs for case study 1 is reported in Table 19. Daily PV profile and PEV charging loads are taken into account to determine proper start of day SOC. With no provision for the prediction of PV and PEV profiles for each day, as well as utilizing a fixed set-point for the energy storage control system, an average SOC of **70%** can be considered as a better starting SOC for the month of November.

Table 19 – Case Study 1: Recommended Daily Start of Day SOC

Day in November	4	5	6	7	8	11	12	13	14	15	18	19	20	21	22
Actual SOC	61%	45%	76%	55%	46%	51%	45%	44%	45%	46%	43%	45%	41%	45%	43%
Optimized SOC	80%	45%	76%	73%	62%	75%	80%	74%	65%	80%	74%	80%	71%	80%	63%

In addition, it is not recommended to use a fixed overnight scheduled charge for the BESS, since there was no control on the start of the day SOC. It was observed that a cloudy day can affect the next day load management operation, even if the next day has a good PV generation. This issue occurred because the starting day SOC would be too low to compensate for the last day's poor operation, since a fixed 20% charge at night time would only be applied. It is highly recommended to ensure SOC target control can manage the SOC to achieve the required start of the day SOC, rather than use a fixed number of hours to charge. For this purpose, battery charging may need to start earlier and last longer, if the day before was cloudy. On the other hand, it may be decided to discharge the energy storage back to the grid if end of day SOC is higher than what is required for the start of the following day.

The daily maximum rate of change of power is summarized in ***Table 20*** below. The low values of 5kW/min variation on November 5 and 6 occurred because the load management mode was successful for the entire day. High rate of change of 11 kW per min was observed for days with very high PV intermittency, when the lower SOC limit of the energy storage was hit and load management mode was not working.

Table 20 – Case Study 1: Daily Maximum Load Changing Rate (Weekdays)

Day in November	4	5	6	7	8	11	12	13	14	15	18	19	20	21	22
Max. Load Rate (kW/min)	7.48	5.01	5.00	5.45	9.82	8.24	10.84	5.72	8.54	6.89	11.00	8.37	10.47	8.04	7.38

On November 5, 2013, a load management goal of 0 kW was achieved for the entire day. On this day, PV generation of 89.45 kWh was higher than study case average while PEV charging of 71.7 kWh was less than the study case's daily average. With more generation than load, the end of the day SOC was increased to 56% from a starting SOC of 45% in the morning.

On November 15, 2013, the load management goal of 0 kW was achieved for only 33% of the time (66% failure). On this day, PV generation of 37.4 kWh was less than half of November 5 and less than the daily average of the study case while there was significant PEV charging, summing to 104 kWh. A starting SOC level of 70%, as opposed to 46%, would have helped the energy storage to maintain Load Management mode for much longer but having limited sunlight would eventually cause failure of the control mode (See Figure 103).

Figure 103 – Battery Performance on Friday, November 15, 2013

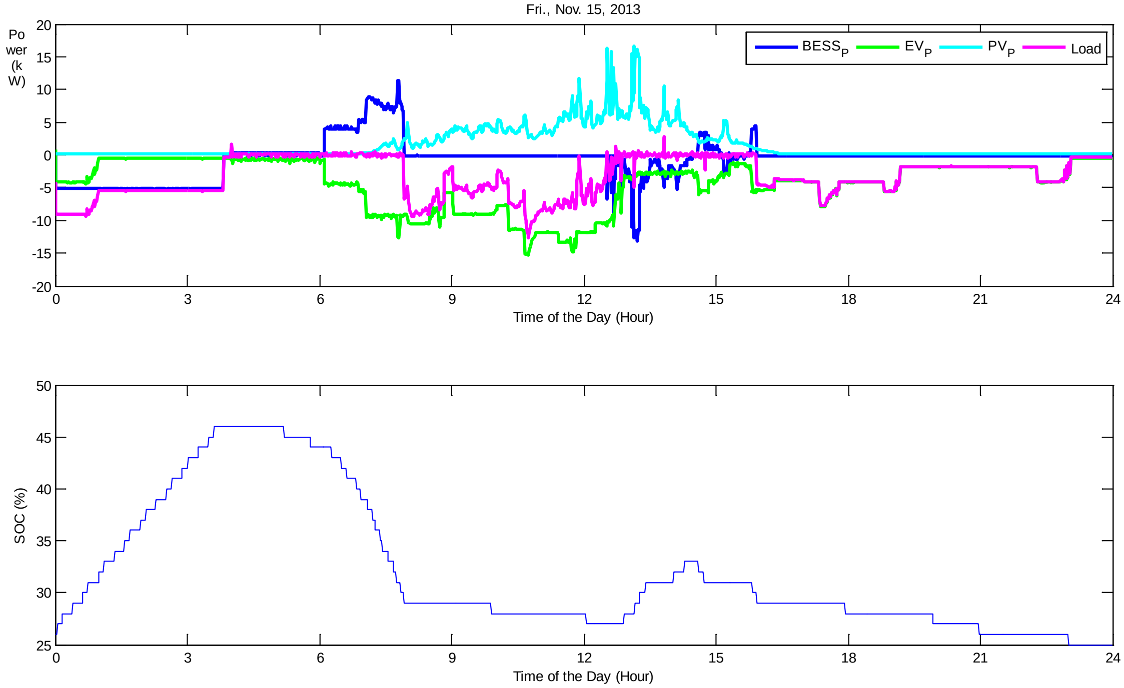

On November 8, 2013, significant PEV charging was observed at 99 kWh, similar to November 15. However, the load management goal of 0 kW was achieved for 90% of the time on this day. This increase in success of the control mode was due to having twice as much PV generation than November 15 at 84.99 kWh. This day could have had 100% success if its Start of Day SOC was higher than 46% (See Figure 104).

Figure 104 – Battery Performance on Friday, November 8, 2013

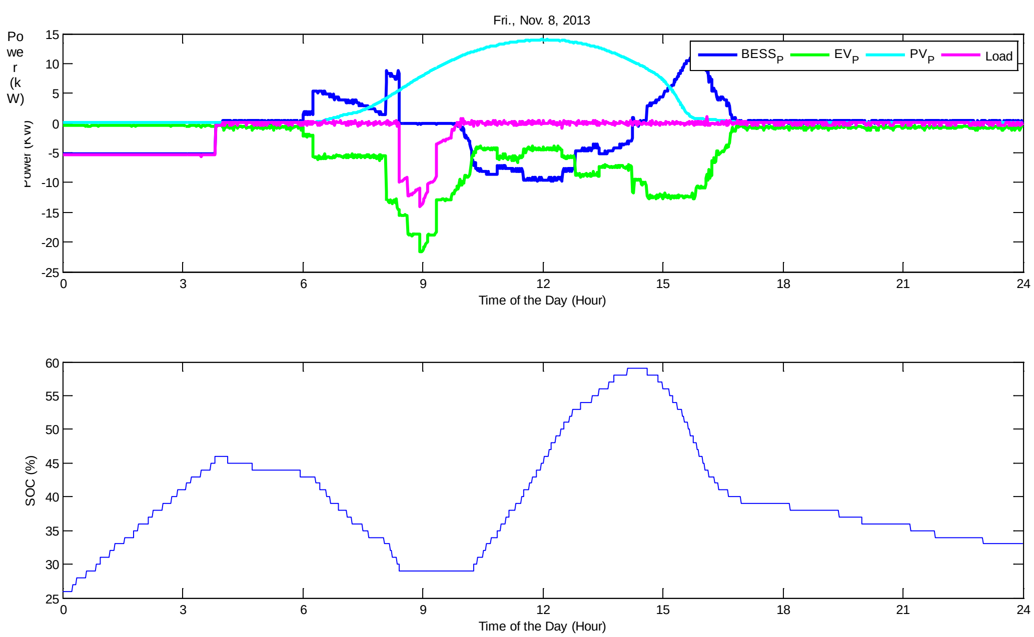

5.2.3 Case Study 2 – Maintaining Load at 5 kW (July 2013)

The performance of the Load Management Control at 5 kW was evaluated for the time period of July 17, 2013 – July 31, 2013. The main objective of the performance evaluation was to quantify the success of the energy storage regulating load flow at 5 kW and to limit the power flow of the main transformer from the grid during the day. The control mode is considered successful when the load meter reports an amount within the load profile set-point of 5 kW ±500. The daytime load management interval is considered from 12:00 pm to 9:00 pm in order to exclude any unusual night activities. This control mode was experimented typically in the afternoon and therefore morning data from 5:00am to 12:00 pm was excluded in the review. A load management set-point of lower than 5 kW or even negative was observed in early morning. Table 21 shows an approximated start time of load management control of 5 kW for each day. Based on the criteria given above, the energy storage load regulation of 5 kW was successful for 63% of the time in the selected 15 day period of Case Study 2. Table 21 provides daily success rates of the energy storage control system and a snapshot of best and worst days of operations.

Table 21 – Case Study 2: Daily Success Rate of Load Regulation

Day in July	17	18	19	20	21	22	23	24	25	26	27	28	29	30	31
Start Time (Hour)	12	10	11	11	10	9.5	11	11.5	10.5	12.5	10	9	10	8.5	12.5
Success rate (%)	75%	59%	50%	99%	88%	69%	83%	66%	81%	58%	51%	34%	43%	54%	30%

July 20 (Best Day)	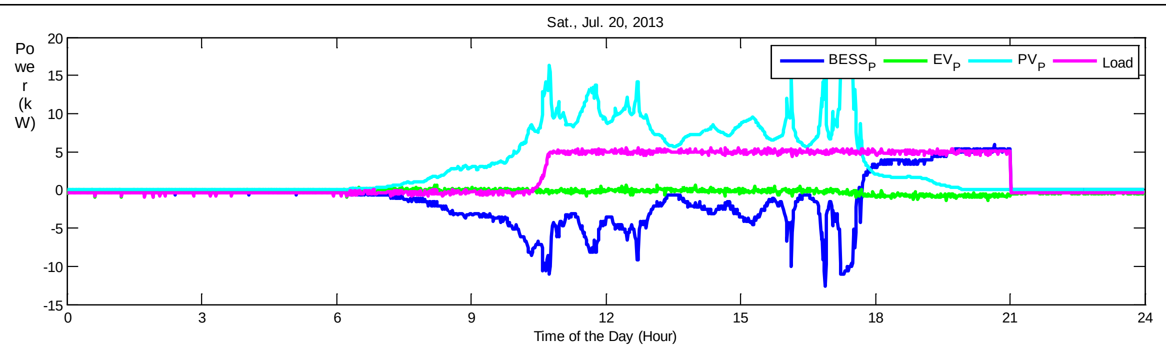
July 31 (Worst Day)	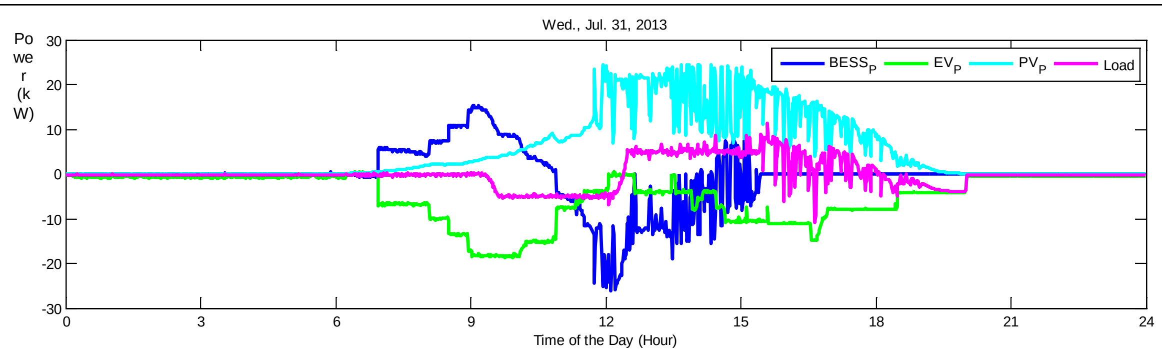

The average daily energy exchange for the BESS, main grid, PV generation, and PEV charging load is summarized in Table 22 below.

Table 22 – Case Study 2: Average Daily System Behavior

PV Generation (kWh)	PEV Charging (kWh)	BESS Charging (kWh)	BESS Discharging (kWh)	Load (+) (kWh)	Load (-) (kWh)
135.97	68.70	40.29	23.83	+66.82	- 14.60

In comparison with Case Study 1 (November 2013), PV generation was almost doubled in the month of July 2013. The control objective for this study case was to limit the load values to 5 kW. The load expects a positive energy flow back to the grid, for instances, when PV generation is higher than PEV charging and the energy storage is fully charged (100% SOC). This positive flow is considerably higher in the month of July compared to November as PV generation is almost double the PEV charging (66.82 kWh daily averages). The negative load flow (demand) of 14.6 kWh is due to load management being successful for only 63% of the time, resulting in the main grid to support the difference between PEV charge and PV generation for 37% of the time. It can be noted that there was no need for overnight charging in this case, since the battery was almost full at the end of the day. The success rate of 63% is less than Case Study 1, due to a lower difference between PV and PEV (high generation month). Further detailed investigation of the SOC is required to properly optimize the load management mode.

In contrast to Case Study 1, load management of 5 kW was also experimented during weekends and holidays for the month of July due to a very high PV generation (See ***Figure 105***). It is difficult for this mode to be successfully applied on the weekends, due to a lack of EV load. The energy storage is expected to absorb the difference between the PV generation and the 5 kW load management set-point for the entire day.

Figure 105 – Battery Performance on Saturday, July 20, 2013

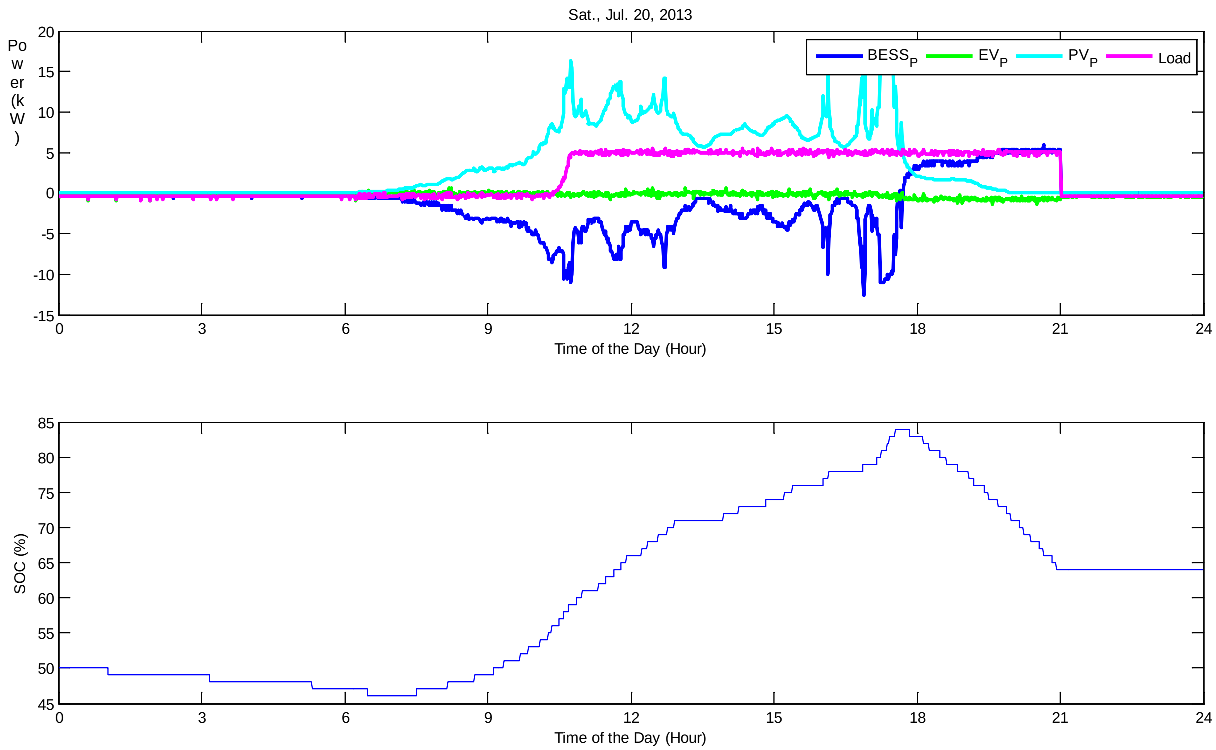

It was observed that the energy storage SOC management was critical for the success of the load management mode. The Start of Day SOC was defined as the battery state of charge at 4:00 am (end of the scheduled overnight charge, if used). The average start of the day SOC for Case Study 2 was approximately 65%. End of Day SOC was calculated at midnight just prior to the scheduled overnight charge, if any. The average End of Day SOC for Case Study 2 was approximately 69%. It was expected that the End of Day SOC be higher as the average PEV charging load was considerably less than PV generation and the energy storage was expected to absorb the difference in PV generation and PEV demand to keep the main grid contribution at 5 kW (see Table 23). No overnight charging was required as the end of the day SOC was typically higher than the start of day charge level.

Table 23 – Case Study 2: Start and End of Day SOC

Day in July	17	18	19	20	21	22	23	24	25	26	27	28	29	30	31
Start of Day SOC	61%	59%	75%	61%	61%	59%	62%	65%	58%	61%	58%	81%	81%	71%	63%
End of Day SOC	56%	81%	50%	64%	52%	81%	71%	68%	52%	50%	84%	84%	73%	84%	81%

Furthermore, SOC distribution for the entire study case 2 was calculated and presented in Table 24. The expectation was to use the entire range of SOC in order to take full advantage of the battery cells. It was observed that energy storage was typically full for the majority of the time due to the difference between the high PV generation and moderate EV load. It was also observed that the lower 20% extreme of SOC was unavailable for the load management mode. Therefore, the load management control was only able to utilize 80% charge of the energy storage.

The SOC was above 70% charge for more than 54% of the time compared to less than 3% of time below 40% charge. Initial observation of higher PV generation than EV charge with the increase of SOC from Start to End of Day suggest the battery required additional overnight discharges to start the day with a lower SOC than 65%. This conclusion does not allow us to have the energy storage start at 0% charge in the morning as there will still be instances of EV load larger than PV generation and therefore the energy storage must discharge the difference.

Table 24 – Case Study 2: Battery SOC Distribution

SOC Interval (%)	0-10	10-20	20-30	30-40	40-50	50-60	60-70	70-80	80-90	90-100
Operation (%)	0%	0%	2%	1%	12%	16%	16%	18%	18%	18%

Daily patterns showed a high PEV charge in early morning when employees returned their electric vehicles to the charging station as well as in the evening just after working hours. With limited PV generation during these stages, the energy storage was expected to compensate a large difference causing an SOC drop. With careful attention to all available data, the SOC can drop by 30% early in the morning. Based on the observations above, the starting SOC should have been considerably less than the average 65% to optimize the amount of time the Load Management Mode is met. With limited prediction of future PV and PEV profiles as well as a fixed set-point available in the energy storage control panel, the 35% average should be the starting SOC for the month of July.

The fixed overnight scheduled charge was not recommended as there is no control on the Start of Day SOC. It is highly recommended to use the SOC management mode to ensure that the Start of Day SOC will always be at the same percentage. The energy storage for the summer season will actually discharge back to the grid since End of Day SOC is higher than what is required at the start of the following day. It is also observed that a fixed 5 kW set-point is difficult to maintain for the entirety of the day regardless of the starting SOC. The energy storage was simply too small to maintain the high discharge of early morning and night as well as the high charge requirements of summer PV generation in the afternoon. A hybrid of various load management step sizes is advisable.

The daily maximum rate of change of power is summarized in Table 25 below. A low value of 5.44 kW/minute variation on July 20 was used because the load management mode was successful for the entire the day. High rate of change of 14.36 kW per minute was observed on a very high PV intermittency day when the upper threshold of SOC limit for the energy storage was hit and load management mode was automatically stopped. The lowest rate of change of 0.97 kW per minute was observed on a smooth PV output day.

Table 25 – Case Study 2: Daily Maximum Load Rate

Day in July	17	18	19	20	21	22	23	24	25	26	27	28	29	30	31
Max. Load Rate (KW/min)	9.03	6.99	3.19	5.44	0.97	5.45	8.02	7.03	5.83	2.88	14.36	5.45	5.47	4.98	12.29

On July 18, 2013, the load regulation goal of 5 kW was achieved for 59% of the day. On this day, the starting SOC was 59%, PV generation was 167.67 kWh (higher than the study case average), while PEV charging equating to 79.95 kWh was observed. With more generation than load, the energy storage reached its full capacity at 2:00 pm. Unable to absorb any more energy, the load management at 5 kW was not followed for the next 4-5 hours. The control mode was able to continue load management in the evening after sundown when EV charging was higher than PV generation (See Figure 106).

Figure 106 – Battery Performance on Thursday, July 18, 2013

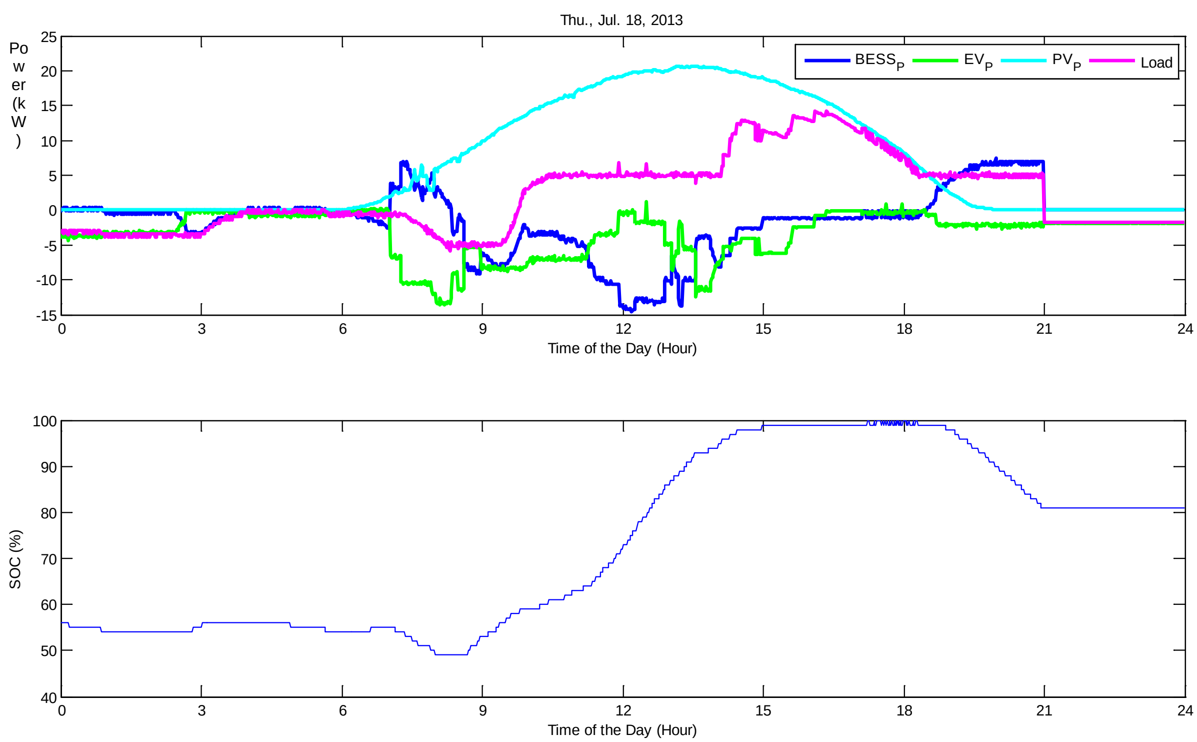

On July 23, 2013, the load regulation goal of 5 kW was achieved for 83% of the time (17% failure). On this day, the starting SOC was 62%, PV generation was 158.08 kWh while experiencing PEV charging of 119.7 kWh. With a smaller difference between PV generation and PEV load of July 18th, the full capacity of the energy storage appeared for less than 2 hours and the control was able to maintain its 5 kW set-point for a longer period (See Figure 107).

Figure 107 – Battery Performance on Tuesday, July 23, 2013

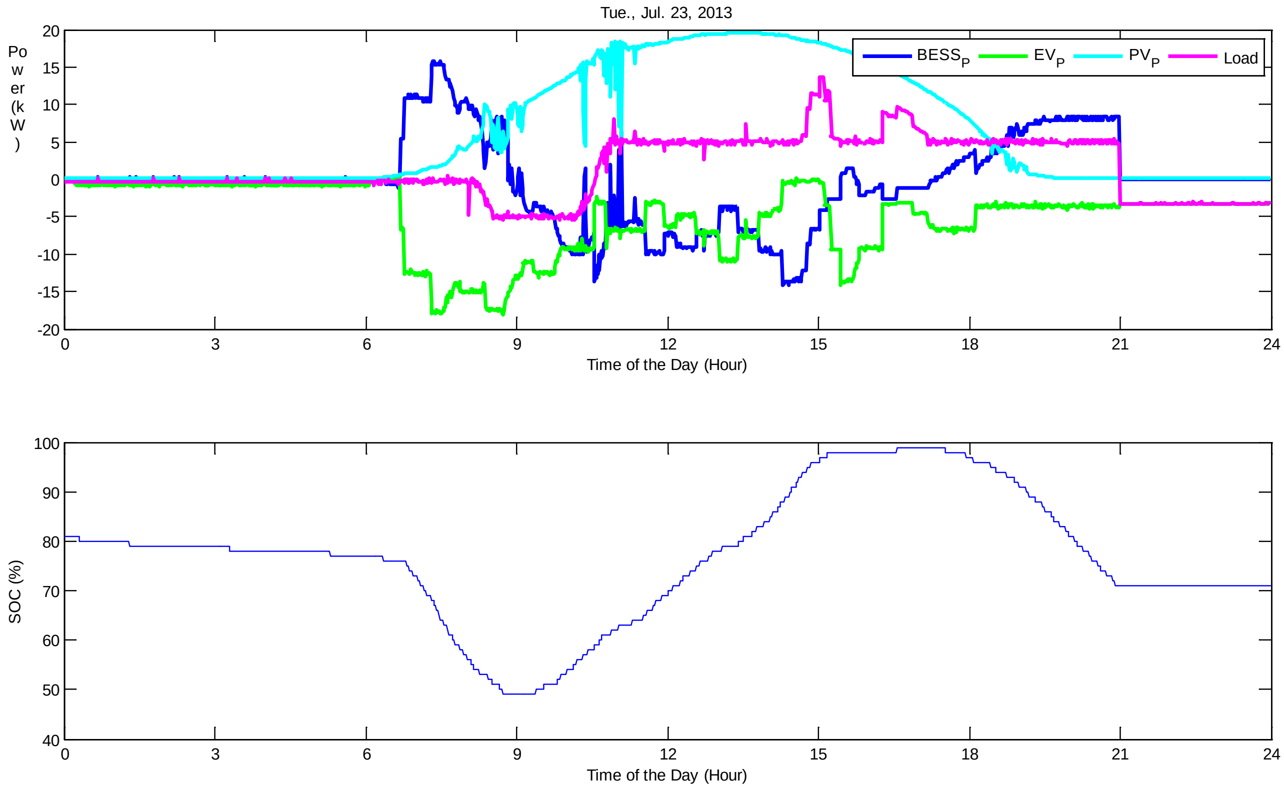

5.2.4 Case Study 3 – Maintaining Load at 10 kW (August 2013)

The performance of the Load Management Control with a 10 kW set-point was evaluated for the time period of August 22, 2013 – August 25, 2013. The main objective of this performance analysis was to monitor the success of the energy storage regulating load flow at 10 kW and to limit the power flow of the main transformer from the grid during the day. The mode was considered successful when the load meter reported an amount within the load profile set-point of 10 kW ± 500 W (accounts for minor fluctuations). Due to a high load management set-point of 10kW and the energy storage's inability to maintain such energy level for an entire day, this study case consists of 4 days with partial 10 kW regulation mode. The approximated duration of this mode for each day is represented in Table 26.

Table 26 – Case Study 3: 10 kW Mode Duration

Day in August	Aug 22	Aug 23	Aug 24	Aug 25
Start Time	10:30 am	12:00 pm	9:30 am	9:30 am
End Time	2:00 pm	4:00 pm	9:00 pm	9:00 pm

Based on the criteria given above, the energy storage load regulation of 10kW was successful for **87%** of the time for the 4 day sampling period used in the Case Study 3. Table 27 provides daily success rate of the energy storage control system and a snapshot of best and worst days of operations.

Table 27 – Case Study 3: Daily Success Rate of Load Regulation (Weekdays)

Day in August	22	23	24	25
Duration of Mode (Hours)	3.50	4.00	11.50	11.50
Success Rate (%)	72%	92%	93%	93%

August 23

(Weekday)

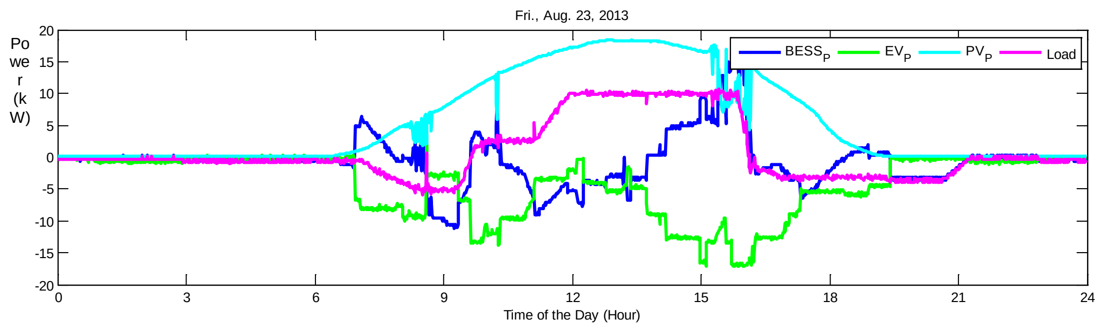

August 25

(Weekend)

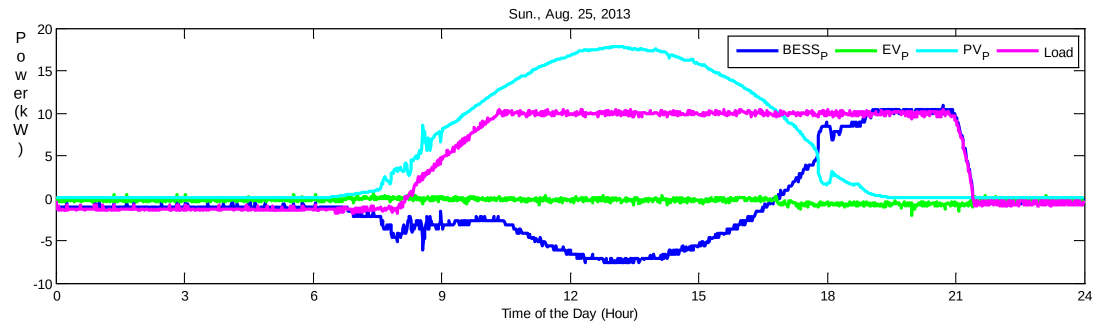

The average daily energy exchange for the BESS main grid, PV generation, and PEV charging load is summarized in Table 28 below.

Table 28 – Case Study 3: Average Daily System Behavior

PV Generation (kWh)	PEV Charging (kWh)	BESS Charging (kWh)	BESS Discharging (kWh)	Load (+) (kWh)	Load (-) (kWh)
137.83	67.66	44.22	29.36	+80.69	- 25.60

In comparison with Case Study 2, PV generation and PEV load are comparable to the month of July 2013. The grid, however, experiences a lower positive energy flow even with a higher set-point of 10 kW compared to the 5 kW regulation of Case Study 2. This is due to the fact that the time interval for 10 kW load management is considerably less than the 5 kW set-point during the day.

It was observed that the average starting SOC for the 10 kW load management on each day was approximately 56%. End of the day SOC was also calculated with an average of 47% (See Table 29).

Table 29 – Case Study 3: Start and End of Day SOC

Day in August	22	23	24	25
Start of Day SOC	56%	58%	54%	55%
End of Day SOC	51%	49%	44%	44%

Furthermore, SOC distribution for the entire study case was calculated and presented in Table 30. Expectation was to use the entire range of SOC in order to take full advantage of the battery cells. It was observed that energy storage was typically full for the majority of the time. The battery charge did not go below 40% for the entirety of 4 days.

In fact, the majority of the time, the SOC fluctuated between the 40% and 60% range. As shown below, the battery load management of 10 kW was timed perfectly for a full half cycle. The energy storage started to charge the battery using the difference between peak PV and 10 kW for the first half of its control mode. Once PV contribution died down, the SOC dropped near to its original starting SOC by discharging a fixed 10 kW back to the grid with minimal PV contribution to assist. However, the energy storage was simply too small to maintain the high load regulation of 10 kW for the entirety of the day. A hybrid of various load management step sizes is advisable.

Table 30 – Case Study 3: Battery SOC Distribution

SOC Interval (%)	0-10	10-20	20-30	30-40	40-50	50-60	60-70	70-80	80-90	90-100
Operation (%)	0%	0%	0%	0%	53%	26%	7%	4%	5%	4%

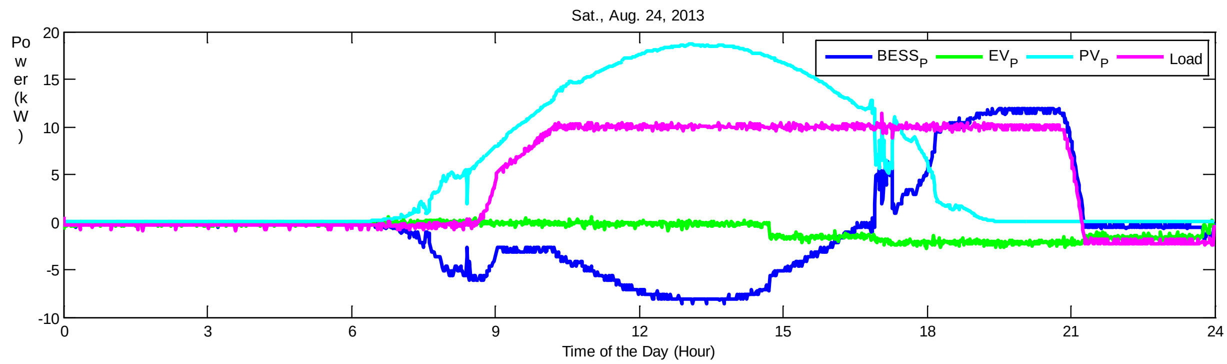

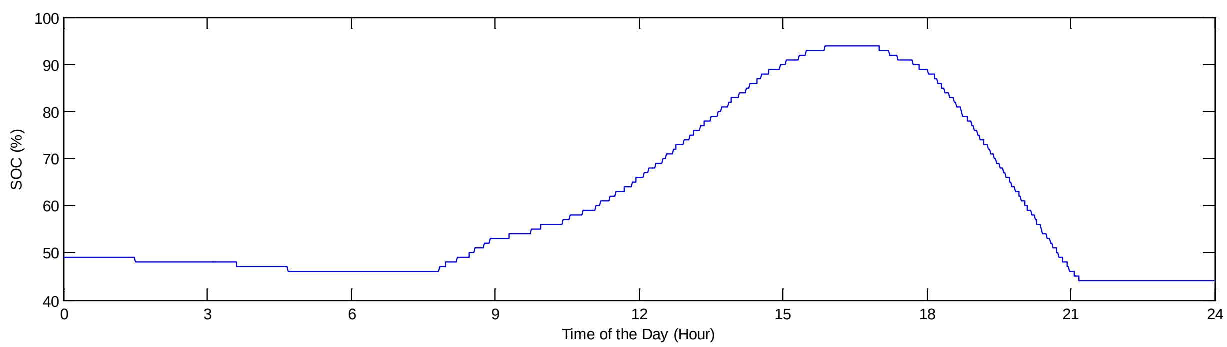

CHAPTER 6: Conclusions

In this project, the impact of Plug-in Electric Vehicles (PEVs) on SDG&E's distribution feeders was studied. Two PEV hardware simulators were designed and built to represent electric vehicles in the field. A Real Time Digital Simulator (RTDS) was used in conjunction with Power Hardware in the Loop (PHIL) and the PEV simulators to accurately simulate the distribution feeder, PEV charging, control functions, and impact and hardware response.

6.1 Distribution Feeder Impact Studies

A survey of SDG&E distribution feeders was conducted, and through the use of a fuzzy inference system, the feeders were ranked according to a set of selected criteria. Circuit A, a 12kV feeder with 41 distributed PV sources and 14 customers with plug-in electric vehicles, was selected for representative testing.

A test plan to evaluate system impact covering various types and sizes of EV chargers installed on the representative distribution circuits was developed and detailed. Changes in primary and secondary voltages, as well as active and reactive power flow through service transformers were measured and reported. Overall, it was assumed that various types of EV chargers were installed and utilized by residential customers or deployed at public locations.

Several test scenarios were proposed and tested, including cases with:

- Single customers utilizing EV chargers
- Multiple customers in vicinity of each other using EV chargers
- Multiple customers supplied from a common service transformer using EV chargers
- All existing customers with EV chargers using their EV chargers
- All represented customers and lumped loads on the circuit using EV chargers

In addition, the sizes of the EV chargers were randomly selected and assigned to service transformers. In areas where roof-top or small commercial PV systems were also available, PV system were modeled and included in the tests and studies.

Two EV utilization scenarios were also incorporated.

- **Scenario 1 (Uncontrolled Scenario)**: Use of EV chargers was assumed to be uncontrolled. In this scenario, EV customers would start charging their vehicles as soon as they arrived at residential or small commercial locations with level 2 AC chargers. To arrive at a more realistic case, the size, start time and end time of the EV charging were randomly selected and incorporated into the test plan to represent a consistent set of test data for various tests and investigations. As a result, most EV chargers would start the charging process during the evening time.

- **Scenario 2 (Controlled Scenarios):** EV chargers had assigned very specific start times, according to the off-peak time of the system, and/or observation of low electricity cost. Selected time, State of Charges (SOC) and starting time of the EV chargers under controlled scenarios were also randomized to represent a realistic case. The EV charging data for this scenario were also incorporated into the test plan (Please see Plan Tables in Section 3.3) to be consistently applied and tested for various conditions.

The EV Simulator Rack 2 was also implemented in a way that smart inverter functionalities and dynamic controls through communications schemes could be tested as stand-alone or with RTDS. Several closed-loop tests were performed with power hardware in the loop to explore commanding and controls through communications.

Some of the main findings from the tests were:

- The main impact of EV charging was noted to be on the transformer current and power flow profile of the circuit. In some cases, the current through transformer was tripled. The 25 kVA transformers were in danger mostly, while the larger transformers (50 kVA and 100 kVA) had more margins for accepting additional demand of the EV charging loads.
- Due to the increased loading, the voltage drops on the secondary circuits were highly observable. If the voltage on secondary circuits was very close to the lower band of the acceptable voltages, additional load of the EV chargers would reduce the voltage beyond the acceptable range. The uncontrolled charging patterns had shown more significant impact on the voltage.
- Because the controlled charging mostly occurred during late evening time, voltage was higher at that time compared to the late afternoon or early evening. Hence, the impact on the secondary voltage drop was lower compared to the un-controlled scenarios.
- In most tested cases, there was less impact on the primary circuit voltages at 12 kV.

Overall, it was shown that the EV Simulator and the power hardware in loop test setup provided a flexible environment for various testing of EV impact on the service transformer and the primary or the secondary circuits. Different circuit arrangements or multiple customer connection points could be represented in the model and test bed, and re-arranged to meet changes in circuit characteristics or the nature of the loads.

6.2 Integration Studies and Mitigation Solutions

The main objective of integrating PEV charging stations with PV and BESS in a hybrid system architecture was to demonstrate load control and power management capabilities of this approach to eliminate resource intermittency and avoid circuit overloading due to extensive loading of PEV charging stations. The demonstration project showed that the hybrid design and integrated PV+PEV+BESS was a viable and beneficial approach. Load control and peak shaving can be performed through this design. BESS was able to maintain the specified load level under certain conditions. Analysis of the performance data for several months of operations have facilitated detailed examination of system design and control behavior.

Because the BESS controls do not have any information (prediction) about the PV production levels, the BESS would not be able to effectively maintain the load level for all seasons. In addition, during the demonstration, the number of charging stations and amount of PEV utilization were significantly increased. Hence, without incorporating additional intelligence into the control schemes to account for seasonal variations and load growth, the control scheme will not be able to compensate for the growing number of charging stations and seasonal PV production.

Analysis of the field measurement data and detailed performance evaluations also showed that some aspects of the control schemes did not perform as described by the vendor. There were discrepancies in the start time and end period of the control scheduler. In several cases, the BESS load management control did not meet the target SOC or failed to match the given load threshold, even though the battery had enough reserve capacity and/or the PV production was sufficient to maintain loading. The control scheme presently utilizes one threshold level for adjusting load, irrespective of the power flow. However, the power flow through the transformer can become negative (reverse flow) due to high PV production and light PEV charging loads. This aspect suggests that a two level approach may be more effective.

The observed control system abnormalities were reported to the BMS vendor for further investigations.

Based on observations from the analysis of the field data, and in the absence of production prediction features, performance of the load management control of the hybrid BESS system can be optimized by using multi-layer load thresholds. The load thresholds will be varied throughout the day to follow expected variations in the PV production and loads. The optimized control mode is intended to keep the load contribution consistently at a pre-selected level for a given period of time, then change the load level to a new level to avoid full charge or complete discharging of the battery and losing the control. This approach will ensure sudden change in transformer load due to changes in the PEV charging and PV intermittencies are eliminated with respect to the grid.

With careful consideration of all the three study cases, it is apparent that a single load management level (0 kW, 5 kW, or 10 kW) is not advisable for the entire day and cannot be maintained in all conditions. This is due to the financial strain of providing bigger energy storage for each PEV charging station as well as very high PV generation in California during certain months.

The proposed scheduled step load management shown in Figure 108 is expected to optimize SOC to control the load on a service transformer, while eliminating PV intermittencies. This control requires SOC management mode to be applied after midnight in order to ensure a starting SOC of 35% at 5:00 am of each day – for the summer season. The target SOC has to be re-defined for each season, since the PV production and energy balancing requirements will be different from season to season. As an example, a look-up table approach can be used for this purpose.

In summer months, it is expected for the energy storage to gradually charge for the entire morning and afternoon, reaching from target SOC (e.g. 35%) to full charge. Later in the afternoon, battery will start discharging because of the increasing demand of the PEVs, as well as the required energy to maintain a scheduled load management of 3 kW during the evening.

It should be noted that starting SOC in winter season should be increased to 70% to compensate for low PV generation.

Figure 108 – Proposed Step Load Management Control in the Absence of PV Production Prediction

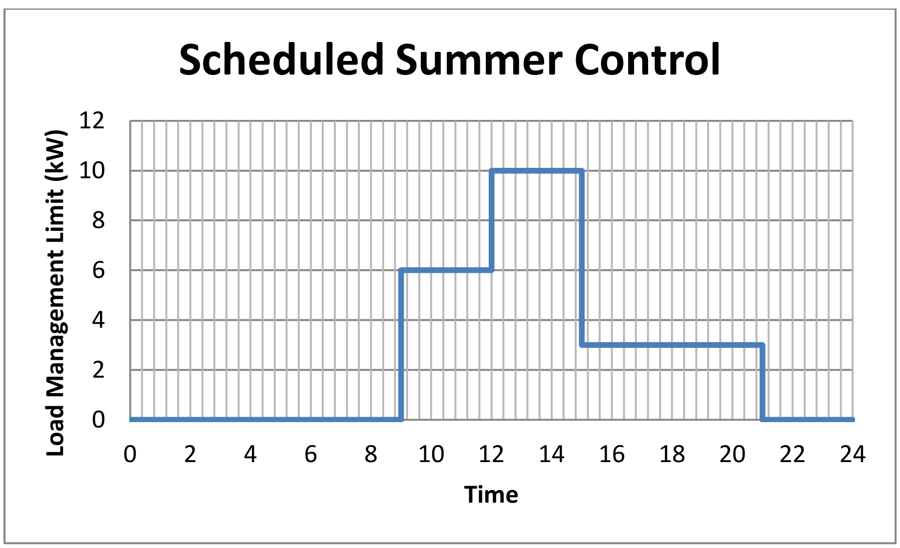

Time of Day	Limit Sent to Grid (kW)
0-9	0
9-12	6
12- 15	10
15-21	3
21-0	0

Starting SOC: 35% @ 5:00 am

6.3 Next Steps - Applicability of EV Simulator for Inverter Testing and Advanced Charging Controls

The PEV Simulators were designed with the use of commercial off-the-shelf PV inverters. The control and communication capabilities of the PV inverters were utilized to produce various charging profiles by adjusting re-generative load of the setup on EV chargers. As a result, EV simulator can also be utilized to investigate various impacts of integrating power electronic based resources (both power electronic generation and electronic loads) on the grid.

The setup can be used to show controllability and remote dispatching of distributed energy resources through smart inverter control functionalities, such as power curtailments, power factor adjustment, and reactive power compensation.

Potential future applications of the EV simulator and power hardware in loop testing test bed are listed below.

- Investigation of various EV price matrices and impact on load shifting
- EV charger as a continuously controllable and dispatchable resource (needs additional remote communications)
- Smart Inverter and electronic load integration testing
- Bi-directional charger for vehicle-to-grid testing (needs minor change in the control and power hardware)

Some applications may need minor enhancement into the user HMI to activate control features. New control options and capabilities can be easily added to the HMI through initial system configuration menu or a quick software upgrade. The control programing follows standard structured text language to ensure future changes can be easily implemented.

GLOSSARY

Term	Definition
AC	Alternating Current
AI	Analog Input
AO	Analog Output
ACSR	Aluminum-conductor steel-reinforced cable
AWG	American wire gauge
BESS	Battery Energy Storage System
BEV	Battery Electric Vehicle
COMM	Communications
D	Depth
d/q	Direct and Quadrature (two dimensional frame)
DC	Direct Current
DI	Digital Input
DO	Digital Output
Energy Commission	California Energy Commission
EPL	Ethernet Powerlink
EV	Electric Vehicle
EVSE	Electric Vehicle Supply Equipment
ft	Feet or foot
FTP	File Transfer Protocol
GTAI	Special Analog Input Card for RTDS
GTAO	Special Analog Output Card for RTDS
GTDI	Special Digital Input Card for RTDS
GTDO	Special Digital Output Card for RTDS
H	Height
HMI	Human Machine Interface
I/O	Input & Output
kg	Kilograms
kVA	Kilovolt Ampere
kVAR	Kilovolt Ampere Reactive
kW	Kilowatt
kWh	Kilowatt Hour
lb	Pounds
LCD	Liquid Crystal Display
PEV	Plug-in Electric Vehicle
PGM	Power Generation Meter
PHEV	Plug-In Hybrid Electric Vehicle
PHIL	Power Hardware-In-Loop
PI	Proportional Integrator

PIER	Public Interest Energy Research
PLC	Programmable Logic Controller
PLL	Phase Locked Loop
PQ	Power Quality
PQM	Power Quality Meter
RD&D	Research, Development and Demonstration
RTDS	Real Time Digital Simulator
RTU	Remote Terminal Unit
SDG&E	San Diego Gas & Electric
sec	Seconds
SOC	State of Charge
TOV	Temporary Overvoltage
TPH	Three Phase (for fault)
V	Volt
W	Width
XFMR	Transformer

REFERENCES

ALCAN, Inc. cable data, https://www.platt.com/CutSheets/Generic/ACSR%20Alum.pdf.

Constantin Von Altrock, (1995). Fuzzy logic and NeuroFuzzy applications explained. Upper Saddle River, NJ: Prentice Hall PTR.

CP solar carport electrical site plans: E-201 – E-203

G. B. Folland, (1999). Real Analysis: Modern techniques and their applications (Second ed.). John Wiley & Sons, Inc.

GS Energy Management System – DESS portal 3.2, user guide, 2013.

J. W. Choi, Y. K. Kim; H. G. Kim, "Digital PLL control for single-phase photovoltaic system," Electric Power Applications, IEEE Proceedings, vol. 153, no.1, pp.40-46, Jan. 2006.

L. Xu, M. Marshall, L. Dow, "A framework for assessing the impact of plug-in electric vehicle to distribution systems", in Proceedings of 2011 IEEE PSCE, Mar 2011, Phoenix, AZ.

Project Report – "Appendix G: Distribution Circuit Survey" (Task 2.2), May 2013.

Project Report – "Appendix H: Grid Impact Testing and Data Analysis" (Tasks 2.5 and 2.6), February 2015.

The MathWorks – Accelerating the pace of Engineering and Science Website, Fuzzy Interface Process R2012b - http://www.mathworks.com/help/fuzzy/fuzzy-inference-process.html.

APPENDIX A:
Detailed Fuzzy Logic Methodology and Example

This section describes the fuzzy inference process. The basic fuzzy algorithm structure applied in this study is shown in the following diagram. Information flows from left to right, from five circuit attributes (only three shown in the figure) to a single output. (i.e., the score for each circuit)

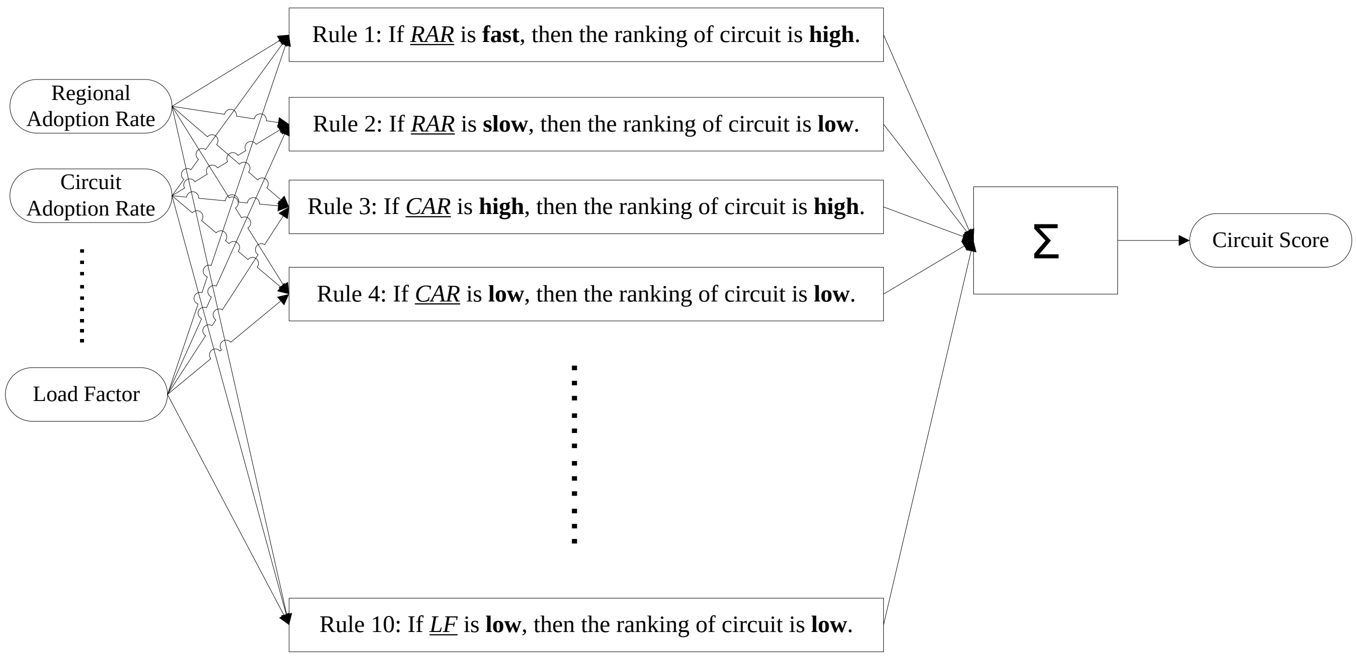

Figure 109 – Fuzzy Inference Diagram

Input Normalization

As indicated earlier, the input data are first normalized to the range of [0, 1] to avoid any potential bias due to different magnitude of input variables. During the normalization process, the smallest value of an attribute is set to 0, the largest value of the attribute is set to 1, and all the remaining values are linearly normalized to a value between 0 and 1. For instance, Table 34 in Appendix B lists the raw data for circuit length. The shortest circuit length is 19,953 ft (Circuit A); its normalized value is 0, as shown in Table 31. The longest circuit length is 54,086 ft (Circuit I); its normalized value is 1. The normalized values of circuit length, along with those of other selected attributes, are input to the fuzzy algorithm. The complete input normalization data are presented in Table 31.

Table 31 – Normalization of Circuit Length

Circuit ID	Circuit Length (ft)	Normalized Input
A	19,953	0.00
B	46,848	0.79
C	30,203	0.30
D	37,472	0.51
E	42,646	0.66
F	27,682	0.23
G	41,352	0.63
H	34,032	0.41
I	54,086	1.00
J	36,690	0.49
K	27,458	0.22

Fuzzy Rules

Basic if-then rules are adopted in this study to define the mapping from circuit features to its likelihood of being impacted by high penetration of PEV charging. The if-then rules utilized in the algorithms are listed below:

- If *PEV regional adoption rate* is **fast**, then the ranking of circuit being both representative and prone to high PEV penetration is **high**.
- If *PEV regional adoption rate* is **slow**, then the ranking of circuit being both representative and prone to high PEV penetration is **low**.
- If *PEV circuit adoption rate* is **high**, then the ranking of circuit being both representative and prone to high PEV penetration is **high**.
- If *PEV circuit adoption rate* is **low**, then the ranking of circuit being both representative and prone to high PEV penetration is **low**.
- If *PEV adoption diversity factor* is **large**, then the ranking of circuit being both representative and prone to high PEV penetration is **high**.
- If *PEV adoption diversity factor* is **small**, then the ranking of circuit being both representative and prone to high PEV penetration is **low**.

- If *Circuit length* is **long**, then the ranking of circuit being both representative and prone to high PEV penetration is **high**.
- If *Circuit length* is **short**, then the ranking of circuit being both representative and prone to high PEV penetration is **low**.
- If *PEV load factor* is **high**, then the ranking of circuit being both representative and prone to high PEV penetration is **high**.
- If *PEV load factor* is **low**, then the ranking of circuit being both representative and prone to high PEV penetration is **low**.

This study is built on ten rules and each of the rules depends on resolving the inputs into a fuzzy linguistic set: regional adoption rate is fast, regional adoption rate is slow, circuit length is long, circuit length is short, and so on. Same to the antecedent part of the rule, the consequent part of the rule is also a fuzzy set: either the circuit score/ranking is high or the circuit score/ranking is low. It is also represented by a membership function. In this study, triangle membership function is also the form used.

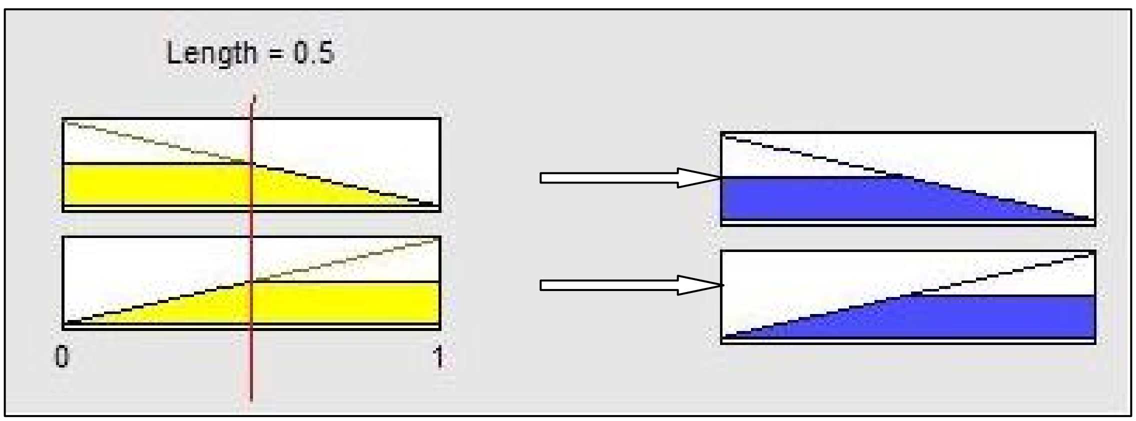

Figure 110 – Fuzzy Rules Implication

Circuit length is used as an example to explain the fuzzy rule inference or implication. In Figure 110, the left part colored in yellow represents the antecedent of the rules and the right part colored in blue represents the consequent of the rules. The top row represents the rule (*If circuit length is short, then the ranking of circuit is low*) and the bottom row represents the rule (*If circuit length is long, then the ranking of circuit is high*). The input for the implication process is a single number given by the antecedent (0.5 in this example) and the output is a fuzzy set. The commonly used implication method is to truncate the output fuzzy set (indicated by blue color). Therefore, the consequent is reshaped using a function associated with the antecedent.

APPENDIX B:
Summary of Raw Circuit Data for Circuit Selection and Study

The following data are used for circuit selection.

Regional Adoption Rate

Table 32 – Raw Data for PEV Regional Adoption Rate

Circuit ID	Substation Name	# PEV	Regional Adoption Rate (% of Total PEV in SDGE[1])
A	DM	63	4.94%
B	NCW	66	5.17%
C	NCW	66	5.17%
D	DM	63	4.94%
E	CC	50	3.92%
F	RN	50	3.92%
G	EN	50	3.92%
H	PO	33	2.59%
I	MRM	14	1.10%
J	CB	14	1.10%
K	EL	21	1.65%

[1]The total number of existing PEV installations as of January 2013 is 1,276 in SDG&E's service territory.

Adoption Diversity Factor

Table 33 – Raw Data for PEV Adoption Diversity Factor

Circuit ID	Circuit PEV/Substation PEV (%)	Adoption Diversity Factor
A	22.22%	4.50
B	34.85%	2.87
C	25.76%	3.88
D	19.05%	5.25
E	22.00%	4.55
F	22.00%	4.55
G	22.00%	4.55
H	45.45%	2.20
I	78.57%	1.27
J	78.57%	1.27
K	52.38%	1.91

Circuit Length

Table 34 – Raw Data for Circuit Length

Circuit ID	OH Length (Feet)	UG Length (Feet)	Total Circuit Length (Feet)
A	14,619	5,334	19,953
B	0	46,848	46,848
C	0	30,203	30,203
D	13,534	23,938	37,472
E	2,140	40,506	42,646
F	4,734	22,948	27,682
G	27,314	14,038	41,352
H	24,114	9,918	34,032
I	0	54,086	54,086
J	27,923	8,767	36,690
K	0	27,458	27,458

Circuit Adoption Rate

Table 35 – Raw Data for PEV Circuit Adoption Rate

Circuit ID	# Residential Customer	Circuit Adoption Rate (PEV/Residential Customer)
A	1,728	0.81%
B	2,199	1.05%
C	2,291	0.74%
D	3,444	0.35%
E	2,730	0.40%
F	2,606	0.42%
G	4,672	0.24%
H	2,020	0.74%
I	3,159	0.35%
J	3,626	0.30%
K	3,337	0.33%

Load Factor

Table 36 – Raw Data for PEV Load Factor

Circuit ID	Historical Load (Amps)	Load Factor PEV/Load (%)
A	189.00	7.41%
B	527.16	4.36%
C	404.08	4.21%
D	474.48	2.53%
E	406.68	2.70%
F	222.12	4.95%
G	473.80	2.32%
H	468.00	3.21%
I	375.60	2.93%
J	385.48	2.85%
K	445.00	2.47%

APPENDIX C:
Primary System Modeling Methodology Details

The development of a RSCAD/RTDS model is subject to limitations imposed by the hardware which would not apply to offline simulation packages such as PSCAD or SynerGEE. To guarantee real time solvability of the system, the RTDS pre-allocates its available hardware resources based on CPU capability. In particular, two restrictions need to be considered:

1. **A Limited Number of Electrical Nodes**: Requires a consideration of what portion of the system should be modeled, and which portion can be simplified or lumped together

2. **A Limited Number of CPU Slots**: Again requires a careful consideration of which elements to model and which elements can be aggregated

The above limitations usually impose a requirement for the simplification of the system under consideration to "fit" within the size resources of the RTDS system. In the case of Circuit A, since the EV locations were the aspect under study, the simplification philosophy was to model the system from source to EV location as accurately as practically possible, and to simplify (lump) other branches. Nodes were maintained at major line splits, EV locations, and Distributed Generation (DG) locations in the direct upstream path of an EV location.

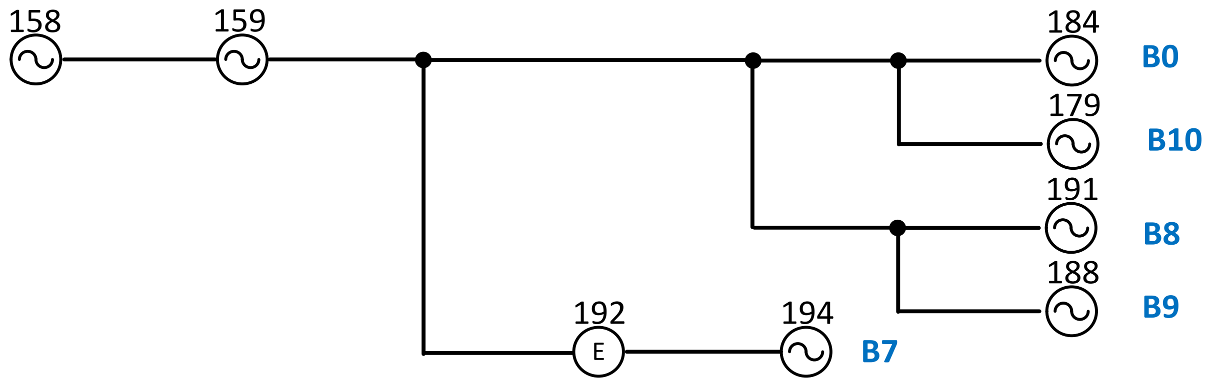

Figure 111 – A Portion of System in the Presence of a Single EV and a Number of Distributed Generators

In the example shown in Figure 111, a number of distributed generators, a single EV, and a number of line splits are present on the portion of the system. Under the selected philosophy, node locations are at:

- **EV 192 Location** – all EV locations are explicitly modeled;
- **Line Split** – major line splits are modeled, downstream portions with no EV can be lumped
- **DGs 159 and 158** – when practical, DGs in the direct upstream path of an EV (EV192 in this case) are modeled

The above considerations would result in four nodes being required to model the system, as shown in Figure 112. The portions of system downstream of the EV location or downstream of the major line split are lumped.

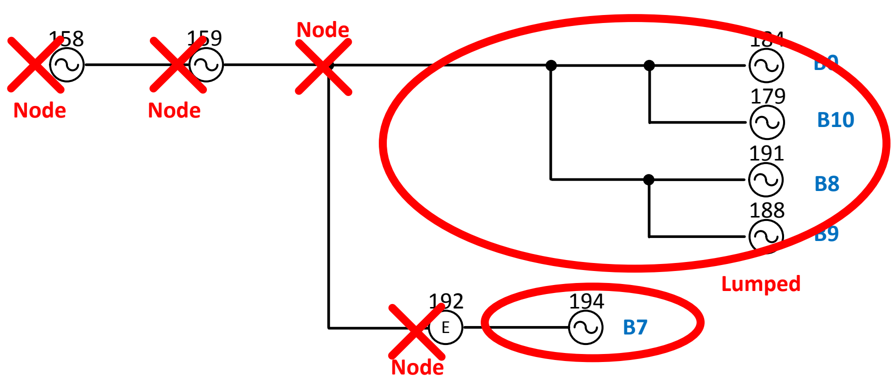

Figure 112 – Required Nodes for Modeling

The simplified portion of the system, modeled in the RTDS, is shown in Figure 113.

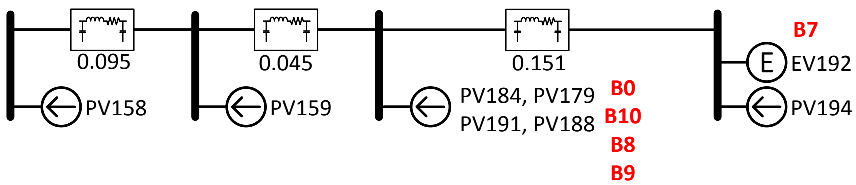

Figure 113 – The Simplified Model of the Portion of System in RTDS

The line segments are modeled as PI segments, with parameters extracted from SynerGEE and calculated as a summation of impedances of the lines in-between the selected nodal points. The methodology is shown in Figure 114 below – parameters for the individual segments are calculated based on conductor and length, and individual segments are summed to obtain an equivalent PI section.

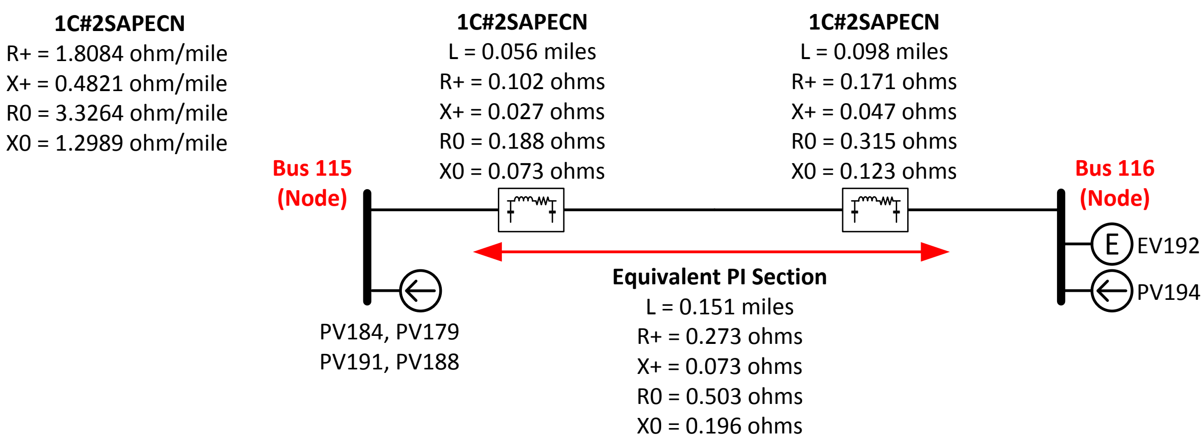

Figure 114 – Parameters Calculation for an Individual Segment of the System

Three-phase loads in RTDS each require one of the limited number of CPU slots. Loads are modeled at bus locations, and by selected convention, all loads between nodal locations, including lumped branches, are shifted downstream to the nearest nodal point. Load size is determined through measurement of the difference in PQ flow at the bounding nodal points. If available CPU resources are an issue, smaller loads are eliminated as they have minimal effect on the system performance.

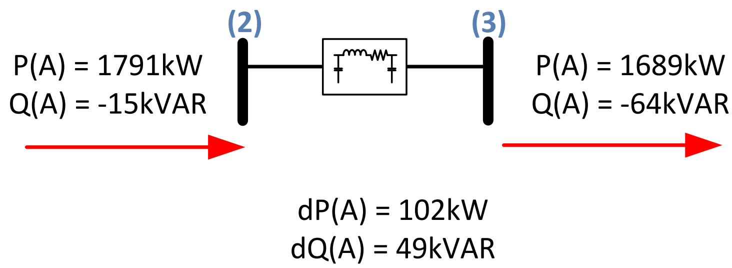

Figure 115 – Active and Reactive Power Measurement to Calculate the Power Consumption Between Two Nodes

In Figure 115, the real and reactive power for Phase A at Bus 2 and Bus 3 are measured. The difference (102 kW and 49 kVAR) is the total power consumed in between the nodes, and is a combination of line loss (generally negligible) and load. To determine the power loss component associated with the line, the simplified RTDS model was first built in a PSCAD offline simulation software package, with loads initially modeled as the full difference in power between the two nodes. Through offline simulation, the power into and out of each equivalent PI section is measured, giving the real and reactive power loss due to line. This is subtracted from the original power difference, giving a more accurate size of the load, as shown in Figure 116 below.

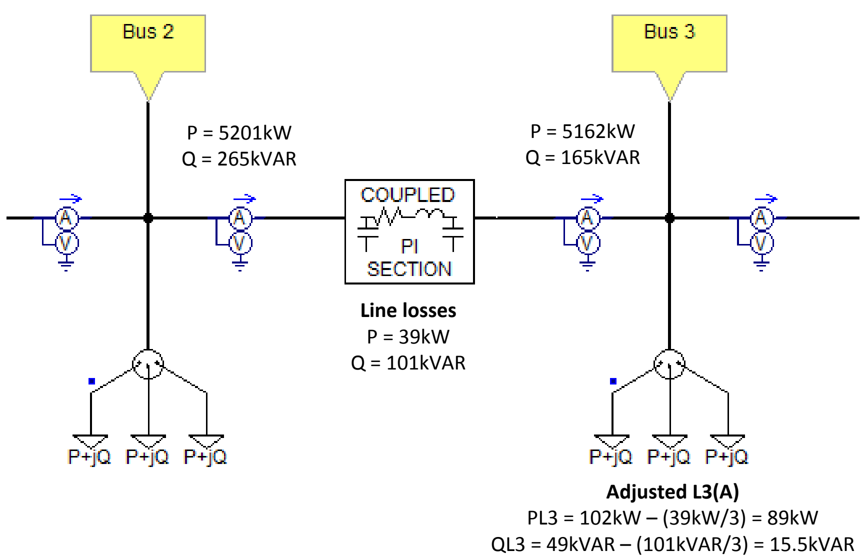

Figure 116 – The PSCAD Model of the Line Segment

The resultant section is modeled in RTDS as shown in Figure 117 below.

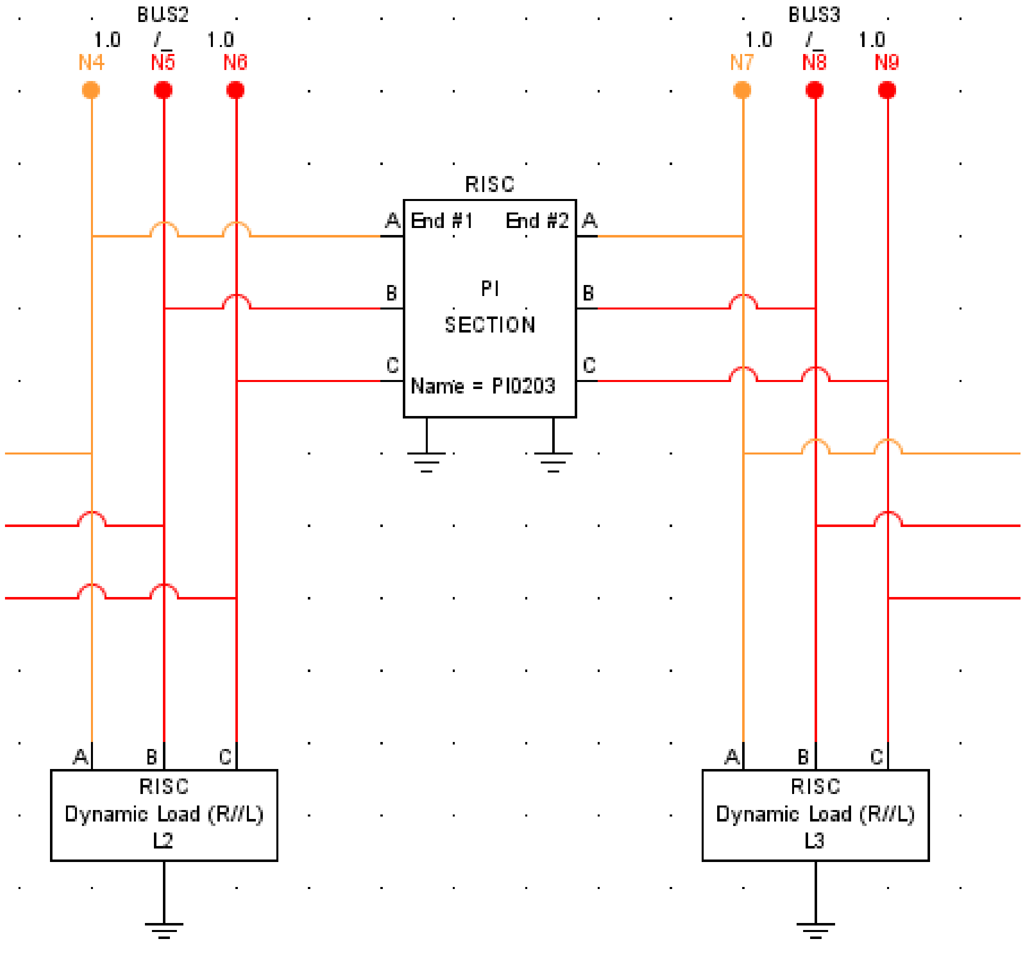

Figure 117 – The Resultant Section Model in RTDS

APPENDIX D:
Load Size and Connection for Secondary systems

Table 37 – Load Size and Connection for Secondary Systems (part I)

Bus #	Transformer kVA (est.)	Connection	Total Load		Total PV	Total EV
			kW	kVAR	kW	#
2		ABC	170	23		
3		ABC	269	34		
4		ABC	146	90		
5		ABC	587	102	30.9	
6		ABC	810	139		
8		ABC	267	46	7.3	
9		ABC	100	19	3.5	
14		ABC	446	77	3.9	
15	50	AB	55	10	12.7	1
16	50	AB	56	9	5.0	
17	50	AB	55	9	6.0	1
20		AC	235	41		1
21	100	B	70	12	4.7	
22	25	B	14	3	3.3	
23	25	B	14	2		1
18	50	A	28	5	1.5	
19	50	A	41	7	3.3	1
10	50	A	55	9	5.9	
11	50	C	28	4	4.6	
12		BC	126	22	3.5	
13	100	A	69	12	9.8	1

Table 38 – Load Size and Connection for Secondary Systems (part II)

Bus #	Transformer kVA (est.)	Connection	Total Load		Total PV	Total EV
			kW	kVAR	kW	#
7		ABC	191	32		
110		ABC	57	9	3.7	
113	50	C	28	5	27.5	
114	50	B	29	6	5.0	
115		ABC	579	99	14.1	
116		A	137	24	13.2	1
111	100	B	84	14	4.6	
112	50	B	28	5	4.7	1
103		ABC	294	51	11.6	
107	50	A	41	7	5.2	
108	50	A	41	7	4.9	
109	50	A	28	5	4.3	1
104	100	B	70	12	10.9	
105	50	B	28	5	5.2	
106	25	B	14	2		1
117					2.9	
118		ABC	111	20	18.9	2
119	50	AB	42	7		1
120	25	C	19	3	5.1	
121	25	C	19	3	5.4	1

APPENDIX E:
Secondary System Implementation in the RTDS

A simplified benchmark system as shown in Figure 118 below is used to test the secondary system for interfacing and integrating the PEV Simulator into the distribution circuit model within the RTDS. The benchmark consists of a 12 kV source with equivalent impedance of the overhead/underground conductor to a given service transformer. The PI line impedances can be adjusted based on the customer interfacing location.

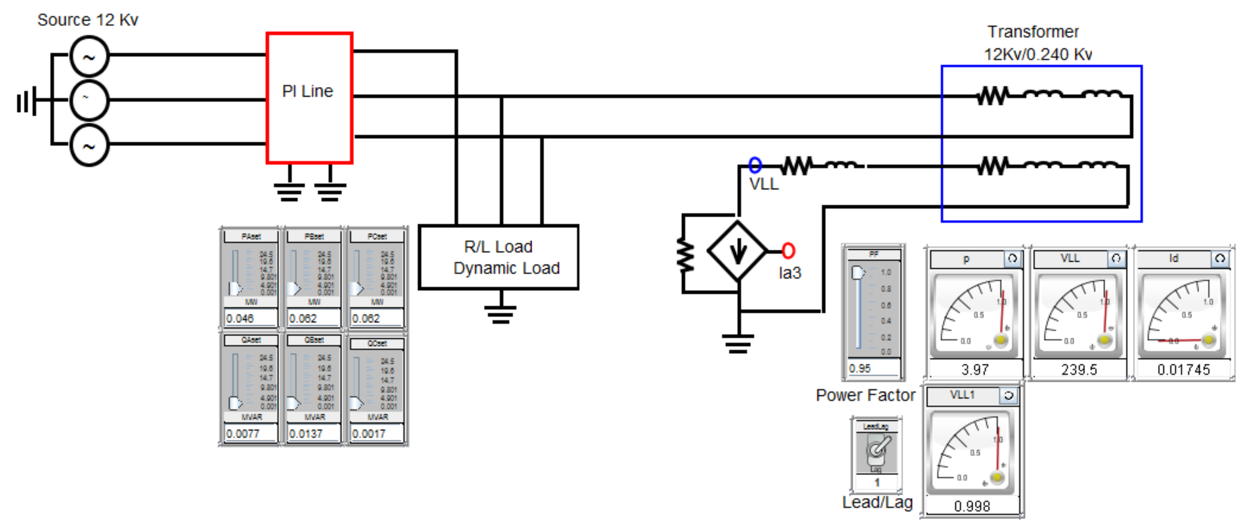

Figure 118 - AC System Diagram for Secondary Testing in RTDS

A 12 kV to 240 V, 50 kV single-phase service transformer is used as an example supply for the end customer. The current feedback from the PEV Simulator is injected through a current source. The voltage measurement at the terminals of the current source is used to synchronize the current injection. The current direction can be changed to create leading or lagging power factor for representing a PEV customer load or a solar PV system. System parameters for the test benchmark are given below.

Table 39 – Benchmark Parameters

Source	12kV, 3Φ, AC, 60 Hz
PI Line	Rp=0.25Ω, Xp=0.573Ω, XCp=9999e6Ω
Transformer	12kV/0.240kV, 1Φ, 50 kVA
Dynamic Load 2 (three phase equivalent load)	Initial Pa=0.042, Pb=0.062, Pc=0.062 MW Initial Qa=0.0077, Qb=0.0137, Qc=0.0017 Mvar
Equal Secondary Network Impedance	0.023 + j 0.0052 Ω

The process of calculating the customer load current (Ia3) is as follows:

1. **Calculation of the Magnitude of Ia3**: The value of the power is read from an excel file and according to the power factor which is defined in the runtime the magnitude is obtained.

2. **Calculation of the Phase Angle of Ia3**: In order to calculate the phase angle, a single phase Phase Locked Loop (PLL) is needed.

In this project, the simplest PLL using the first-order filter method [7] has been implemented. The PLL, the Power factor and lead/lag switch are defined in the run-time page of RTDS, where the phase angle was calculated and applied. The test results from the benchmark in RTDS are provided in the following illustrations.

Figure 119 - Shows the Vds and Vqs which are obtained from the PLL. The angle which is calculated according to the power factor, the Lead/Lag switch and using PLL is shown in Figure 120.

Figure 122 - For validating the PLL performance, a sinusoidal source is used as Vin3 that has the phase angle from the output of PLL. Vin3 completely follows the reference voltage. (An offset is used here in order to be able to show two waveforms separately).

Figure 123 - Finally, the calculated Ia3 which simulates a dynamic load current in phase or out of phase with the terminal voltage is show in this figure.

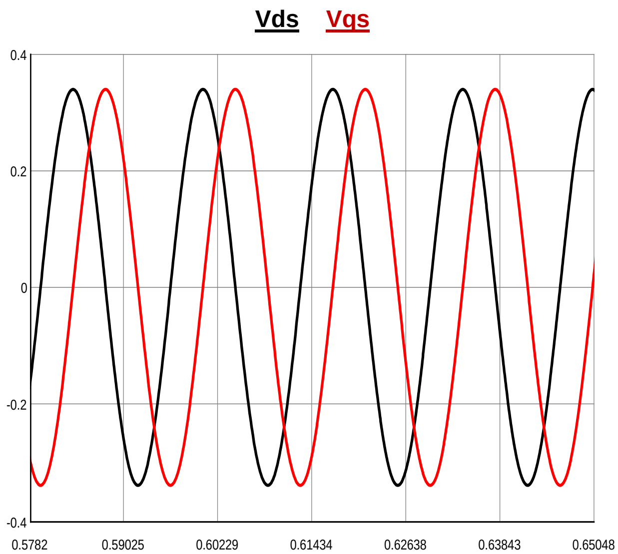

Figure 119 – d/q Components of the Terminal Voltages Corresponding to PLL

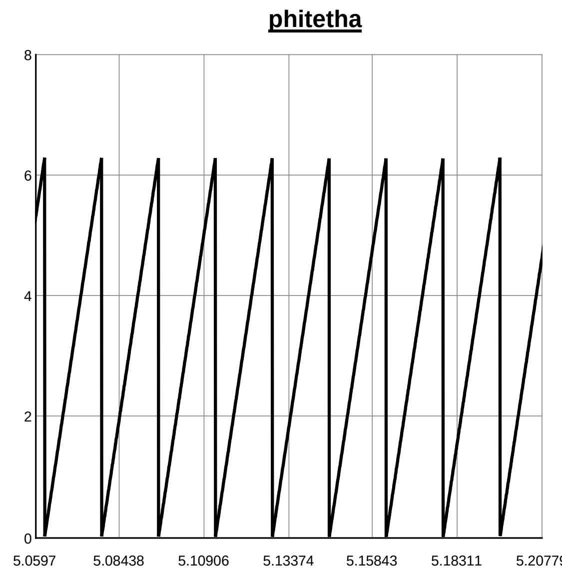

Figure 120 – Phase Angle Estimation for Ia3

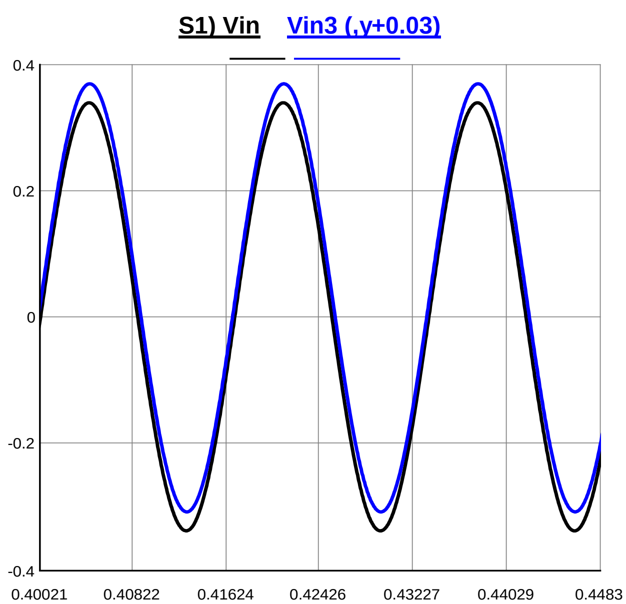

Figure 121 - Terminal Voltage vs. Load Voltage

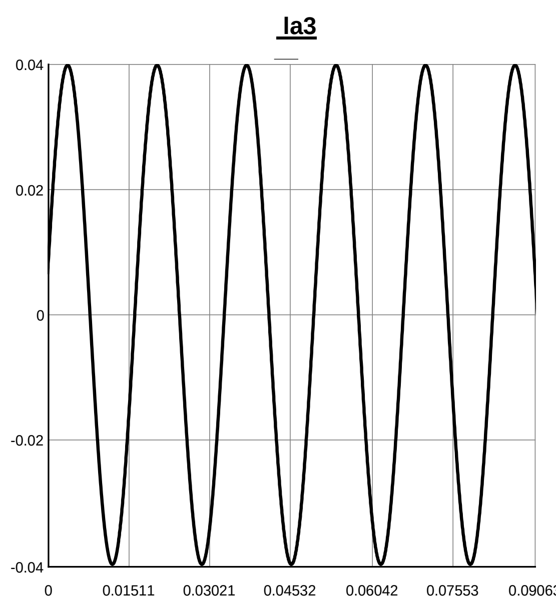

Figure 122 –Load Current

APPENDIX F: Technology Transfer Activities

Technology transfer for this demonstration project is a priority at SDG&E. The testing and impact analysis of various types and sizes of EV chargers installed on the distribution network will contribute to advancements in the system planning and investigation of mitigation solutions to ensure proper asset utilization, as well as producing a variety of benefits and consumer options for California's electricity ratepayers.

The key topics for technology transfer have been as follows:

Project Fact Sheet – A project fact sheet was developed to describe the project objectives, approach and findings in a short, 3-page format. The fact sheet was handed out to laboratory visitors during the project demonstration and tour of the test facility.

PEV Simulator Application – A quick user guide was developed to describe how to use the simulator for any potential testing applications involving electric vehicles. Possible future enhancement and added features were also identified.

Methodology for Distribution Circuit Survey and Circuit Selection - Distribution survey methodology was presented to the planning group. The method can be readily applied.

Test Bed Design - Test bed design summary including RTDS model and power hardware-in-the-loop testing approach were discussed and demonstrated to the participants.

Results - The study results of RTDS testing was shared with audiences.

Integration - The results of the field demonstration and integration testing with the Solar Carport, the Energy Storage and the employee and fleet electric vehicle chargers were presented to the planning and field engineers.

Applicability - Applicability of PEV simulator for testing smart inverter functionalities was shown through the setup development. This is an area that can provide benefit to engineers for understanding and testing grid integration aspects, which is a valuable and interesting aspect of this project for the industry, research and policy makers.

Next Steps – Using the information from the laboratory and field testing to improve the utility-industry collaboration in enhancing the EVSE design and structuring possible charging rates that attracts shifting the load to off-peak time.

Table 40 below represents a summary of specific technology and outreach activities conducted by the project team.

Table 40 - Technology Transfer & Outreach Activities

Date	Location	Topic	Presented by	Audience Served
June 19, 2013	Web Conference	Energy Commission PEV 500-11-007	SDG&E	CPR Stakeholders Meeting
July 24, 2013	Vancouver, BC	IEEE PES General Meeting 2013	SDG&E, Quanta	Work was presented in a special panel on EV and Utility infrastructure. A wide range of industry, academia and international researchers attended the panel.
Oct 2013	San Diego, CA	Plug-in 2013	SDG&E	The Plug-in 2013 conference brought together automotive industry experts and researchers to answer this question by discussing the state of the industry, and what it will take to get more PEVs on roadways.
March 31, 2014	San Diego, CA	PEV Knowledge Transfer Seminar & Training	SDG&E	SDG&E Management, Engineers, Project Managers
Sept 8, 2014	San Diego, CA	PEV Simulator – Transition Meetings	SDG&E	SDG&E Project Manager
Sept 12, 2014	San Diego, CA	PEV Simulator – Transition Meetings	SDG&E	SDG&E Project Manager
Sept 12, 2014	San Diego, CA	PEV Simulator – Transition Meetings	SDG&E	Administration Team
Sept 15, 2014	Web Conference	Energy Commission Critical Project Review Meeting for PEV Grid Impacts (500-11-007)	SDG&E, Quanta	SDG&E, Energy Commission, Quanta
Sept 15, 2014	San Diego, CA	PEV Simulator – Transition Meetings	SDG&E	Distributed Energy Resource Manager & Team
Sept 17, 2014	San Diego, CA	PEV Simulator – Plug-in Electric Vehicle Simulation	SDG&E	SDG&E Internal Departments, Directors, Engineers & Management
Sept 18, 2014	San Diego, CA	PEV Simulator – Transition Meetings	SDG&E	SDG&E Management, Engineers, Project Managers
Sept 18, 2014	San Diego, CA	PEV Simulator – Transition Meetings	SDG&E	SDG&E Management, Engineers, Project Managers

Date	Location	Topic	Presented by	Audience Served
Sept 23, 2014	San Diego, CA	PEV Simulator – Transition Meetings	SDG&E	SDG&E Management, Engineers, Project Managers
Mar 24, 2015	San Diego, CA	PEV Simulator –– Final Presentation	SDG&E, Quanta	Energy Commission Project Management Team and Guests
Mar 24, 2015	San Diego, CA	Tour of Integrated Test Facility and Demonstration of the PEV Simulator Project	SDG&E, Quanta	Pacific Gas & Electric Personnel
Mar 31, 2015	San Diego, CA	PEV Simulator – Final Report Submission	SDG&E	Energy Commission Project Management Team
May 6, 2015	SDG&E Lunch & Learn Presentation	PEV Simulator – Final Report	SDG&E	SDG&E Internal Departments, Directors, Engineers & Management
April 17, 2015	San Diego, CA	PEV Simulator – Final Report	SDG&E	SDG&E Electric Distribution Engineering (Standards)
April 2015	SDG&E Smart Grid Website	PEV Grid Impacts – Final Report & PowerPoint Presentation	Posted on SDG&E Smart Grid Website	Internal and Public Access – Please search “PEV Charging Simulator”, “500-11-007”, and/or “PIER” on SDG&E’s website
May 29, 2015	San Diego, CA	PEV Simulator – Final Report	SDG&E	Jonathan Woldemariam, Electric Transmission & Distribution Engineering Director; Neal Bartek, Distributed Energy Resources Manager
June 29, 2015	San Diego, CA	PEV Simulator – Tour at the Integrated Test Facility	SDG&E	UCLA - Rajit Gadh, PhD Professor, Founder & Director, UCLA Smart Grid Energy Research Center (SMERC)

APPENDICES

Appendix G: Distribution Circuit Survey

Appendix H: Grid Impact Testing and Data Analysis

These appendices are available as separate volumes, publication numbers CEC-500-2015-093-APG and CEC-500-2015-093-APH.